



HAL
open science

Sparse multidimensional analysis using blind and adaptive processing

Nacerredine Lassami

► **To cite this version:**

Nacerredine Lassami. Sparse multidimensional analysis using blind and adaptive processing. Signal and Image Processing. Ecole nationale supérieure Mines-Télécom Atlantique, 2019. English. NNT : 2019IMTA0139 . tel-03276296

HAL Id: tel-03276296

<https://theses.hal.science/tel-03276296>

Submitted on 2 Jul 2021

HAL is a multi-disciplinary open access archive for the deposit and dissemination of scientific research documents, whether they are published or not. The documents may come from teaching and research institutions in France or abroad, or from public or private research centers.

L'archive ouverte pluridisciplinaire **HAL**, est destinée au dépôt et à la diffusion de documents scientifiques de niveau recherche, publiés ou non, émanant des établissements d'enseignement et de recherche français ou étrangers, des laboratoires publics ou privés.

THESE DE DOCTORAT DE

L'ÉCOLE NATIONALE SUPERIEURE MINES-TELECOM ATLANTIQUE
BRETAGNE PAYS DE LA LOIRE - IMT ATLANTIQUE
COMUE UNIVERSITE BRETAGNE LOIRE

ECOLE DOCTORALE N° 601
*Mathématiques et Sciences et Technologies
de l'Information et de la Communication*
Spécialité : *Signal, image, vision*

Par

Nacerredine LASSAMI

**Représentations parcimonieuses et analyse multidimensionnelle :
méthodes aveugles et adaptatives**

Thèse présentée et soutenue à Brest, le 11 Juillet 2019
Unité de recherche : UMR CNRS 6285 Lab-STICC
Thèse N° : 2019IMTA0139

Rapporteurs avant soutenance :

Rémy BOYER Professeur, Université de Lille
Roland BADEAU Professeur, Télécom ParisTech

Composition du Jury :

Président :	Karine AMIS	Professeur, IMT Atlantique
Examineurs :	Abdel-Ouahab BOUDRAA	Professeur, Ecole navale de Brest
Rapporteurs :	Rémy BOYER	Professeur, Université de Lille
	Roland BADEAU	Professeur, Télécom ParisTech
Dir. de thèse :	Abdeldjalil AISSA-EL-BEY	Professeur, IMT Atlantique
Co-dir. de thèse :	Karim ABED-MERAIM	Professeur, Université d'Orléans

Acknowledgments

I WOULD like to express my sincerest thanks and appreciation to all the members of the Signal and Communications department for welcoming me in your laboratory. I have met many people inside and outside the work sphere that made the Ph.D an enjoyable adventure.

I am deeply grateful to my supervisors, Dr. Abdeldjalil AISSA EL BEY and Dr. Karim Abed-Meraim, for their invaluable advice, kindness, encouragements, patience and support during these three years. Their profound scientific knowledge, invaluable insight and experience have had a great impact on the success of the thesis. There is no doubt in my mind that without their comments, criticisms and guidance, my Phd will not be accomplished. I am also indebted to them for giving me the opportunity to improve my research background and experience. I am very lucky to have had the opportunity to work with them. It was always a pleasure to share an unforgettable moments rich with new results.

Furthermore, i would also like to thank my family members, especially my wife Amina and my mother, who have believed in me and who have been encouraging me all the time.

In addition, i would also like to thank my friends in Brest from both inside and outside the school with whom we had a good time, Zahran, RÃ©da, Malek, Rabie, Mohamed, Nicolas, Thomas, Sabrina, Fiona, Khalil...

Last, I dedicate this work to my newborn girl Lyne an to the soul of my dead father.

List of Figures

1.1	Global devices and connections growth from Cisco VNI Global IP Traffic Forecast, 2017-2022	6
1.2	The DOA estimation problem for a linear array antenna	8
1.3	Speech signal and its STFT spectrogram	11
1.4	Example of the "hibiscus" image and its 6-level wavelet decomposition using 2-D Daubechies-4.	12
1.5	Different enhancing sparsity penalty functions	13
2.1	Blind source separation scheme	29
3.1	Subspace performance $\rho(t)$, norm ℓ_1 of $\mathbf{W}(t)$, ℓ_0 sparsity ratio $S(\mathbf{W}(t))_\alpha$ with $\alpha = 0.05$ and the recovery error $\Gamma(\mathbf{A}^\# \mathbf{W}(t))$ in terms of dB versus time with \mathbf{A} non-orthogonal and $(d = 16, p = 9, SNR = 15dB)$	61
3.2	Subspace performance $\rho(t)$, norm ℓ_1 of $\mathbf{W}(t)$, ℓ_0 sparsity ratio $S(\mathbf{W}(t))_\alpha$ with $\alpha = 0.05$ and the recovery error $\Gamma(\mathbf{A}^\# \mathbf{W}(t))$ in terms of dB versus time with \mathbf{A} orthogonal and $(d = 16, p = 9, SNR = 15dB)$. .	62
3.3	Phase diagram of: -left- SS-FAPI for non-orthogonal \mathbf{A}_0 -right- OSS-FAPI for orthogonal \mathbf{A}_0 , with sparsity parameter $\theta = 0.3$ and $p \in \{16, 20, 24, 28, 32\}$	63
3.4	Norm ℓ_1 of $\mathbf{W}(t)$ versus time for $(d = 16, p = 9, SNR = 15dB)$ with different values μ for SS-FAPI	64
3.5	ℓ_1 -norm of $\mathbf{W}(t)$ versus time for $(d = 16, p = 9, SNR = 15dB)$ with different numbers of Givens rotations	64
3.6	Subspace performance $\rho(t)$ and norm ℓ_1 of $\mathbf{W}(t)$ versus SNR for $(d = 16, p = 9, T = 3000)$	65
3.7	Norm ℓ_1 of $\mathbf{W}(t)$ versus time for $(d = 16, p = 9, SNR = 15dB)$ with same convergence limit	66
3.8	Subspace performance $\rho(t)$ and norm ℓ_1 of $\mathbf{W}(t)$ versus time for $(d = 16, p = 9, SNR = 15dB)$ of SS-FAPI compared to SPCA algorithms .	67
3.9	Subspace performance $\rho(t)$ and norm ℓ_1 of $\mathbf{W}(t)$ versus time for $(d = 16, p = 9, SNR = 15dB)$ of FAPI algorithms vs LORAF algorithms .	68
3.10	Subspace performance $\rho(t)$ and norm ℓ_1 of $\mathbf{W}(t)$ versus time for the NIPS dataset	69

4.1	Example of source signals (solid blue lines) and their separated versions (red points) for $d = 16$, $p = 4$ and $SNR = 10dB$	83
4.2	Mean rejection level I_{pref} versus time for $d = 16$, $p = 4$ and $SNR = 20dB$	83
4.3	Mean rejection level I_{pref} versus SNR for $d = 16$, $p = 4$ after 2000 iterations.	84
4.4	Mean rejection level I_{pref} versus time for $d = 10$, $p = 4$ and $SNR = 10dB$	84
4.5	Mean rejection level I_{pref} versus Time for $d = 20$, $p = 8$ and $SNR = 10dB$	85
4.6	Amplitude of the speech source signals versus time in seconds.	85
4.7	Amplitude of a received signal (top) and its corresponding transformed version (bottom) versus time in seconds.	86
4.8	Amplitude of the separated signals versus time in seconds.	86
4.9	Mean rejection level I_{pref} versus Time for speech signals with $d = 10$, $p = 4$ and $SNR = 10dB$	87
5.1	Example of sparse SIMO channel used in simulation with $N_r = 3$ and $L = 25$	102
5.2	NMSE in dB versus time for $(N_r = 3, L = 15)$ and $SNR = 20dB$	103
5.3	NMSE in dB versus time for $(N_r = 3, L = 30)$ and $SNR = 20dB$	104
5.4	NMSE in dB versus SNR en dB for $(N_r = 3, L = 15)$	105
5.5	NMSE in dB of AMAP-adapt algorithm versus time for $(N_r = 3, L = 60)$ and $SNR = 20dB$	105
5.6	NMSE in dB and BER performance of the regularized-DML proposed approach versus SNR for BPSK modulation and $(N_t = 3, N_r = 8, L = 10)$ and $T = 1000$	106
5.7	NMSE in dB and BER performance of the regularized-DML proposed approach versus SNR for 4-QAM modulation and $(N_t = 3, N_r = 8, L = 10)$ and $T = 1000$	107
5.8	NMSE in dB and BER performance of the regularized-DML proposed approach with different number of iterations versus SNR for BPSK modulation and $(N_t = 3, N_r = 8, L = 10)$ and $T = 1000$	108
5.9	NMSE in dB and BER performance of the regularized-DML proposed approach versus SNR for BPSK modulation and sparse channel with $(N_t = 3, N_r = 8, L = 20)$ and $T = 1000$	109
5.10	NMSE in dB and MSE in dB performance of the regularized-DML proposed approach versus SNR for sparse signals with $(N_t = 3, N_r = 8, L = 10)$ and $T = 1000$	110

5.11 NMSE in dB and MSE in dB performance of the regularized-DML proposed approach versus SNR for sparse signals and sparse channels with $(N_t = 3, N_r = 8, L = 20)$ and $T = 1000$	111
---	-----

List of Tables

3.1	Summary of the computational complexity per iteration of sparse subspace tracking algorithms	69
4.1	Summary of the computational complexity of the proposed algorithms for adaptive blind sparse source separation	82
A.1	Résumé des complexités de calcul par itération des algorithmes proposés et s'il considère la contrainte d'orthogonalité	139
A.2	Résumé des Complexités de calcul par itération pour les algorithmes proposés pour la séparation aveugle de sources parcimonieuses	141

List of Algorithms

1	Projection Approximation Subspace Tracking PAST algorithm	23
2	Orthogonal Projection Approximation Subspace Tracking OPAST algorithm	23
3	Fast Approximated Power Iterations FAPI algorithm	25
4	ℓ_1 -norm Projection Approximation Subspace Tracking ℓ_1 -PAST algorithm	27
5	System matrix Sparsity algorithm based on FAPI SS-FAPI	46
6	System matrix Sparsity algorithm based on FAPI SS-FAPI2	48
7	System matrix Sparsity algorithm based on FAPI and Shear-Givens rotations SGSS-FAPI	50
8	Orthogonal System matrix Sparsity algorithm based on FAPI OSS-FAPI	52
9	System matrix Sparsity algorithm based on FAPI and Givens rotations GSS-FAPI	55
10	Data Sparsity algorithm based on OPAST for adaptive blind source separation DS-OPAST	76
11	Data Sparsity algorithm based on OPAST for adaptive blind source separation DS-OPAST2	78
12	Data Sparsity algorithm based on FAPI and Shear-Givens rotations for adaptive blind source separation SGDS-FAPI	80
13	blind sparse channel identification algorithm based on (approximated) adaptive maximum a posteriori approach MAP-adapt & AMAP-adapt	95

Acronyms

M2M Machine-to-Machine

IoT Internet of things

fECG foetal ElectroCardioGram

EVD EigenValue Decomposition

SVD Singular Value Decomposition

MUSIC MUltiple SIngal Characterization algorithm

DOA Direction-Of-Arrival

TWRI Through-the-Wall Radar Imaging

SVMs Support Vector Machines

MAC Multiply-ACcumulate

PAST Projection Approximation Subspace Tracking

OPAST Orthogonal Projection Approximation Subspace Tracking

LORAF2 LOw Rank Adaptive Filter method

NP3 Natural Power method

API Approximated Power Iterations algorithm

FAPI Fast Approximated Power Iterations algorithm

QRI sQuare-Root Inverse iteration algorithm

FRANS fast generalized Rayleigh's quotient adaptive noise subspace method

HFRANS Householder transformation-based implementation of FRANS

NOOJA Normalized Orthogonal OJA method

FDPM Fast Data Projection Method

YAST Yet Another Subspace Tracker method

OPERA OPErator Restriction Algorithm

AIC Akaike information criterion

-
- CS** Compressed Sensing
- PCA** Principal Component Analysis
- SPCA** Sparse PCA
- CSI** Channel State Information
- HDTV** High Definition TeleVision
- FIR** Finite Impulse Response
- SIMO** Single Input, Multiple Output
- MIMO** Multiple Input, Multiple Output
- ML** Maximum Likelihood
- DML** Deterministic Maximum Likelihood
- SNR** Signal-to-Noise Ratio
- PDF** Probability Distribution Function
- AWGN** additive white Gaussian noise
- STFT** Short-Time Fourier Transform
- Gpower** Generalized power Method for SPCA
- IMRP** Iterative Minimization of Rectangular Procrustes algorithm
- MM** Minimization-maximization framework
- OIST** Oja's algorithm with Iterative Soft Thresholding
- STAP** Space-Time Adaptive Processing
- BSS** Blind Source Separation
- BSSS** Blind Sparse Source Separation
- ICA** Independent Component Analysis
- SCA** Sparse Component Analysis
- i.i.d** Identically Independently Distributed
- KL** Kullback-Leibler divergence

- JADE** Joint Approximation Diagonalization of Eigenmatrices algorithm
- EASI** Equivalent Adaptive Separation via Independence algorithm
- Infomax** Information maximization algorithm
- MAP** Maximum A Posteriori estimator
- MCA** Morphological Component Analysis
- DCT** Discrete Cosine Transform
- HOS** Higher Order Statistics
- SOS** Second Order Statistics
- CR** Cross Relation method
- TSML** Two-Step Maximum Likelihood method
- SS-FAPI** System matrix Sparsity algorithm based on FAPI
- SGSS-FAPI** System matrix Sparsity algorithm based on FAPI and Shear-Givens rotations
- SGSS-FAPI-iter** SGSS-FAPI with parameter optimization
- OSS-FAPI** Orthogonal System matrix Sparsity algorithm based on FAPI
- GSS-FAPI** System matrix Sparsity algorithm based on FAPI and Givens rotations
- DS-OPAST** Data Sparsity algorithm based on OPAST for adaptive blind source separation
- SGDS-FAPI** Data Sparsity algorithm based on FAPI and Shear-Givens rotations for adaptive blind source separation
- OFDM** Orthogonal Frequency Division Multiplexing
- MAP** Maximum a Posteriori
- MAP-adapt** blind sparse channel identification algorithm based on adaptive Maximum A Posteriori approach
- AMAP-adapt** Approximated MAP-adapt
- SCR-adapt** CR-based adaptive algorithm
- IQML** Iterative Quadratic Maximum Likelihood algorithm

MLBA Maximum Likelihood Block Algorithm

MLAA) Maximum Likelihood Adaptive Algorithm

LARS Least Angle Regression algorithm

BER Bit Error Rate

MSE Mean Squared Error

NMSE Normalized Mean Squared Error

BPSK Binary Phase Shift Keying modulation

M-QAM M Quadrature Amplitude Modulation

LS Least Squares method

Notations

Symbol	Description
$(.)^H$	Hermitian transposition operator
$(.)^T$	Transposition operator
$ \cdot $	Absolute value of a number
$\ \cdot\ _p$	ℓ_p -norm of a vector or matrix
$\ \cdot\ _F$	The Frobenius norm
$\mathbb{E}[\cdot]$	Expectation operator
$\mathcal{R}(\cdot)$	Real part of the complex argument
$\mathcal{I}(\cdot)$	Imaginary part of the complex argument
$\text{Sign}(\cdot)$	Sign function of the argument
$\text{Tri}(\cdot)$	Hermitian transposed version of the upper triangular is copied to the another lower triangular part.
x	Complex or real number
\mathbf{x}	Complex or real vector
\mathbf{x}_i	The i^{th} element of the vector \mathbf{x}
\mathbf{X}	Complex or real matrix
$\text{Tr}(\cdot)$	Trace of the input matrix
$(.)^\#$	Moore-Penrose pseudo inverse operator
\mathbf{I}_n	$n \times n$ Identity matrix
\mathbb{C}	Field of complex numbers
\mathbb{R}	Field of real numbers

List of Publications

Journal Papers

Submitted

- N. Lassami, A. Aissa-El-Bey and K. Abed-Meraim, "Low Cost Sparse Subspace Tracking Algorithms", submitted to *IEEE Transactions on Signal Processing*. (Part of Chap 3).

In preparation

- N. Lassami, A. Aissa-El-Bey and K. Abed-Meraim, "Regularized deterministic maximum likelihood joint estimation of MIMO channels and input data"(in preparation). (Part of Chap 5).

Conference Papers

Submitted

- N. Lassami, A. Aissa-El-Bey and K. Abed-Meraim , "Fast Sparse Subspace Tracking Algorithm based on Shear and Givens Rotations", submitted to *Asilomar Conference on Signals, Systems, and Computers, 2019*.

Published

- N. Lassami, K. Abed-Meraim and A. Aissa-El-Bey, "Low cost subspace tracking algorithms for sparse systems", *2017 25th European Signal Processing Conference (EUSIPCO), Kos, 2017, pp. 1400-1404*. (Part of Chap 3 and part of Chap 4).

- N. Lassami, K. Abed-Meraim and A. Aissa-El-Bey, "Algorithmes de poursuite de sous-espace avec contrainte de parcimonie", *26ème colloque du Groupement de Recherche en Traitement du Signal et des Images (GRETSI)*, Juan-Les-Pins, France, 2017. (Part of Chap 3).

- N. Lassami, A. Aissa-El-Bey and K. Abed-Meraim , "Adaptive Blind Identification of Sparse SIMO Channels using Maximum a Posteriori Approach", *2018 52nd Asilomar Conference on Signals, Systems, and Computers*, Pacific Grove, CA, USA, 2018, pp. 137-141. (Part of Chap 5).

- N. Lassami, A. Aissa-El-Bey and K. Abed-Meraim, "Low Cost Sparse Subspace Tracking Algorithm based on Shear and Givens Rotations", *1st Conference on Electrical Engineering*, Algiers, Algeria, 2019. (Part of Chap 3).

- N. Lassami, A. Aissa-El-Bey and K. Abed-Meraim, "Adaptive Blind Sparse Source separation Based on Shear and Givens Rotations". *ICASSP 2019 - 2019*

IEEE International Conference on Acoustics, Speech and Signal Processing (ICASSP),
Brighton, United Kingdom, 2019, pp. 4225-4229. (Part of Chap 4).

Contents

List of Figures	ii
List of Tables	vi
List of Algorithms	viii
1 Introduction	5
1.1 Introduction	5
1.2 Multidimensional array signal processing and subspace methods . . .	7
1.3 Sparsity in signal processing	10
1.3.1 Sparsity and regularization	11
1.3.2 Sparse representations	13
1.3.3 Sparse principal component analysis	14
1.3.4 Sparsity for channel state information estimation	15
1.4 Scope of the thesis	15
1.5 Outline of the thesis	17
2 State-of-the-art: Sparsity and blind system identification	19
2.1 Introduction	19
2.2 Subspace Tracking Algorithms	20
2.2.1 Data model	21
2.2.2 Projection Approximation Subspace Tracking and Orthogonal PAST algorithms	21
2.2.3 Fast Approximated Power Iterations algorithm	24
2.2.4 Sparse Principal Component Analysis algorithms	25
2.2.5 ℓ_1 -norm Projection Approximation Subspace Tracking algorithm	27
2.3 Blind source separation	27
2.3.1 Data model	28
2.3.2 Independent Component Analysis ICA based blind source sep- aration	29
2.3.3 Sparse/Morphological Component Analysis SCA/MCA based blind source separation	31
2.4 Blind FIR channel identification	32
2.4.1 Data model	33
2.4.2 Classical approaches	35
2.4.3 Sparse approaches	37
2.5 Conclusion	38

3	Low-cost sparse subspace tracking algorithms	41
3.1	Introduction	41
3.2	Non-orthogonal sparse subspace tracking algorithms	43
3.2.1	System matrix Sparsity algorithm based on FAPI SS-FAPI	45
3.2.2	System matrix Sparsity algorithm based on FAPI SS-FAPI2	47
3.2.3	System matrix Sparsity algorithm based on FAPI and Shear-Givens rotations SGSS-FAPI	48
3.3	Orthogonal sparse subspace tracking algorithms	51
3.3.1	Orthogonal System matrix Sparsity algorithm based on FAPI OSS-FAPI	51
3.3.2	System matrix Sparsity algorithm based on FAPI and Givens rotations GSS-FAPI	52
3.4	Theoretical analysis	55
3.4.1	Convergence analysis of FAPI algorithm	55
3.4.2	Convergence analysis of the ℓ_1 minimization	56
3.5	Simulation results	58
3.5.1	Performance factors	58
3.5.2	Synthetic data	59
3.5.3	Real data	67
3.6	Discussion	68
3.7	Conclusion	72
4	Blind sparse source separation	73
4.1	Introduction	73
4.2	Data Sparsity algorithm based on OPAST for adaptive blind source separation DS-OPAST	74
4.3	Data Sparsity algorithm based on FAPI and Shear-Givens rotations for adaptive blind source separation SGDS-FAPI	77
4.4	Simulation results	82
4.5	Conclusion	87
5	Blind identification of sparse systems	89
5.1	Introduction	89
5.2	Adaptive blind identification of sparse SIMO channels using the maximum a posteriori approach	91
5.2.1	Computational complexity reduction	93
5.2.2	Gradient step optimization	94
5.3	Regularized deterministic maximum likelihood based joint estimation of MIMO channels and input data	95

5.3.1	Blind deterministic maximum likelihood DML estimation approach	97
5.3.2	Regularized blind deterministic maximum likelihood DML estimation approach	98
5.3.3	Initialization and resolving ambiguities in subspace-based blind identification of MIMO channels	101
5.4	Simulation results	102
5.5	Conclusion	109
6	Conclusions & Perspectives	113
6.1	Conclusions	113
6.2	Perspectives	115
A	Connexion with the Natural Gradient	117
	Bibliography	119

Introduction

Contents

1.1	Introduction	5
1.2	Multidimensional array signal processing and subspace methods	7
1.3	Sparsity in signal processing	10
1.3.1	Sparsity and regularization	11
1.3.2	Sparse representations	13
1.3.3	Sparse principal component analysis	14
1.3.4	Sparsity for channel state information estimation	15
1.4	Scope of the thesis	15
1.5	Outline of the thesis	17

1.1 Introduction

Recent years have seen a huge increase in our needs for transmitting more data with less latency. Wireless communications and internet services have infiltrated the society and changed our life exceeding all expectations. In addition, the demand of reliable and efficient array signal processing is still growing rapidly, especially with new contexts of Massive M2M (Machine-to-Machine) and Internet of things (IoT). By 2022, according to Cisco's annual Visual Networking Index, M2M connections that support IoT applications will account for more than half of the world's 28.5 billion connected devices [1]. Fig. 1.1 shows the forecast of the number of connected devices until 2022 by category based on 2017 numbers.

Despite electronic hardware and computer system advances, which allows most of theoretical work on signal array processing and wireless communication systems to be deployed, the requirement of more effective processing and transmitting systems keeps draining resources such as the spectral efficiency, the density of the components of integrated circuits and their power consumption. Hence, there is a crucial need

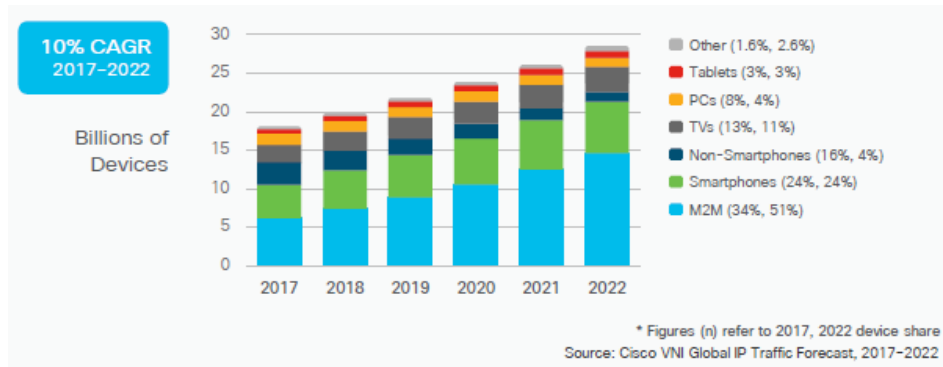


Figure 1.1: Global devices and connections growth from Cisco VNI Global IP Traffic Forecast, 2017-2022

to develop new accurate array signal processing techniques in response to these challenges.

From the signal processing point of view, future algorithmic solutions must have low computational complexity and adaptive schemes where the outputs can be updated based on previous outputs without repeating all the processing. This is important to reduce the power consumption of the calculation hardware and to be able to keep the processing accurate even in case of non-stationary environments.

In wireless communications, the most common problem faced by designers of wireless communication systems is how to estimate Channel State Information (CSI). Solutions based on pilot sequences are generally used, despite lost in bandwidth efficiency. Blind solutions are suitable because of their capacity to give the transmitter more flexibility where it can reduce or totally get rid of the pilot sequences to have a better bandwidth efficiency. Blind techniques are also recommended in case of military communications to avoid sending pilot sequences. They enable us also to treat problems where we cannot influence the input such as the extracting of the foetal electrocardiogram (fECG).

In order those signal processing methods to be more accurate, all available information should be used. In various applications, sparsity *a priori* has been successfully used to enhance algorithms performance. Sparse representation has attracted much attention from researchers in fields of signal processing, image processing, computer vision and pattern recognition [2–6]. Despite the amount of work dedicated to sparsity-based methods, the potential of the sparsity *a priori* is remaining not fully exploitable and some problems are still widely open [7].

Motivated by the above ideas, this thesis combines the recent advances in sparse representations/estimation and array signal processing methods, especially those

based on subspace techniques to meet the challenge of developing more accurate blind low-cost solutions. We have investigated three major topics: sparse principal subspace tracking, blind sparse source separation and blind sparse channel identification. Each time, we have targeted solutions that are adaptive and have low computational cost.

In this chapter, we first present a brief introduction and a chronology of development of the main subjects investigated in this thesis, in particular, subspace methods and sparsity based methods. Then, a small scope of the thesis followed by the organization of the manuscript is presented.

1.2 Multidimensional array signal processing and subspace methods

Beside the fact that array antenna design and array processing have experienced five decades of intensive research, they are still an active and open topic. As a matter of fact, the recent technological advances have made the realization of array systems (ground/air/space borne) and real-time processing possible [8]. Riding on the wave of electronic hardware and computer system advances, the scientific interest in the realization of complex systems such as antenna array and real-time signal processing has grown enormously in the recent years. So far, antenna array design as well as array signal processing has obtained fruitful achievements in theory, algorithm and hardware. However, the need for faster and more accurate signal processing routines as well as the need for more efficient and miniaturized antennas and sensors still continues [8].

Most of the classical statistical estimation methods in array signal processing can be divided into maximum likelihood (ML), least-squares and moment methods. Maximum likelihood is based on statistical setting, least-squares is derived from geometrical considerations, whereas the method of moments exploits properties of the moments of the observed data in an ad-hoc fashion. The subspace-based approach to parameter estimation is more close to the moment method class compared to the other classes. However, in the literature, subspace-based methods usually get their own class. Their motivation is similar to the moment-based approach, though: a geometrical relation involving the exact moments of the data is set up. Most commonly, the covariance matrix of the data is used, although to suppress the effects of noise, one can also consider higher-order moments. The desired signal parameters are then extracted by solving the geometrical relation in some approximate sense, and using sample moments instead of the exact ones. The distinguishing feature of subspace-based methods is that the underlying geometrical relation involves a

low-rank 'moment matrix' of the data. However, when the moments are estimated using a finite number of noisy samples, the resulting matrix has full rank. Thus, the low-rank structure is restored using the eigenvalue decomposition (EVD) of the sample covariance matrix or the truncated singular value decomposition (SVD) of the data matrix before any further processing. This non-parametric data reduction is the first step of all subspace-based methods. The motivation is that by applying a preliminary noise cleaning step using rank truncation, it becomes less critical how the desired signal parameters are extracted later [9].

The introduction of MUSIC (MUltiple SIgnal Characterization algorithm) in [10] marked the beginning of the 'subspace era' in signal processing. It was introduced in order to solve the problem of direction of arrival DOA estimation. The goal of DOA estimation is to use the data received at the d -array antenna to estimate the DOA's $\theta_1, \dots, \theta_p$ of the p emitting sources as showed in Fig. 1.2 for the case of a linear array.

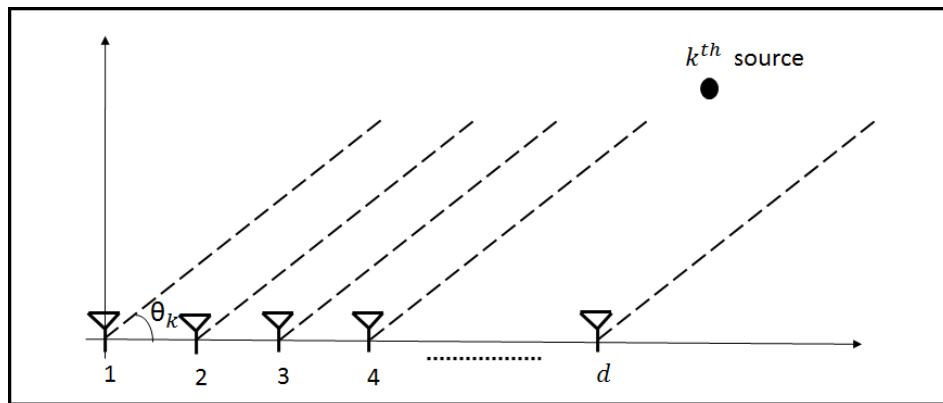


Figure 1.2: The DOA estimation problem for a linear array antenna

advantages in terms of performance (high resolution for DOA estimation) versus complexity, as compared to traditional methods, have been documented both analytically and experimentally [11, 12]. The ideas have been brought into diverse areas as smart antennas for wireless communication, sensor arrays, multiuser detection, time delay estimation, image segmentation, speech enhancement, learning systems, magnetic resonance spectroscopy and radar systems [11, 12].

Subspace methods remain interesting research area nowadays, especially with the explosion of problem dimension which makes the low rank dimensionality reduction feature of subspace methods more appreciated. For example, we can mention recent work about: channel estimation of Large Millimeter-Wave MIMO Systems [13], wall clutter mitigation in Through-the-Wall Radar Imaging (TWRI) [14] and Support

Vector Machines (SVMs) for hyperspectral image classification [15].

Most of subspace methods are based on EVD or SVD decompositions. Unfortunately, such decompositions require a lot of calculation especially when the problem has high dimension. In fact, if d is the dimension of the observed data vector (number of sensors), then, the EVD/SVD decomposition complexity¹ is of order $\mathcal{O}(d^3)$ flops. In case of time-varying system, we deal frequently with non-stationary signals and we have to update the estimation of the subspace every time we receive new observations. Hence, using repeated EVD or SVD based subspace methods is very time consuming task. This is unsuitable because the processing time can exceed the time where the system is considered unchanged (coherence time for communications systems where the channel impulse response is essentially invariant). Many subspace tracking algorithms were proposed to replace the EVD/SVD decomposition in the adaptive case by updating the previous subspace estimation at every received data sample without a huge computational cost.

The subspace tracking algorithms can be classified according to the targeted subspace to principal (signal or dominant) subspace trackers, minor (noise) subspace trackers and subspace trackers which can be used to estimate both minor and principal subspaces. For example, we can mention the projection approximation subspace tracking (PAST) algorithm [16], the orthogonal PAST (OPAST) [17], the low rank adaptive filter (LORAF2) [18], the natural power method (NP3) [19], the approximated power iterations (API) algorithm [20] and its fast version (FAPI) [21] as principal subspace trackers. Whereas the square-root inverse iteration algorithm (QRI) [22], the fast generalized Rayleigh's quotient adaptive noise subspace (FRANS) [23] and a Householder transformation-based implementation (HFRANS) [24] algorithms belong to minor subspace trackers. Other algorithms such as OJA [25], normalized orthogonal OJA (NOOJA) [26], fast data projection method (FDPM) [27] and yet another subspace tracker (YAST) [28] can handle both principal and minor subspace tracking.

The subspace tracking algorithms can also be classified according to their complexities to three classes. If p denotes the rank of the principal or minor subspace that we would like to estimate, since usually $p \ll d$, then it is classic to refer to the three classes by their computation complexity i.e. algorithms which have a computational complexity of order $\mathcal{O}(d^2)$ or $\mathcal{O}(pd^2)$ per update such as Jacobi SVD method [29], the transposed QR-iteration [30] and [31]. Algorithms which have a computational complexity of order $\mathcal{O}(dp^2)$ such as Karasalo's algorithm [32], the operator restriction algorithm (OPERA) [33] and the natural power method

¹Operations counts are expressed in terms of multiply-accumulate (MAC) operations. Only the dominant cost is presented

NP2 [19]. Finally the less time-consuming algorithms which have a linear computational complexity of order $\mathcal{O}(dp)$ such as PAST [16], OPAST [17], NP3 [19] and FAPI [21].

Estimating the subspace adaptively requires the use of a certain processing window such as the exponential window or the truncated sliding window. The type of the processing window can also be another criterion to classify the subspace tracking algorithms. The exponential window has a forgetting factor which is used to control the impact of the previous estimation on the new one. Algorithms which use the exponential window have smaller computational complexity and memory needs compared to algorithms which use a truncated sliding window. However, the truncated sliding window is more appreciated for fast tracking of signal parameter changes. It is worth mentioning that some algorithms such as FAPI [21] are derived for both the exponential window or the truncated sliding window.

1.3 Sparsity in signal processing

In its most general definition, the principle of sparsity, or parsimony, consists of representing some phenomenon with as few variables as possible. Numerous tools have been developed by statisticians to build models of physical phenomena with good predictive power. Models are usually learned from observed data, and their generalization performance is evaluated on test data. Among a collection of plausible models, the simplest one is often preferred, and the number of underlying parameters is used as a criterion to perform model selection as is the case with the Akaike information criterion (AIC).

A discrete signal can be considered as sparse if only a small number its elements are non-zero, compared to its dimension. Common situation in the case of real-world signals is that the number of significant coefficients is small as compared to the number of other components. These coefficients could be neglected or set to zero for the purpose of compression, denoising or to get a simpler representation which is easier to manipulate. Otherwise, most of signals can be decomposed in a certain representation domain in order to be sparse. For example, speech signals are known to be sparse in the temporal domain. However, speech signals transformed with the short-time Fourier transform (STFT), have a sparser representation as it is shown in Fig. 1.3 where we present a speech signal and its STFT spectrogram. Same remarks can be seen for natural images after the wavelet transform as we show in Fig. 1.4. This sparsity resulted in a simple and an effective procedure for image denoising where we use thresholding methods in order to set to zero the negligible wavelet coefficients.

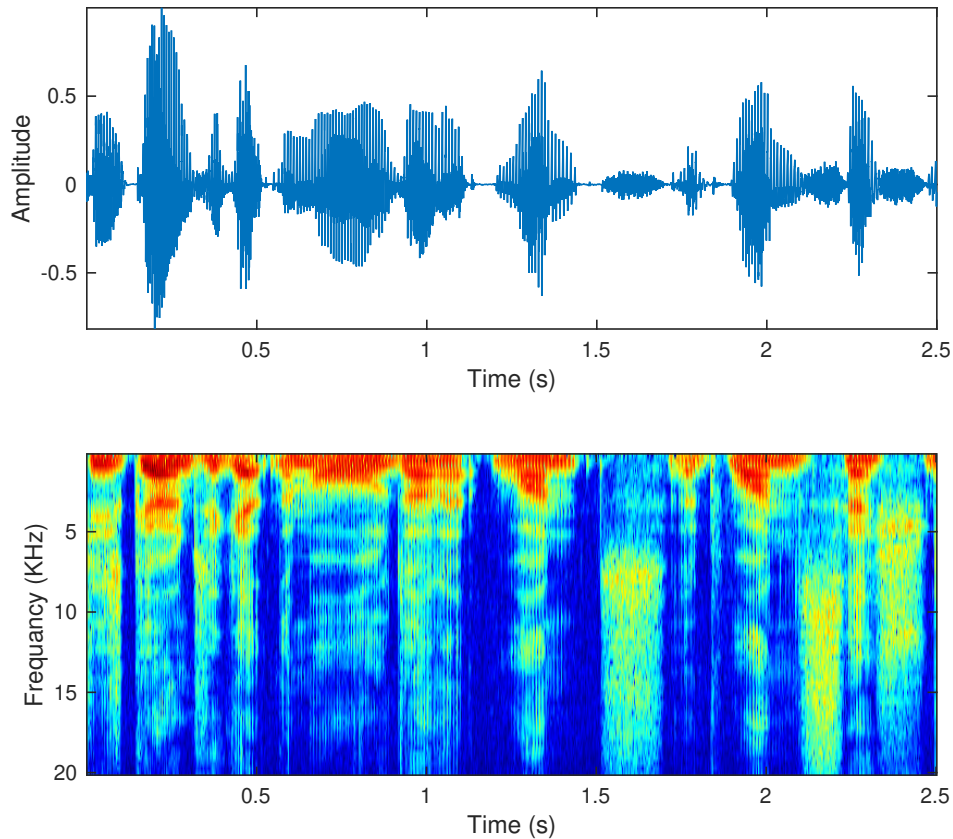


Figure 1.3: Speech signal and its STFT spectrogram

The obvious applications of the sparsity are modelling and compression. Nevertheless, sparsity is often used to solve ill-conditioned (underdetermined) inverse problems based on the regularization technique. The use of the sparsity principle has also led to state-of-the-art algorithms in denoising, inpainting, deconvolution, sampling, etc. In this section, we will give some insight about the sparsity benefits from the point of view of: regularization, sparse representation, sparse principal component analysis and sparse channel estimation.

1.3.1 Sparsity and regularization

In signal and image processing, one can often encounter problems formulated as such underdetermined linear systems of equations where one has fewer equations than unknowns. Clearly, there are infinitely many possible solutions that may 'explain' the observations, among which there are some that may look better than others. In order to narrow this choice to one well-defined solution, additional criteria are needed. A familiar way to do this is regularization, where a penalty function that

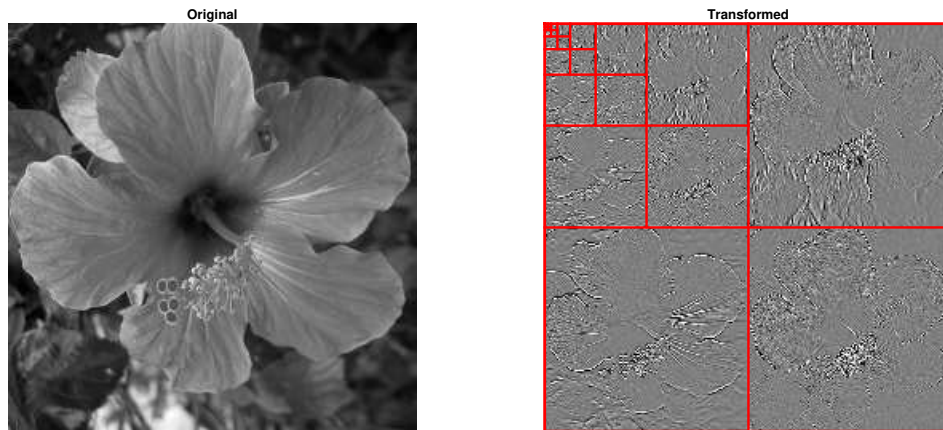


Figure 1.4: Example of the "hibiscus" image and its 6-level wavelet decomposition using 2-D Daubechies-4.

evaluates the desirability of a would-be solution is introduced, with smaller values being preferred (minimization of the penalty function). Classical penalty function would be the ℓ_2 -norm of the solution vector which leads to the so called minimum-norm solution [34]. This function was widely used due to its convexity and simplicity leading to closed-form and unique solution. In many instances, it is known that the solution is sparse or compressible. For example, in a biological experiment, one could measure changes of expression in 30,000 genes and expect at most a couple hundred genes with a different expression level [35]. Attracted by the convexity of ℓ_p -norms for $p \geq 1$, such norms were also used as regularization penalty functions [34]. The special case of ℓ_1 -norm, which in addition to guaranteeing the uniqueness of the solution due to the convexity property, promotes sparse solutions. In order to get sparser solutions than the ℓ_1 -norm, we can use regularization penalty functions based on ℓ_p -norms for $0 \leq p < 1$ (no longer formal norms as the triangle inequality is no longer satisfied). However, these functions are not convex which leads to more complicated optimization problems. The extreme case of ℓ_0 -norm is a very simple and intuitive measure of sparsity counting the number of nonzero entries in a vector. The term ℓ_0 -norm is misleading, as this function does not satisfy all the axiomatic requirements of a norm. In addition to optimization difficulty of the regularization problem, the ℓ_0 -norm is not necessarily the right notion for empirical work [34]. A vector of real data would rarely be representable by a vector of coefficients containing many zeros. A more relaxed and forgiving notion of sparsity can and should be built on the notion of approximately representing a vector using a small number of non-zeros such as the ℓ_p -norms described above [34]. Other penalty functions were also proposed in literature and showed their superiority compared to ℓ_1 -norm in

enhancing sparse solutions such as reweighted ℓ_1 [35] or smooth ℓ_0 [36]. Figure 1.5 illustrates the behaviour of different enhancing sparsity penalty functions.

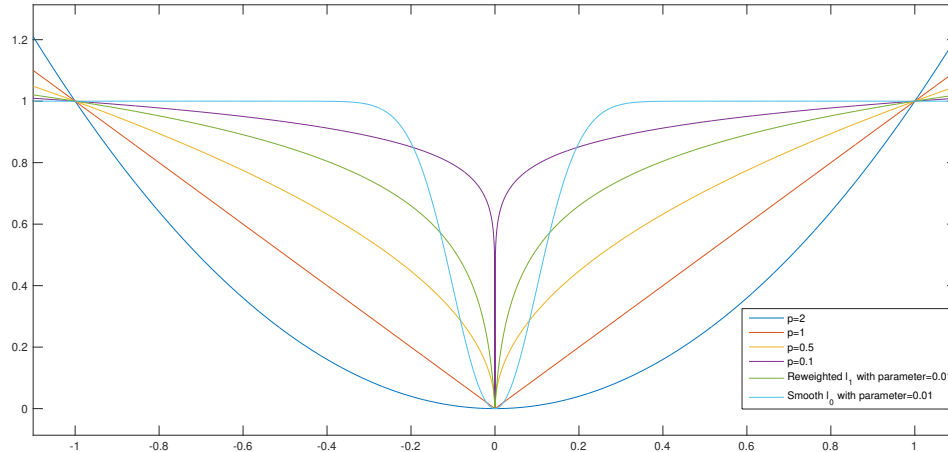


Figure 1.5: Different enhancing sparsity penalty functions

1.3.2 Sparse representations

In parallel with the regularization approach, another insight has been developed in signal and image processing, where it has been found that many media types (imagery, video, acoustic) can be sparsely represented using transform-domain methods [34]. In fact many important tasks dealing with such media can fruitfully be viewed as finding sparse solutions to underdetermined systems of linear equations. Each signal is approximated by a sparse linear combination of the transformation matrix columns called dictionary elements or atoms, resulting in simple and compact models or representations.

In various instances in signal processing, an important part of the processing is achieved by an efficient representation of the considered signal. Sparse representation has attracted much attention from researchers in fields of signal processing, image processing, computer vision and pattern recognition [34]. Sparse representation, from the viewpoint of its origin, is directly related to time-frequency analysis where signals are studied in both the time and frequency domains simultaneously. The time-frequency analysis is equivalent to projecting an observed signal on the analysis chosen base. This idea was also extended later to time-scale analysis and went from orthonormal analysis bases such as local Cosin and wavelet to overcomplete dictionaries such as Gabor atoms. In the overcomplete case, signals can have more than one possible representation due to their redundancy. Hence, the sparsity information is desired to force a unique representation with the lowest number of

atoms. This problem has the same formulation as the regularization ℓ_0 problem discussed above.

Research has focused on three aspects of the sparse representation: pursuit methods for solving the optimization problem, such as matching pursuit [37], orthogonal matching pursuit [38], basis pursuit [39], LARS/homotopy methods [40]. Methods for designing and learning the adequate dictionary from the observed data instead of a predefined dictionary, such as the K-SVD method [2]. The applications of the sparse representation for different tasks, such as signal separation [3,6], denoising [5], coding [41], etc. The well known media encoding standards JPEG and its successor, JPEG2000 are based on the notion of transform encoding that leads to a sparse representation.

Compressed Sensing (CS) is a recent branch that separated from sparse and redundant representations, becoming a centre of interest of its own. It is one of the most popular topics in recent years. In a recent work that emerged in 2006 by Emmanuel Candes, Justin Romberg, Terence Tao, David Donoho [42–44], and others that followed, the theory and practice of this field were beautifully formed. CS theory suggests that if a signal is sparse or compressive, the original signal can be reconstructed by exploiting a few measured values. Exploiting sparse representation of signals, their sampling can be made far more effective compared to the classical Nyquist-Shannon sampling. This main result explains the popularity of CS researches in the recent years.

1.3.3 Sparse principal component analysis

Sparsity has been successfully applied to different signal processing topics as we mentioned above. In case of Principal Component Analysis (PCA), the sparsity was also introduced to correct some weakness of the classical PCA. In fact, PCA is a statistical procedure that uses an orthogonal transformation to convert a set of observations of possibly correlated variables into a set of values of linearly uncorrelated variables called principal components. PCA is widely used for data processing and dimensionality reduction. However, it suffers from the fact that each principal component is a linear combination of all the original variables, thus it is often difficult to interpret the results. In addition, datasets often have number of input variables comparable with or even much larger than the number of samples. It has been shown that if their ratio does not converge to zero, the classical PCA is not consistent i.e. the PCA loadings does not match with the dominant eigenvectors of the covariance matrix of the dataset. To address the drawbacks of classic PCA, various modified PCA methods have been proposed to form principal components where each one is the linear combination of a small subset of the variables while still explain high

percentage of data variance. Such methods are designed by Sparse PCA (SPCA). Moreover, besides the interpretability and high-dimensional estimation consistency would not be the only advantage of SPCA, we can discard the variables with zero loadings in all of the PCs, so it will lead to an automatic feature selection. SCoT-LASS proposed in [45], a quite natural extension to classic PCA, which maximizes the explained variances with ℓ_1 constraints on the loadings, as well as orthogonal conditions on subsequent loadings. D'Aspremont *et al.* [46] suggested a semidefinite programming problem as a relaxation to the ℓ_0 -penalty for sparse covariance matrix. The SPCA developed by Zou *et al.* [47] formulates PCA as a regression-type optimization problem, and then to obtain sparse loadings by imposing the Lasso or Elastic-net penalty on the regression coefficients. More algorithms for SPCA were proposed later such as GPower [48] and IMRP [49]. The interest in SPCA solutions has increased with the growth of the datasets size and the need to more efficient dimensionality reduction algorithms.

1.3.4 Sparsity for channel state information estimation

Wireless communication systems have to be designed in such way that the adverse effect of multipath fading is minimized. Fortunately, multipath can be seen as a blessing depending on the amount of Channel State Information (CSI) available to the system. However, in practise CSI is seldom available *a priori* and needs to be estimated. On the other hand, a wireless channel can often be modelled as a sparse channel in which the delay spread could be very large, but the number of significant paths is normally very small. Such channels are encountered in many communication applications. High Definition television (HDTV) channels are hundreds of data symbols long but there are only a few nonzero taps. Hilly terrain delay profile has a small number of multipath in the broadband wireless communication and underwater acoustic channels are also known to be sparse and long. The prior knowledge of the channel sparseness can be effectively used to improve the channel estimation using regularization techniques such in [50] or the Compressed Sensing theory [51].

1.4 Scope of the thesis

In the course of last decade, mathematical and statistical study of sparse representations and their applications in audio, in image, in video, in sources separation and in communication systems knew an intensive activity. However, the potential of the sparsity *a priori* is remaining not fully exploitable and some problems are still widely open such as blind separation and identification problems. In the

other hand, the interest in low-cost and adaptive solutions to array signal processing problems such as subspace-based estimation and dimensionality reduction methods keeps growing, especially with the notable increase in problems dimensions. This thesis is motivated by those new opportunities and the challenge to find low-cost and blind solutions to array signal processing problems by combining the recent advances in subspace-based estimation and dimensionality reduction methods with the *a priori* sparsity information in order to enhance the processing performances. We have undertaken three main studies:

The first challenge in this thesis aims to solve is sparse principal subspace tracking. After a deep state-of-the-art, we proposed low-cost solutions based on a two-step approach where at every received data we update the principal subspace, then, the sparse desired basis. The proposed algorithms have different characteristics such as the sparsity performance (speed and limit of convergence), the computational complexity and the orthogonality of the solution. In addition, we show that under some mild conditions, they are able to recover the sparse ground truth mixing matrix. They outperform the state-of-the-art schemes in terms of low computational complexity (suitable for the adaptive context) and they achieve both good convergence and estimation performance.

The second line of research is adaptive blind sparse source separation. Our goal is to use the information about the source signals sparsity in order to blindly separate them adaptively. Contrary to most of the literature on the blind sparse source separation, we are interested in the overdetermined case where subspace methods can be used to estimate the principal subspace of the received data. We have followed a similar two step-approach as for sparse principal subspace tracking where we start by estimating the principal subspace then we calculate the separating matrix. We have proposed two algorithms that have low computational complexity which make them suitable for adaptive processing. Simulations are carried out to evaluate the performance of the resulting algorithms compared to the state-of-the-art.

The third subject that we have treated is the blind identification of Finite Impulse Response (FIR) systems. We started by proposing a new solution to adaptively estimate Single Input, Multiple Output (SIMO) channel impulse response using the sparsity additional information. The proposed algorithm has low computational complexity. In addition, it is robust to the overestimation of the channel order errors. Later, we investigated the problem of blindly estimating both the Multiple Input, Multiple Output (MIMO) channel impulse responses and the input data. We have considered the Deterministic maximum likelihood (DML) formulation and add some regularization penalty functions to exploit the *a priori* information such as the finite source alphabet simplicity property or/and the sparsity of the channel re-

sponses. After an initialization done by some state-of-the-art method, the resulting criterion is alternatively optimized over the channel and data due to the convexity of the used formation in each parameter separately. Both proposed algorithms are compared to state-of-the-art solutions.

1.5 Outline of the thesis

The document is organized as follows:

Chapter 2 is dedicated to introduce the investigated problems and to present their state-of-the-art. We start by the problem of subspace tracking algorithms under a sparsity constraint on the weight matrix. Then, the blind source separation problem is considered with a sparsity *a priori* on the source signals. After that, the blind FIR channel identification problem is addressed with a focus on the sparse channel case. We stress weak and strong points of some of the latest literature solutions in each case.

In Chapter 3, we address the sparse principal subspace tracking problem. We exploit the sparsity information to design multiple algorithms. First, the sparse subspace is considered non-orthogonal which is most likely the case in blind source separation with a sparse mixing matrix. Then, we consider the orthogonal case which is much closer to SPCA case. A comparison in terms of complexity is done and conditions of successfully recover the sparse ground truth mixing matrix are investigated.

Chapter 4 is devoted to blind sparse source separation. The sparsity information about the sources is used to allow the blind separation. In order to enable an adaptive separation, we focus on low-cost solutions. Simulations are conducted to compare the two proposed algorithms with state-of-the-art solutions.

In Chapter 5, we investigate the problem of blind identification of FIR systems. First, we consider the SIMO case, where the sparsity information is used to adaptively estimate the channel impulse response. For the MIMO case, we present a bilinear approach based on a regularized DML formation of the problem. This formulation allows us to alternatively estimate the channel impulse responses and the input data using the *a priori* information about the problem as a regularization penalty. Different *a priori* are considered such as sparse channel and finite alphabet simplicity of the input data. The proposed solutions are compared to existing methods in different simulations scenarios.

Finally Chapter 6 concludes the document and gives some perspectives.

State-of-the-art: Sparsity and blind system identification

Contents

2.1	Introduction	19
2.2	Subspace Tracking Algorithms	20
2.2.1	Data model	21
2.2.2	Projection Approximation Subspace Tracking and Orthogonal PAST algorithms	21
2.2.3	Fast Approximated Power Iterations algorithm	24
2.2.4	Sparse Principal Component Analysis algorithms	25
2.2.5	ℓ_1 -norm Projection Approximation Subspace Tracking algorithm	27
2.3	Blind source separation	27
2.3.1	Data model	28
2.3.2	Independent Component Analysis ICA based blind source sep- aration	29
2.3.3	Sparse/Morphological Component Analysis SCA/MCA based blind source separation	31
2.4	Blind FIR channel identification	32
2.4.1	Data model	33
2.4.2	Classical approaches	35
2.4.3	Sparse approaches	37
2.5	Conclusion	38

2.1 Introduction

Blind system identification is a fundamental signal processing technology and has received an increasing research interest. Most of the work tends to explore to a higher degree the diversities inherent in multiple-output systems. At the same time,

making use of the sparsity information in some signal processing applications has been very successful. Hence, the combination of these two ideas is really interesting, especially, in response to the challenge of developing more accurate methods under more 'real-time' constraints. The three main subjects in this thesis are: tracking the sparse principal subspace, where we consider an instantaneous mixture with a sparsity information of the system mixing matrix. The second subject is blind sparse source separation which considers the same instantaneous mixture but with a sparsity information on the input data. The third subject is blind sparse FIR channel identification which is a more complicated problem due to the considered convolutive mixture model. In this case, the sparsity information is on the FIR channel.

In this section, we will give some hints about each one of the three blind problems in a classical way (without the sparsity information). We will present some of the popular approaches to solve these problems, and which we may need later in the next chapters to develop our proposed methods. After that, we will develop how the sparsity has been brought to treat each type of these problems and how it impacts the processing. Finally, we will present some state-of-the-art solutions that will be used later as a benchmark for the proposed methods.

2.2 Subspace Tracking Algorithms

Subspace estimation plays an important role in a variety of modern signal processing applications. It has been applied successfully in a variety of problems. Typical examples are the MUSIC [10] and the ESPRIT [52] algorithms for estimating frequencies of sinusoids or directions of arrival (DOA) of plane waves impinging an antenna array. Both mentioned algorithms have as first step the estimation of a correlation matrix, then calculating its eigen-decomposition. If we consider a tracking context where the sources are moving, we have to estimate the DOA's more frequently. However, this could be complicated due to the computational complexity of the decomposition needed. In fact, the implementations of these techniques have been based on the batch EVD of the sample correlation matrix or on the batch SVD of the data matrix. This is unsuitable for adaptive processing because it requires repeated EVD/SVD, which is a task that is very time consuming. In order to overcome this difficulty, a number of adaptive algorithms for subspace tracking has been developed. In chapter 1, we have proposed a brief historical overview on the subspace tracking algorithms. Now, we will present the data model, as well as the used state-of-the-art algorithms for principal subspace tracking.

2.2.1 Data model

Let $\mathbf{x}(t)$ be a d -random data vector observed at the t^{th} snapshot. For example, $\mathbf{x}(t)$ may represent the samples of an array of d sensors $\mathbf{x}(t) = [x_1(t), \dots, x_d(t)]^T$ in spatial domain. It can also be in time domain, a vector of d consecutive samples of a time series $\mathbf{x}(t) = [x(t), x(t-1), \dots, x(t-d+1)]^T$. We assume $\mathbf{x}(t)$ satisfying the following very common observation signal model:

$$\mathbf{x}(t) = \mathbf{A}(t)\mathbf{s}(t) + \mathbf{n}(t) \quad (2.1)$$

where $\mathbf{s}(t) = [s_1(t), \dots, s_p(t)]^T$ is the p -dimensional ($p < d$) zero-mean random signal vector with its covariance matrix $\mathbf{C}_s(t) = \mathbb{E}[\mathbf{s}(t)\mathbf{s}(t)^H]$ non singular. The vector $\mathbf{n}(t)$ is zero-mean additive random white noise uncorrelated with the signal and $\mathbf{A}(t)$ is a $d \times p$ full rank mixing matrix which describes the p signals. The covariance matrix of the observation vector is given by :

$$\mathbf{C}_x(t) = \mathbb{E}[\mathbf{x}(t)\mathbf{x}(t)^H] = \mathbf{A}(t)\mathbf{C}_s(t)\mathbf{A}^H(t) + \sigma_n^2\mathbf{I}_d \quad (2.2)$$

with σ_n^2 is the power of the white additive noise. Applying EVD on $\mathbf{C}_x(t)$ yields to:

$$\mathbf{C}_x(t) = \begin{bmatrix} \mathbf{U}_s(t) & \mathbf{U}_n(t) \end{bmatrix} \begin{bmatrix} \mathbf{\Delta}_s(t) + \sigma_n^2\mathbf{I}_p & 0 \\ 0 & \sigma_n^2\mathbf{I}_{d-p} \end{bmatrix} \begin{bmatrix} \mathbf{U}_s^H(t) \\ \mathbf{U}_n^H(t) \end{bmatrix} \quad (2.3)$$

where $\mathbf{\Delta}_s(t) + \sigma_n^2\mathbf{I}_p$ is the diagonal matrix of the p dominant eigenvalues of $\mathbf{C}_x(t)$. $\mathbf{U}_s(t)$ is the $d \times p$ orthonormal basis for the signal subspace of $\mathbf{C}_x(t)$ and $\mathbf{U}_n(t)$ is the $d \times (d-p)$ orthonormal basis for the noise (minor) subspace of $\mathbf{C}_x(t)$. So far, we have assumed:

- **A1:** Linear overdetermined data model with $d > p$.
- **A2:** Having the knowledge of the sources number p .
- **A3:** Non singularity of the covariance matrix $\mathbf{C}_s(t)$.
- **A4:** $\mathbf{n}(t)$ is an additive white noise.

The objective of principal subspace tracking algorithms is estimating the instantaneous full column rank weight $d \times p$ matrix $\mathbf{W}(t)$ which spans the same subspace as $\mathbf{A}(t)$ and $\mathbf{U}_s(t)$.

2.2.2 Projection Approximation Subspace Tracking and Orthogonal PAST algorithms

In order to solve the principal subspace tracking problem, Yang has proposed in [16] to minimize the weighted quadratic error of reconstruction given by:

$$J_{PS}(\mathbf{W}(t)) = \sum_{i=1}^t \beta^{t-i} \left\| \mathbf{x}(i) - \mathbf{W}(t)\mathbf{W}^H(t)\mathbf{x}(i) \right\|_2^2 \quad (2.4)$$

22 Chapter 2. State-of-the-art: Sparsity and blind system identification

where $0 < \beta < 1$ is the forgetting factor used to afford the tracking capability when the system operates in a non-stationary environment (the index ‘PS’ stands for Principal Subspace). Without loss of generality, we assume $\mathbf{W}(t) \in \mathbb{C}^{d \times p}$ to have full rank p . Otherwise, if the rank of $\mathbf{W}(t)$ is $\tilde{p} < p$, $\mathbf{W}(t)$ in Eq. (2.4) can always be replaced by a full rank $d \times \tilde{p}$ matrix $\tilde{\mathbf{W}}(t)$ satisfying $\tilde{\mathbf{W}}(t)\tilde{\mathbf{W}}^H(t) = \mathbf{W}(t)\mathbf{W}^H(t)$. It is shown in [16] that:

- $\mathbf{W}(t)$ is a stationary point of $J_{PS}(\mathbf{W}(t))$ if and only if $\mathbf{W}(t) = \mathbf{V}_p \mathbf{Q}$, where \mathbf{V}_p is a $d \times p$ matrix containing p distinct eigenvectors of $\mathbf{C}_x(t)$, and \mathbf{Q} is any $p \times p$ unitary matrix.
- Every stationary point of $J_{PS}(\mathbf{W}(t))$ is a saddle point, except when \mathbf{V}_p contains the p dominant eigenvectors of $\mathbf{C}_x(t)$ (equal to $\mathbf{U}_s(t)$ up to a matrix rotation). In this case $J_{PS}(\mathbf{W}(t))$ attains the global minimum.

An iterative optimization of Eq. (2.4) leads to the solution

$$\mathbf{W}(t) = \mathbf{C}_x(t)\mathbf{W}(t-1)\left(\mathbf{W}^H(t-1)\mathbf{C}_x(t)\mathbf{W}(t-1)\right)^{-1} \quad (2.5)$$

The instantaneous covariance matrix $\mathbf{C}_x(t)$ is estimated in the PAST algorithm according to the exponential window having β as forgetting factor, and it is updated by:

$$\hat{\mathbf{C}}_x(t) = \sum_{i=1}^t \beta^{t-i} \mathbf{x}(i)\mathbf{x}(i)^T = \beta \hat{\mathbf{C}}_x(t-1) + \mathbf{x}(t)\mathbf{x}(t)^T \quad (2.6)$$

PAST algorithm is based on Eq. (2.5), Eq. (2.6), the matrix inversion lemma and the projection approximation

$$\hat{\mathbf{C}}_x(t)\mathbf{W}(t) \approx \hat{\mathbf{C}}_x(t)\mathbf{W}(t-1) \quad (2.7)$$

The PAST algorithm is summarized in Algorithm 1 where the $\text{Tri}(\cdot)$ operator indicates that only the upper (or lower) triangular part of $\mathbf{Z}_{PAST}(t) = \mathbf{C}_y^{-1}(t)$ is calculated and its Hermitian transposed version is copied to the another lower (or upper) triangular part ($\mathbf{C}_y(t) = \mathbb{E}[\mathbf{y}(t)\mathbf{y}(t)^H]$). In almost all situations the PAST method converges to an orthogonal matrix whose column vectors spans the principal subspace. However, in some particular cases, it may have an oscillatory behavior and not converge [17, 19]. To solve this problem (i.e., ensure the overall convergence of the method) and, more importantly, to ensure the orthogonality of the weight matrix at each iteration, the authors in [17] proposed a new orthogonal PAST (OPAST) method.

The OPAST method is based on the same cost function as the one in Eq. (2.4) for PAST algorithm, but with the orthogonality constraint over the weight matrix

Algorithm 1 Projection Approximation Subspace Tracking PAST algorithm

Require: $\mathbf{x}(t)$ data vector, β the forgetting factor, $\mathbf{W}_{PAST}(t-1)$ and $\mathbf{Z}_{PAST}(t-1)$ previous outputs.

Ensure: $\mathbf{W}_{PAST}(t)$ and $\mathbf{Z}_{PAST}(t)$

- 1: $\mathbf{y}(t) = \mathbf{W}_{PAST}(t-1)^H \mathbf{x}(t)$
 - 2: $\mathbf{a}(t) = \mathbf{Z}_{PAST}(t-1) \mathbf{y}(t)$
 - 3: $\mathbf{g}(t) = \frac{\mathbf{a}(t)}{\beta + \mathbf{y}(t)^T \mathbf{a}(t)}$
 - 4: $\mathbf{Z}_{PAST}(t) = \frac{1}{\beta} \text{Tri} \left\{ \mathbf{Z}_{PAST}(t-1) - \mathbf{g}(t) \mathbf{a}^H(t) \right\}$
 - 5: $\mathbf{e}(t) = \mathbf{x}(t) - \mathbf{W}_{PAST}(t-1) \mathbf{y}(t)$
 - 6: $\mathbf{W}_{PAST}(t) = \mathbf{W}_{PAST}(t-1) + \mathbf{e}(t) \mathbf{g}^H(t)$
-

Algorithm 2 Orthogonal Projection Approximation Subspace Tracking OPAST algorithm

Require: $\mathbf{x}(t)$ data vector, β the forgetting factor, $\mathbf{W}_{OPAST}(t-1)$ and $\mathbf{Z}_{OPAST}(t-1)$ previous outputs.

Ensure: $\mathbf{W}_{OPAST}(t)$ and $\mathbf{Z}_{OPAST}(t)$

- 1: $\mathbf{y}(t) = \mathbf{W}_{OPAST}(t-1)^H \mathbf{x}(t)$
 - 2: $\mathbf{g}(t) = \frac{1}{\beta} \mathbf{Z}_{OPAST}(t-1) \mathbf{y}(t)$
 - 3: $\gamma = \frac{1}{1 + \mathbf{y}^H(t) \mathbf{g}(t)}$
 - 4: $\tau = \frac{1}{\|\mathbf{g}(t)\|^2} \left(\frac{1}{\sqrt{1 + \|\mathbf{g}(t)\|^2 \gamma^2 (\|\mathbf{x}(t)\|^2 - \|\mathbf{y}(t)\|^2)}} - 1 \right)$
 - 5: $\mathbf{e}(t) = \mathbf{W}_{OPAST}(t-1) \left(\tau \mathbf{g}(t) - \gamma (1 + \tau \|\mathbf{g}(t)\|^2) \mathbf{y}(t) \right) + \left(1 + \tau \|\mathbf{g}(t)\|^2 \right) \gamma \mathbf{x}(t)$
 - 6: $\mathbf{Z}_{OPAST}(t) = \frac{1}{\beta} \mathbf{Z}_{OPAST}(t-1) - \gamma \mathbf{g}(t) \mathbf{g}^H(t)$
 - 7: $\mathbf{W}_{OPAST}(t) = \mathbf{W}_{OPAST}(t-1) + \mathbf{e}(t) \mathbf{g}^H(t)$
-

$\mathbf{W}_{OPAST}^H(t) \mathbf{W}_{OPAST}(t) = \mathbf{I}_p$. Hence, The OPAST algorithm is a modified version of the PAST algorithm where the weight matrix $\mathbf{W}_{OPAST}(t)$ is forced to be orthonormal at each iteration by means of:

$$\mathbf{W}_{OPAST}(t) = \mathbf{W}_{PAST} \left(\mathbf{W}_{PAST}^H \mathbf{W}_{PAST} \right)^{-1/2} \quad (2.8)$$

In order to avoid the direct calculations of the matrix square root inverse $\left(\mathbf{W}_{PAST}^H \mathbf{W}_{PAST} \right)^{-1/2}$, further simplifications were introduced which led to the OPSAT algorithm as is summarized in Algorithm 2. PAST [16] and OPSAT [17] algorithms have a linear computational complexity equals to $3dp + \mathcal{O}(p^2)$ for PAST and $4dp + \mathcal{O}(p^2)$ for OPAST.

2.2.3 Fast Approximated Power Iterations algorithm

The FAPI [20] [21] algorithm is based on the power iteration and on a new projection approximation compared to the one used previously in PAST and OPAST algorithms. FAPI algorithm has a low (linear) computational complexity but provides a better estimation of the principal subspace (compared to algorithms having the same computational complexity order). The classical power iteration technique converges globally and exponentially to the signal subspace and it alternates between two steps that update the estimation of the weight matrix $\mathbf{W}(t-1)$ to $\mathbf{W}(t)$. In the first step corresponding to Eq. (2.9), $\mathbf{C}_{xy}(t)$ (data compression) is calculated, then $\mathbf{W}(t)$ is estimated by a fast QR decomposition of $\mathbf{C}_{xy}(t)$ in the second one corresponding to Eq. (2.10) (orthogonalization).

$$\mathbf{C}_{xy}(t) = \mathbf{C}_x(t)\mathbf{W}(t-1) \quad (2.9)$$

$$\mathbf{W}(t)\mathbf{R}(t) = \mathbf{C}_{xy}(t) \quad (2.10)$$

where $\mathbf{R}(t)$ is a $p \times p$ upper triangular matrix and $\mathbf{C}_{xy}(t)$ is the $d \times p$ correlation matrix between the data vectors $\mathbf{x}(i)$ and the projected data vectors $\mathbf{y}(i) = \mathbf{W}(t-1)^H \mathbf{x}(i)$ for $i = 1, \dots, t$. Despite its interesting convergence properties, a direct implementation of Eq. (2.9) and Eq. (2.10) would lead to a high computational complexity of order $\mathcal{O}(d^2 p)$ flops per iteration. In [21], the authors proposed to reduce the computation cost by using the recursive update of $\hat{\mathbf{C}}_x(t)$, a new projection approximation trick and the matrix inversion lemma. The instantaneous covariance matrix $\hat{\mathbf{C}}_x(t)$ is updated either by Eq. (2.6) corresponding to the exponential window or by Eq. (2.12) corresponding to a truncated window (sliding window which have an exponential decrease).

$$\hat{\mathbf{C}}_x(t) = \sum_{i=t-L+1}^t \beta^{t-i} \mathbf{x}(i)\mathbf{x}(i)^H \quad (2.11)$$

$$= \beta \hat{\mathbf{C}}_x(t-1) + \mathbf{x}(t)\mathbf{x}(t)^H - \beta^L \mathbf{x}(t-L)\mathbf{x}(t-L)^H \quad (2.12)$$

where L is the width of the window.

Remark: One should choose the exponential window in case of slowly changing signal parameters since it tends to smooth the variations of the desired parameters. The truncated (sliding) window is preferred for faster tracking of signal parameter changes, but it leads to a higher computational complexity and needs more memory than the exponential window.

Note that the projection approximation of Eq. (2.7) proposed in PAST [16] and used later in OPAST [17] is more restrictive compared to the one used in FAPI [21]

given by

$$\mathbf{W}(t) \approx \mathbf{W}(t-1)\mathbf{\Theta}(t) \quad (2.13)$$

$$\mathbf{R}^H(t) \approx \mathbf{C}_y(t)\mathbf{\Theta}(t) \quad (2.14)$$

where the $r \times r$ matrix $\mathbf{\Theta}(t)$ is defined by $\mathbf{\Theta}(t) \triangleq \mathbf{W}(t-1)^H \mathbf{W}(t)$ and $\mathbf{C}_y(t)$ is the correlation matrix of the projected data $\mathbf{y}(i)$ for $i = 1, \dots, t$. This explains the better tracking capability of the FAPI algorithm compared to PAST and OPAST. Using this projection approximation with the rank-one update of the covariance matrix $\hat{\mathbf{C}}_x(t)$, leads to a linear computational complexity equal to $3dp + \mathcal{O}(p^2)$ with the exponential window and to $6dp + 4Lp + \mathcal{O}(p^2)$ with the truncated window. The exponential window version of FAPI algorithm is summarized in Algorithm 3 (see [20, 21] for more details).

Algorithm 3 Fast Approximated Power Iterations FAPI algorithm

Require: $\mathbf{x}(t)$ data vector, β the forgetting factor, $\mathbf{W}_{FAPI}(t-1)$ and $\mathbf{Z}_{FAPI}(t-1)$ previous outputs.

Ensure: $\mathbf{W}_{FAPI}(t)$ and $\mathbf{Z}_{FAPI}(t)$

- 1: $\mathbf{y}(t) = \mathbf{W}_{FAPI}(t-1)^H \mathbf{x}(t)$
 - 2: $\mathbf{a}(t) = \mathbf{Z}_{FAPI}(t-1) \mathbf{y}(t)$
 - 3: $\mathbf{g}(t) = \frac{\mathbf{a}(t)}{\beta + \mathbf{y}(t)^H \mathbf{a}(t)}$
 - 4: $\varepsilon^2(t) = \|\mathbf{x}(t)\|^2 - \|\mathbf{y}(t)\|^2$
 - 5: $\tau(t) = \frac{\varepsilon^2(t)}{1 + \varepsilon^2(t)\|\mathbf{g}(t)\|^2 + \sqrt{1 + \varepsilon^2(t)\|\mathbf{g}(t)\|^2}}$
 - 6: $\eta(t) = 1 - \tau(t)\|\mathbf{g}(t)\|^2$
 - 7: $\mathbf{y}'(t) = \eta(t)\mathbf{y}(t) + \tau(t)\mathbf{g}(t)$
 - 8: $\mathbf{a}'(t) = \mathbf{Z}_{FAPI}(t-1)^H \mathbf{y}'(t)$
 - 9: $\mathbf{f}(t) = \frac{\tau(t)}{\eta(t)} \left(\mathbf{Z}_{FAPI}(t-1)\mathbf{g}(t) - \left(\mathbf{a}'(t)^H \mathbf{g}(t) \right) \mathbf{g}(t) \right)$
 - 10: $\mathbf{Z}_{FAPI}(t) = \frac{1}{\beta} \left(\mathbf{Z}_{FAPI}(t-1) - \mathbf{g}(t)\mathbf{a}'(t)^H + \mathbf{f}(t)\mathbf{g}(t)^H \right)$
 - 11: $\mathbf{e}(t) = \eta(t)\mathbf{x}(t) - \mathbf{W}_{FAPI}(t-1)\mathbf{y}'(t)$
 - 12: $\mathbf{W}_{FAPI}(t) = \mathbf{W}_{FAPI}(t-1) + \mathbf{e}(t)\mathbf{g}(t)^H$
-

2.2.4 Sparse Principal Component Analysis algorithms

The sparsity constraint over the weight matrix $\mathbf{W}(t)$ is considered for principal subspace tracking. This was already discussed, but in the context of SPCA as it was mentioned in Chapter 1. Most of the proposed solutions for SPCA are batch algorithms which process all the received data as one block. However, in non-stationary systems, the estimating parameters changes with time and the result of such an approach is suboptimal. Hence, adaptive processing must be done after

receiving each data sample. It is worth mentioning that the adaptive principal component analysis problem is closely related to subspace tracking problem. In fact, if we consider the orthogonality of the loadings constraint and we drop the non-correlation of the projected data constraint, the two problems are equivalent and their solutions are equal up to a unitary rotation matrix. In addition, it is known that SPCA can not verify both the orthogonality and the non-correlation constraints at the same time [53] as the classical PCA .

As SPCA batch algorithms, we will use later for comparison GPower [48] and IMRP [49]. The authors of [48] proposed the so-called as Generalized Power Method for SPCA (Gpower), where the single-component (component by component with a deflation scheme) and the block (multiple component at the same time which is equivalent to sparse principal subspace) SPCA problems are formulated as an optimization program involving maximization of a convex function on a compact set either for the ℓ_0 -norm or the ℓ_1 -norm. Then, a simple gradient method is proposed for the optimization task. Convergence properties were provided in the case when either the objective function or the feasible set are strongly convex, which is the case with the single-component formulations and can be enforced in the block case. Iterative Minimization of Rectangular Procrustes (IMRP) algorithm was proposed in [49], where the authors considered the problem of SPCA with the orthogonality constraint. They apply the minimization-maximization (MM) framework where they iteratively maximize a tight lower bound surrogate function (approximate the ℓ_0 -norm by a differentiable function) of the objective function over the Stiefel manifold. The inner maximization problem has the form of the rectangular Procrustes problem, which has a closed-form solution.

Among the existing adaptive solutions, one can mention the OIST [54] (Oja's algorithm with Iterative Soft Thresholding) algorithm which considers only the single-component (a rank one subspace) model and is based on Oja's algorithm [25] followed by a soft thresholding step. To use such an algorithm for subspace tracking, one needs to use an iterative deflation method (every column is considered alone) which generally leads to poor subspace tracking performance and to the lost of the weight matrix orthogonality. Another algorithm called streaming SPCA via row truncation, proposed in [55], focuses on row sparsity of the weight matrix by using a sliding rectangular window, a row truncation operator based on ℓ_0 -norm and a QR decomposition is realized at each iteration which increases considerably the computational cost. Additionally, the proposed version for the global case in [55] where the columns of the weight matrix are all sparse but their supports are nearly disjoint, is also based on an iterative deflation method.

Algorithm 4 ℓ_1 -norm Projection Approximation Subspace Tracking ℓ_1 -PAST algorithm

Require: $\mathbf{x}(t)$ data vector, β the forgetting factor, κ the sparsity parameter,

$\mathbf{W}_{\ell_1\text{-PAST}}(t-1)$ and $\mathbf{Z}_{\ell_1\text{-PAST}}(t-1)$ previous outputs.

Ensure: $\mathbf{W}_{\ell_1\text{-PAST}}(t)$ and $\mathbf{Z}_{\ell_1\text{-PAST}}(t)$

- 1: $\mathbf{y}(t) = \mathbf{W}_{\ell_1\text{-PAST}}(t-1)^H \mathbf{x}(t)$
 - 2: $\mathbf{a}(t) = \mathbf{Z}_{\ell_1\text{-PAST}}(t-1) \mathbf{y}(t)$
 - 3: $\mathbf{g}(t) = \frac{\mathbf{a}(t)}{\beta + \mathbf{y}(t)^T \mathbf{a}(t)}$
 - 4: $\mathbf{S} = \mathbf{Z}_{\ell_1\text{-PAST}}(t-1) - \mathbf{g}(t) \mathbf{a}^H(t)$
 - 5: $\mathbf{Z}_{\ell_1\text{-PAST}}(t) = \frac{1}{\beta} \text{Tri} \left\{ \mathbf{Z}_{\ell_1\text{-PAST}}(t-1) - \mathbf{g}(t) \mathbf{a}^H(t) \right\}$
 - 6: $\mathbf{e}(t) = \mathbf{x}(t) - \mathbf{W}_{\ell_1\text{-PAST}}(t-1) \mathbf{y}(t)$
 - 7: $\tilde{\mathbf{W}}_{\ell_1\text{-PAST}}(t) = \mathbf{W}_{\ell_1\text{-PAST}}(t-1) + \mathbf{e}(t) \mathbf{g}^H(t) + \kappa \left(1 - \frac{1}{\beta}\right) \text{sign} \left(\mathbf{W}_{\ell_1\text{-PAST}}(t-1) \right) \mathbf{S}$
 - 8: $\mathbf{W}_{\ell_1\text{-PAST}}(t) = \text{Orth} \left(\tilde{\mathbf{W}}_{\ell_1\text{-PAST}}(t) \right)$
-

2.2.5 ℓ_1 -norm Projection Approximation Subspace Tracking algorithm

The ℓ_1 -PAST algorithm is proposed in [56] to solve the principal subspace tracking problem under a sparsity constraint on the weight matrix. It was developed for the STAP (space-time adaptive processing) application for Airborne Phased Array Radar. A new objective function is proposed, consisting of the sum of the weighted quadratic error of signal reconstruction, similar to the one proposed in PAST [16] and the ℓ_1 -norm of the weight matrix. It is given by:

$$J_{\ell_1\text{-PAST}}(\mathbf{W}(t)) = \sum_{i=1}^t \beta^{t-i} \left\| \mathbf{x}(i) - \mathbf{W}(t) \mathbf{W}^H(t) \mathbf{x}(i) \right\|_2^2 + 2\kappa \left\| \mathbf{W}(t) \right\|_1 \quad (2.15)$$

$$= J_{PS}(\mathbf{W}(t)) + 2\kappa \left\| \mathbf{W}(t) \right\|_1 \quad (2.16)$$

Based on the sub-gradient calculation and some simplifications under the assumption of slowly changing system, the resulting algorithm is summarized in Algorithm 4. The ℓ_1 -PAST algorithm has a complexity equal to $2dp^2 + \mathcal{O}(p^2)$ flops per iteration if the orthogonal processing by Gram-Schmidt method is considered.

2.3 Blind source separation

Blind source separation (BSS) is a signal processing technology which has been intensively used recently in several areas [57], such as biomedical engineering [58],

audio (music and speech) processing [59] and communication applications [60]. The main objective of source separation is to recover unknown transmitted source signals from the observations received at a set of sensors. In BSS neither the sources nor the mixing matrix are known, i.e. it exploits only the information carried by the received signals and a prior information about the statistics or the nature of transmitted source signals (e.g. decorrelation, independence, sparsity, morphological diversity, etc).

In this section, we present the data model considered in the blind source separation problem. After that, we give a quick review of independent component analysis (ICA) and sparse component analysis (SCA) techniques.

2.3.1 Data model

Let $\mathbf{x}(t) = [x_1(t), \dots, x_d(t)]^T$ be a random data vector observed at the t^{th} snapshot over an array of d sensors. The measured array output is a mapped version of the unobserved sources, $\mathbf{s}(t) = [s_1(t), \dots, s_p(t)]^T$, assuming zero mean and stationarity.

$$\mathbf{x}(t) = \mathcal{A}(\mathbf{s}(t)) \tag{2.17}$$

where \mathcal{A} is an unknown mapping from the p -space of \mathbf{s} to the d -space of \mathbf{x} . Various mixture models have been considered, initially the linear instantaneous mixtures, then the linear convolutive mixtures and more recently the nonlinear models [57]. It is clear that without this a priori information, the BSS problem is ill-posed. Hence, one needs to restore the well-posedness of the problem by imposing somehow a diversity between sources. For instantaneous (memoryless) linear mixtures corrupted by $\mathbf{n}(t)$ which is a realization of a zero-mean additive random white noise, the model is given by:

$$\mathbf{x}(t) = \mathbf{A}\mathbf{s}(t) + \mathbf{n}(t) \tag{2.18}$$

Depending on the number of sources p and sensors d , the model (2.18) is overdetermined ($d > p$) or underdetermined ($d < p$). Solving the blind source separation problem means to find a $p \times d$ separation matrix \mathbf{B} (or equivalently, identifying \mathbf{A} and applying its pseudo-inverse $\mathbf{A}^\#$) such that $\hat{\mathbf{s}}(t) = \mathbf{B}\mathbf{x}(t)$ is an estimation of the source signals.

Note that complete blind identification of separating matrix is possible only up to permutation and scaling ambiguity i.e. \mathbf{B} is a solution if:

$$\hat{\mathbf{s}}(t) = \mathbf{B}\mathbf{x}(t) = \mathbf{P}\mathbf{A}\mathbf{s}(t) \tag{2.19}$$

where \mathbf{P} is a permutation matrix and \mathbf{A} is a non-singular diagonal matrix.

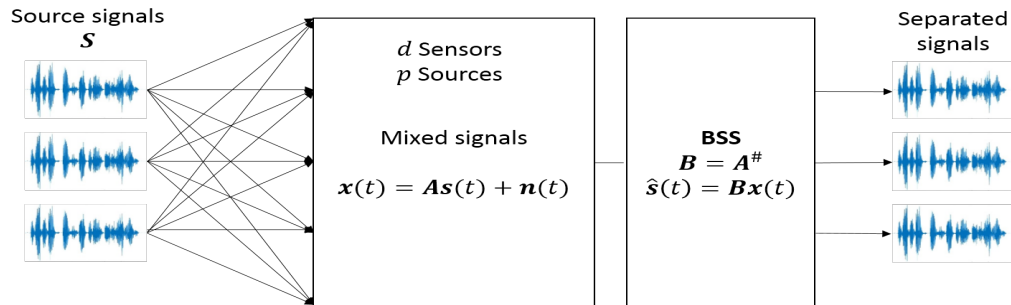


Figure 2.1: Blind source separation scheme

2.3.2 Independent Component Analysis ICA based blind source separation

In the previous section, we discussed PCA as a dimensionality reduction technique and we noticed that PCA does not look for (and usually does not find) components with direct physical meaning contrary to ICA. In fact, the ICA technique tries to recover the original sources by estimating a linear transformation assuming a statistical independence among the unknown sources. The ICA framework is clearly related to the BSS problem, where the sources are assumed to be temporally i.i.d (identically independently distributed) and non-Gaussian¹. If the sources admit a probability density function (pdf), then the joint pdf can be factorized as the product of the marginal pdf's:

$$f_{\mathbf{s}}(\mathbf{s}_1, \mathbf{s}_2, \dots, \mathbf{s}_p) = \prod_{i=1}^p f_{s_i}(\mathbf{s}_i) \quad (2.20)$$

Actually the above independence criterion is not convenient, since it not only requires equality of two multivariate functions, but also requires their perfect knowledge to start with. Consequently, other independence measures based on the second characteristic function or the Kullback-Leibler (KL) divergence, lead to more convenient criteria and contrast functions, which always involve (explicitly or implicitly) higher-order statistics. The KL divergence from the joint density $f_{\mathbf{s}}(\mathbf{s}_1, \mathbf{s}_2, \dots, \mathbf{s}_p)$ to the product of its marginal density is a popular measure of statistical independence and it is given by:

$$J(\mathbf{s}) = \mathcal{K} \left[f_{\mathbf{s}}(\mathbf{s}_1, \mathbf{s}_2, \dots, \mathbf{s}_p), \prod_{i=1}^p f_{s_i}(\mathbf{s}_i) \right] \quad (2.21)$$

$$= \int_{\mathbf{s}} f_{\mathbf{s}}(\mathbf{s}_1, \mathbf{s}_2, \dots, \mathbf{s}_p) \log \left(\frac{f_{\mathbf{s}}(\mathbf{s}_1, \mathbf{s}_2, \dots, \mathbf{s}_p)}{\prod_{i=1}^p f_{s_i}(\mathbf{s}_i)} \right) d\mathbf{s} \quad (2.22)$$

¹Darmois [61] showed that the problem has no solution for Gaussian and temporally iid sources

The KL can be decomposed into two terms [62] as follows:

$$J(\mathbf{s}) = \mathcal{C}(\mathbf{s}) - \sum_{i=1}^p \mathcal{G}(\mathbf{s}_i) + c \quad (2.23)$$

where c is a constant and $\mathcal{C}(\mathbf{s}) = \mathcal{K}[\mathcal{N}(\mathbb{E}(\mathbf{s}), \mathbf{\Sigma}_s), \mathcal{N}(\mathbb{E}(\mathbf{s}), \text{diag}(\mathbf{\Sigma}_s))]$ and $\mathcal{G}(\mathbf{s}_i) = \mathcal{K}[f_{\mathbf{s}_i}(\mathbf{s}_i), \mathcal{N}(\mathbb{E}(\mathbf{s}_i), \sigma_{\mathbf{s}_i}^2)]$ where $\sigma_{\mathbf{s}_i}^2$ is the variance of \mathbf{s}_i and $\mathcal{N}(\mathbf{m}, \mathbf{\Sigma})$ is the normal probability density function with mean \mathbf{m} and covariance $\mathbf{\Sigma}$. The first term in Eq. (2.23) vanishes when the sources are decorrelated. The second term measures the marginal Gaussianity of the sources. This decomposition of the KL entails that maximizing independence is equivalent to minimizing the correlation between the sources and maximizing their non-Gaussianity. Note that, intuitively, mixing independent signals should lead to a kind of Gaussianity with respect to the central limit theorem. Hence, it is natural to think that source separation leads to deviation from Gaussian processes.

In the ICA setting, the mixing matrix is generally square and invertible. Otherwise, the overdetermined BSS problem can be reduced to a square problem by using a PCA stage. Among most popular batch ICA methods:

- The fixed point algorithm FastICA [63] is often used in 'real time' applications because of the possible parallel implementation. FastICA uses kurtosis for the independent components estimation. A prewhitening step is usually performed on data before the execution of the algorithm
- The Joint Approximation Diagonalization of Eigenmatrices algorithm (JADE) [64] is based on joint diagonalization of eigenmatrices that are computed by the fourth order cumulants of whitened signals.

We are more interested in the adaptive ICA algorithms. The main motivation behind adaptive methods is their ability to track variations of the mixing system in non-stationary environments, if the non-stationarity is mild enough. A variety of adaptive ICA algorithms have been proposed. Update formulas of some popular algorithms are presented below:

- The natural gradient learning algorithm proposed in [65]

$$\mathbf{B}(t+1) = \mathbf{B}(t) + \mu [\mathbf{I}_p - \mathbf{y}(t)\mathbf{u}^H(t)] \mathbf{B}(t)$$

- The Equivalent Adaptive Separation via Independence (EASI) algorithm proposed in [66]

$$\mathbf{B}(t+1) = \mathbf{B}(t) + \mu [\mathbf{I}_p - \mathbf{u}(t)\mathbf{u}^H(t) + \mathbf{u}(t)\mathbf{y}^H(t) - \mathbf{y}(t)\mathbf{u}^H(t)] \mathbf{B}(t)$$

- The Information maximization (Infomax) algorithm proposed in [67]

$$\mathbf{B}(t+1) = \mathbf{B}(t) + \mu [\mathbf{B}(t)^{-H} - \mathbf{y}(t)\mathbf{x}(t)^H]$$

where $\mathbf{u}(t) = \mathbf{B}(t)\mathbf{x}(t)$, $\mathbf{y}(t) = g(\mathbf{u}(t))$ and $g(\cdot)$ is a nonlinear function known as the score function, which depends on the pdf of the source signals.

Despite its theoretical strength and elegance, ICA suffers from several limitations:

- The sources to be processed in practice are perhaps actually not independent.
- Since ICA algorithms are based on statistical independence, they require to take into account higher (than 2) order statistics.
- ICA algorithms cannot separate independent Gaussian sources.

2.3.3 Sparse/Morphological Component Analysis SCA/MCA based blind source separation

Sparse decomposition techniques for signals and images underwent considerable development during the flourishing of wavelet-based compression and denoising methods in the early 1990s. Later, these techniques have been exploited for blind source separation. Their main impact is that they provide a relatively simple framework for separating a number of sources exceeding the number of observed mixtures. Also they greatly improve quality of separation in the case of square (or overdetermined) mixing matrix [57].

The sparsity has been first introduced as an alternative to standard contrast functions of ICA in [68], where a fully Bayesian framework is used. Each source is assumed to be sparsely represented in a basis (e.g. orthogonal wavelet basis) Φ :

$$\forall i = 1, \dots, p; \quad \mathbf{s}_i(t) = \sum_{k=1}^K c_{ik} \Phi_k(t) \quad (2.24)$$

where coefficients c_{ik} are supposed to be sparse. This sparsity is modeled by the prior distribution:

$$f_i(c_{ik}) \propto e^{-g(c_{ik})} \quad \text{with} \quad g(c) = |c|^\gamma, \quad \gamma \leq 1 \quad (2.25)$$

A Maximum A Posteriori (MAP) estimator is used to estimate the mixing matrix and the coefficients signals. Inspired by the idea of Basis Pursuit the problem is written in its matrix form:

$$\min_{\mathbf{A}, \mathbf{C}} \frac{1}{2\sigma^2} \|\mathbf{AC}\Phi - \mathbf{X}\|_F^2 + \sum_{i,k} g(c_{ik}) \quad \text{Subject to} \quad \|A\| \leq 1 \quad (2.26)$$

where \mathbf{C} is the matrix which has as entries the sparse coefficients c_{ik} and the noise is assumed zero-mean gaussian with a covariance equals to $\sigma^2\mathbf{I}_p$. Later, the so-called the Relative Newton Algorithm [4] was proposed to optimize more efficiently the above objective function.

Many recent researches in SCA extended the basis Φ to an overcomplete dictionary and use the redundancy to enhance the sparsity of the coefficients. Combining the ICA based BSS previous results and the recent advances in sparse representations area, helped a lot in developing new SCA techniques.

The perfect sparse case assumes that the sources have mutually disjoint supports (sets of nonzero samples) in the sparse or transformed domain. Nonetheless, this simple case requires highly sparse signals. Unfortunately, this is not the case for large classes of classes of highly structured data and especially in image processing [6]. Furthermore, over the past ten years, new tools have emerged from modern computational harmonic analysis : wavelets, ridgelets, curvelets, bandlets, contourlets, to name a few. It was tempting to combine several representations to build a larger dictionary of waveforms that will enable the sparse representation of larger classes of signals.

In [69], the authors proposed a practical algorithm known as Morphological Component Analysis (MCA) aiming at decomposing signals in overcomplete dictionaries made of a union of bases. For instance, a piece-wise smooth source (cartoon picture) is well sparsified in a curvelet tight frame, while a warped globally oscillating source (texture) is better represented using a discrete cosine transform (DCT). Morphological diversity then relies on the sparsity of those morphological components in specific bases. Theoretical arguments as well as experiments were given in [6, 69, 70] showing that MCA provides at least as good results as Basis Pursuit for sparse overcomplete decompositions in a union of bases. Moreover, MCA turns out to be clearly much faster than Basis Pursuit. Then, MCA is a practical alternative to classical sparse overcomplete decomposition techniques.

2.4 Blind FIR channel identification

Reliable communication often requires the identification of the channel impulse response. Such identification can facilitate channel equalization as well as maximum likelihood sequence detection. The so-called blind channel identification means that the channel is identified without using a training signal; instead, the identification is achieved by using only the channel output along with certain *a priori* statistical information on the input. Such methods have the potential to increase the transmission capability due to the elimination of training signals. The need for

blind channel identification arises from a number of applications such as in data communications [71], speech recognition [72], image restoration [73], seismic signal processing [74], etc. The blind channel identification problem has received a lot of attention over the last two decades and many efficient solutions exist for Single Input, Multiple Output (SIMO) and Multiple Input, Multiple Output (MIMO) systems in the literature. We can distinguish two main classes of Blind System Identification BSI methods: higher order statistics (HOS) and second order statistics (SOS) techniques. In general, HOS-based methods require large sample sizes to achieve 'better' estimation performances than the SOS-based methods [75]. Among the famous SOS-based techniques, one can mention the cross-relation (CR) method [76], the subspace method [77], and the two-step maximum likelihood (TSML) method [78]. Unfortunately, it seems likely that in case of very long impulse response and sparse channel, these methods perform poorly. Such sparse channels can be encountered in many communication applications including High-Definition television (HDTV) channels and underwater acoustic channels [79]. Recently, solutions have been proposed to handle this case by adapting the 'classical' blind identification methods to the sparse case.

Next, we present the considered data model and some classical approaches to solve the blind channel identification problem such as the maximum likelihood method TSML [78], the CR method [76], the subspace method [77]. Also, solutions that consider the channel sparsity are discussed such as the sparse CR method [80], The MAP method [81] and its adaptive version [82].

2.4.1 Data model

Our focus is on the SIMO/MIMO channels in a blind identification context. We present the global MIMO case which includes also the SIMO case by considering only one transmitter. We consider a mathematical model where the input and the output are both discrete but we have access only to the output. The system is driven by N_t input sequences $\mathbf{s}_1(t), \dots, \mathbf{s}_{N_t}(t)$, and yields N_r output sequences $\mathbf{x}_1(t), \dots, \mathbf{x}_{N_r}(t)$ at time t . We assume that the discrete channels between the N_t transmit antennas and the N_r receive antennas are modeled as an $N_r \times N_t$ FIR filter with L as the upper bound on the orders of these channels i.e. $\mathbf{H} = [\mathbf{H}^T(0), \dots, \mathbf{H}^T(L)]^T$ with

$$\mathbf{H}(l) = \begin{bmatrix} h_{11}(l) & \dots & h_{1N_t}(l) \\ \vdots & & \vdots \\ h_{N_r1}(l) & \dots & h_{N_rN_t}(l) \end{bmatrix}$$

The system can be described by:

$$\mathbf{x}(t) = \sum_{k=0}^L \mathbf{H}(k)\mathbf{s}(t-k) + \mathbf{n}(t) = [\mathbf{H}(z)]\mathbf{s}(t) + \mathbf{n}(t) \quad (2.27)$$

where

$$[\mathbf{H}(z)] = \sum_{k=0}^L \mathbf{H}(k)z^{-k} \quad (2.28)$$

and $\mathbf{n}(t)$ is an additive N_r -dimensional white noise, independent from the symbol sequences with $\mathbb{E}[\mathbf{w}(t)\mathbf{w}^T(t)] = \sigma^2\mathbf{I}_{N_r}$, where σ^2 is the unknown power noise.

We denote stacked observations over a window of length N by the vector $\mathbf{x}_N(t) = [\mathbf{x}^T(t), \mathbf{x}^T(t-1), \dots, \mathbf{x}^T(t-N+1)]^T$. The following linear model holds:

$$\mathbf{x}_N(t) = \mathcal{T}(\mathbf{H})\mathbf{s}_N(t) + \mathbf{n}_N(t) \quad (2.29)$$

with $\mathbf{s}_N(t) = [\mathbf{s}^T(t), \mathbf{s}^T(t-1), \dots, \mathbf{s}^T(t-N+1)]^T$ and $\mathbf{n}_N(t) = [\mathbf{n}^T(t), \dots, \mathbf{n}^T(t-N+1)]^T$. The $(NN_r) \times (N(L+1)N_t)$ block-Toeplitz matrix $\mathcal{T}(\mathbf{H})$ associated with the filter \mathbf{H} is given by:

$$\mathcal{T}(\mathbf{H}) = \begin{bmatrix} \mathbf{H}(0) & \dots & \mathbf{H}(L) & & 0 \\ & \ddots & & \ddots & \\ 0 & & \mathbf{H}(0) & \dots & \mathbf{H}(L) \end{bmatrix} \quad (2.30)$$

From now on, we make the following important assumptions:

- $\mathbf{H}(z)$ is irreducible ($\text{Rank}(\mathbf{H}(z)) = N_t; \forall z$) and $\mathbf{H}(L)$ is of full column rank
- The channels have a known maximum order L .
- Number of sensors is strictly greater than the number of sources $N_r > N_t$
- Large enough observation Window $N > (L+1)N_t$

Under these assumptions, $\mathcal{T}(\mathbf{H})$ is full column rank and the channel matrix \mathbf{H} is identifiable up to a $N_t \times N_t$ constant full rank matrix [83].

For the SIMO case ($N_t = 1$), we introduce another notation corresponding to stacking observations with respect to sensor number:

$$\mathbf{x}_{N_r}(t) = \mathcal{H}_{N_r}\mathbf{s}_N(t) + \mathbf{n}_{N_r}(t) \quad (2.31)$$

where $\mathbf{x}_{N_r}(t) = [\mathbf{x}_1^T(t), \dots, \mathbf{x}_{N_r}^T(t)]^T$ with $\mathbf{x}_i(t) = [x_i(t), \dots, x_i(t-N+1)]^T$ for $i = 1, \dots, N_r$. The noise vector $\mathbf{n}_{N_r}(t)$ is constructed in the same way as the observations by $\mathbf{n}_{N_r}(t) = [\mathbf{n}_1^T(t), \dots, \mathbf{n}_{N_r}^T(t)]^T$ with $\mathbf{n}_i(t) = [n_i(t), \dots, n_i(t-N+1)]^T$ for $i = 1, \dots, N_r$. The matrix $\mathcal{H}_{N_r} = [\mathcal{T}(\mathbf{h}_1)^T, \dots, \mathcal{T}(\mathbf{h}_{N_r})^T]^T$ is a block Sylvester matrix, $\mathcal{T}(\mathbf{h}_i)$ being the Sylvester matrix of the i -th channel given by $\mathbf{h}_i = [h_i(0), \dots, h_i(L)]^T$ for $i = 1, \dots, N_r$.

2.4.2 Classical approaches

We now introduce some popular techniques for blindly identifying SIMO ($\mathbf{N}_t = 1$) FIR channel, in particular the deterministic maximum-likelihood (ML) method TSML [78] method and the noise subspace method [77,83] (we investigate the MIMO case later).

SIMO system

The ML method is a classic approach applicable to any parameter estimation problem where the pdf of the available data is known. Assuming that the system output vector is corrupted by additive circular white Gaussian noise vector \mathbf{n} allows us to write the log-likelihood:

$$f(\mathbf{x}_{N_r}(t); \mathcal{H}_{\mathbf{N}_r}, \mathbf{s}_N(t)) = \frac{1}{2\sigma^2} \left\| \mathbf{x}_{N_r}(t) - \mathcal{H}_{\mathbf{N}_r} \mathbf{s}_N(t) \right\|_2^2 + \text{constant} \quad (2.32)$$

It then follows that the channel output vector $\mathbf{x}_{N_r}(t)$ is Gaussian distributed with the mean vector $\mathcal{H}_{\mathbf{N}_r} \mathbf{s}_N(t)$ and the covariance matrix $\sigma^2 \mathbf{I}$. The ML criterion is expressed as:

$$\left(\mathcal{H}_{\mathbf{N}_r}, \mathbf{s}_N(t) \right) = \arg \max_{\mathcal{H}_{\mathbf{N}_r}, \mathbf{s}_N(t)} f(\mathbf{x}_{N_r}(t); \mathcal{H}_{\mathbf{N}_r}, \mathbf{s}_N(t)) \quad (2.33)$$

$$= \arg \min_{\mathcal{H}_{\mathbf{N}_r}, \mathbf{s}_N(t)} \left\{ \left\| \mathbf{x}_{N_r}(t) - \mathcal{H}_{\mathbf{N}_r} \mathbf{s}_N(t) \right\|_2^2 \right\} \quad (2.34)$$

Let's define \mathcal{G}_{N_r} by

$$\mathcal{G}_2^H = \left[-\overline{\mathcal{T}}(\mathbf{h}_1), \overline{\mathcal{T}}(\mathbf{h}_2) \right] \quad (2.35)$$

and

$$\mathcal{G}_q^H = \left[\begin{array}{cc|c} \mathcal{G}_{q-1}^H & & 0 \\ -\overline{\mathcal{T}}(\mathbf{h}_q) & & \overline{\mathcal{T}}(\mathbf{h}_1) \\ & \ddots & \vdots \\ 0 & & -\overline{\mathcal{T}}(\mathbf{h}_q) \quad \overline{\mathcal{T}}(\mathbf{h}_{q-1}) \end{array} \right] \quad (2.36)$$

for $q = 3, \dots, N_r$, where $\overline{\mathcal{T}}(\mathbf{h}_q)$ is the top-left $(N-L) \times N$ sub-matrix of $\mathcal{T}(\mathbf{h}_q)$.

Under the necessary identifiability conditions [83] and by using projection techniques and commutativity property of linear convolution, Eq. (2.34) yields the equivalent problem:

$$\mathbf{h}_{\text{ML}} = \arg \min_{\|\mathbf{h}\|_2=1} \left\{ \mathbf{h}^H \mathcal{X}_{N_r}^H \left(\mathcal{G}_{N_r}^H \mathcal{G}_{N_r} \right)^\# \mathcal{X}_{N_r} \mathbf{h} \right\} \quad (2.37)$$

where $\mathbf{h} = [\mathbf{h}_1^T, \dots, \mathbf{h}_{N_r}^T]^T$ and $(\cdot)^\#$ refers to the pseudo inverse operator. The matrix \mathcal{X}_{N_r} is defined by

$$\mathcal{X}_2 = \left[\mathbf{X}_2, -\mathbf{X}_1 \right] \quad (2.38)$$

and

$$\mathcal{X}_q = \left[\begin{array}{cc|c} \mathcal{X}_{q-1} & & 0 \\ \mathbf{X}_q & & -\mathbf{X}_1 \\ & \ddots & \vdots \\ 0 & & \mathbf{X}_q & -\mathbf{X}_{q-1} \end{array} \right] \quad (2.39)$$

for $q = 3, \dots, N_r$, where \mathbf{X}_q is given by:

$$\mathbf{X}_q = \begin{bmatrix} x_q(t) & \dots & x_q(t-L) \\ \vdots & & \vdots \\ x_q(t-N+L+1) & \dots & x_q(t-N+1) \end{bmatrix}. \quad (2.40)$$

The cost function is optimized under the constraint $\|\mathbf{h}\|_2 = 1$ to avoid the scalar indeterminacy². The TSML method [78] uses an two-step estimation procedure to solve Eq. (2.37) efficiently as shown below:

- Minimization: $\mathbf{h}_{\text{CR}} = \arg \min_{\|\mathbf{h}\|_2=1} \left\{ \mathbf{h}^H \mathcal{X}_{N_r}^H \mathcal{X}_{N_r} \mathbf{h} \right\}$
- Minimization: $\mathbf{h}_{\text{ML}} = \arg \min_{\|\mathbf{h}\|_2=1} \left\{ \mathbf{h}^H \mathcal{X}_{N_r}^H \left(\mathcal{G}_{\text{CR}}^H \mathcal{G}_{\text{CR}} \right)^\# \mathcal{X}_{N_r} \mathbf{h} \right\}$

where \mathcal{G}_{CR} is \mathcal{G}_{N_r} constructed from \mathbf{h}_{CR} according to Eq. (2.35) and Eq. (2.36).

The first step of the TSML method is known to coincide with a method based on a 'cross-relation' (CR) property of the SIMO system. This cross relation is as follows:

$$\mathbf{x}_i(t) * \mathbf{h}_j = \mathbf{x}_j(t) * \mathbf{h}_i \quad 1 \leq i \neq j \leq N_r \quad (2.41)$$

under the noise free model. By collecting all possible pairs of N_r channels, one can easily establish a set of linear equations. In matrix form, this set of equations can be expressed as:

$$\mathcal{X}_{N_r} \mathbf{h} = 0 \quad (2.42)$$

where \mathcal{X}_{N_r} turns out to be the same as defined by Eq. (2.38) and Eq. (2.39). In presence of noise, the solution to the above equation can be naturally replaced by the least-squares (LS) solution:

$$\mathbf{h}_{\text{CR}} = \arg \min_{\|\mathbf{h}\|_2=1} \left\{ \mathbf{h}^H \mathcal{X}_{N_r}^H \mathcal{X}_{N_r} \mathbf{h} \right\} \quad (2.43)$$

The Channel Subspace (CS) Method was proposed in [77] and it is based on estimating the observed signals covariance matrix \mathcal{R}_x given by

$$\mathcal{R}_x = \mathbb{E}[\mathbf{x}_{N_r}(t)\mathbf{x}_{N_r}^T(t)] \approx \frac{1}{T-N+1} \sum_{t=0}^{T-N} \mathbf{x}_{N_r}(t)\mathbf{x}_{N_r}^T(t) \quad (2.44)$$

²The SIMO noise free model is identifiable up to a scalar indeterminacy i.e. $\hat{\mathbf{h}} = \alpha \mathbf{h}$ for a given scalar coefficient α .

where T is the number of the observed samples (N is the length of the window). Then, the eigen-decomposition of \mathcal{R}_x allows us to identify the $NN_r \times (NN_r - N - L)$ \mathbf{V}_n noise subspace matrix which should be orthogonal to the signal subspace spanned by $\mathcal{H}_{\mathbf{N}_r}$. Using this orthogonality and under the necessary identifiability conditions [83], the channel vector can be estimated by:

$$\mathbf{h}_{\text{CS}} = \arg \min_{\|\mathbf{h}\|_2=1} \|\mathbf{V}_n^H \mathcal{H}_{\mathbf{N}_r}\|_F^2 \quad (2.45)$$

This is resolved by constructing the matrix \mathcal{V}_n which verifies $\|\mathbf{V}_n^H \mathcal{H}_{\mathbf{N}_r}\|_F^2 = \|\mathcal{V}_n^H \mathbf{h}\|_2^2$. Hence, the solution \mathbf{h}_{CS} is the eigenvector corresponding to the smallest eigenvalue of $(\mathcal{V}_n \mathcal{V}_n^H)$.

MIMO system

The identification conditions for the MIMO case was discussed for the subspace method in [83]. The indeterminacy for the MIMO case is such that the solution is found up to a $N_t \times N_t$ full rank matrix \mathbf{Q} i.e. $\hat{\mathbf{H}}_{\text{CS}} = \mathbf{H}\mathbf{Q}$.

The subspace method stays valid for the MIMO case with some changes. The signals covariance matrix is calculated in the same way but using $\mathbf{x}_N(n)$ as defined in Eq. (2.29). The $NN_r \times ((NN_r) - (N(L+1)N_t))$ noise subspace matrix \mathbf{V}_n is calculated by tanking the $((NN_r) - (N(L+1)N_t))$ eigenvectors corresponding to the smallest eigenvalues of \mathcal{R}_x . The solution \mathbf{H}_{CS} is determined by calculating the N_t eigenvectors of $(\mathcal{V}_n \mathcal{V}_n^H)$ corresponding to the N_t smallest eigenvalues with \mathcal{V}_n constructed in the same way as in SIMO case.

The deterministic ML approach can also be used for MIMO channels. In such case the ML criterion is given by:

$$\left(\mathcal{T}(\mathbf{H}), \mathbf{s}_N(t) \right) = \arg \max_{\mathcal{T}(\mathbf{H}), \mathbf{s}_N(t)} f(\mathbf{x}_N(t); \mathcal{T}(\mathbf{H}), \mathbf{s}_N(t)) \quad (2.46)$$

$$= \arg \min_{\mathcal{T}(\mathbf{H}), \mathbf{s}_N(t)} \left\{ \left\| \mathbf{x}_N(t) - \mathcal{T}(\mathbf{H})\mathbf{s}_N(t) \right\|_2^2 \right\} \quad (2.47)$$

The joint optimization of the likelihood function in both the channel and the source parameter spaces is difficult. Fortunately, the observation is linear in both the channel and the input parameters. In other words, we have a separable nonlinear LS problem, which allows us to reduce the complexity considerably. The ML approaches can be made very effective by including the subspace and other suboptimal approaches as initialization procedures.

2.4.3 Sparse approaches

In case of very long impulse response and sparse channel, classical methods perform poorly. In addition, some methods (such as subspace method) need a correct estima-

tion of channel order and suffer in case of order overestimation. Recently, solutions have been proposed to handle this case by adapting classical blind identification methods to the sparse case by using a specular channel parametric model such as in [84], or by constraining the desired solution through a ℓ_p -norm (with $0 < p \leq 1$) such as in [80], where the CR cost function is considered:

$$\mathbf{h}_{\text{SCR}} = \arg \min_{\|\mathbf{h}\|_2=1} \left\{ \mathbf{h}^H \mathcal{X}_{N_r}^H \mathcal{X}_{N_r} \mathbf{h} + \lambda \|\mathbf{h}\|_p^p \right\} \quad (2.48)$$

where λ is a weighting parameter which controls the tradeoff between approximation error and sparsity. Then, a stochastic gradient technique is proposed to solve this minimization problem efficiently.

Another solution was proposed in [81], where a channel sparsity measure is used together with the ML criterion to improve the estimation quality. Based on the Maximum a Posteriori (MAP) approach and using the generalized Laplacian distribution model to approximate the sparse channel PDF, leads to the following objective function:

$$\mathbf{h}_{\text{MAP}} = \arg \min_{\|\mathbf{h}\|_2=1} \left\{ \mathbf{h}^H \mathcal{X}_{N_r}^H (\mathcal{G}_{\text{CR}}^H \mathcal{G}_{\text{CR}})^{\#} \mathcal{X}_{N_r} \mathbf{h} + \lambda \|\mathbf{h}\|_p^p \right\} \quad (2.49)$$

Similarly to the ML method, the above cost function is optimized in two steps; the first one is equivalent to Eq. (2.48) where $(\mathcal{G}_{\text{CR}}^H \mathcal{G}_{\text{CR}})^{\#}$ is replaced by an identity matrix. Then, the estimated channel at the first step is used to construct $(\mathcal{G}_{\text{CR}}^H \mathcal{G}_{\text{CR}})^{\#}$ and to optimize Eq. (2.49) using a stochastic gradient minimization. Furthermore, an extension was proposed in [50] to deal adaptively with such system identification based on the sparse CR method in the case of SIMO channel.

For the MIMO case, we can mention the solution proposed in [50] which is based on the subspace method. The sparsity is induced by adding the ℓ_p -norm penalty or the Reweighted ℓ_1 penalty [35] to the cost function in Eq. (2.45) for the MIMO case. A gradient based solution is used for the optimization. A semi-blind solution is introduced in the same paper to improve the performance and to resolve the indeterminacy of the problem.

2.5 Conclusion

In this chapter, we have introduced the three main problems investigated in this thesis. First, we discussed the principal subspace tracking problem and the data model considered. Then, three solutions from the state-of-the-art are presented: PAST, OPAST and FAPI algorithms. SPCA algorithms and the ℓ_1 -PAST are introduced as solutions to the problem of principal subspace tracking under the sparsity

constraint of the system. The second discussed problem is blind source separation where we introduced the classical ICA based separation solutions. Then, we showed how sparse decomposition techniques affected this problem and led to SCA and MCA based separation solutions. The third problem treated is blind FIR channel identification where we exposed the SIMO/MIMO model. We presented three classical approaches to this problem: TSML method, CR method and noise subspace method. For the sparse channel problem, we have presented some methods from the state-of-the-art, which are, in general, just an adaptation of the classical methods with additional constraints to induce the sparsity. In the next chapter, we will present the different methods proposed in order to solve the problem of tracking the principal subspace under the sparsity constraint and the performance comparison with the state-of-the-art algorithms.

Low-cost sparse subspace tracking algorithms

Contents

3.1	Introduction	41
3.2	Non-orthogonal sparse subspace tracking algorithms	43
3.2.1	System matrix Sparsity algorithm based on FAPI SS-FAPI	45
3.2.2	System matrix Sparsity algorithm based on FAPI SS-FAPI2	47
3.2.3	System matrix Sparsity algorithm based on FAPI and Shear-Givens rotations SGSS-FAPI	48
3.3	Orthogonal sparse subspace tracking algorithms	51
3.3.1	Orthogonal System matrix Sparsity algorithm based on FAPI OSS-FAPI	51
3.3.2	System matrix Sparsity algorithm based on FAPI and Givens rotations GSS-FAPI	52
3.4	Theoretical analysis	55
3.4.1	Convergence analysis of FAPI algorithm	55
3.4.2	Convergence analysis of the ℓ_1 minimization	56
3.5	Simulation results	58
3.5.1	Performance factors	58
3.5.2	Synthetic data	59
3.5.3	Real data	67
3.6	Discussion	68
3.7	Conclusion	72

3.1 Introduction

In many recent applications, the data dimensions are becoming huge and that raises some important questions about the estimation accuracy, the computational cost

and the lack of interpretation of the signal processing techniques. This is the case, for example, for principal component analysis (PCA) and its financial or biological applications [85]. One of the ways to enhance the quality of processing and its interpretability is to use all the known information about our system. In our work, we have considered the sparsity information. More precisely, in this chapter, our main objective is to solve the principal subspace tracking problem under a sparsity constraint over the weight matrix. This will be crucial in two major cases: when we deal with the lack of interpretability. For example, in high-dimensional genomic research, the traditional PCA is often difficult to interpret as principal components loadings are linear combinations of all available variables (the number of genes is generally very large for genomic data) [86]. Hence, we want to have principal components that involve only a few genes, so researchers can focus on these specific genes for further analysis [86]. In the second case, we want to recover the ground truth mixing matrix as is the case in source separation when the mixing matrix is sparse, in sparse channel identification or generally in blind sparse system identification [87]. Many solutions have been proposed for batch sparse subspace estimation known generally as SPCA methods. Unlike the batch case, there is not a lot of work that has been done for the adaptive scheme. After the state-of-the-art presented in the previous chapter, we present here the proposed methods to solve the considered problem. We first start with the non-orthogonal case i.e. there is no orthogonality constraint on the weight matrix which corresponds to the problem of blind sparse system identification. However, most applications of subspace tracking methods require or prefer to use an orthogonal weight matrix, e.g. the MUSIC [10] and the minimum-norm [88] algorithms in the context of DOA (directions of arrival) or frequency estimation. Hence, we have proposed solutions to the problem of tracking the sparse principal subspace under the orthogonality constraint of the weight matrix.

Most of the methods proposed in the literature suffer from a trade-off between the subspace performance and the targeted level of sparsity. A two-step approach is used to solve this problem, where the first one uses the Fast Approximated Power Iteration subspace tracking algorithm FAPI [21] for an adaptive extraction of an orthonormal basis of the principal subspace. Then, under the sparsity constraint, an estimation of the desired weight matrix is done in the second step using different optimization techniques. The resulting algorithms have different characteristics such as the sparsity performance (speed and limit of convergence), the computational complexity and the orthogonality of the solution. Therefore, they are able to treat many applications depending on the imposed constraints. Under some mild conditions, a theoretical convergence analysis shows that the proposed two step approach

allows us to recover the sparse ground truth mixing matrix. Also, the proposed algorithms have a low computational complexity (suitable for the adaptive context) and they achieve both good convergence and estimation performance as compared to the state-of-the-art solutions.

In this chapter, we start by deriving the proposed algorithms for both cases: with or without the orthogonality constraint over the weight matrix. Afterwards, we discuss the theoretical analysis of the proposed two-step approach and we show the efficiency of the proposed scheme compared to the state-of-the-art algorithms in different simulations scenarios.

From now on, we will suppose without any loss of generality only the real case of the data model of Eq. (2.1) i.e. $\mathbf{A}(t)$, $\mathbf{x}(t)$, $\mathbf{s}(t)$ and $\mathbf{n}(t)$ have real entries. We can easily extend the derived equation to the complex model at the cost of an increased computational complexity.

3.2 Non-orthogonal sparse subspace tracking algorithms

The proposed solutions to the problem of tracking the signal subspace with a sparsity constraint over the weight matrix are based on a two-step approach corresponding to:

1. An adaptive extraction of an orthonormal basis of the principal subspace of the instantaneous covariance matrix $\mathbf{C}_x(t)$.
2. Estimation of the sparse weight matrix that spans the same subspace.

In the first step, the objective function to minimize is equivalent to the one given by Eq. (2.4) under the orthogonality constraint of the weight matrix $\mathbf{W}(t)^T \mathbf{W}(t) = \mathbf{I}_p$ in the exponential window case (equivalent formulation can also be expressed in case of truncated window). The resulting weight matrix from this first step is denoted $\mathbf{W}_{PS}(t)$. The first version of the proposed solutions was based on OPAST [17]. Later, we replaced OPAST by FAPI [21] which has better tracking capabilities with the same computational complexity.

For the second step, we search for the desired sparse weight matrix in the form $\mathbf{W}(t) = \mathbf{W}_{PS}(t)\mathbf{Q}(t)$ where the non-singular matrix $\mathbf{Q}(t) \in \mathbb{R}^{p \times p}$ is introduced in order to optimize the chosen sparsity criterion and it is computed in such a way we

minimize the cost function¹

$$\begin{aligned} J_{SS}(\mathbf{Q}(t)) &= \|\mathbf{W}(t)\|_1 = \|\mathbf{W}_{PS}(t)\mathbf{Q}(t)\|_1 \\ \text{s.t. } \mathbf{Q}(t) &\text{ is non-singular with unit norm columns} \end{aligned} \quad (3.1)$$

It is known that the ℓ_0 pseudo-norm is more appropriate to represent the sparsity of $\mathbf{W}(t)$ but it will make the objective function non convex, non continuous and hard to optimize. Therefore, we use the ℓ_1 -norm relaxation which is the tightest convex relaxation of the ℓ_0 pseudo-norm [89] and it makes the optimization of the objective function easier as compared to the ℓ_0 -based version. It is important also to notice that the signal subspace spanned by $\mathbf{W}_{PS}(t)\mathbf{Q}(t)$ is the same one spanned by $\mathbf{W}_{PS}(t)$ when $\mathbf{Q}(t)$ is non-singular. In fact the orthogonal projection matrix of the principal subspace estimate is given by

$$\mathbf{\Pi}_s(t) = \mathbf{W}(t)\mathbf{W}^\#(t) \approx \mathbf{W}_{PS}(t)\mathbf{Q}(t)\mathbf{Q}^\#(t)\mathbf{W}_{PS}^\#(t) \quad (3.2)$$

$$= \mathbf{W}_{PS}(t)\mathbf{W}_{PS}^T(t) \quad (3.3)$$

because $\mathbf{Q}(t)\mathbf{Q}^\#(t) = \mathbf{I}_p$ when $\mathbf{Q}(t)$ is non-singular.

This is one of the reasons why we have chosen the two-step scheme. Indeed, most of the proposed methods in the literature suffer from a trade-off between the subspace performance and the targeted level of sparsity. By choosing the two-step approach, we seek the sparse basis matrix without disturbing the first step responsible of the subspace tracking. Hence, the proposed method has the same subspace performance (i.e. the linear complexity as well as the good estimation accuracy) as the considered tracking method (FAPI).

Note that depending on the applications, the orthogonality is not necessarily aligned with the sparsity constraint of the weight matrix. Indeed, in this work, we confirmed experimentally the hypothesis that looking for the best orthogonal subspace in most of the considered situations is not the sparsest one, and trying to reach both goals of sparsity and orthogonality at the same time generally leads to sub-optimal solutions. For that reason, we have considered the two-step approach with two different weight matrices $\mathbf{W}_{PS}(t)$ and $\mathbf{W}(t)$. The first one keeps tracking the principal subspace and the second one estimates the sparse weight matrix. We have proposed five different techniques to minimize the cost function $J_{SS}(\mathbf{Q}(t))$ which leads to five algorithms described below: SS-FAPI, SS-FAPI2, SGSS-FAPI for Shear-Givens rotations based SS-FAPI, OSS-FAPI for Orthogonal SS-FAPI and GSS-FAPI for Givens rotations based SS-FAPI. The comparative behavior of these algorithms will be illustrated and discussed in sections 3.5 and 3.6.

¹SS stands for System matrix Sparsity. The unit-norm column constraint of $\mathbf{Q}(t)$ is necessary here because we replaced the ℓ_0 pseudo-norm by the more tractable ℓ_1 norm.

3.2.1 System matrix Sparsity algorithm based on FAPI SS-FAPI

The optimization of the ℓ_1 norm criterion $J_{SS}(\mathbf{Q}(t))$ is achieved here by using a natural gradient approach [90] (see the Appendix A for more details about the natural gradient and its relation with SS-FAPI). Hence, we search for the updated matrix $\mathbf{Q}(t)$ in the form $\mathbf{Q}(t) = \mathbf{Q}(t-1)(\mathbf{I}_p + \boldsymbol{\varepsilon})$ where $\boldsymbol{\varepsilon} \in \mathbb{R}^{p \times p}$ is a matrix which has small valued entries (depending on the gradient step) that can be computed using a first order approximation according to:

$$\hat{\boldsymbol{\varepsilon}} = \arg \min_{\boldsymbol{\varepsilon}} \left\| \mathbf{W}_{PS}(t)\mathbf{Q}(t-1) + \mathbf{W}_{PS}(t)\mathbf{Q}(t-1)\boldsymbol{\varepsilon} \right\|_1 \quad (3.4)$$

Letting $\mathbf{M} = \mathbf{W}_{PS}(t)\mathbf{Q}(t-1)$, then (3.4) yields

$$\hat{\boldsymbol{\varepsilon}} = \arg \min_{\boldsymbol{\varepsilon}} \left\| \mathbf{M} + \mathbf{M}\boldsymbol{\varepsilon} \right\|_1 \quad (3.5)$$

$$= \arg \min_{\boldsymbol{\varepsilon}} \sum_{i=1}^d \sum_{j=1}^p \left| m_{ij} + \sum_{k=1}^p m_{ik}\varepsilon_{kj} \right| \quad (3.6)$$

If we assume that two scalars x and z have the same sign or $|z| \leq |x|$, one can say that $|x+z| = |x| + \text{sign}(x)z$. This remains approximately true when $|z|$ is slightly bigger than $|x|$. Using this approximation in (3.6) (m_{ij} as x and $\sum_{k=1}^p m_{ik}\varepsilon_{kj}$ as z) leads to:

$$\hat{\boldsymbol{\varepsilon}} \approx \arg \min_{\boldsymbol{\varepsilon}} \sum_{i=1}^d \sum_{j=1}^p \left(|m_{ij}| + \text{sign}(m_{ij}) \sum_{k=1}^p m_{ik}\varepsilon_{kj} \right) \quad (3.7)$$

The idea is to look for an expression of $\boldsymbol{\varepsilon}$ that ensures a decreasing direction of the objective function. We can see that:

$$\begin{aligned} & \sum_{i=1}^d \sum_{j=1}^p \left(\text{sign}(m_{ij}) \sum_{k=1}^p m_{ik}\varepsilon_{kj} \right) \\ &= \sum_{j=1}^p \sum_{k=1}^p \left(\varepsilon_{kj} \sum_{i=1}^d \text{sign}(m_{ij}) m_{ik} \right) \end{aligned} \quad (3.8)$$

$$= \sum_{j=1}^p \sum_{k=1}^p \varepsilon_{kj} b_{kj} = \text{Tr}(\boldsymbol{\varepsilon} \mathbf{B}^T) \quad (3.9)$$

with $\mathbf{B} = \mathbf{M}^T \text{sign}(\mathbf{M})$. By applying a simple gradient on (3.9), we can take $\hat{\boldsymbol{\varepsilon}} = -\mu \frac{\mathbf{B}}{\|\mathbf{B}\|_F^2}$ with $\mu > 0$ to ensure a local decrease of the cost function. On the other hand, the value of μ should be small enough for the linear approximation to hold and to preserve the non-singularity of matrix \mathbf{Q} . In fact, using a first order approximation, one can write:

$$\det(\mathbf{Q}(t)) \approx \det(\mathbf{Q}(t-1)) \left(1 - \mu \frac{\text{Tr}(\mathbf{B})}{\|\mathbf{B}\|_F^2} \right)$$

Algorithm 5 System matrix Sparsity algorithm based on FAPI SS-FAPI

Require: $\mathbf{x}(t)$ data vector, β the forgetting factor, $\mathbf{W}_{PS}(t-1)$, $\mathbf{Z}_{PS}(t-1)$ and $\mathbf{Q}(t-1)$ from the previous iteration.

Ensure: $\mathbf{W}_{PS}(t)$, $\mathbf{Z}_{PS}(t)$, $\mathbf{Q}(t)$ and the sparse weight matrix $\mathbf{W}(t)$

- 1: Find $\mathbf{W}_{PS}(t)$ using FAPI
 - 2: $\mathbf{M} = \mathbf{W}_{PS}(t)\mathbf{Q}(t-1)$
 - 3: $\mathbf{B} = \mathbf{M}^T \text{sign}(\mathbf{M})$ then $\mathbf{B} = \frac{\mathbf{B}}{\|\mathbf{B}\|_F^2}$
 - 4: $\mathbf{Q}(t) = \mathbf{Q}(t-1)(\mathbf{I}_p - \mu\mathbf{B})$
 - 5: Columns normalization of $\mathbf{Q}(t)$
 - 6: $\mathbf{W}(t) = \mathbf{W}_{PS}(t)\mathbf{Q}(t)$.
-

Therefore, one can choose heuristically $\mu = c\|\mathbf{B}\|_F^2/\text{Tr}(\mathbf{B})$ where $c < 1$ (typically $c = 0.1$) is a given small coefficient. The full SS-FAPI algorithm is summarized in Algorithm 5.

Note that, after every iteration, it is important to normalize the columns of $\mathbf{Q}(t)$ to better control the conditioning of matrix $\mathbf{W}(t)$ and to meet the constraint condition of Eq. (3.1). This columns normalization can be seen as a projection onto the set $\{Q : \|q_i\| = 1\}$, i.e., the set of matrices with unit norm columns, which makes the followed scheme similar to the projected gradient scheme. However, instead of the ordinary gradient (sub-gradient), we use the natural gradient (see the Appendix A for the relation with the natural gradient).

Although the complexity² of the first stage (FAPI algorithm) is only $\mathcal{O}(dp)$, the global complexity of our algorithm is $\mathcal{O}(dp^2)$ because the second stage dominates the overall complexity. Thus, two improvement directions on SS-FAPI are possible by:

- Replacing the FAPI algorithm used in the first stage's by a more efficient subspace tracker of complexity $\mathcal{O}(dp^2)$ which leads to the same global complexity with better subspace estimation. Thus, following this idea, we have proposed a variant called SS-LORAF2 where we use the algorithm LORAF2 [18] to track the subspace in the first stage while keeping the second stage unchanged.
- Or otherwise, reducing the computational complexity of the second stage responsible of the ℓ_1 minimization to keep the linear global complexity, which we propose here in the second algorithm SS-FAPI2.

²Operations counts are expressed in terms of multiply-accumulate (MAC) operations. Only the dominant cost of the SS-FAPI second stage is presented under the assumption $p \ll d$.

3.2.2 System matrix Sparsity algorithm based on FAPI SS-FAPI2

Based of SS-FAPI, the idea here is to avoid using all the matrix $\mathbf{B} = \mathbf{M}^T \text{sign}(\mathbf{M})$ to update $\mathbf{Q}(t)$ but selecting only two entries which have (i, j) and (j, i) as indices with $i \neq j$. This is equivalent to minimize only the ℓ_1 -norm of the i^{th} and the j^{th} columns of the matrix $\mathbf{W}(t)$ in Eq. (3.1). The choice of i and j is done according to an automatic (incremental) selection throughout the iterations in such a way all indices values are visited periodically with $1 \leq i < j \leq p$. Hence, if (l, m) are the indices at time instant $(t - 1)$, then at the current time instant, we will have

$$(i, j) = \begin{cases} (l, m + 1) & \text{if } m < p \\ (l + 1, l + 2) & \text{if } m = p \text{ and } l < p - 1 \\ (1, 2) & \text{if } m = p \text{ and } l = p - 1 \end{cases} \quad (3.10)$$

Using this update in (3.4) and (3.7), we can see that only b_{ij} and b_{ji} need to be calculated. For that, one needs only to evaluate the two columns \mathbf{m}_i and \mathbf{m}_j of the matrix \mathbf{M} .

$$\mathbf{m}_i = \mathbf{w}_i(t - 1) + \tilde{g}_i \mathbf{e} \quad \text{and} \quad \mathbf{m}_j = \mathbf{w}_j(t - 1) + \tilde{g}_j \mathbf{e} \quad (3.11)$$

$$b_{ij} = \mathbf{m}_i^T \text{sign}(\mathbf{m}_j) \quad \text{and} \quad b_{ji} = \mathbf{m}_j^T \text{sign}(\mathbf{m}_i) \quad (3.12)$$

where $\mathbf{w}_j(t - 1)$ is the j^{th} column of the sparse weight matrix of the previous iteration and \tilde{g}_j is the j^{th} element of vector $\tilde{\mathbf{g}} = \mathbf{Q}(t - 1)^T \mathbf{g}$ (\mathbf{g} and \mathbf{e} are rank-one update vectors issued from the last step of FAPI). Then, we normalize by $b_{ji}^2 + b_{ij}^2 = 1$ (same normalization as $\frac{\mathbf{B}}{\|\mathbf{B}\|_F^2}$ in SS-FAPI) and we update $\mathbf{Q}(t)$ by $\mathbf{Q}(t) = \mathbf{Q}(t - 1) - \mu \mathbf{Z}$ with \mathbf{Z} is given by $\mathbf{Z} = [0, \dots, b_{ji} \mathbf{q}_j(t - 1), 0, \dots, b_{ij} \mathbf{q}_i(t - 1), \dots, 0]$. Finally, $\mathbf{W}(t)$ is given by

$$\begin{aligned} \mathbf{W}(t) &= \left(\mathbf{W}_{PS}(t - 1) + \mathbf{e} \mathbf{g}^T \right) \left(\mathbf{Q}(t - 1) - \mu \mathbf{Z} \right) \\ &= \mathbf{W}(t - 1) + \mathbf{e} \tilde{\mathbf{g}}^T - \mu \tilde{\mathbf{W}} \end{aligned} \quad (3.13)$$

with $\tilde{\mathbf{W}} = \mathbf{W}_{PS}(t) \mathbf{Z} = [0, \dots, d_{ji} \mathbf{m}_j, 0, \dots, d_{ij} \mathbf{m}_i, \dots, 0]$. This version is called SS-FAPI2 and it is summarized in Algorithm 6. The global complexity of SS-FAPI2 is $4dp + \mathcal{O}(p^2)$ which is linear and comparable to the complexity of simple FAPI (i.e. $3dp + \mathcal{O}(p^2)$). However, it is clearly smaller than the complexity of SS-FAPI which is $\mathcal{O}(dp^2)$.

Note that other selection strategies for the rotation indices can be considered. For example, at each iteration, one can select the indices (i, j) corresponding to the columns \mathbf{m}_i and \mathbf{m}_j of matrix \mathbf{M} having the maximum ℓ_1 norms (i.e. the ones that deviate the most from the target sparsity objective).

Algorithm 6 System matrix Sparsity algorithm based on FAPI SS-FAPI2

Require: $\mathbf{x}(t)$ data vector, β the forgetting factor, $\mathbf{W}(t-1)$, $\mathbf{W}_{PS}(t-1)$, $\mathbf{Z}_{PS}(t-1)$ and $\mathbf{Q}(t-1)$ from the previous iteration.

Ensure: $\mathbf{W}_{PS}(t)$, $\mathbf{Z}_{PS}(t)$, $\mathbf{Q}(t)$ and the sparse weight matrix $\mathbf{W}(t)$

- 1: $\mathbf{W}_{PS}(t) = \mathbf{W}_{PS}(t-1) + \mathbf{e}\mathbf{g}^T$ last step of FAPI
- 2: $\tilde{\mathbf{g}} = \mathbf{Q}(t-1)^T \mathbf{g}$
- 3: Update indices (i, j) using automatic selection strategy according to Eq. (3.10)
- 4: $\mathbf{m}_i = \mathbf{w}_i(t-1) + \tilde{g}_i \mathbf{e}$ and $\mathbf{m}_j = \mathbf{w}_j(t-1) + \tilde{g}_j \mathbf{e}$
- 5: $b_{ij} = \mathbf{m}_i^T \text{sign}(\mathbf{m}_j)$ and $b_{ji} = \mathbf{m}_j^T \text{sign}(\mathbf{m}_i)$
- 6: $b_{ij} = \frac{b_{ij}}{\sqrt{b_{ij}^2 + b_{ji}^2}}$ and $b_{ji} = \frac{b_{ji}}{\sqrt{b_{ij}^2 + b_{ji}^2}}$
- 7: $\mathbf{Z} = [0, \dots, b_{ji} \mathbf{q}_j(t-1), 0, \dots, b_{ij} \mathbf{q}_i(t-1), \dots, 0]$
- 8: $\mathbf{Q}(t) = \mathbf{Q}(t-1) - \mu \mathbf{Z}$
- 9: $\tilde{\mathbf{W}} = [0, \dots, b_{ji} \mathbf{m}_j, 0, \dots, b_{ij} \mathbf{m}_i, \dots, 0]$
- 10: $\mathbf{W}(t) = \mathbf{W}(t-1) + \mathbf{e}\tilde{\mathbf{g}}^T - \mu \tilde{\mathbf{W}}$

3.2.3 System matrix Sparsity algorithm based on FAPI and Shear-Givens rotations SGSS-FAPI

The SGSS-FAPI (Shear-Givens rotations SS-FAPI) algorithm is based on the same two-step approach as in the previous algorithms. However, in this work, the sparsity criterion is optimized by means of Givens and Shear (hyperbolic givens) rotations. The Jacobi-like techniques are attractive due to their numerical stability, their low computational cost and their facility to be parallelized. Such techniques have been already used in the context of blind source separation [91, 92] but with different *a priori* information on source signals.

In order to minimize $J_{SS}(\mathbf{Q}(t))$, we propose to write the matrix $\mathbf{Q}(t)$ as a product of elementary Givens and Shear matrices:

$$\mathbf{Q}(t) = \prod_{1 \leq i < j \leq p} \mathcal{G}_{ij} \mathcal{S}_{ij} \quad (3.14)$$

Indeed, any non singular matrix (up to a scalar constant) can be decomposed into product of Shear \mathcal{S}_{ij} and Givens \mathcal{G}_{ij} rotation matrices for $1 \leq i < j \leq p$ which are defined as an identity matrix except for their $(i, i)^{th}$, $(i, j)^{th}$, $(j, i)^{th}$ and $(j, j)^{th}$ entries given by:

$$\begin{bmatrix} \mathcal{G}_{ij}(i, i) & \mathcal{G}_{ij}(i, j) \\ \mathcal{G}_{ij}(j, i) & \mathcal{G}_{ij}(j, j) \end{bmatrix} = \begin{bmatrix} \cos(\theta) & -e^{i\alpha} \sin(\theta) \\ e^{-i\alpha} \sin(\theta) & \cos(\theta) \end{bmatrix} \quad (3.15)$$

$$\begin{bmatrix} \mathcal{S}_{ij}(i, i) & \mathcal{S}_{ij}(i, j) \\ \mathcal{S}_{ij}(j, i) & \mathcal{S}_{ij}(j, j) \end{bmatrix} = \begin{bmatrix} \cosh(\phi) & e^{i\beta} \sinh(\phi) \\ e^{-i\beta} \sinh(\phi) & \cosh(\phi) \end{bmatrix} \quad (3.16)$$

where (θ, α) and (ϕ, β) are Givens and Shear parameters ($\alpha = \beta = 0$ in the real case). Next, we present the case of using just one Shear-Givens rotation every time iteration for simplicity and then we generalize to the case where we consider more than one rotation. Hence, we can write that

$$\mathbf{Q}(t) = \mathbf{Q}(t-1)\mathcal{G}_{ij}\mathcal{S}_{ij} \quad (3.17)$$

for the selected indices (i, j) at the t^{th} time iteration.

In order to minimize the objective function $J_{SS}(\mathbf{Q}(t))$, one needs to specify how the rotation indices are chosen at each iteration as well as how the parameters (θ, ϕ) are optimized. We can propose to use the automatic selection strategy for the rotation indices already used for SS-FAPI2 and expressed in Eq. (3.10) which allows us to scan all the $p(p-1)/2$ possible values periodically.

Hence, after fixing the indices (i, j) , finding $\mathbf{Q}(t)$ resumes in estimating the parameters (θ, ϕ) which minimize:

$$J(\theta, \phi) = \left\| \mathbf{W}_{PS}(t)\mathbf{Q}(t-1)\mathcal{G}_{ij}\mathcal{S}_{ij} \right\|_1 \quad (3.18)$$

$$= \left\| \begin{bmatrix} \mathbf{m}_i & \mathbf{m}_j \end{bmatrix} \begin{bmatrix} \cos(\theta) & -\sin(\theta) \\ \sin(\theta) & \cos(\theta) \end{bmatrix} \begin{bmatrix} \cosh(\phi) & \sinh(\phi) \\ \sinh(\phi) & \cosh(\phi) \end{bmatrix} \right\|_1 \quad (3.19)$$

where \mathbf{m}_i and \mathbf{m}_j are the i^{th} and j^{th} columns of the product $\mathbf{W}_{PS}(t)\mathbf{Q}(t-1)$ available from the previous iteration. We can expand the equation to:

$$\begin{aligned} J(\theta, \phi) = & \left\| \begin{aligned} & \left(\cos(\theta) \cosh(\phi) - \sin(\theta) \sinh(\phi) \right) \mathbf{m}_i + \\ & \left(\cos(\theta) \sinh(\phi) + \sin(\theta) \cosh(\phi) \right) \mathbf{m}_j \end{aligned} \right\|_1 + \\ & \left\| \begin{aligned} & \left(\cos(\theta) \sinh(\phi) - \sin(\theta) \cosh(\phi) \right) \mathbf{m}_i + \\ & \left(\cos(\theta) \cosh(\phi) + \sin(\theta) \sinh(\phi) \right) \mathbf{m}_j \end{aligned} \right\|_1 \end{aligned} \quad (3.20)$$

$J(\theta, \phi)$ is a scalar function of two variables with no simple analytic solution for its minimum point. In order to minimize $J(\theta, \phi)$, we propose to use a numerical optimization method for unconstrained multivariate cost functions.

Now, we will resume the scheme to follow in order to reach a linear computational complexity for both steps. The main idea is to run the FAPI algorithm independently and to update the weight matrix by

$$\mathbf{W}(t) = \mathbf{W}_{PS}(t)\mathbf{Q}(t) \quad (3.21)$$

$$= \left(\mathbf{W}_{PS}(t-1) + \mathbf{e}\mathbf{g}^T \right) \mathbf{Q}(t-1)\mathcal{G}_{ij}\mathcal{S}_{ij} \quad (3.22)$$

$$= \mathbf{W}(t-1)\mathcal{G}_{ij}\mathcal{S}_{ij} + \mathbf{e}\mathbf{g}^T\mathbf{Q}(t) \quad (3.23)$$

Algorithm 7 System matrix Sparsity algorithm based on FAPI and Shear-Givens rotations SGSS-FAPI

Require: $\mathbf{x}(t)$ data vector, forgetting factor β , $\mathbf{W}_{PS}(t-1)$ and $\mathbf{Z}_{PS}(t-1)$ previous FAPI outputs. Previous indices (l, m) and outputs $\mathbf{Q}(t-1)$, $\mathbf{W}(t-1)$.

Ensure: $\mathbf{W}_{PS}(t)$, $\mathbf{Z}_{PS}(t)$, indices (i, j) , $\mathbf{Q}(t)$ and $\mathbf{W}(t)$

- 1: Run FAPI : $\mathbf{W}_{PS}(t) = \mathbf{W}_{PS}(t-1) + \mathbf{e}'(t)\mathbf{g}(t)^H$
 - 2: Update indices (i, j) using automatic selection strategy according to Eq. (3.10)
 - 3: Computing \mathbf{m}_i and \mathbf{m}_j
 - 4: Find $(\hat{\theta}, \hat{\phi}) = \arg \min J(\theta, \phi)$
 - 5: $\mathbf{Q}(t) = \mathbf{Q}(t-1)\mathcal{G}_{ij}\mathcal{S}_{ij}$
 - 6: $\mathbf{W}(t) = \mathbf{W}(t-1)\mathcal{G}_{ij}\mathcal{S}_{ij} + \mathbf{e}\mathbf{g}^T\mathbf{Q}(t)$
-

where \mathbf{e} and \mathbf{g} are the FAPI rank one update vectors. The matrix-matrix multiplication in Eq. (3.23) involves only two columns of the matrix $\mathbf{W}(t-1)$ which gives us a linear global computational complexity of order $4dp + O(p^2)$ flops per iteration or $7dp + 4Lp + O(p^2)$ if we use the truncated window version of FAPI. (L is the length of the data window approximated by $\frac{1}{1-\beta}$). The proposed algorithm referred to as SGSS-FAPI (Shear-Givens rotations based algorithm for System matrix Sparsity) is summarized in Algorithm 7.

Remark 1: It is possible to optimize separately the Givens parameter θ then the Shear parameter ϕ . This leads to a slight loss in terms of estimation quality but helps reducing the computational cost since one replaces the 2D search by two 1D parameter optimization. This version is referred to as SGSS-FAPI-iter.

Remark 2: In case where we consider more than one Shear-Givens rotation every time iteration, two possible solutions can be adopted. First, we can consider a sequential solution by repeating steps 2-6 of Algorithm 7. Otherwise, we can use the parallelization capability of the Jacobi-like techniques, which allows us run simultaneously steps 3-6 of Algorithm 7 for multiple pairs of indices selected according to more sophisticated selection strategy (pairs should not share any column index).

Remark 3: In the complex case, the ℓ_1 cost function depends on four parameters $(\theta, \phi, \alpha, \beta)$, which means that the joint optimization used in SGSS-FAPI is harder and more time-consuming. In this case, the iterative optimization (parameter per parameter) used in SGSS-FAPI-iter is more interesting, especially knowing that the parameters (θ, α, β) are angles bounded by $[-\frac{\pi}{2}, \frac{\pi}{2}]$.

3.3 Orthogonal sparse subspace tracking algorithms

Until now, we have not put any orthogonality constraint on the output weight matrix in order to reach the maximum of the weight matrix sparsity. However, most applications of subspace tracking require or prefer to use an orthogonal weight matrix as is the case for most of SPCA applications and also DOA estimators MUSIC [10] and minimum-norm [88]. Hence, we have modified SS-FAPI to force the output orthogonality in the next algorithm called OSS-FAPI.

3.3.1 Orthogonal System matrix Sparsity algorithm based on FAPI OSS-FAPI

The goal is to keep the same scheme as SS-FAPI but ensure also the orthogonality of the weight matrix. We already knew that the output of the FAPI algorithm $\mathbf{W}_{PS}(t)$ is orthogonal and the columns of $\mathbf{Q}(t)$ are normalized. Thus, the orthogonality constraint of $\mathbf{W}(t)$ requires that $\mathbf{Q}(t)$ to be orthonormal. Under the assumption that $\mathbf{Q}(t-1)^T \mathbf{Q}(t-1) = \mathbf{I}_p$, we want the update $\mathbf{Q}(t) = \mathbf{Q}(t-1) \left(\mathbf{I}_p - \mu \mathbf{B} \right)$ such that it minimizes the sparsity criterion while preserving the orthogonality of $\mathbf{Q}(t)$. For that we will exploit the fact that a square matrix \mathbf{R} is a skew-symmetric matrix (i.e. $\mathbf{R}^T = -\mathbf{R}$) if and only if $\exp(\mathbf{R})$ is a unitary matrix. We use the same updating trick considered in [93], to replace $\mathbf{Q}(t) = \mathbf{Q}(t-1) \left(\mathbf{I}_p - \mu \mathbf{B} \right)$ by the new update form $\mathbf{Q}(t) = \mathbf{Q}(t-1) \exp(-\mu \mathbf{B})$. If we take a small enough gradient step μ , it is simple to prove that the two forms are approximately equal:

$$\mathbf{Q}(t) = \mathbf{Q}(t-1) \exp(-\mu \mathbf{B}) \quad (3.24)$$

$$= \mathbf{Q}(t-1) \left(\mathbf{I}_p - \mu \mathbf{B} + \frac{\mu^2}{2!} \mathbf{B}^2 - \frac{\mu^3}{3!} \mathbf{B}^3 + \dots \right) \quad (3.25)$$

$$\approx \mathbf{Q}(t-1) \left(\mathbf{I}_p - \mu \mathbf{B} \right) \quad (3.26)$$

Hence, our new aim is to search for a skew-symmetric matrix \mathbf{B} that minimizes (3.5). It is known that a skew-symmetric matrix $-\mu \mathbf{B}$ can be decomposed into the sum $-\mu \mathbf{B} = \boldsymbol{\varepsilon} - \boldsymbol{\varepsilon}^T$ where $\boldsymbol{\varepsilon} \in \mathbb{R}^{p \times p}$. So, we simply change $\boldsymbol{\varepsilon}$ in (3.5) by $\boldsymbol{\varepsilon} - \boldsymbol{\varepsilon}^T$ which gives

$$\hat{\boldsymbol{\varepsilon}} = \arg \min_{\boldsymbol{\varepsilon}} \left\| \mathbf{M} + \mathbf{M}(\boldsymbol{\varepsilon} - \boldsymbol{\varepsilon}^T) \right\|_1 \quad (3.27)$$

Using the same development as in (3.7), we get this time

$$\hat{\boldsymbol{\varepsilon}} \approx \arg \min_{\boldsymbol{\varepsilon}} \sum_{i=1}^d \sum_{j=1}^p |m_{ij}| + \text{sign}(m_{ij}) \sum_{k=1}^p m_{ik} \varepsilon_{kj} - \text{sign}(m_{ij}) \sum_{k=1}^p m_{ik} \varepsilon_{jk} \quad (3.28)$$

Algorithm 8 Orthogonal System matrix Sparsity algorithm based on FAPI OSS-FAPI

Require: $\mathbf{x}(t)$ data vector, β the forgetting factor, $\mathbf{W}_{PS}(t-1)$, $\mathbf{Z}_{PS}(t-1)$ and $\mathbf{Q}(t-1)$ from the previous iteration.

Ensure: $\mathbf{W}_{PS}(t)$, $\mathbf{Z}_{PS}(t)$, $\mathbf{Q}(t)$ and the sparse-orthogonal weight matrix $\mathbf{W}(t)$

- 1: Find $\mathbf{W}_{PS}(t)$ using FAPI
 - 2: $\mathbf{M} = \mathbf{W}_{PS}(t)\mathbf{Q}(t-1)$
 - 3: $\mathbf{B} = \mathbf{M}^T \text{sign}(\mathbf{M})$
 - 4: $\mathbf{F} = \mathbf{B} - \mathbf{B}^T$ then $\mathbf{F} = \frac{\mathbf{F}}{\|\mathbf{F}\|_F^2}$
 - 5: $\mathbf{Q}(t) = \mathbf{Q}(t-1)\exp(-\mu\mathbf{F})$
 - 6: $\mathbf{W}(t) = \mathbf{W}_{PS}(t)\mathbf{Q}(t)$.
-

then the second term can be rewritten as

$$\begin{aligned} & \sum_{i=1}^d \sum_{j=1}^p \text{sign}(m_{ij}) \sum_{k=1}^p m_{ik} \varepsilon_{kj} - \text{sign}(m_{ij}) \sum_{k=1}^p m_{ik} \varepsilon_{jk} \\ &= \sum_{j=1}^p \sum_{k=1}^p \varepsilon_{kj} \sum_{i=1}^d \left(\text{sign}(m_{ij}) m_{ik} - \text{sign}(m_{ik}) m_{ij} \right) \end{aligned} \quad (3.29)$$

$$= \sum_{j=1}^p \sum_{k=1}^p \varepsilon_{kj} f_{kj} = \text{Tr}(\boldsymbol{\varepsilon} \mathbf{F}^T) \quad (3.30)$$

where $\mathbf{F} = \mathbf{M}^T \text{sign}(\mathbf{M}) - \text{sign}(\mathbf{M})^T \mathbf{M}$. Applying a simple gradient on (3.30) leads to $\hat{\boldsymbol{\varepsilon}} = -\mu \frac{\mathbf{F}}{\|\mathbf{F}\|_F^2}$ which ensures a local decreasing of the objective function. The full OSS-FAPI algorithm is summarized in Algorithm 8.

Initially $\mathbf{Q}(t) = \mathbf{Q}(t-1)\exp(-\mu(\boldsymbol{\varepsilon} - \boldsymbol{\varepsilon}^T))$ with $\boldsymbol{\varepsilon} = -\mu \frac{\mathbf{F}}{\|\mathbf{F}\|_F^2}$, but we have remarked that $\boldsymbol{\varepsilon} - \boldsymbol{\varepsilon}^T = 2 \frac{\mathbf{F}}{\|\mathbf{F}\|_F^2}$ because \mathbf{F} is already a skew-symmetric. Hence, we are omitting the calculation of $\boldsymbol{\varepsilon} - \boldsymbol{\varepsilon}^T$ and integrate the multiplication by 2 in the normalization step before multiplying by μ .

Note that numerical complexity of OSS-FAPI is $\mathcal{O}(dp^2)$ as in SS-FAPI, this can be explained by the fact that the only difference between the two algorithms is the matrix exponential calculation which costs $\mathcal{O}(p^3)$ flops ($dp^2 \gg p^3$ under the assumption $d \gg p$).

3.3.2 System matrix Sparsity algorithm based on FAPI and Givens rotations GSS-FAPI

Following the same spirit as for SS-FAPI2, we aim now to reduce the computational complexity of OSS-FAPI from $\mathcal{O}(dp^2)$ to $\mathcal{O}(dp)$. To achieve this objective,

we propose to update at each iteration only two entries of matrix $\boldsymbol{\varepsilon} - \boldsymbol{\varepsilon}^T$. Hence, the latter matrix has zero-valued entries except for its (i, j) -th and (j, i) -th entries that are equal to θ and $-\theta$, respectively. In that case, the exponential matrix $\exp(-\mu(\boldsymbol{\varepsilon} - \boldsymbol{\varepsilon}^T))$ coincides with a unitary Givens rotation according to the equality:

$$\exp\left(-\begin{bmatrix} 0 & \theta \\ -\theta & 0 \end{bmatrix}\right) = \begin{bmatrix} \cos(\theta) & -\sin(\theta) \\ \sin(\theta) & \cos(\theta) \end{bmatrix}.$$

Based on this, the considered $p \times p$ unitary matrix will be decomposed into a product of elementary Givens rotations

$$\mathbf{Q}(t) = \prod_{1 \leq i < j \leq p} \mathcal{G}_{ij} \quad (3.31)$$

where, \mathcal{G}_{ij} is defined as in Eq. (3.15), i.e. an identity matrix except for their $(i, i)^{th}$, $(i, j)^{th}$, $(j, i)^{th}$ and $(j, j)^{th}$ entries given by:

$$\begin{bmatrix} \mathcal{G}_{ij}(i, i) & \mathcal{G}_{ij}(i, j) \\ \mathcal{G}_{ij}(j, i) & \mathcal{G}_{ij}(j, j) \end{bmatrix} = \begin{bmatrix} c & -s \\ s & c \end{bmatrix}$$

where $c = \cos(\theta)$ and $s = \sin(\theta)$ for some angle θ and the coordinate pair (i, j) takes all the $p(p-1)/2$ possible values in the range $1 \leq i < j \leq p$. It is clear that those matrices are orthonormal and the product $\mathbf{W}_{PS}(t)\mathcal{G}_{ij}$ will span the same subspace as $\mathbf{W}_{PS}(t)$. Givens-based (Jacobi-like) techniques are known also for their numerical stability, their facility to be parallelized and their low operation count when dealing with very sparse matrices.

Next, we present the case of using just one rotation every time iteration for simplicity and then we generalize to the case where we consider more than one rotation. In the first stage we keep using the FAPI [21] algorithm as a subspace tracker, then in the second stage we seek the matrix \mathcal{G}_{ij} that minimizes the objective function $J_{SS}(\mathcal{G}_{ij}) = \|\mathbf{W}_{PS}(t)\mathcal{G}_{ij}\|_1$.

We have used the same automatic (incremental) selection strategy throughout the iterations for the rotation indices (i, j) as the one used in SS-FAPI2 (according to (3.10)), which allows us to select all the $p(p-1)/2$ possible values periodically. Thus, finding \mathcal{G}_{ij} resumes in finding the angle θ which minimizes:

$$\hat{\theta} = \arg \min_{\theta} \|\mathbf{W}_{PS}(t)\mathcal{G}_{ij}\|_1 \quad (3.32)$$

$$= \arg \min_{\theta} \left\| \begin{aligned} &\mathbf{w}_{PS1}(t) \dots c\mathbf{w}_{PSi}(t) + s\mathbf{w}_{PSj}(t) \dots \\ &\dots c\mathbf{w}_{PSj}(t) - s\mathbf{w}_{PSi}(t) \dots \mathbf{w}_{PSp}(t) \end{aligned} \right\|_1 \quad (3.33)$$

$$= \arg \min_{\theta} \left\| \begin{aligned} &\cos(\theta)\mathbf{w}_{PSi}(t) + \sin(\theta)\mathbf{w}_{PSj}(t) \\ &\cos(\theta)\mathbf{w}_{PSj}(t) - \sin(\theta)\mathbf{w}_{PSi}(t) \end{aligned} \right\|_1 \quad (3.34)$$

where $\mathbf{w}_{PSj}(t)$ is the j^{th} column of matrix $\mathbf{W}_{PS}(t)$.

It is clear that J_{SS} is a $\pi/2$ periodic scalar function of a single variable θ . There is no simple analytical solution to this problem, so we have used a numerical search solution which minimizes a scalar continuous function over a fixed interval of a single variable. The cost of this minimization is relatively low because it is a scalar function with only one bounded variable ($\theta \in [-\frac{\pi}{4}, \frac{\pi}{4}]$). Since we are using a numerical solution, we can also change the ℓ_1 norm penalty by other functions to enhance the sparsity as the one used in reweighted ℓ_1 -norm minimization [35] where they consider $P(\mathbf{w}_j) = \sum_{i=1}^d \log(1 + \frac{|w_{ij}|}{\nu})$ with $0 < \nu \ll 1$ or the one proposed in [49] which is also based on a sum of logs but handle additionally its non-smoothness (non-differentiable at 0) by using a quadratic approximation around 0.

After estimating \mathcal{G}_{ij} , the update form in GSS-FAPI is based on the implementation of the API [20] (Approximated Power Iteration) algorithm, the parent version of FAPI [21] by adapting both outputs ($\mathbf{W}(t)$ and $\mathbf{Z}(t)$). Indeed, the update equations for $\mathbf{W}(t)$ and $\mathbf{Z}(t)$ in API are

$$\mathbf{Z}_{PS}(t) = \frac{1}{\beta} \mathbf{\Theta}(t)^T (\mathbf{I}_p - \mathbf{g} \mathbf{y}^T) \mathbf{Z}_{PS}(t-1) \mathbf{\Theta}(t)^{-T} \quad (3.35)$$

$$\mathbf{W}_{PS}(t) = (\mathbf{W}_{PS}(t-1) + \mathbf{e} \mathbf{g}^T) \mathbf{\Theta}(t) \quad (3.36)$$

with \mathbf{y} , \mathbf{g} , \mathbf{e} and $\mathbf{\Theta}(t)$ are given by the first equations in the algorithm API [20].

In our case, we need to add the calculation of the product $\mathbf{W}(t) = \mathbf{W}_{PS}(t) \mathcal{G}_{ij}$ to the update form. Hence, it is equivalent to use a new matrix $\hat{\mathbf{\Theta}}(t) = \mathbf{\Theta}(t) \mathcal{G}_{ij}$ in the previous update equations which gives us:

$$\mathbf{Z}(t) = \frac{1}{\beta} \mathcal{G}_{ij}^T \mathbf{\Theta}(t)^T (\mathbf{I}_p - \mathbf{g} \mathbf{y}^T) \mathbf{Z}_{PS}(t-1) \mathbf{\Theta}(t)^{-T} \mathcal{G}_{ij} \quad (3.37)$$

$$\mathbf{W}(t) = (\mathbf{W}_{PS}(t-1) + \mathbf{e} \mathbf{g}^T) \mathbf{\Theta}(t) \mathcal{G}_{ij} \quad (3.38)$$

with $\mathcal{G}_{ij}^{-T} = \mathcal{G}_{ij}$ because it is an orthonormal matrix. This can be rewritten as:

$$\mathbf{Z}(t) = \mathcal{G}_{ij}^T \mathbf{Z}_{PS}(t) \mathcal{G}_{ij} \quad (3.39)$$

$$\mathbf{W}(t) = \mathbf{W}_{PS}(t) \mathcal{G}_{ij} \quad (3.40)$$

This update applies also for the FAPI algorithm. We note also that the multiplication by \mathcal{G}_{ij} can be calculated simply by updating the i -th and j -th columns or rows of the multiplied matrix depending of the direction of the multiplication which will reduce considerably the computational cost. The GSS-FAPI algorithm is summarized in Algorithm 9.

Algorithm 9 System matrix Sparsity algorithm based on FAPI and Givens rotations GSS-FAPI

- 1: Find $[\mathbf{W}_{PS}(t), \mathbf{Z}_{PS}(t)] = FAPI(\mathbf{x}(t), \mathbf{W}(t), \mathbf{Z}(t), \beta)$
 - 2: Update indices (i, j) using automatic selection strategy according to Eq. (3.10)
 - 3: Find the angle θ according to (3.34)
 - 4: $\mathbf{w}_k(t) = \mathbf{w}_{PSk}(t)$ for $k \notin \{i, j\}$
 - 5: $\mathbf{w}_i(t) = \cos(\theta)\mathbf{w}_{PSi}(t) + \sin(\theta)\mathbf{w}_{PSj}(t)$
 - 6: $\mathbf{w}_j(t) = -\sin(\theta)\mathbf{w}_{PSi}(t) + \cos(\theta)\mathbf{w}_{PSj}(t)$
 - 7: $\mathbf{s}_k = \mathbf{z}_{PSk}(t)$ for $k \notin \{i, j\}$
 - 8: $\mathbf{s}_i = \cos(\theta)\mathbf{z}_{PSi}(t) + \sin(\theta)\mathbf{z}_{PSj}(t)$
 - 9: $\mathbf{s}_j = -\sin(\theta)\mathbf{z}_{PSi}(t) + \cos(\theta)\mathbf{z}_{PSj}(t)$
 - 10: $\mathbf{Z}(t) = \mathbf{S}$
 - 11: $\mathbf{Z}_{i,:}(t) = \cos(\theta)\mathbf{S}_{i,:} + \sin(\theta)\mathbf{S}_{j,:}$ ($\mathbf{S}_{i,:}$: being the i -th row of \mathbf{S})
 - 12: $\mathbf{Z}_{j,:}(t) = -\sin(\theta)\mathbf{S}_{i,:} + \cos(\theta)\mathbf{S}_{j,:}$
-

One can see that the computational complexity of GSS-FAPI is now linear of order $\mathcal{O}(dp)$. Additionally, GSS-FAPI has less needs in memory storage because it stores only $\mathbf{W}(t)$ and $\mathbf{Z}(t)$, contrary to the previous algorithms where we had to keep also $\mathbf{W}_{PS}(t)$ and $\mathbf{Q}(t)$. In case of using multiple ($nb_{rot} > 1$) Givens rotation matrices, we need only to repeat steps 2 until 12 nb_{rot} times and use the output indices, $\mathbf{W}(t)$ and $\mathbf{Z}(t)$ of the previous rotation as inputs for the next one.

3.4 Theoretical analysis

The algorithms proposed in the previous sections are all based on the same two-step scheme, therefore, we will analyze the convergence behavior of each stage separately. In the first part, we are interested in the convergence of the FAPI algorithm to the principal subspace. In the second part, we will provide more details about the ℓ_1 minimization problem and its convergence.

3.4.1 Convergence analysis of FAPI algorithm

The FAPI algorithm is a simplified version of the QR power iteration algorithm which is related to the natural power method. In fact, the direct implementation of the natural power method is equivalent (up to a unitary rotation) to the QR power method. The global and exponential convergence property of the natural power method was shown in [19]. It has been also analyzed in [16] where the convergence analysis of PAST algorithm (that uses, like FAPI, a power iteration approach) is provided.

3.4.2 Convergence analysis of the ℓ_1 minimization

Let us assume that FAPI converged to \mathbf{U}_s , the orthogonal principal subspace which spans the same subspace as \mathbf{A}_0 the mixing matrix. The ℓ_1 minimization tends to recover the ground truth (original) mixing matrix \mathbf{A}_0 which is assumed to be sparse by finding the invertible matrix \mathbf{Q}_0 which rotates \mathbf{U}_s into $\mathbf{A}_0 = \mathbf{U}_s \mathbf{Q}_0$.

$$\arg \min_{\mathbf{Q}} \left\| \mathbf{U}_s \mathbf{Q} \right\|_1 \quad \text{s.t.} \quad \mathbf{Q} \in \mathcal{Q} \quad (3.41)$$

with $\mathcal{Q} = \left\{ \mathbf{Q} \text{ invertible and } \|\mathbf{q}_i\|_2 = 1 \quad i = 1, \dots, p \right\}$ and \mathbf{q}_i being the i -th column vector of \mathbf{Q} . It is important to study first the identifiability of the objective function, then the convergence property of the gradient scheme used in SS-FAPI.

Identifiability

The main idea here is to transform our problem to match the shape of a sparse dictionary learning problem or a matrix factorization problem in order to take advantage of their available theoretical identification studies. First, let $\mathbf{W} = \mathbf{U}_s \mathbf{Q}$, then we can write that $\mathbf{U}_s = \mathbf{W} \mathbf{Q}^{-1}$ (\mathbf{Q} is invertible). By taking the transpose we found $\mathbf{U}_s^T = \mathbf{Q}^{-T} \mathbf{W}^T$ and problem (3.41) can be seen as:

$$\arg \min_{\mathbf{Q}} \left\| \mathbf{W} \right\|_1 \quad \text{s.t.} \quad \mathbf{U}_s^T = \mathbf{Q}^{-T} \mathbf{W}^T, \quad \mathbf{Q} \in \mathcal{Q} \quad (3.42)$$

The previous problem has the same shape as the sparse dictionary learning problem where we seek the sparse representation \mathbf{W}^T and the dictionary \mathbf{Q}^{-T} by separating the observations \mathbf{U}_s^T into $\mathbf{U}_s^T = \mathbf{Q}^{-T} \mathbf{W}^T$. It can also be seen as a simplified matrix factorization problem given \mathbf{U}_s and the *a priori* sparsity information of \mathbf{W} . Recent works [94–101] have considered the characterization of \mathbf{A}_0 such that the local minima of (3.42) can only be found at around \mathbf{Q}_0 , which would guarantee that numerical optimization algorithms cannot be trapped in spurious local minima, and would converge independently of their initialization. This raises two new smaller issues: first, the uniqueness, i.e. which conditions guarantee that, when \mathbf{Q} is a local minimum of the cost function, it must match \mathbf{Q}_0 ? Second, the local identifiability, i.e. which conditions on \mathbf{A}_0 (and \mathbf{Q}_0) guarantee that \mathbf{Q}_0 is a local minimum of the cost function?

The uniqueness of such factorization has been studied for the first time in the context of dictionary learning for the ℓ_0 problem in [94] [95] with a combinatorial approach, then in [96] where they considered the case of complete dictionary. This is equivalent to the ℓ_0 version of (3.42) where the complete dictionary corresponds to the invertible matrix \mathbf{Q} . The authors in [96] consider the noiseless case and use the Bernoulli-Subgaussian model to characterize the sparsity defined by:

Definition 1 *The matrix \mathbf{A}_0 satisfies the Bernoulli-Gaussian model with parameter θ if $\mathbf{A}_0 = \mathbf{\Omega} \odot \mathbf{R}$, where $\mathbf{\Omega}$ is an iid Bernoulli matrix with parameter θ , and \mathbf{R} is an independent random matrix whose entries are i.i.d $\mathcal{N}(0, 1)$.*

The authors in [96, Theorem 3] provide a tighter lower bound on the number of samples required (dimension of the system in our case) compared to [94] [95] for a certain sparsity level of \mathbf{A}_0 that guarantees the uniqueness of the solution for the ℓ_0 factorization problem. In the same spirit of [96, Theorem 3], one can find a lower bound on the number of sensors d (dimension of the system) required to recover 'uniquely' the pair $(\mathbf{Q}_0, \mathbf{A}_0)$ for a certain number p of signals and sparsity level of \mathbf{A}_0 . First, we need to define the matrices $\mathbf{\Pi}$ and $\mathbf{\Delta}$, where $\mathbf{\Pi}$ is a permutation matrix, with a single non-zero element (which equals 1) in each row and column. The matrix $\mathbf{\Delta}$ is a diagonal sign matrix, with a diagonal entries equal to ± 1 .

Theorem 1 *Suppose that \mathbf{A}_0 follows the Bernoulli-Gaussian model with parameter θ . If $\frac{1}{p} \leq \theta \leq \frac{1}{C}$ and $d > Cp \log(p)$ for C large enough, then, with probability at least $1 - \exp(-c'd)$, any alternative factorization $\mathbf{U}_s^T = \mathbf{Q}^{-T} \mathbf{W}^T$ such that $\max_i \left(\|\mathbf{W} \mathbf{e}_i\|_0 \right) \leq \max_i \left(\|\mathbf{A}_0 \mathbf{e}_i\|_0 \right)$ can be decomposed as $\mathbf{W} = \mathbf{A}_0 \mathbf{\Pi} \mathbf{\Delta}$ and $\mathbf{Q} = \mathbf{Q}_0 \mathbf{\Pi} \mathbf{\Delta}$, for some permutation matrix $\mathbf{\Pi}$ and sign matrix $\mathbf{\Delta}$.*

where \mathbf{e}_i is the standard basis vector that is non-zero in coordinate i ($i = 1, \dots, p$) and C, c' are positive constants which depend on the sparsity parameter θ and the system dimensions (d, p) . For C large enough, (d large) the probability $1 - \exp(-c'd)$ tends to 1. The proof of theorem 1 is based on an obvious idea; since \mathbf{W} spans the same subspace as \mathbf{A}_0 , it can be seen as a linear combination of its columns. Or a linear combination of distinct sparse columns of \mathbf{A}_0 with disjoint sparsity patterns (different indices for the non-zero entries), can only deteriorate the sparsity of the result (increase the number of non-zero entries). A formal proof is established in [96, Appendix A] for the case of dictionary learning.

As a result for Theorem 1, while solving our problem, we focus on the local identifiability of the whole equivalence class defined by the transformations described above in Theorem 1. Extending the previous result to the ℓ_1 objective function is an open research problem and more results can be found in literature of dictionary learning such as [97] [98]. Having established the basis for uniqueness of the solution, we now turn to discuss the convergence.

Convergence

The local convergence was first discussed for the complete dictionary case in [99] where they developed necessary and sufficient algebraic conditions on a dictionary

coefficient pair (\mathbf{A}_0 and \mathbf{Q}_0) to constitute a local minimum of the ℓ_1 dictionary learning criterion. After that, most of works focused on the extension to the over-complete case [100] (which does not interest us because \mathbf{Q}_0 is square) and the robustness to noise and outliers [101].

One of the most recent results was introduced in [101] where the authors formulate the problem as LASSO minimization function to handle the noisy case in addition to outliers. They provide an asymptotic as well as precise finite-sample analysis of the local minima under certain mild assumptions. It was found that the resulting dictionary converges locally to the reference dictionary \mathbf{Q}_0 with a certain resolution r , (i.e. $\|\hat{\mathbf{Q}} - \mathbf{Q}_0\|_F \leq r$) which depends on the limited coherence³ of \mathbf{Q}_0 , limited number of non-zeros in \mathbf{A}_0 and small enough LASSO regularization parameter λ . More details can be found in [101, Theorem 1-2].

The gradient descent used in SS-FAPI is similar to the natural gradient step as we explain in the Appendix. Using the results discussed above on the uniqueness and the local convergence, we can conclude that under certain constraints the proposed gradient descent method will converge asymptotically to the local minima which is equivalent to \mathbf{Q}_0 up to a permutation and sign transformation. These constraints are over the system size ($d > Cp \log p$), the sparsity of the ground truth \mathbf{A}_0 and its coherence (same as coherence of \mathbf{Q}_0).

3.5 Simulation results

We present in this section some numerical simulations to assess the performance of the proposed algorithms. They are compared to FAPI [21] as subspace tracking algorithm without sparsity constraint and ℓ_1 -PAST as representative of the state-of-art of low-complexity sparse subspace tracking algorithms. Also, we compare SS-FAPI to the SPCA batch algorithms: GPower [48] and IMRP [49] and the adaptive algorithm Streaming-SPCA [55].

3.5.1 Performance factors

In order to measure the estimation error of the principal subspace, we adopt the following normalized quadratic error of reconstruction:

$$\rho(t) = \frac{1}{r} \sum_{i=1}^r \frac{\text{Tr}\left(\mathbf{W}_i^\#(t) \left(\mathbf{I}_n - \mathbf{W}_{ex} \mathbf{W}_{ex}^T\right) \mathbf{W}_i(t)\right)}{\text{Tr}\left(\mathbf{W}_i^\#(t) \mathbf{W}_{ex} \mathbf{W}_{ex}^T \mathbf{W}_i(t)\right)} \quad (3.43)$$

³The maximum absolute value of the cross-correlations between the normalized columns of \mathbf{Q} i.e. $\max_{i \neq j} |\mathbf{q}_i^T \mathbf{q}_j|$.

where r is the number of Monte Carlo runs, $\mathbf{W}_i(t)$ is the sparse weight matrix of the estimated subspace at sample i and iteration t . \mathbf{W}_{ex} is the exact orthogonal subspace computed from the exact mixing matrix \mathbf{A} (in synthetic data simulation) or extracted from the principal eigenvector subspace of the whole data set (in real data application).

As we explained in the previous section, though ℓ_0 is the most appropriate sparsity measure, all our algorithms are based on minimizing the ℓ_1 penalty function. Hence, the resulting matrix has probably a lot of non-zero small values, therefore, a thresholding step must be applied to present well the ℓ_0 sparsity of our solutions. By choosing a well adjusted threshold α , one can use the following ratio to express the ℓ_0 sparsity

$$S(\mathbf{W}(t))_\alpha = \frac{1}{dp} \left\| (|w_{ij}(t)| < \alpha) \right\|_0 \quad (3.44)$$

where $((w_{ij}(t) < \alpha))$ is the (i, j) -th entry of a $d \times p$ binary matrix equal to zero or otherwise one if the inequality is satisfied. $w_{ij}(t)$ refers here to the (i, j) -th element of the matrix $\mathbf{W}(t)$. This metric depends of the parameter α and the time iteration t which will yield 3-dimensional graphs to have a full vision of the function evolution. To have simpler results presentation, most of the plots in this section are in function of time iteration, so we choose as a sparsity measure the ℓ_1 -norm of the weight matrix with columns normalized to 1 which is a parameter free metric.

In order to measure the capability of the proposed methods to recover the ground truth mixing matrix, we define the recovery error Γ by:

$$\Gamma(\mathbf{A}^\# \mathbf{W}) = \frac{1}{p(p-1)} \sum_{i=1}^p \left(\sum_{j=1}^p \frac{(\mathbf{A}^\# \mathbf{W})_{ij}^2}{\max_j ((\mathbf{A}^\# \mathbf{W})_{ij}^2)} - 1 \right) \quad (3.45)$$

which is similar to the global rejection level proposed in [102] in the context of blind source separation.

3.5.2 Synthetic data

We consider tracking the principal subspace of rank p (number of sources) within a d dimensional system (number of sensors) with $d > p$. We use the data model $\mathbf{x}(t) = \mathbf{A}(t)\mathbf{s}(t) + \mathbf{n}(t)$ with $\mathbf{A} \in \mathbb{R}^{d \times p}$ a random sparse mixing matrix generated according to the Bernoulli-Gaussian model with parameter θ . The vector $\mathbf{s}(t)$ of source signals is generated according to a Gaussian distribution, with zero mean and unit variance, and $\mathbf{n}(t)$ is a white Gaussian noise with a variance σ^2 . We generate T snapshots $\mathbf{x}(t)$ for every Monte Carlo run with $r = 100$. In the following, the matrices $\mathbf{W}(0)$, $\mathbf{Z}(0)$, $\mathbf{W}_{PS}(0)$, $\mathbf{Z}_{PS}(0)$ and $\mathbf{Q}(0)$ are initialized by an identity

matrix. The signal to noise ratio SNR for our data model is defined by

$$SNR(dB) = 10 \log_{10} \frac{\mathbb{E} \left[\left\| \mathbf{A}(t) \mathbf{r}(t) \right\|_2^2 \right]}{\mathbb{E} \left[\left\| \mathbf{n}(t) \right\|_2^2 \right]} \quad (3.46)$$

In the first simulation, we consider the parameters: $d = 16$, $p = 9$, $\theta = 0.3$ i.e. 30% of the matrix \mathbf{A} entries are non-zero, SNR=15dB, $\beta = 0.99$ as forgetting factor, $\mu_{SS-FAPI} = 1$, $\mu_{SS-FAPI2} = 0.1$, $\mu_{OSS-FAPI} = 1$, $\kappa_{l_1-PAST} = 1$ and one rotation per iteration for SGSS-FAPI and GSS-FAPI. We study two cases: \mathbf{A} is non-orthogonal corresponding to the results shown in Fig. 3.1 and \mathbf{A} is orthogonal which the results are shown in Fig. 3.2. It is clear from the subspace performance in Fig. 3.1 and Fig. 3.2, that all the proposed algorithms have the same subspace error as FAPI [21] which is in agreement with our claim and they out-perform the ℓ_1 -PAST [56] algorithm. In terms of the ℓ_1 norm, in both cases, SS-FAPI, SS-FAPI2 and SGSS-FAPI reach lower error levels as compared to OSS-FAPI and GSS-fapi. Furthermore, they can reach ℓ_1 -norm limits smaller than the mean of ℓ_1 -norms of the matrices \mathbf{A} used in the simulation. The identity initialization explains the low sparsity level in the early iterations for all the algorithms. We provide also the ℓ_0 sparsity ratio $S(\mathbf{W}(t))_\alpha$ to confirm that the ℓ_1 -norm is sufficient to express the sparsity behavior which is demonstrated in Fig. 3.1 and Fig. 3.2 by an arbitrarily chosen threshold $\alpha = 0.05$. We provide also the recovery error of the ground truth matrix \mathbf{A} for the orthogonal and the non-orthogonal cases. We can notice that the proposed methods outperform the ℓ_1 -PAST [56] algorithm.

In order to show the capability of the proposed methods to recover the ground truth mixing matrix \mathbf{A} , we calculate the recovery error defined in (3.45) and then we decide with an ad-hoc threshold ($-20dB$) if \mathbf{A}_0 was well recovered or not. In each simulation, we consider the noiseless case and we change the system size (d, p) by fixing $p \in \{16, 20, 24, 28, 32\}$ and changing d between $0.5p \log(p) < d < 4p \log(p)$. For each pair (d, p) , 200 iterations are carried out with a sparsity parameter (Bernoulli parameter in the Bernoulli-Subgaussian model) $\theta = 0.3$. Figure 3.3 shows the phase diagram of SS-FAPI with \mathbf{A} being non-orthogonal on the left and OSS-FAPI with \mathbf{A} being orthogonal on the right. The simulation results confirm the theoretical study presented above and we see that above a certain number of sensors $d > Cp \log(p)$, the ground truth matrix \mathbf{A} is correctly recovered up to a sign and a permutation transformation.

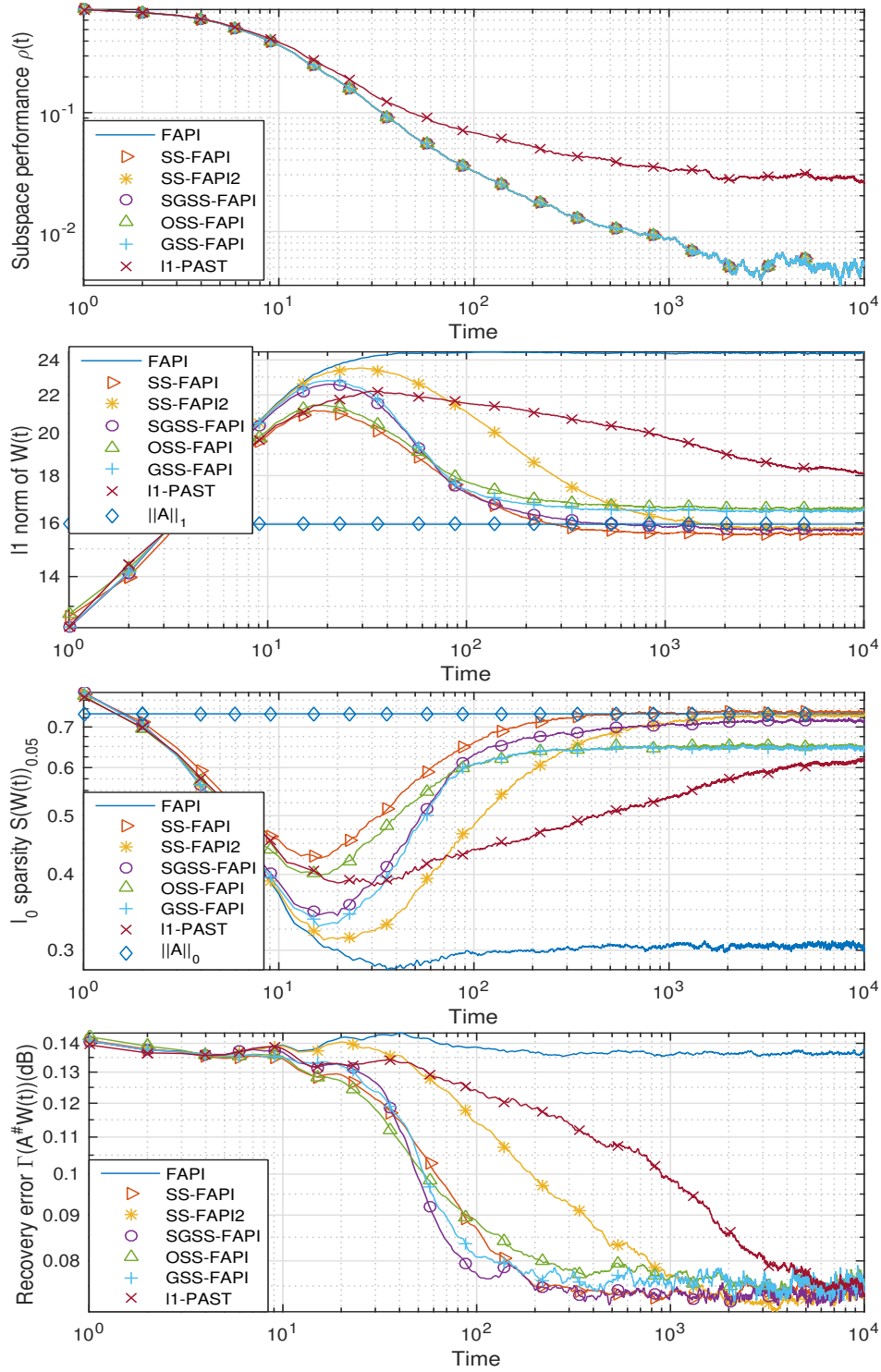


Figure 3.1: Subspace performance $\rho(t)$, norm l_1 of $\mathbf{W}(t)$, l_0 sparsity ratio $S(\mathbf{W}(t))_\alpha$ with $\alpha = 0.05$ and the recovery error $\Gamma(\mathbf{A}^\#\mathbf{W}(t))$ in terms of dB versus time with \mathbf{A} non-orthogonal and ($d = 16, p = 9, SNR = 15dB$)

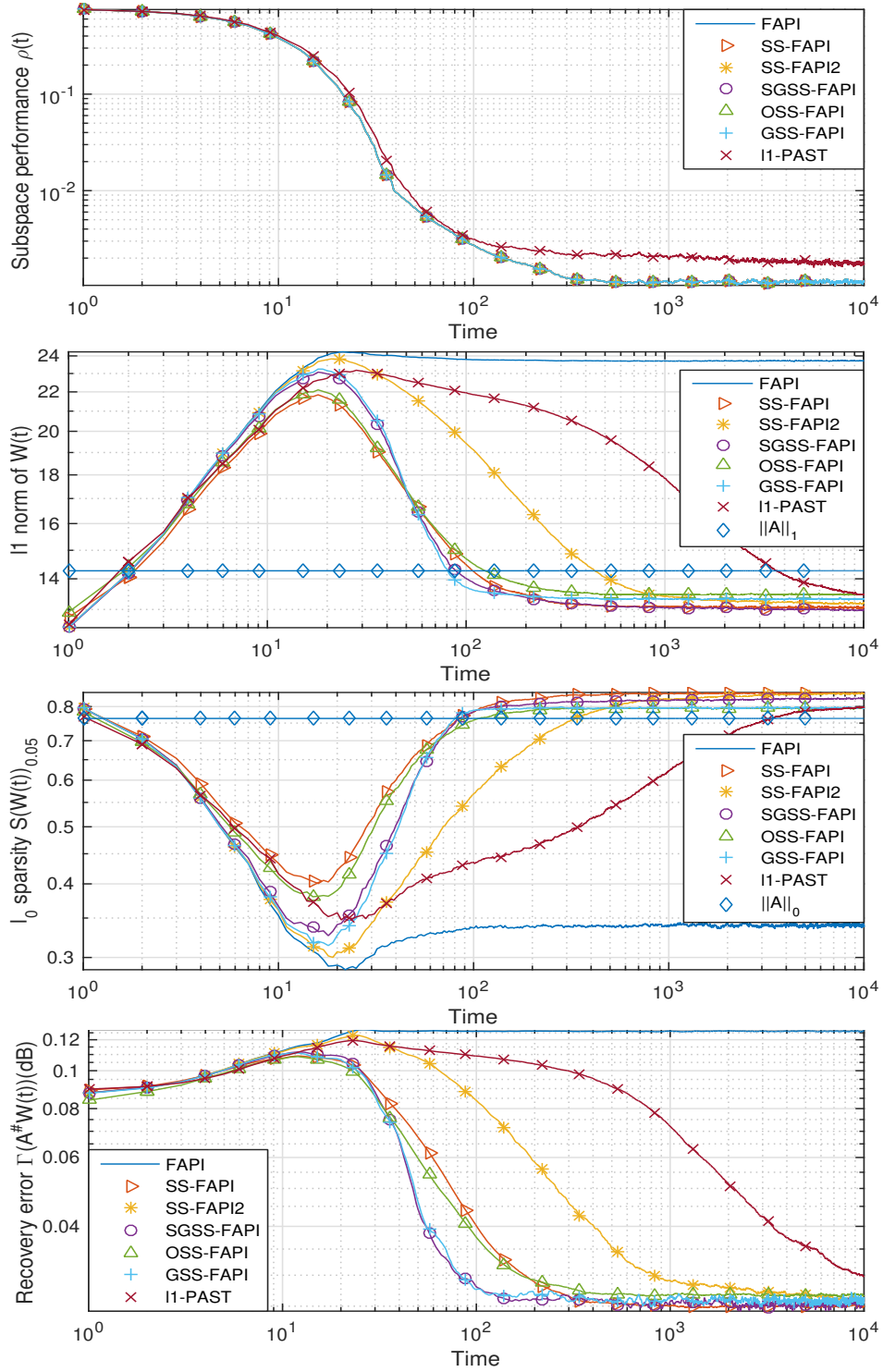


Figure 3.2: Subspace performance $\rho(t)$, norm ℓ_1 of $\mathbf{W}(t)$, ℓ_0 sparsity ratio $S(\mathbf{W}(t))_\alpha$ with $\alpha = 0.05$ and the recovery error $\Gamma(\mathbf{A}^\# \mathbf{W}(t))$ in terms of dB versus time with \mathbf{A} orthogonal and $(d = 16, p = 9, SNR = 15dB)$

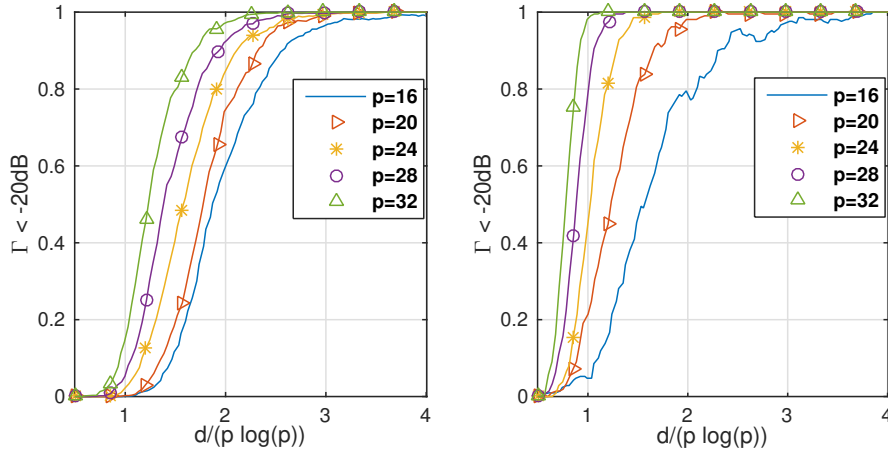


Figure 3.3: Phase diagram of: -left- SS-FAPI for non-orthogonal \mathbf{A}_0 -right- OSS-FAPI for orthogonal \mathbf{A}_0 , with sparsity parameter $\theta = 0.3$ and $p \in \{16, 20, 24, 28, 32\}$

The performances of the proposed algorithms SS-FAPI, SS-FAPI2 and OSS-FAPI depend heavily on the chosen optimization step μ . In Fig. 3.4, we investigate the influence of taking different step values $\mu \in \{0.01, 0.1, 1, 5, 10, 20, 0.1 \frac{\|\mathbf{B}\|_F^2}{\text{Tr}(\mathbf{B})}\}$ on SS-FAPI performance with $d = 16$, $p = 9$ and $SNR = 15dB$. Actually, small μ values yield to low convergence rates and large μ values would degrade the algorithm's performance due to the non-validity of the considered first order approximation. Also, increasing the value of μ can lead to losing the rank constraint of the solution, e.g. for $\mu = 20$ we obtained $\det(\mathbf{Q}) \approx 10^{-8}$ in the steady state regime. Thus, the choice of μ needs to achieve a good compromise between convergence speed and estimation accuracy while preserving the non-singularity of matrix \mathbf{Q} . The tuning parameter for SGSS-FAPI and GSS-FAPI is the number of rotations per iteration. In fact, the low complexity of searching the rotation optimal angle is what allows us to consider the choice of several rotations instead of one. To analyze the influence of taking multiple rotations, we run GSS-FAPI for the same simulation settings ($d = 16$, $p = 9$ and $SNR = 15dB$) with different numbers of rotations $\{1, 2, 5, 10, 15, 25\}$ knowing that a full search will require $\frac{p(p-1)}{2} = 36$ rotations.

We notice in Fig.3.5 that changing the number of rotations per iteration does not affect the limit of convergence, however, the convergence speed to that limit increases with the number of rotations. Hence, one can achieve a good compromise between the speed of convergence of GSS-FAPI and the computational cost thanks to an appropriate choice of the number of rotations.

In the next simulation, we analyze the influence of the SNR on the convergence limit of our algorithms by running the same simulation with $d = 16$, $p = 9$ for

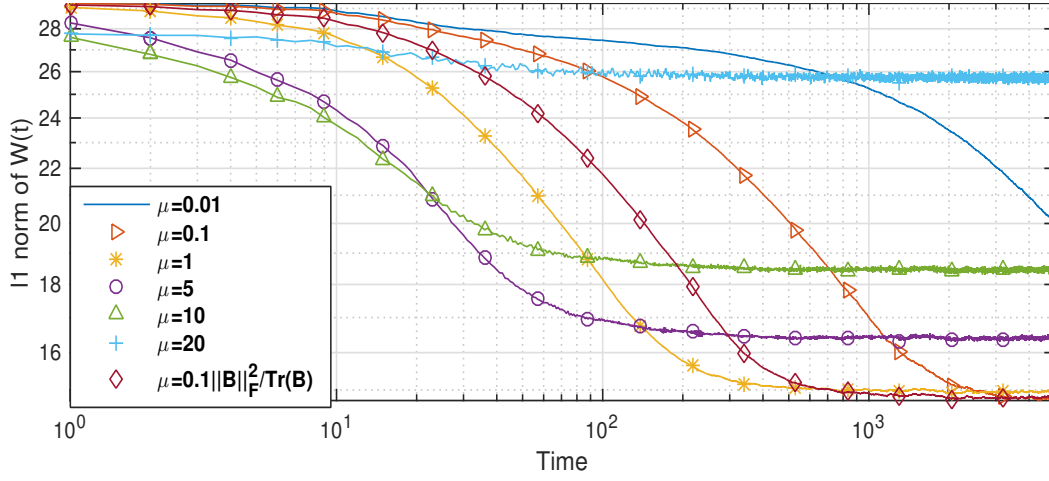


Figure 3.4: Norm ℓ_1 of $\mathbf{W}(t)$ versus time for $(d = 16, p = 9, SNR = 15dB)$ with different values μ for SS-FAPI

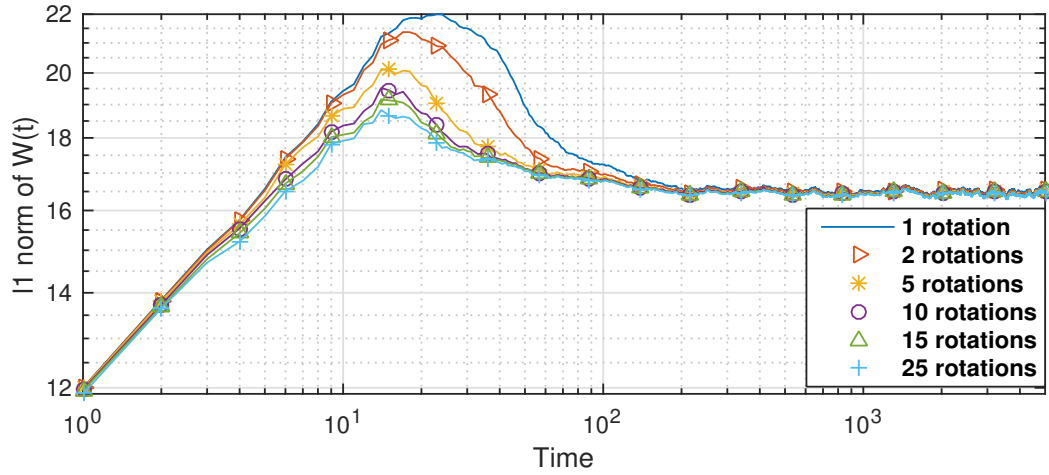


Figure 3.5: ℓ_1 -norm of $\mathbf{W}(t)$ versus time for $(d = 16, p = 9, SNR = 15dB)$ with different numbers of Givens rotations

$T = 3000$ iterations. Fig.3.6 shows the subspace performance and the ℓ_1 -norm of $\mathbf{W}(t)$ after T iterations versus the SNR for the different algorithms with the same parameters as in the first simulation ($\beta = 0.99$ forgetting factor, $\mu_{SS-FAPI} = 1$, $\mu_{SS-FAPI2} = 0.1$, $\mu_{OSS-FAPI} = 1$, $\kappa_{\ell_1-PAST} = 1$ and one rotation per iteration for SGSS-FAPI and GSS-FAPI). We notice that increasing the SNR will have better impact on our algorithms than on the ℓ_1 -PAST especially from the subspace performance point of view.

In order to correctly compare the different algorithms from the point of view of convergence speed, we adjust the parameters of every algorithm to reach the

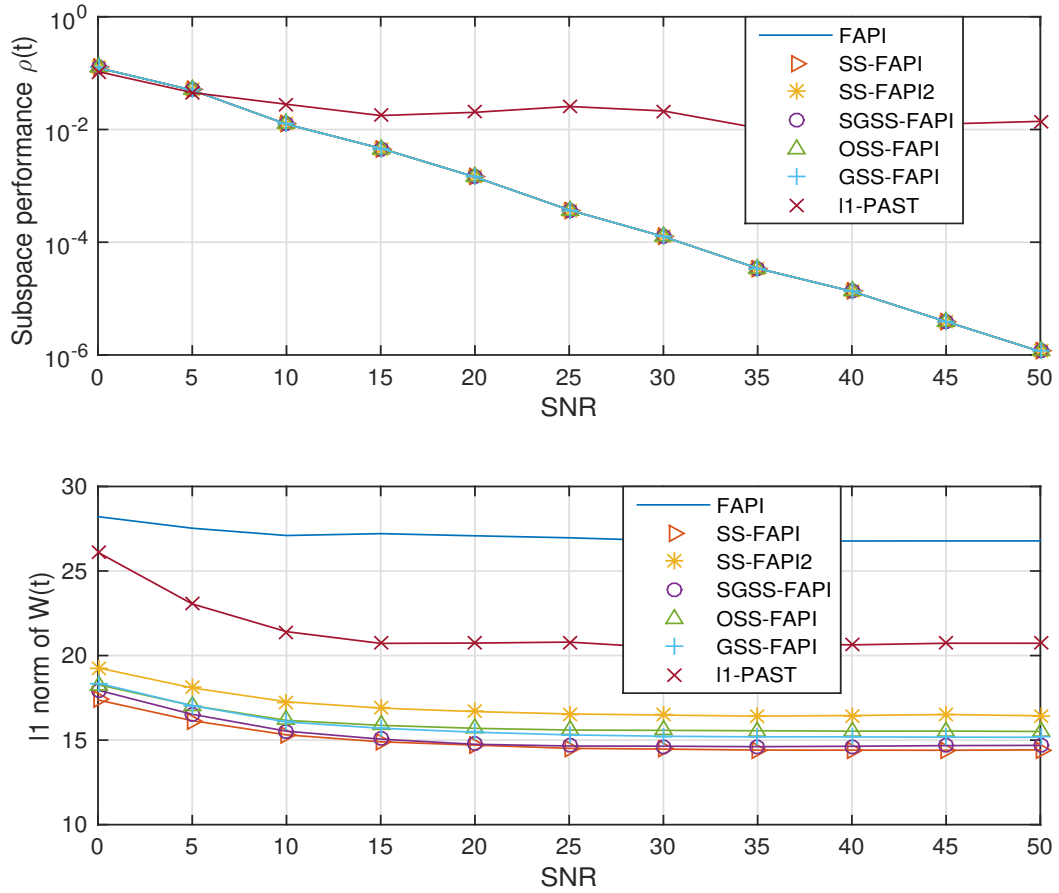


Figure 3.6: Subspace performance $\rho(t)$ and norm ℓ_1 of $\mathbf{W}(t)$ versus SNR for ($d = 16, p = 9, T = 3000$)

same limit of sparsity. Fig.3.7 presents the evolution of the norm ℓ_1 for the proposed algorithms with $\mu_{SS-FAPI} = 1.5$, $\mu_{SS-FAPI2} = 0.08$, $\mu_{OSS-FAPI} = 0.5$, $\kappa_{I1-PAST} = 1.2$ and one rotation then four per iteration for SGSS-FAPI and GSS-FAPI. One can notice that depending on the selected algorithm, we reach approximately the same convergence limit with different speeds. We can observe that: ℓ_1 -PAST and SS-FAPI2 are the slowest ones, SS-FAPI, SGSS-FAPI and GSS-FAPI with 4 rotations are the fastest ones and OSS-FAPI and GSS-FAPI with one rotation have approximately the same speed.

As we mentioned in the introduction, our algorithms can be compared to those proposed for SPCA problems. We use a system with $d = 16, p = 4$ and $SNR = 15dB$ to compare SS-FAPI ($\mu_{SS-FAPI} = 1$) with:

- The Gpower [48] algorithm by using as entry of every iteration all the data that have been already received and a sparsity parameter $\gamma = 0.15$.
- The IMRP [49] algorithm by using as entry a covariance matrix calculated from

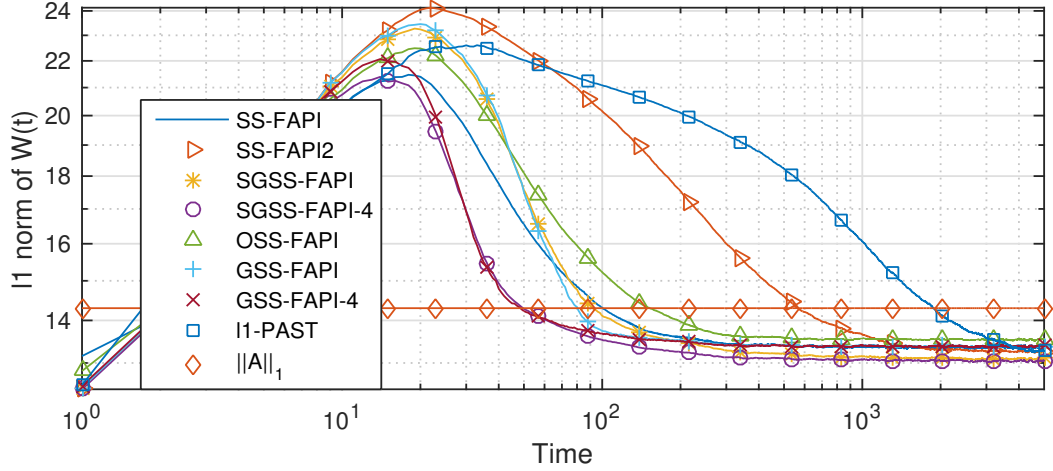


Figure 3.7: Norm ℓ_1 of $\mathbf{W}(t)$ versus time for $(d = 16, p = 9, SNR = 15dB)$ with same convergence limit

all the data that have been received with algorithm parameters $(\rho = 0.08, p = 0.5)$ and $\varepsilon = 0.001$).

- The Streaming-SPCA algorithm by using a sliding rectangular data window of length 500 and fixing the number of the truncated rows to 9 from $d = 16$.

In order to show the tracking capability of our adaptive approach over the SPCA algorithms, we change the used mixing matrix $\mathbf{A}(t)$ after $t = 800$. Unlike the batch algorithms (Gpower and IMRP), one can observe in Fig.3.8 that Streaming-SPCA keeps tracking the principal subspace after changing the mixing matrix. However, the row sparsity structure considered is not always satisfied (not in our simulation anyway), which explains the failure of reaching low ℓ_1 norm levels. Even if comparing batch algorithms performances to those of SS-FAPI is not really proper due to their high computational cost, this will help us to have an idea about the limits of our method and how far our algorithms are from ‘optimality’. Fig.3.8 shows that SS-FAPI needs only 100 iterations to outperform the subspace estimation and obviously the tracking capability of Gpower and IMRP with the same sparsity levels.

Until now, we have used only FAPI [20] as subspace tracker for the proposed algorithms. As we mentioned earlier, in SS-FAPI, the second step which consists in minimizing the ℓ_1 norm, is the costliest in term of computational complexity and costs $\mathcal{O}(dp^2)$. As long as we keep the global complexity $\mathcal{O}(dp^2)$, one can propose to switch FAPI [20] which has complexity of order $\mathcal{O}(dp)$, by a more efficient subspace tracker of higher complexity of order $\mathcal{O}(dp^2)$. By choosing LORAF2 [18] as new subspace tracker, we get alternative solutions to SS-FAPI, SGSS-FAPI, OSS-FAPI and GSS-FAPI called respectively SS-LORAF, SGSS-LORAF, OSS-LORAF and

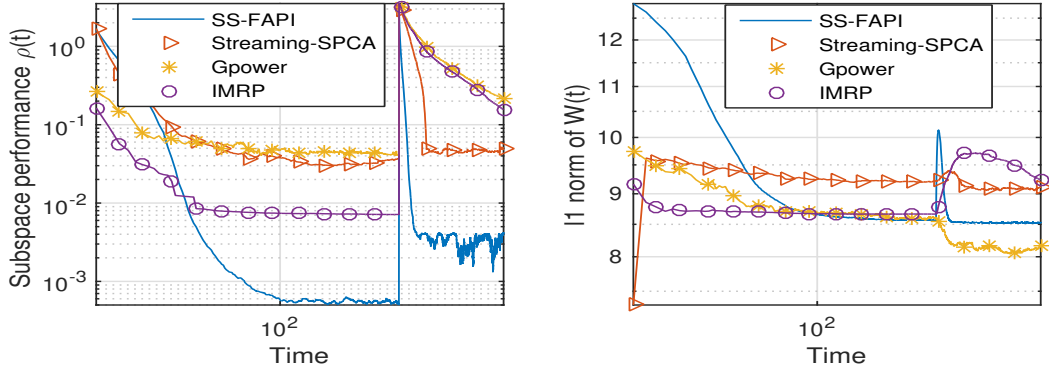


Figure 3.8: Subspace performance $\rho(t)$ and norm l_1 of $\mathbf{W}(t)$ versus time for ($d = 16, p = 9, SNR = 15dB$) of SS-FAPI compared to SPCA algorithms

GSS-LORAF. Indeed we can observe in Fig.3.9, that LORAF-like algorithms have better subspace performances as we expected. However, the sparsity performance of the LORAF-like algorithms is poor as compared to FAPI-based algorithms. Indeed, the natural gradient approach used for enhancing the sparsity in the second step, is poorly adapted to the rapid changes of $\mathbf{W}_{PS}(t)$ noticed in the LORAF-like algorithms.

3.5.3 Real data

In order to confront our algorithms with a real situation, we consider now an application related to the text data. By doing sparse principal subspace tracking on these text data, we aim to find a p interpretable principal components (classes) which will be the words that best represent the text dataset and can be used to summarize, classify and explore the large corpora. Also, the dataset we choose is large and it will keep being enriched over time, which makes it a good application for our adaptive algorithms. We use the NIPS conference papers 1987-2015 dataset [103] publicly available from the UCI Machine Learning Repository. This large dataset records word occurrences in the form of bags-of-words⁴. It contains the distribution of words in the full text of the NIPS conference papers published from 1987 to 2015. The dataset is in the form of a 11463×5812 matrix of word counts, containing 11463 words and 5811 NIPS conference papers (keeping only words occurring more than 50 times). The number of classes p depends on the targeted data, in our case it can represent the number of most interesting research topics that the NIPS conference papers discuss (we choose for the simulation $p = 10$). We compare the performance

⁴The bag-of-words model is a simplifying representation used in natural language processing. In this model, a text (such as a sentence or a document) is described by the occurrence of words within a document disregarding grammar and even word order but keeping only multiplicity.

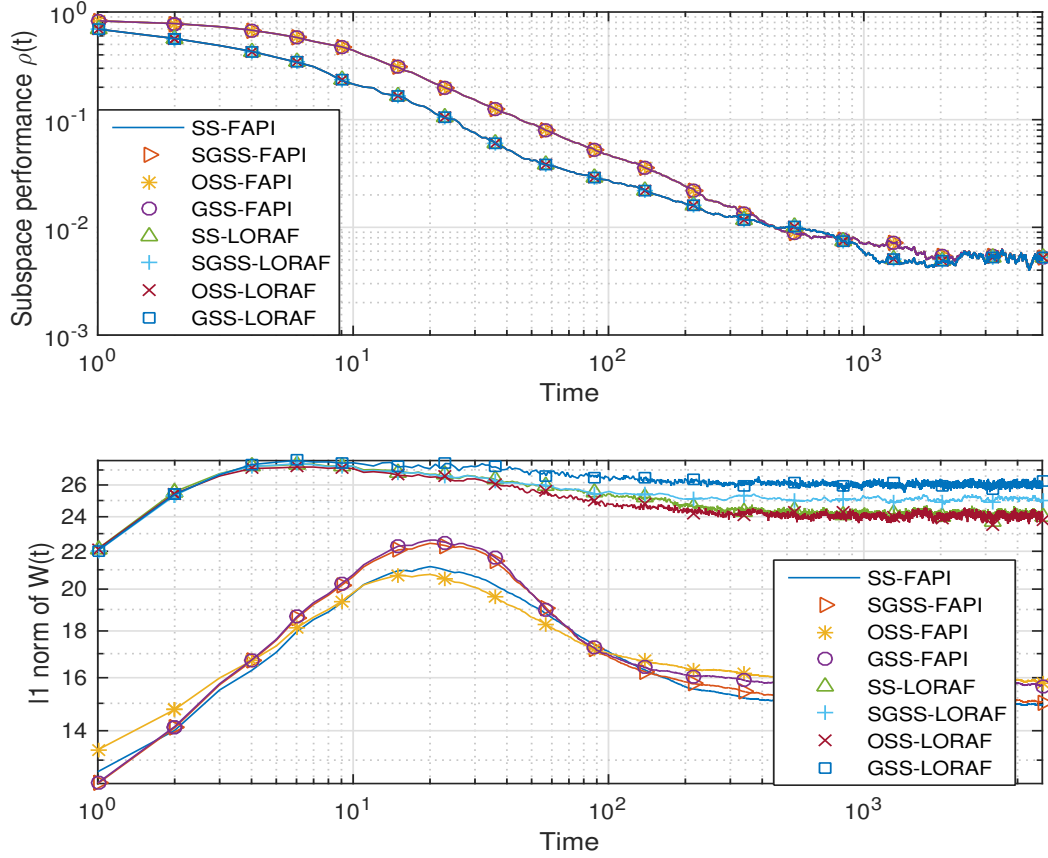


Figure 3.9: Subspace performance $\rho(t)$ and norm ℓ_1 of $\mathbf{W}(t)$ versus time for ($d = 16, p = 9, SNR = 15dB$) of FAPI algorithms vs LORAF algorithms

of ℓ_1 -PAST as state of art to SS-FAPI, OSS-FAPI and GSS-FAPI. Fig. 3.10 shows us that even in that case where we have more variables $d = 11463$ (number of words) than samples $T = 5812$ (number of articles) our algorithms keep tracking the subspace and reach lower ℓ_1 -norm than ℓ_1 -PAST, resulting in a sparser and more interpretable solution. We can also note that OSS-FAPI and GSS-FAPI have approximately the same results while SS-FAPI has the best sparsity over all.

3.6 Discussion

In this section, we provide comments on the behavior of every proposed algorithm and in which context should we use it. Let us start by evaluating the subspace and the sparsity performances of the proposed algorithms compared to the existing algorithms in the literature.

The proposed algorithms (SS-FAPI, SS-FAPI2, SGSS-FAPI, OSS-FAPI and GSS-

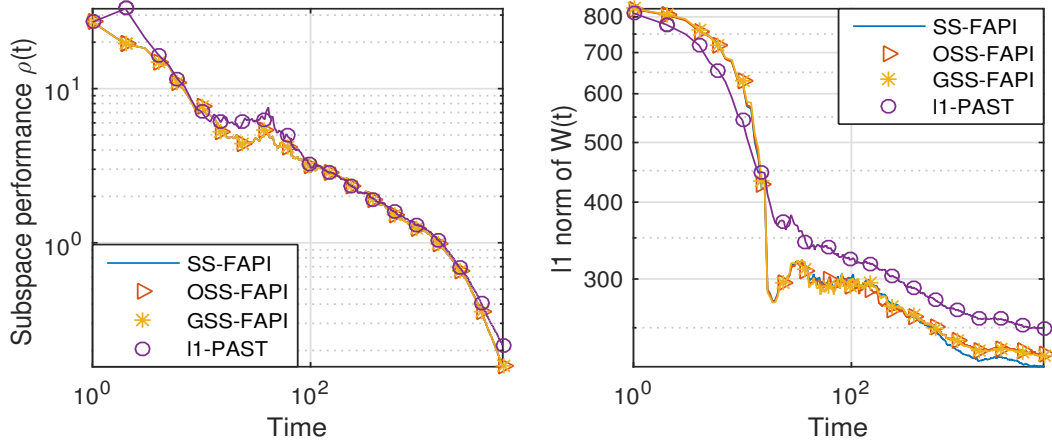


Figure 3.10: Subspace performance $\rho(t)$ and norm ℓ_1 of $\mathbf{W}(t)$ versus time for the NIPS dataset

FAPI) have improved the subspace tracking capability and achieve better sparsity performance than the algorithm ℓ_1 -PAST. Also, the computational complexity of ℓ_1 -PAST [56] is comparable to the complexity of SS-FAPI and OSS-FAPI, however, it is higher than that of SS-FAPI2, SGSS-FAPI and GSS-FAPI. Table A.1 summarizes the computational complexity per iteration of each algorithm when considering the exponential window. Finding the angles θ in GSS-FAPI and (θ, ϕ) (alternatively) in SGSS-FAPI have a complexity of $4\alpha d$ and $8\alpha d$ respectively. The scalar α is the number of the iterations needed to reach the targeted precision. For instance, using the golden section method we need about $\alpha = 15$ iterations to reach a precision of 10^{-4} . The joint optimization proposed in SGDS-FAPI is more complicated and needs more function evaluations to converge compared to the iterative case.

Algorithm	Computational complexity per iteration
FAPI	$3dp + \mathcal{O}(p^2)$
ℓ_1 -PAST	$3dp^2 + 3dp + \mathcal{O}(p^2)$
SS-FAPI	$2dp^2 + 4dp + \mathcal{O}(p^2)$
SS-FAPI2	$4dp + \mathcal{O}(p^2)$
SGSS-FAPI	$4dp + 8\alpha d + \mathcal{O}(p^2)$
OSS-FAPI	$2dp^2 + 3dp + \mathcal{O}(p^3)$
GSS-FAPI	$4dp + 4\alpha d + \mathcal{O}(p^2)$

Table 3.1: Summary of the computational complexity per iteration of sparse subspace tracking algorithms

In terms of ground truth recovery, above a certain number of sensors $d >$

$Cp \log(p)$, our algorithms recover correctly the ground truth matrix up to a sign and a permutation transformation. The constant C depends on the system dimensions and the sparsity of the ground truth matrix [96].

The subspace performance of Streaming-SPCA depends essentially on the length of the sliding window, so it can be better than the FAPI [21] algorithm if we take a larger window. However, this will deteriorate the tracking capabilities to rapid changes and increases significantly the computational cost and the complexity will be comparable to a batch algorithm. The poor sparsity performance of Streaming-SPCA [55] can be explained by the row sparsity constraint which is a more restrictive structural form of sparsity than the full sparsity that we are seeking by the proposed algorithms.

Even with its high computational complexity, the batch algorithm Gpower [48] does not achieve a subspace estimation comparable to the one we are getting with the proposed algorithms (with the same sparsity limits). This can be explained by the iterative deflation method followed in Gpower [48] to extend the case of one principal component to multiple components (principal subspace).

The IMRP [49] algorithm has the closest performance compared to the proposed algorithms. Indeed, this batch algorithm, based on SVD decomposition (solution to Rectangular Procrustes), has a subspace error close to the one given by an eigenvalue decomposition solution without any sparsity which is the best estimation that we can reach. Additionally, IMRP [49] is one of the most efficient and latest proposed batch algorithms for the sparse principal subspace problem. Nevertheless, our algorithms have the advantages of the low computational cost and the tracking capability.

We have decided to omit the comparison with the OIST [54] algorithm which was proposed to track only the first principal component and not all the subspace which is our objective. We could use the iterative deflation method to use OIST [54] on all the subspace column by column, but this generally leads to poor subspace estimation.

So far, we have positioned the performance of the proposed algorithms regarding the state of the art methods. Now, we focus on our algorithms and the advantages of using every one of them. Let us start by recalling that the subspace estimation error of the proposed algorithms is the same as the error of the FAPI [21] algorithm which is one of the best subspace trackers with a linear $\mathcal{O}(dp)$ computational complexity. Hence, the comparison criteria are the sparsity performance (speed and limit of convergence), the computational complexity and the orthogonality of the solution.

First, if we seek the sparsest solution in a fast time-varying context without taking into account the orthogonality constraint, we should use SS-FAPI which has a complexity of $\mathcal{O}(dp^2)$. The SS-FAPI2 is a less computational greedy solu-

tion $\mathcal{O}(dp)$ than SS-FAPI and can reach the same sparsity levels but with slower convergence speed (it would be a more appropriate choice for slowly time-varying subspace situations). The SGSS-FAPI has both a linear computational complexity of order $\mathcal{O}(dp)$ and a faster tracking capability compared to SS-FAPI2 which can be more enhanced by considering more than one Shear-Givens rotation per iteration despite the increase of the computational cost. As we mentioned earlier, the speed of convergence depends essentially on the system dimensions and the choice of the optimization step that we consider. Note that if we take $\mu = 0$, we get the same result as FAPI [21] without sparsity, and if μ is too large we get a better sparsity but we can either contradict the assumptions used for the first order expansion or lose the constraint on the solution rank (i.e. $\text{rank}(\mathbf{W}) = p$) since the weight matrix becomes close to singular when we run the algorithm for a long period.

Secondly, if we are dealing with applications requiring an orthogonality constraint, we have the choice between the two proposed algorithms: OSS-FAPI or GSS-FAPI. The first one is an extended version of SS-FAPI where we have a trade-off between the low ℓ_1 norm levels and the orthogonality of the solution. The GSS-FAPI algorithm reaches the same levels of ℓ_1 norm as OSS-FAPI with linear computational complexity of order $\mathcal{O}(dp)$. However, The OSS-FAPI algorithm has a better convergence speed than GSS-FAPI especially when the dimension of the system grows. A particularity of GSS-FAPI is the ability to enhance the rate of convergence without changing the final limit by increasing the number of Givens rotations used per iteration. We recall that this increment in the number of rotations will negatively affect the computational cost. It is also worth mentioning that as long as we are using a numerical solution in GSS-FAPI to solve (3.34), one can use other sparsity penalty functions, such as the reweighed ℓ_1 minimization [35] or the approximation of ℓ_0 used in [49].

The algorithms we presented here can be easily modified to fit with other adaptive subspace algorithms such as PAST [16], OPAST [17] or LORAF2 [18]. As we showed in Fig. 3.9, the LORAF-like algorithms have better subspace performances as compared to FAPI-based algorithms, however, their sparsity performance are poor. The failure of SS-LORAF, SGSS-LORAF, OSS-LORAF and GSS-LORAF to reach low sparsity levels can be explained by the rapid variation in the output of the LORAF algorithm. Indeed, the choice of the FAPI [21] algorithm was not only based on its good subspace performance, but also on the slow variation property of the solution. This last one is fundamental to the proper functioning of our algorithms because of the natural gradient used in the second stage (in general, the gradient type algorithms are poorly adapted to rapid changes).

One of the important things to observe in the simulation results is the ability of

reaching lower sparsity levels with the solutions which does not respect the orthogonality constraint compared to the ones which respect it. Indeed, if the target matrix is sparse but not orthogonal, the latter constraint would decrease the sparsity level of the estimated weight matrix.

3.7 Conclusion

In this chapter, tracking principal subspace algorithms under sparsity constraint of the weight matrix has been studied. Compared to other methods proposed in the literature, our algorithms have the advantage of low computational cost and improved performances in terms of subspace estimation accuracy and the sparsity of the results. They allow us to recover the original sparse mixing matrix under some mild constraints. Finally, the diversity of the proposed methods makes them adaptable to many applications depending on the problem's imposed constraints such as the computational complexity and the weight matrix orthogonality.

Aside from the sparsity constraint on the weight matrix, the sparsity constraint can be also on the source signals in the same data model. In the next chapter, we will consider the problem of blind source separation using the sparsity of the source signals as a contrast function.

Blind sparse source separation

Contents

4.1	Introduction	73
4.2	Data Sparsity algorithm based on OPAST for adaptive blind source separation DS-OPAST	74
4.3	Data Sparsity algorithm based on FAPI and Shear-Givens rotations for adaptive blind source separation SGDS-FAPI	77
4.4	Simulation results	82
4.5	Conclusion	87

4.1 Introduction

Separation of sources consists of recovering a set of signals when only their mixture is observed. Different models can be considered for source separation depending on the nature of the mixture which can be linear or non-linear. In the linear case, we can distinguish the convolutive mixtures and the instantaneous mixtures which will be considered in this chapter. In many situations, no *a priori* information on the mixing matrix is available: the linear mixture should be 'blindly' processed. In Blind Source Separation (BSS), we have to exploit only the information carried by the received signals and prior information about the statistics or the nature of transmitted source signals (e.g. decorrelation, independence, sparsity, morphological diversity, etc.) [57]. Recently, sparsity has emerged as a novel and effective source of diversity for BSS [68, 70, 79]. Although the sparse source separation can be particularly useful for separating under-determined mixtures (more sources than sensors), it is also potentially interesting for the noisy over-determined mixture (more sensors than sources) in which case sparsity is exploited to improve the source separation quality [57].

In this chapter, we address the problem of adaptive blind sparse source separation in the noisy over-determined case. We introduce two algorithms based on the same two-step approach used for tracking sparse principal subspace previously.

The first algorithm is DS-OPAST (DS stands for Data Sparsity) based on a natural gradient scheme, whereas the second algorithm is SGDS-FAPI based on the Shear and Givens rotations. Numerical simulations are presented where we show that the proposed algorithms outperform existing solutions in both convergence speed and estimation quality.

We recall that we are using the data model presented in section 2.3 and we assume from now on that all the vectors and matrices have real values for the simplicity of the equations. In case of complex values problem, we can either extend the derived equation or simply transfer it to its real equivalent form using the following equation:

$$\begin{pmatrix} \mathcal{R}(\mathbf{x}(t)) \\ \mathcal{I}(\mathbf{x}(t)) \end{pmatrix} = \begin{pmatrix} \mathcal{R}(\mathbf{A}) & -\mathcal{I}(\mathbf{A}) \\ \mathcal{I}(\mathbf{A}) & \mathcal{R}(\mathbf{A}) \end{pmatrix} \begin{pmatrix} \mathcal{R}(\mathbf{s}(t)) \\ \mathcal{I}(\mathbf{s}(t)) \end{pmatrix} \quad (4.1)$$

where $\mathcal{R}(\cdot)$ and $\mathcal{I}(\cdot)$ represent the real and the imaginary operators for complex values. The latter can be combined with the structure preserving technique shown in [104]. In order to consider the separation in an adaptive context, we assume also a time-varying mixing matrix \mathbf{A} (we omit the time index (t) to reduce the amount of notation).

Solving the blind source separation problem adaptively means to update the estimation of the $p \times d$ separation matrix $\mathbf{B}(t)$ (or equivalently, identifying \mathbf{A} and use its pseudo-inverse $\mathbf{A}^\#$) after receiving each observation vector $\mathbf{x}(t)$ such that $\hat{\mathbf{s}}(t) = \mathbf{B}\mathbf{x}(t)$ is an estimation of the source signals.

4.2 Data Sparsity algorithm based on OPAST for adaptive blind source separation DS-OPAST

The First proposed algorithm to solve the adaptive blind source separation problem is the DS-OPAST where we write the separation matrix $\mathbf{B}(t)$ on the form of $\mathbf{B}(t) = \mathbf{Q}^T(t)\mathbf{W}_{PS}^T(t)$. It is based on a two-step approach corresponding to:

1. An adaptive extraction of an orthonormal basis of the principal subspace $\mathbf{W}_{PS}(t)$ of the instantaneous covariance matrix $\mathbf{C}_x(t)$.
2. Estimation the non-singular matrix $\mathbf{Q}(t)$ and the separation matrix $\mathbf{B}(t)$ using the sources sparsity information.

In the first step, the objective function to minimize is the one given by Eq. (2.4) under the orthogonality constraint of the weight matrix $\mathbf{W}(t)^T\mathbf{W}(t) = \mathbf{I}_p$ in the exponential window case (equivalent formulation can also be expressed in case of truncated window). The resulting weight matrix from this first step is denoted $\mathbf{W}_{PS}(t)$.

The optimization task can be done with different principal subspace trackers. The first version of the proposed solution was based on OPAST [17]. Nevertheless, one can replace OPAST by other subspace trackers that have better tracking capabilities with the same computational complexity such as FAPI [21] but should have the slow variation property of the solution because of the natural gradient used in the second stage (in general, the gradient type algorithms are poorly adapted to rapid changes).

In the second step, we search for $\mathbf{B}(t) = \mathbf{W}^T(t)$, the desired separation matrix which extracts the sparse source signals in the form $\mathbf{W}(t) = \mathbf{W}_{PS}(t)\mathbf{Q}(t)$ where the non-singular matrix $\mathbf{Q}(t) \in \mathbb{R}^{p \times p}$ is introduced in order to optimize the sparsity criterion of the source signals which is represented by the cost function:

$$\begin{aligned} J_{DS}(\mathbf{Q}(t)) &= \left\| (\mathbf{W}_{PS}(t)\mathbf{Q}(t))^T \mathbf{X}(t) \right\|_1 \\ &= \left\| \mathbf{Q}^T(t) \mathbf{W}_{PS}^T(t) \mathbf{X}(t) \right\|_1 \\ \text{s.t. } \mathbf{Q}(t) &\text{ is non-singular with unit norm columns} \end{aligned} \quad (4.2)$$

where $\mathbf{X}(t) = [\beta^{L-1}\mathbf{x}(t-L+1), \beta^{L-2}\mathbf{x}(t-L+2), \dots, \mathbf{x}(t)]$ is the windowed data matrix (exponential when $L = t$ and truncated when $L < t$).

The ℓ_1 -norm is used instead of the pseudo ℓ_0 -norm because of the convexity (ℓ_1 is the tightest convex relaxation of the ℓ_0 pseudo-norm [89]) and the easier optimization task compared to the ℓ_0 -based version. The unit-norm column constraint of $\mathbf{Q}(t)$ is necessary here for the uniqueness of the ℓ_1 minimization solution.

Using a natural gradient approach [90] similar to the one used in the previous section, we search for the updated matrix $\mathbf{Q}(t)$ in the form $\mathbf{Q}(t) = \mathbf{Q}(t-1)(\mathbf{I}_p + \boldsymbol{\varepsilon})$ where $\boldsymbol{\varepsilon} \in \mathbb{R}^{p \times p}$ is a matrix which has small valued entries (depending on the gradient step) that can be computed using a first order approximation according to:

$$\hat{\boldsymbol{\varepsilon}} = \arg \min_{\boldsymbol{\varepsilon}} \left\| \mathbf{Q}^T(t) \mathbf{W}_{PS}^T(t) \mathbf{X}(t) \right\|_1 \quad (4.3)$$

$$= \arg \min_{\boldsymbol{\varepsilon}} \left\| (\mathbf{I}_p + \boldsymbol{\varepsilon})^T \mathbf{Q}^T(t-1) \mathbf{W}_{PS}^T(t) \mathbf{X}(t) \right\|_1 \quad (4.4)$$

$$= \arg \min_{\boldsymbol{\varepsilon}} \left\| \boldsymbol{\varepsilon}^T \mathbf{Y}(t) + \mathbf{Y}(t) \right\|_1 \quad (4.5)$$

with $\mathbf{Y}(t) = \mathbf{Q}^T(t-1) \mathbf{W}_{PS}^T(t) \mathbf{X}(t)$. Using the same development and approximation as in Eq. (3.6) and Eq. (3.7), we get:

$$\hat{\boldsymbol{\varepsilon}} = \arg \min_{\boldsymbol{\varepsilon}} \sum_{i=1}^p \sum_{j=t-L+1}^t |\mathbf{Y}(t)_{ij}| + \sum_{i=1}^p \sum_{k=1}^p \varepsilon_{ki} \left(\mathbf{Y}(t) \text{sign}(\mathbf{Y}^T(t)) \right)_{ki} \quad (4.6)$$

$$= \arg \min_{\boldsymbol{\varepsilon}} \left\| \mathbf{Y}(t) \right\|_1 + Tr(\boldsymbol{\varepsilon} \mathbf{R}^T(t)) \quad (4.7)$$

Algorithm 10 Data Sparsity algorithm based on OPAST for adaptive blind source separation DS-OPAST

Require: $\mathbf{x}(t)$ data vector, β the forgetting factor, $\mathbf{W}_{PS}(t-1)$, $\mathbf{Z}_{PS}(t-1)$, $\mathbf{Q}(t-1)$ and $\mathbf{R}(t-1)$ from the previous iteration.

Ensure: $\mathbf{W}_{PS}(t)$, $\mathbf{Z}_{PS}(t)$, $\mathbf{Q}(t)$, $\mathbf{R}(t)$ and $\mathbf{W}(t)$

- 1: Find $\mathbf{W}_{PS}(t)$ using OPAST
 - 2: $\mathbf{y}(t) = \mathbf{Q}^T(t-1)\mathbf{W}_{PS}^T(t)\mathbf{x}(t)$
 - 3: $\mathbf{R}(t) = \beta\mathbf{R}(t-1) + \mathbf{y}(t)\text{sign}(\mathbf{y}^T(t))$ then $\mathbf{R}(t) = \frac{\mathbf{R}(t)}{\|\mathbf{R}(t)\|_F}$
 - 4: $\mathbf{Q}(t) = \mathbf{Q}(t-1)\left(\mathbf{I}_p - \mu\mathbf{R}(t)\right)$
 - 5: Columns normalization of $\mathbf{Q}(t)$
 - 6: $\mathbf{W}(t) = \mathbf{W}_{PS}(t)\mathbf{Q}(t)$.
-

where $\mathbf{R}(t) = \mathbf{Y}(t)\text{sign}(\mathbf{Y}^T(t))$. By applying a simple gradient on Eq. (4.7), we can take $\hat{\boldsymbol{\varepsilon}} = -\mu\frac{\mathbf{R}(t)}{\|\mathbf{R}(t)\|_F^2}$ with $\mu > 0$ to ensure a local decrease of the cost function. On the other hand, the value of μ should be small enough for the linear approximation to hold and to preserve the non-singularity of matrix $\mathbf{Q}(t)$. However, since the dimension of $\mathbf{Y}(t)$ grows linearly with time, a direct computation of matrix $\mathbf{R}(t)$ would be prohibitive. To reduce the cost, we use the projection approximation as shown below:

$$\begin{aligned} \mathbf{R}(t) &= \mathbf{Q}^T(t-1)\mathbf{W}_{PS}^T(t)\left[\beta\mathbf{X}(t-1), \mathbf{x}(t)\right] \\ &\quad \times \text{sign}\left(\left[\beta\mathbf{X}(t-1), \mathbf{x}(t)\right]^T\mathbf{W}_{PS}(t)\mathbf{Q}(t-1)\right) \end{aligned} \quad (4.8)$$

$$\begin{aligned} &= \beta\mathbf{Q}^T(t-1)\mathbf{W}_{PS}^T(t)\mathbf{X}(t-1)\text{sign}\left(\beta\mathbf{X}^T(t-1)\mathbf{W}_{PS}(t)\mathbf{Q}(t-1)\right) \\ &\quad + \mathbf{Q}^T(t-1)\mathbf{W}_{PS}^T(t)\mathbf{x}(t)\text{sign}\left(\mathbf{x}^T(t)\mathbf{W}_{PS}(t)\mathbf{Q}(t-1)\right) \end{aligned} \quad (4.9)$$

Under the assumption

$$\mathbf{W}_{PS}(t)\mathbf{Q}(t-1) \approx \mathbf{W}_{PS}(t-1)\mathbf{Q}(t-2) \quad (4.10)$$

we can write that

$$\mathbf{R}(t) \approx \beta\mathbf{R}(t-1) + \mathbf{y}(t)\text{sign}(\mathbf{y}^T(t)) \quad (4.11)$$

with $\mathbf{y}(t) = \mathbf{Q}^T(t-1)\mathbf{W}_{PS}^T(t)\mathbf{x}(t)$. The full algorithm is summarized in Algorithm 10.

Note that the computational cost of DS-OPAST is of order $\mathcal{O}(dp)$ per iteration without step 5. Now, if the update of the weight matrix $\mathbf{W}(t) = \mathbf{W}_{PS}(t)\mathbf{Q}(t)$ is needed, the latter cost would be of order $\mathcal{O}(dp^2)$ due to the previous matrix product. However, by using the updating equations in steps 3 and 4 of Algorithm 10 together

with the projection approximation used earlier in Eq. (4.10) (which is valid with small choice of gradient step μ), one can avoid the matrix - matrix product and preserve the linear complexity $\mathcal{O}(dp)$. This is done by introducing a new matrix $\mathbf{F}(t) = \mathbf{W}_{PS}(t)\mathbf{Q}(t-1)\mathbf{R}(t)$. Hence, step 5 of the previous algorithm can be written as:

$$\mathbf{W}(t) = \mathbf{W}_{PS}(t)\mathbf{Q}(t-1) - \mu\mathbf{W}_{PS}(t)\mathbf{Q}(t-1)\mathbf{R}(t) \quad (4.12)$$

$$= \mathbf{W}(t-1) + \mathbf{e}\tilde{\mathbf{g}}^T - \mu\mathbf{F}(t) \quad (4.13)$$

The vector $\tilde{\mathbf{g}}$ is given by $\tilde{\mathbf{g}} = \mathbf{Q}(t-1)^T\mathbf{g}$ with \mathbf{g} and \mathbf{e} are rank-one update vectors issued from the last step of the OPAST algorithm 2. Then, the update of the matrix $\mathbf{F}(t)$ is approximated by:

$$\mathbf{F}(t) = \mathbf{W}_{PS}(t)\mathbf{Q}(t-1)\mathbf{R}(t) \quad (4.14)$$

$$= \frac{1}{\alpha}\mathbf{W}_{PS}(t)\mathbf{Q}(t-1)\left(\beta\mathbf{R}(t-1) + \mathbf{y}(t)\text{sign}\left(\mathbf{y}^T(t)\right)\right) \quad (4.15)$$

$$\approx \frac{\beta}{\alpha}\mathbf{F}(t-1) + \frac{1}{\alpha}\mathbf{W}_{PS}(t)\mathbf{Q}(t-1)\mathbf{y}(t)\text{sign}\left(\mathbf{y}^T(t)\right) \quad (4.16)$$

with $\alpha = \left\|\beta\mathbf{R}(t-1) + \mathbf{y}(t)\text{sign}\left(\mathbf{y}^T(t)\right)\right\|_F^2$. Using Eq. (4.13) and Eq. (4.16) allows us to avoid all matrix-matrix products and to have a global complexity of order $\mathcal{O}(dp)$. This version is referred to as DS-OPAST2 and it is summarized in Algorithm 11. Note that a columns normalization of the matrix $\mathbf{W}(t)$ is essential because of the approximation errors.

4.3 Data Sparsity algorithm based on FAPI and Shear-Givens rotations for adaptive blind source separation SGDS-FAPI

The proposed algorithms DS-OPAST and DS-OPAST2 have low computational cost but the use of the exponential window, the OPAST algorithm and the gradient method result in slow convergence speed. This is can be problematic, especially if we have quick changes in the system mixing matrix. In order to enhance the convergence speed, we introduce our second proposed solution for the problem of adaptive blind sparse source separation in the noisy over-determined case denoted SGDS-FAPI (SGDS stands for Data Sparsity algorithm based on Shear-Givens rotations). This algorithm is based on a two-step approach as the DS-OPAST algorithm which we have proposed earlier in the previous section. However, in this work, the used subspace tracker is more accurate and the sparsity criterion is optimized by means of Givens and Shear (hyperbolic givens) rotations.

Algorithm 11 Data Sparsity algorithm based on OPAST for adaptive blind source separation DS-OPAST2

Require: $\mathbf{x}(t)$ data vector, β the forgetting factor, $\mathbf{W}_{PS}(t-1)$, $\mathbf{Z}_{PS}(t-1)$, $\mathbf{Q}(t-1)$, $\mathbf{R}(t-1)$, $\mathbf{F}(t-1)$ and $\mathbf{W}(t-1)$ from the previous iteration.

Ensure: $\mathbf{W}_{PS}(t)$, $\mathbf{Z}_{PS}(t)$, $\mathbf{Q}(t)$, $\mathbf{R}(t)$, $\mathbf{F}(t)$ and $\mathbf{W}(t)$

- 1: Find $\mathbf{W}_{PS}(t) = \mathbf{W}_{PS}(t-1) + \mathbf{e}(t)\mathbf{g}(t)^T$ using OPAST
 - 2: $\mathbf{y}(t) = \mathbf{Q}^T(t-1)\mathbf{W}_{PS}^T(t)\mathbf{x}(t)$
 - 3: $\mathbf{R}(t) = \beta\mathbf{R}(t-1) + \mathbf{y}(t)\text{sign}(\mathbf{y}^T(t))$ then $\mathbf{R}(t) = \frac{\mathbf{R}(t)}{\alpha}$ with $\alpha = \|\mathbf{R}(t)\|_F$
 - 4: $\mathbf{Q}(t) = \mathbf{Q}(t-1)(\mathbf{I}_p - \mu\mathbf{R}(t))$
 - 5: $\mathbf{v}_1 = \mathbf{Q}(t-1)\mathbf{y}(t)$
 - 6: $\mathbf{v}_2 = \mathbf{W}_{PS}(t)\mathbf{v}_1$
 - 7: $\mathbf{F}(t) = \frac{1}{\alpha}(\beta\mathbf{F}(t-1) + \mathbf{v}_2\text{sign}(\mathbf{y}^T(t)))$
 - 8: $\tilde{\mathbf{g}} = \mathbf{Q}(t-1)^T\mathbf{g}$
 - 9: $\mathbf{W}(t) = \mathbf{W}(t-1) + \mathbf{e}\tilde{\mathbf{g}}^T - \mu\mathbf{F}(t)$
 - 10: Columns normalization of $\mathbf{W}(t)$ and $\mathbf{Q}(t)$.
-

In the first step, our aim is to track the principal subspace matrix $\mathbf{W}(t)$ which should span the same subspace as the one spanned by the p dominant eigenvectors i.e. which correspond to the p greater eigenvalues of the covariance matrix $\mathbf{C}_x = \mathbb{E}[\mathbf{x}(t)\mathbf{x}^H(t)]$. The later matrix is adaptively updated either by using the exponential data window or the truncated (sliding) data window. Contrary to DS-OPAST algorithm where we have used OPAST [17] as a subspace tracker, the FAPI [20,21] algorithm is used for SGDS-FAPI. The FAPI algorithm [20,21] resolves the problem of tracking the signal subspace of dimension $p < d$ under the orthogonality constraint of the weighting matrix $\mathbf{W}(t)$ for both types of windows. The choice of FAPI was encouraged by its linear complexity and capability to guarantee the orthonormality of the subspace weighting matrix $\mathbf{W}(t)$ at each time step. In fact, FAPI has one of the best trade-off between quality of estimation and complexity of calculation (for more details see subsection 2.2.3).

The FAPI output matrix $\mathbf{W}_{PS}(t)$ should also span the same subspace as our mixing matrix \mathbf{A} and we can write that

$$\mathbf{A} = \mathbf{W}_{PS}(t)\mathbf{Q}(t) \quad (4.17)$$

where $\mathbf{Q}(t)$ is a non singular square matrix. Note also that finding the matrix $\mathbf{A}^\#$ (with permutation and scaling ambiguity) is somehow equivalent to finding \mathbf{B} the separation matrix. Therefore, in this second step the non singular matrix $\mathbf{Q}(t)$ is introduced in order to optimize the criterion which describes the sparsity of the

separated sources. Hence, the objective function considered to restore the sparsity of the source signals (estimated as $\mathbf{A}^\# \mathbf{x}(t)$) is given by:

$$\begin{aligned} J_{DS2}(\mathbf{Q}(t)) &= \left\| (\mathbf{W}(t)\mathbf{Q}(t))^\# \mathbf{X}(t) \right\|_1 \\ &= \left\| \mathbf{Q}(t)^{-1} \mathbf{W}(t)^T \mathbf{X}(t) \right\|_1 \\ \text{s.t. } \mathbf{Q}(t) &\text{ is non-singular with unit norm columns} \end{aligned} \quad (4.18)$$

where $\mathbf{X}(t) = [\beta^{L-1} \mathbf{x}(t-L+1), \beta^{L-2} \mathbf{x}(t-L+2), \dots, \mathbf{x}(t)]$ is the windowed data matrix (exponentially when $L = t$ and truncated when $L < t$). Note that the above function is slightly different from J_{DS} used in DS-OPAST where \mathbf{Q}^T is replaced by $\mathbf{Q}^{-1}(t)$.

In order to optimize the criterion of Eq. (4.18) with respect to $\mathbf{Q}(t)$, we propose to write the matrix $\mathbf{Q}(t)^{-1}$ as a product of elementary Givens and Shear matrices:

$$\mathbf{Q}(t)^{-1} = \prod_{1 \leq i < j \leq p} \mathcal{S}_{ij} \mathcal{G}_{ij} \quad (4.19)$$

where the Shear \mathcal{S}_{ij} and the Givens \mathcal{G}_{ij} elementary matrices are described by Eq. (3.15) and Eq. (3.16) respectively. Indeed, any non singular matrix can be decomposed into product of Shear \mathcal{S}_{ij} and Givens \mathcal{G}_{ij} elementary matrices (up to a constant factor) for $1 \leq i < j \leq p$. The Givens-based (Jacobi-like) techniques are attractive due to their numerical stability, their facility to be parallelized and their low computational cost. Such techniques have been already used in the context of BSS [91,92] but with other a prior information than sparsity.

Next, we present the case of using just one Shear-Givens rotation every time iteration for simplicity and then we generalize to the case where we consider more than one rotation. Hence, we can write that

$$\mathbf{Q}^{-1}(t) = \mathbf{H}(t) = \mathcal{S}_{ij} \mathcal{G}_{ij} \mathbf{H}(t-1) \quad (4.20)$$

for the selected indices (i, j) at the t^{th} time iteration.

In order to minimize the objective function $J_{DS2}(\mathbf{Q}(t))$, one needs to specify how the rotation indices are chosen at each iteration as well as how the parameters (θ, ϕ) are optimized. One can choose the same automatic selection strategy for the rotation indices as the one used for in SS-FAPI2 expressed by Eq. (3.10). Hence, all the $p(p-1)/2$ possible search indices values are visited periodically by an automatic incrementation of indices throughout the iterations.

After fixing the indices (i, j) , finding $\mathbf{H}(t)$ resumes in estimating the parameters (θ, ϕ) which minimize:

$$J(\theta, \phi) = \left\| \mathcal{S}_{ij} \mathcal{G}_{ij} \mathbf{H}(t-1) \mathbf{W}_{PS}^T(t) \mathbf{X}(t) \right\|_1 \quad (4.21)$$

Algorithm 12 Data Sparsity algorithm based on FAPI and Shear-Givens rotations for adaptive blind source separation SGDS-FAPI

Require: $\mathbf{x}(t)$ data vector, parameters β and L , $\mathbf{W}_{PS}(t-1)$ and $\mathbf{Z}_{PS}(t-1)$ previous FAPI outputs. Previous indices (l, m) and outputs $\mathbf{H}(t-1)$, $\mathbf{B}(t-1)$.

Ensure: $\mathbf{W}_{PS}(t)$, $\mathbf{Z}_{PS}(t)$, indices (i, j) , $\mathbf{H}(t)$ and $\mathbf{B}(t)$

- 1: Run FAPI : $\mathbf{W}_{PS}(t) = \mathbf{W}_{PS}(t-1) + \mathbf{e}(t)\mathbf{g}(t)^T$
 - 2: Update indices (i, j) using automatic selection strategy described in Eq. (3.10)
 - 3: Computing \mathbf{y}_i and \mathbf{y}_j using (4.25)
 - 4: Find $(\hat{\theta}, \hat{\phi}) = \arg \min J(\theta, \phi)$
 - 5: $\mathbf{H}(t) = \mathcal{S}_{ij}\mathcal{G}_{ij}\mathbf{H}(t-1)$
 - 6: $\mathbf{B}(t) = \mathcal{S}_{ij}\mathcal{G}_{ij}\mathbf{B}(t-1) + \mathbf{H}(t)\mathbf{g}(t)\mathbf{e}'(t)^T$
-

$$= \left\| \begin{bmatrix} \cosh(\phi) & \sinh(\phi) \\ \sinh(\phi) & \cosh(\phi) \end{bmatrix} \begin{bmatrix} \cos(\theta) & \sin(\theta) \\ -\sin(\theta) & \cos(\theta) \end{bmatrix} \begin{bmatrix} \mathbf{y}_i \\ \mathbf{y}_j \end{bmatrix} \right\|_1 \quad (4.22)$$

where \mathbf{y}_i and \mathbf{y}_j are the i^{th} and j^{th} rows of the product $\mathbf{H}(t-1)\mathbf{W}_{PS}^T(t)\mathbf{X}(t)$ available from the previous iteration. We can expand the equation to:

$$\begin{aligned} J(\theta, \phi) = & \left\| \left(\cos(\theta) \cosh(\phi) - \sin(\theta) \sinh(\phi) \right) \mathbf{y}_i + \right. \\ & \left. \left(\cos(\theta) \sinh(\phi) + \sin(\theta) \cosh(\phi) \right) \mathbf{y}_j \right\|_1 + \\ & \left\| \left(\cos(\theta) \sinh(\phi) - \sin(\theta) \cosh(\phi) \right) \mathbf{y}_i + \right. \\ & \left. \left(\cos(\theta) \cosh(\phi) + \sin(\theta) \sinh(\phi) \right) \mathbf{y}_j \right\|_1 \end{aligned} \quad (4.23)$$

$J(\theta, \phi)$ is a scalar function of two variables with no simple analytic solution for its minimum point, so we have used a numerical search method to find the minimum of this unconstrained optimization problem.

Remark: It is possible to optimize separately the Givens parameter θ then the Shear parameter ϕ . This leads to a slight loss in terms of estimation quality but helps reducing the computational cost since one replaces the 2D search by two 1D parameter optimization. In addition, the cost function is $\pi/2$ -periodic in θ and we knew also that ϕ is also bounded between $-\gamma \leq \phi \leq \gamma$. One can include those bounds to reduce the research set for each parameter. This version is referred to as SGDS-FAPI2.

Combining both steps

Now, we will resume the scheme to follow in order to reach a linear computational complexity for both steps. The main idea is to run the FAPI algorithm

independently and to update the separation matrix

$$\mathbf{B}(t) = \mathbf{H}(t)\mathbf{W}_{PS}^T(t) \quad (4.24)$$

at every iteration. Note that Eq. (4.23) includes only the two rows \mathbf{y}_i and \mathbf{y}_j of the product $\mathbf{H}(t-1)\mathbf{W}_{PS}^T(t)\mathbf{X}(t)$, which means that we need only the i^{th} and j^{th} rows of $\mathbf{H}(t-1)\mathbf{W}_{PS}^T(t)$. We can write:

$$\mathbf{H}(t-1)\mathbf{W}_{PS}^T(t) = \mathbf{B}(t-1) + \mathbf{H}(t-1)\mathbf{g}(t)\mathbf{e}(t)^T \quad (4.25)$$

with $\mathbf{g}(t)$ and $\mathbf{e}(t)$ are the FAPI rank one update vectors. Next, we calculate the rows \mathbf{y}_i and \mathbf{y}_j which will have $\mathcal{O}(dL)$ complexity with L the size of the data window ($L = 1/(1 - \beta)$ in the case of the exponential window or the width of the truncated window). After that, one needs to optimize the function $J(\theta, \phi)$ and to update the outputs: i.e., $\mathbf{H}(t)$ by means of Eq. (4.20) and $\mathbf{B}(t)$ by combining Eq. (4.24) and Eq. (4.25). Note that the left multiplication by $\mathcal{S}_{ij}\mathcal{G}_{ij}$ can be summed up in changing the i^{th} and j^{th} rows. The global complexity of the proposed algorithm is $5dp + 2dL + \mathcal{O}(p^2)$ if we use the exponentially window version of FAPI or $8dp + 6dL + \mathcal{O}(p^2)$ if we use the truncated window version. The proposed algorithm is summarized in Algorithm 12.

Besides their low computational complexity, the Jacobi-like techniques are also known for their ability to be easily parallelizable. This can be really useful in the case where we consider more than one Shear-Givens rotation every time iteration. In this case, one needs to be careful with the indices selection strategy used and repeat the steps 3-6 of Algorithm 12. Otherwise, one can just do this sequentially by repeating steps 2-6 of Algorithm 12. The latter has been tested in the sequel to assess the algorithm's performance in that case.

Remark: Note that other selection strategies for the rotation indices can be considered but are omitted due to space limitation. For example, at each iteration, one can select the indices (i, j) corresponding to row vectors \mathbf{y}_i and \mathbf{y}_j of maximum ℓ_1 norms (i.e. the ones that deviate the most from the target sparsity objective).

Table A.2 summarizes the computational complexity of the proposed algorithms in this chapter. Finding the angles (θ, ϕ) iteratively in SGDS-FAPI2 has a complexity of $8\alpha_2 d$ with α_2 being the number of the iterations to reach the targeted precision. For instance, using the golden section method we need about $\alpha_2 = 15$ iterations to reach a precision of 10^{-4} . The joint optimization proposed in SGDS-FAPI is more complicated and needs more function evaluations to converge which means that $\alpha_1 \gg \alpha_2$.

Algorithm	Computational complexity per iteration
DS-OPAST	$dp^2 + 4dp + \mathcal{O}(p^3)$
DS-OPAST2	$5dp + \mathcal{O}(p^3)$
SGDS-FAPI	$5dp + 2dL + 8\alpha_1d + \mathcal{O}(p^2)$
SGDS-FAPI2	$5dp + 2dL + 8\alpha_2d + \mathcal{O}(p^2)$

Table 4.1: Summary of the computational complexity of the proposed algorithms for adaptive blind sparse source separation

4.4 Simulation results

In order to assess the performance of the proposed algorithms, we present here some numerical simulation results. The batch algorithm JADE [91] which was re-applied at each time instant t to all samples from 1 to t , is used for comparison. We consider the data model presented in section 2.3 with the sparse signals generated according to the Bernoulli-Gaussian distribution (SPRANDN Matlab function). The performance index used is the mean rejection level [57], which is defined by $\mathcal{I}_{perf} \stackrel{def}{=} \sum_{p \neq q} \mathcal{I}_{pq}$ where \mathcal{I}_{pq} measures the ratio of the power of the interference of the q^{th} source to the power of the p^{th} source signal. In our case, since the sources are generated with the same power, they are defined as $\mathcal{I}_{pq} = \mathbf{E}|(\hat{\mathbf{A}}^\# \mathbf{A})_{pq}|$ (where $\hat{\mathbf{A}}^\# = \mathbf{H}(t)\mathbf{W}_{PS}^T(t)$ for the SGSS-FAPI algorithm and $\hat{\mathbf{A}}^\# = \mathbf{Q}^T(t)\mathbf{W}_{PS}^T(t)$ for the DS-OPAST algorithm). We simulated 100 times the data with p sparse sources, d sensors in each experiment of the following results.

Figure 4.1 shows an example of source signals and their corresponding separated signals by means of SGDS-FAPI for a $SNR = 10dB$ (after adjusting the amplitude and put every output signal with its correspondent source signal to remove the inherent ambiguities of BSS). In order to show the adaptive separation capability of our algorithms, we change randomly the mixing matrix \mathbf{A} after 2000 iterations. Figure 4.2 illustrates the improved performance of the SGDS-FAPI compared to DS-OPAST and JADE algorithms. SGDS-FAPI2 corresponds to the truncated window version of SGDS-FAPI with $L = 50$ (with truncated version of FAPI) which explains its higher sensitivity to noise as compared to SGDS-FAPI. Fig. 4.3 shows the results after 2000 iterations versus the SNR . It is clear that the SGDS-FAPI algorithm reaches lower mean rejection levels than the other adaptive algorithms and even outperforms, in that context, the batch algorithm JADE for $SNR > 10dB$.

Fig. 4.4 illustrates the influence of the choice of the gradient parameter μ on the performance of DS-OPAST and DS-OPAST2. It is clear that there is a trade-off between the achievable limit of mean rejection level and the speed of convergence

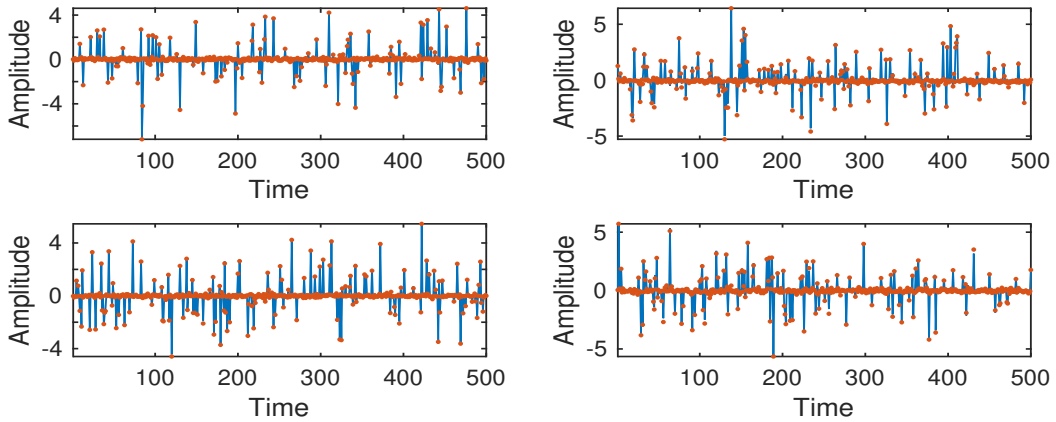


Figure 4.1: Example of source signals (solid blue lines) and their separated versions (red points) for $d = 16$, $p = 4$ and $SNR = 10dB$.

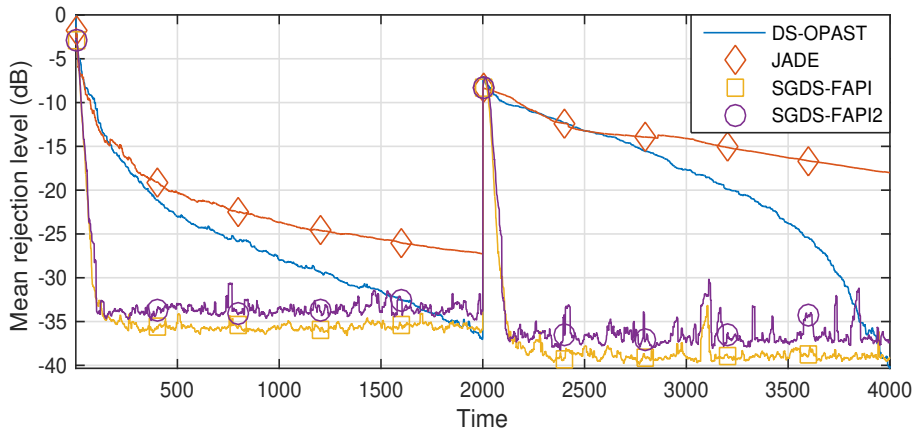


Figure 4.2: Mean rejection level I_{pref} versus time for $d = 16$, $p = 4$ and $SNR = 20dB$.

to that limit. In order to show the effect of using multiple rotations per iteration on the speed of convergence of SGDS-FAPI, we change the mixing matrix (randomly) two times: at time instants 200 and 400 with the parameters $d = 20$, $p = 8$ and $SNR = 10dB$. Fig.4.5 shows that the more rotations per iteration we consider, the faster the convergence rate is. The computational complexity should increase with such a solution, unless we use a parallel scheme with an appropriate indices selection strategy.

Until now, we have considered that source signals are sparse in the time domain. However, this is not true in most cases, hence, generally source signals are assumed to be sparsely represented in another basis. For example, the orthogonal wavelet basis is a good choice when dealing with image processing, or the DCT when processing

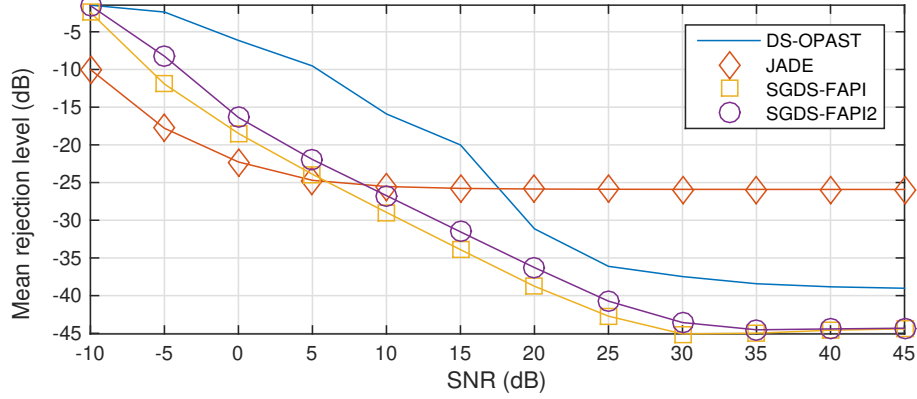


Figure 4.3: Mean rejection level I_{pref} versus SNR for $d = 16$, $p = 4$ after 2000 iterations.

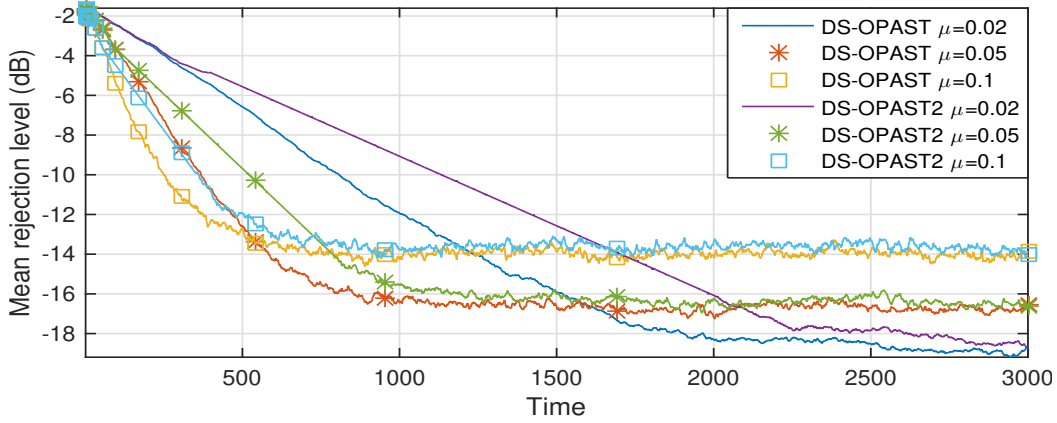


Figure 4.4: Mean rejection level I_{pref} versus time for $d = 10$, $p = 4$ and $SNR = 10dB$.

speech signals. The next experiment was performed with source signals from four speakers $p = 4$, sampled at $20kHz$, of $2.5s$ duration and presented in Fig. 4.6. The mixing matrix \mathbf{A} which is generated randomly with $d = 10$ sensors, changes completely after receiving $1.5s$ of the signals. The received data are corrupted by a white Gaussian noise with $SNR = 10dB$. We proposed an adaptive framework to separate the sources, where the received signals are treated block per block every time frame. The window duration of this frame is typically between $10 - 30ms$ because of the quasi-stationary assumption on the speech signals. We consider sliding rectangular windows of length $20ms$ which is equivalent to 400 samples and with an overlapping of 50%. The received signals at every time frame are projected using a 400×50 rectangular DCT matrix which is equivalent to low resolution DCT transformation. In addition to enhancing the sparsity, this projection will allow us to

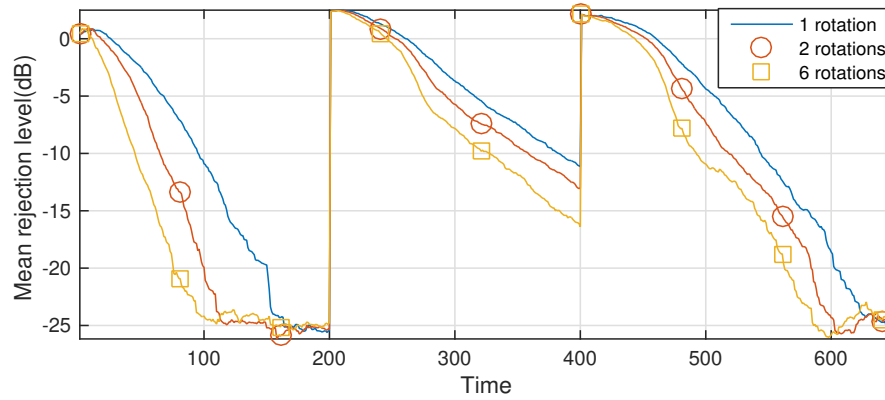


Figure 4.5: Mean rejection level I_{pref} versus Time for $d = 20$, $p = 8$ and $SNR = 10dB$.

reduce the number of samples to process from 400 to 50 per time frame. In Fig. 4.7, we can see an example of a received signal and its corresponding transformed version which is clearly more sparse.

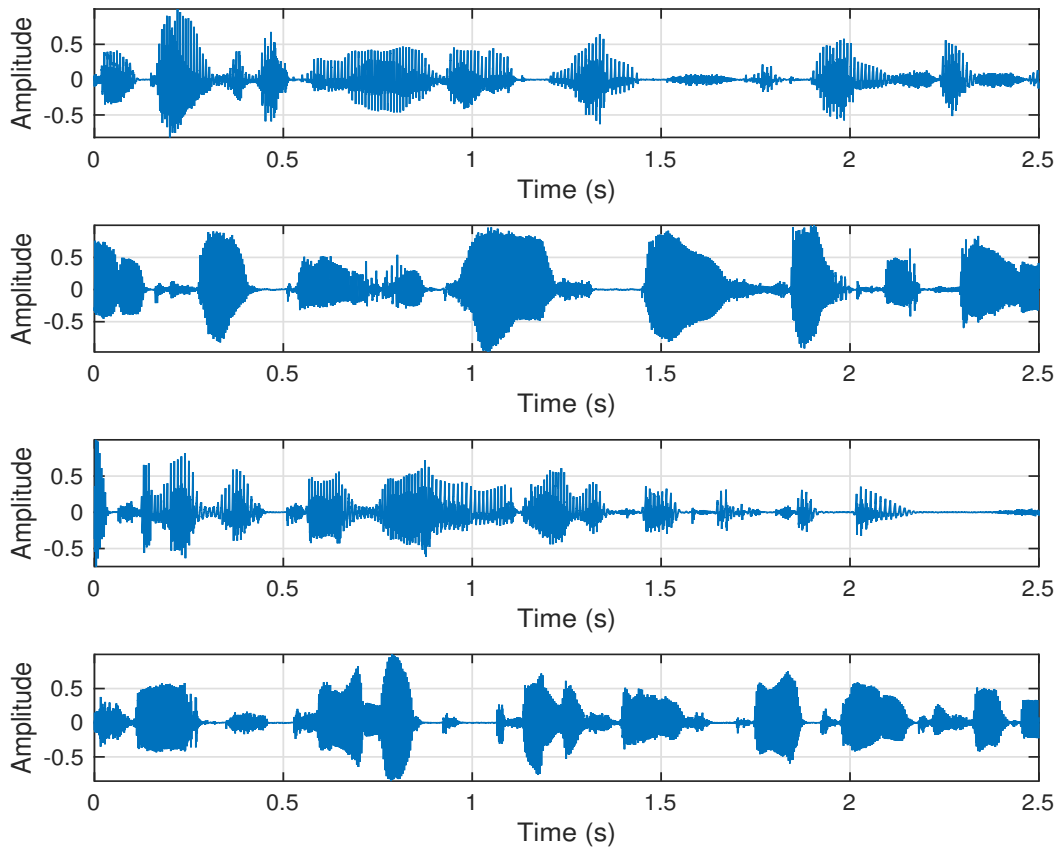


Figure 4.6: Amplitude of the speech source signals versus time in seconds.

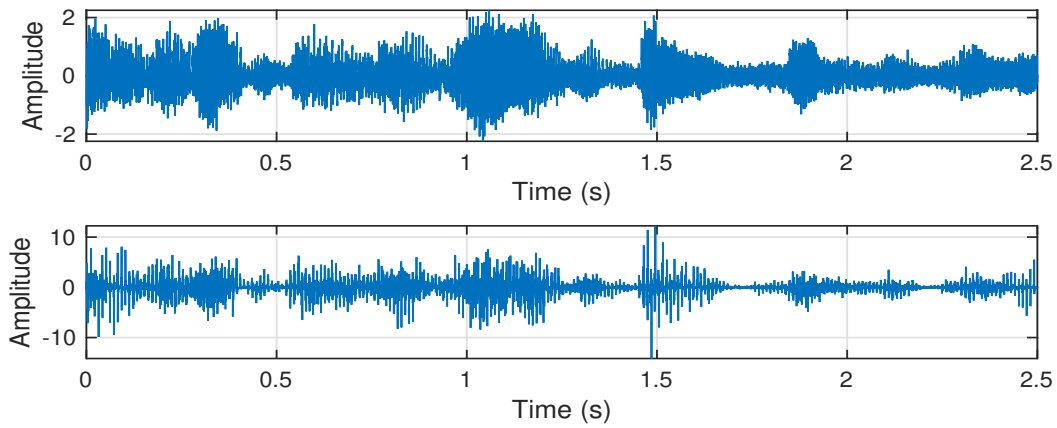


Figure 4.7: Amplitude of a received signal (top) and its corresponding transformed version (bottom) versus time in seconds.

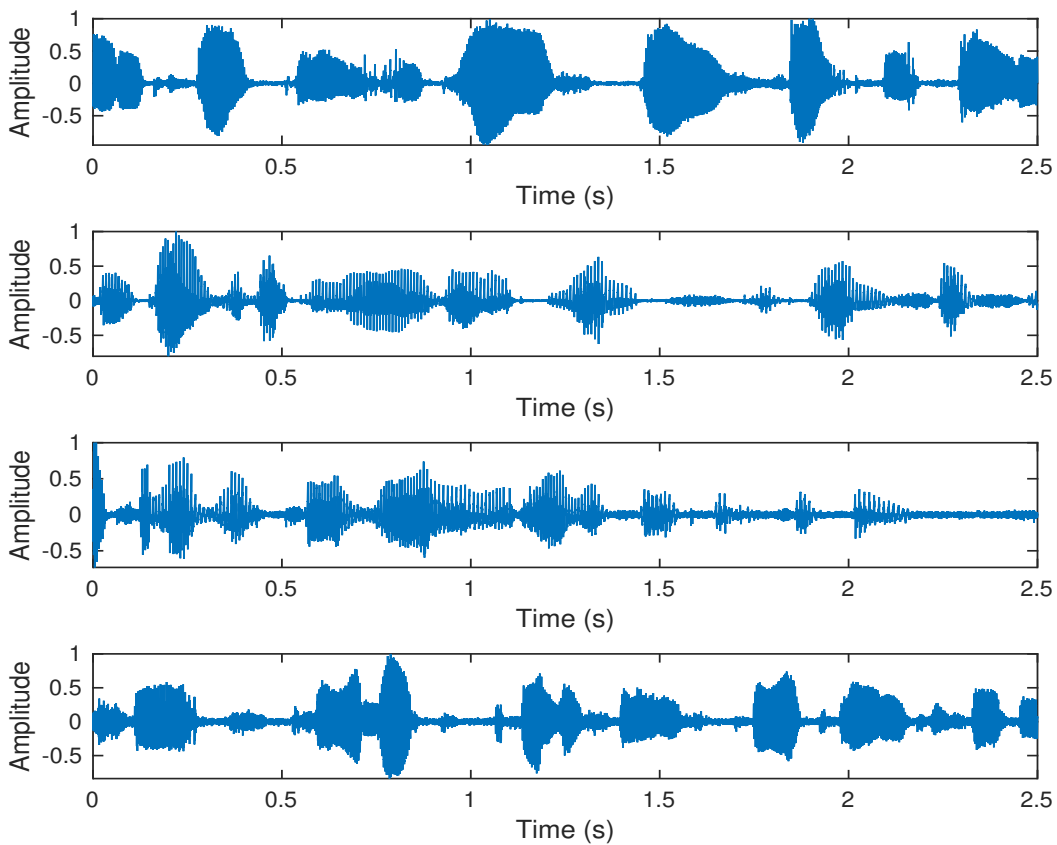


Figure 4.8: Amplitude of the separated signals versus time in seconds.

Next, we apply DS-OPAST and SGSS-FAPI on the transformed signals using as an initialization the results from the previous time frame. Fig. 4.8 shows an example of the separated signals with the DS-OPAST algorithm where we can distinguish

the recovery of the source signals in a different order. For a more quantitative comparison, we have used the batch algorithm JADE [91] on all the received signals from the first sample until time t (without the transformation).

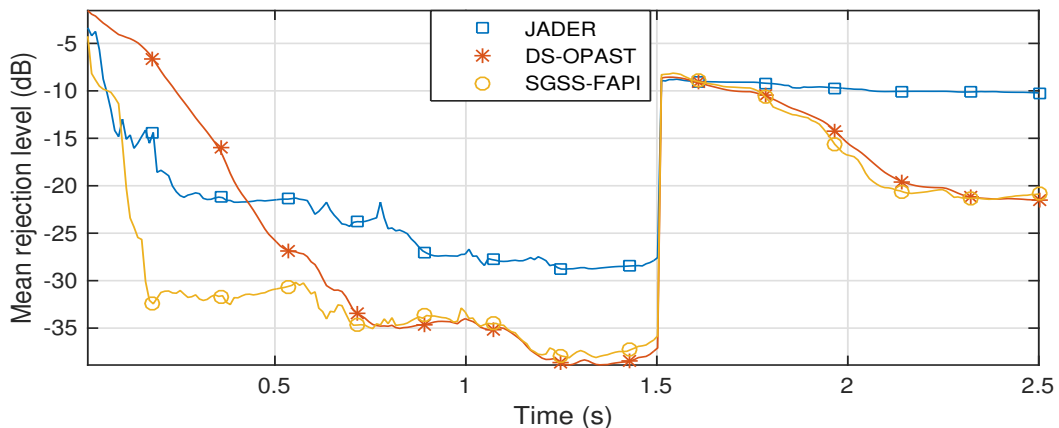


Figure 4.9: Mean rejection level I_{pref} versus Time for speech signals with $d = 10$, $p = 4$ and $SNR = 10dB$.

Fig. 4.9 shows that both DS-OPAST and SGSS-FAPI separate successfully the sources with a slight advantage to SGSS-FAPI in terms of the speed of tracking changes over the separating matrix. Nevertheless, both proposed methods have better performance compared to batch algorithm JADE, especially after the change in the mixing matrix. It is worth mentioning that after separating the received signals at the current time frame, one will have the task to correctly assign each separated signal in the actual time frame with the previously separated signals. One of the possible solutions to this problem is to check for higher correlation between previous and current separated signals.

4.5 Conclusion

The problem of blind adaptive sparse source separation has been studied in this chapter. The over-determined instantaneous noisy mixture has been considered. Based on a two step approach, we have proposed the two main algorithms: DS-OPAST and SGDS-FAPI. Different extensions were also discussed to reduce the complexity and enhance the tracking capabilities of these algorithms. The first step of the proposed algorithms allows us to project the data on the signal subspace estimated by means of FAPI algorithm. Then, the sparsity of the source signals which is represented by an ℓ_1 criterion is optimized. A natural Gradient method is used in DS-OPAST for the optimization of the ℓ_1 criterion. An adaptive method based on Shear and Givens rotations is used in SGDS-FAPI algorithm. In addition to the low

computational cost, the proposed algorithms have shown improved performance as compared to existing solutions.

After considering the blind instantaneous mixture model in both chapter 3 and chapter 4 with the sparsity *a priori* on the system matrix or on the sources, in the next chapter, we will consider the blind convolutive mixture model where we will be interested in the blind sparse channel identification problem.

Blind identification of sparse systems

Contents

5.1	Introduction	89
5.2	Adaptive blind identification of sparse SIMO channels using the maximum a posteriori approach	91
5.2.1	Computational complexity reduction	93
5.2.2	Gradient step optimization	94
5.3	Regularized deterministic maximum likelihood based joint estimation of MIMO channels and input data	95
5.3.1	Blind deterministic maximum likelihood DML estimation approach	97
5.3.2	Regularized blind deterministic maximum likelihood DML estimation approach	98
5.3.3	Initialization and resolving ambiguities in subspace-based blind identification of MIMO channels	101
5.4	Simulation results	102
5.5	Conclusion	109

5.1 Introduction

Blind system identification (BSI) problems are receiving considerable interest from both signal processing and communications communities since accurate channel estimation is likely to become more challenging in future generation wireless systems, which will likely have both increased spatial diversity and decreased coherence times. Furthermore, in some communication systems, the synchronization between the receiver and the transmitter is not possible; thus training sequences are not exploitable. Blind techniques present reduced need for overhead information which increases the bandwidth efficiency. Development of blind receivers also

has applications in military communication systems when the transmitted symbols have to be estimated in a blind fashion. Blind techniques also enable us to treat problems where we cannot influence the input such as the extracting of the foetal electrocardiogram (fECG). Many methods have been proposed to solve blind channel estimation problems, and we can distinguish two main classes of BSI methods: higher order statistics (HOS) and second order statistics (SOS) techniques. In general, HOS-based methods require large sample sizes to achieve 'better' estimation performances than the SOS-based methods [83]. Unfortunately, it seems likely that in case of very long impulse response and sparse channel, most of the state-of-the-art methods perform poorly. Such sparse channels can be encountered in many communication applications including High-Definition television (HDTV) channels and underwater acoustic channels. In this chapter, we present our contributions to solve the sparse channel identification problem in both Single Input, Multiple Output (SIMO) and Multiple Input, Multiple Output (MIMO) cases.

First, in the case of sparse SIMO channel, we extend the work in [81] by considering the SIMO case of a time varying sparse channel. A generalized Laplacian distribution is considered to enhance the sparsity of the channel coefficients with a Maximum A Posteriori (MAP) approach. Then, an adaptive technique based on the gradient descent method is proposed to estimate efficiently the sparse channel coefficients. The robustness against channel overestimation errors will also be discussed.

However, even if some training sequence exists, combining it with blind techniques often leads to improved performance which explains the increased interest for joint estimation of channels and the data referred to as data-aided channel estimation [105–109]. Our second contribution aims to estimate jointly the channel state information and the transmitted data in the case of MIMO channels using a regularized Deterministic Maximum Likelihood (DML) formulation based on different prior types. This regularization can be on the transmitted signals and/or on the channel impulse response. For instance, most of digital communications are based on transmitted signals that belong to a finite-alphabet set. Hence, the simplicity property was considered for the recovery of finite-alphabet signals as is the case in [110] for large-scale MIMO systems. The sparsity property was also used in [68] for blind source separation when the sources are known to be sparse or can be sparsely represented. For the transmitted signals, we will consider either the simplicity property in the case of finite-alphabet signals or the sparsity property in the case of sparse signals. For the channel impulse response, we will consider the sparsity prior which was already used in the context of blind and semi-blind channel identification, for example, in [50] for MIMO channels with orthogonal frequency

division multiplexing (OFDM).

5.2 Adaptive blind identification of sparse SIMO channels using the maximum a posteriori approach

Our focus is on the SIMO sparse channel case in a blind identification context. We aim to estimate the channel state information using only the observation data and the sparsity information of the channel coefficients. Considering the mathematical model presented in section 2.4 with $N_t = 1$ for the SIMO case,

$$\mathbf{x}_{N_r}(t) = \mathcal{H}_{N_r} \mathbf{s}_N(t) + \mathbf{n}_{N_r}(t) \quad (5.1)$$

where $\mathbf{x}_{N_r}(t) = [\mathbf{x}_1^T(t), \dots, \mathbf{x}_{N_r}^T(t)]^T$ with $\mathbf{x}_i(t) = [x_i(t), \dots, x_i(t - N + 1)]^T$ for $i = 1, \dots, N_r$. The noise vector $\mathbf{n}_{N_r}(t)$ is constructed in the same way as the observations by $\mathbf{n}_{N_r}(t) = [\mathbf{n}_1^T(t), \dots, \mathbf{n}_{N_r}^T(t)]^T$ with $\mathbf{n}_i(t) = [n_i(t), \dots, n_i(t - N + 1)]^T$ for $i = 1, \dots, N_r$. The matrix $\mathcal{H}_{N_r} = [\mathcal{T}(\mathbf{h}_1)^T, \dots, \mathcal{T}(\mathbf{h}_{N_r})^T]^T$ is a block Sylvester matrix, $\mathcal{T}(\mathbf{h}_i)$ being the Sylvester matrix of the i -th channel given by $\mathbf{h}_i = [h_i(0), \dots, h_i(L)]^T$ for $i = 1, \dots, N_r$.

The main idea of the Maximum a Posteriori (MAP) approach is to estimate the channel vector \mathbf{h} using its conditional probability distribution as follows:

$$\hat{\mathbf{h}}_{MAP} = \arg \max_{\mathbf{h}} \left\{ \frac{f(\mathbf{x}_{N_r} | \mathbf{h}) f(\mathbf{h})}{\int f(\mathbf{x}_{N_r} | \mathbf{h}') f(\mathbf{h}') d\mathbf{h}'} \right\} \quad (5.2)$$

$$= \arg \max_{\mathbf{h}} \left\{ f(\mathbf{x}_{N_r} | \mathbf{h}) f(\mathbf{h}) \right\} \quad (5.3)$$

Generally speaking, the MAP allows us to exploit prior information about the desired parameter. Hence, one needs to *a priori* know the probability distribution function $f(\mathbf{h})$ of the channel vector. This *a priori* depends on the application context and its physical environment. In our case, it is the channel vector sparsity that we model by representing the channel pdf with the generalized Laplacian distribution given by:

$$f(\mathbf{h}) = \left[2\gamma \Gamma\left(1 + \frac{1}{p}\right) \right]^{-N_r(L+1)} \exp\left(-\frac{\|\mathbf{h}\|_p^p}{\gamma^p}\right) \quad (5.4)$$

where $\gamma > 0$ is a scale parameter, $0 < p \leq 1$ and $\Gamma(z) = \int_0^\infty t^{z-1} e^{-t} dt$, $z > 0$ is the Gamma function. Using this pdf, one increases the chances to get channel coefficients close to zero. Combining equations (2.32), (5.3) and (5.4) leads to the following objective function:

$$\mathcal{J}(\mathbf{h}) = \arg \min_{\|\mathbf{h}\|_2=1} \left\{ \mathbf{h}^H \mathcal{X}_{N_r}^H \left(\mathcal{G}_{N_r}^H \mathcal{G}_{N_r} \right)^\# \mathcal{X}_{N_r} \mathbf{h} + \lambda \|\mathbf{h}\|_p^p \right\} \quad (5.5)$$

where $\lambda = \frac{\sigma^2}{\gamma^p}$ is a good approximation to the 'optimal' weighting parameter which controls the trade-off between the ML term and the penalty term. The matrices \mathcal{X}_{N_r} and \mathcal{G}_{N_r} were already introduced in section 2.4. The cost function is optimized under the constraint $\|\mathbf{h}\|_2 = 1$ to avoid the scalar indeterminacy. We can also use other types of constraints such as fixing the first element of the vector \mathbf{h} to one. The minimization of such a problem is computationally expensive and may be even intractable when the channel impulse responses are long and the number of channels is large.

For a slowly varying channel, one can reduce the computational cost and track the channel variations by using a stochastic adaptive gradient technique to solve the previous minimization problem efficiently.

Let $\mathbf{h}(t)$ be the solution after the t -th iteration, then the solution at the $(t+1)$ -th iteration is given by:

$$\mathbf{h}(t+1) = \mathbf{h}(t) - \mu \nabla \mathcal{J}(\mathbf{h}(t)) \quad (5.6)$$

where μ is a small positive optimization step and the gradient $\nabla \mathcal{J}(\mathbf{h}(t))$ is given by:

$$\begin{aligned} \nabla \mathcal{J}(\mathbf{h}(t)) = & 2\mathcal{X}_{N_r}^H(t+1) \left(\mathcal{G}_{N_r}^H(t) \mathcal{G}_{N_r}(t) \right)^\# \mathcal{X}_{N_r}(t+1) \mathbf{h}(t) \\ & + \lambda p \tilde{\mathbf{h}}(t) \end{aligned} \quad (5.7)$$

where $\tilde{h}_i = \text{sign}(h_i) |h_i|^{p-1}$ for $i = 1, \dots, N_r(L+1)$.

We define the matrix:

$$\mathcal{Q}_z(t+1) = \mathcal{X}_{N_r}^H(t+1) \mathbf{Z}(t) \mathcal{X}_{N_r}(t+1) \quad (5.8)$$

with $\mathbf{Z}(t) = \left(\mathcal{G}_{N_r}^H(t) \mathcal{G}_{N_r}(t) \right)^\#$.

A more elegant way to update $\mathcal{Q}_z(t+1)$ is to use the adaptive exponential window

$$\mathcal{X}_{N_r}(t+1) = \left[\sqrt{\beta} \mathcal{X}_{N_r}(t)^T, \bar{\mathcal{X}}_{N_r}(t+1)^T \right]^T \quad (5.9)$$

with $0 < \beta < 1$ a forgetting factor and $\bar{\mathcal{X}}_{N_r}(t+1)$ is given by:

$$\bar{\mathcal{X}}_2(t+1) = \left[\bar{\mathbf{x}}_2(t+1), -\bar{\mathbf{x}}_1(t+1) \right] \quad (5.10)$$

and

$$\bar{\mathcal{X}}_q(t+1) = \left[\begin{array}{ccc|c} \bar{\mathcal{X}}_{q-1}(t+1) & & & 0 \\ \hline \bar{\mathbf{x}}_q(t+1) & & 0 & -\bar{\mathbf{x}}_1(t+1) \\ & \ddots & & \vdots \\ 0 & & \bar{\mathbf{x}}_q(t+1) & -\bar{\mathbf{x}}_{q-1}(t+1) \end{array} \right] \quad (5.11)$$

for $q = 3, \dots, N_r$ with $\bar{\mathbf{x}}_q(t) = [x_q(t), \dots, x_q(t-L)]$.

Hence, combining equation (5.8) and (5.9) yields:

$$\begin{aligned} \mathcal{Q}_z(t+1) &= \beta \mathcal{X}_{N_r}^H(t) \mathbf{Z}(t) \mathcal{X}_{N_r}(t) \\ &+ \bar{\mathcal{X}}_{N_r}^H(t+1) \mathbf{Z}(t) \bar{\mathcal{X}}_{N_r}(t+1) \end{aligned} \quad (5.12)$$

Using the approximation $\mathcal{Q}_z(t) \approx \mathcal{X}_{N_r}^H(t) \mathbf{Z}(t) \mathcal{X}_{N_r}(t)$, we can rewrite:

$$\mathcal{Q}_z(t+1) = \beta \mathcal{Q}_z(t) + \bar{\mathcal{X}}_{N_r}^H(t+1) \mathbf{Z}(t) \bar{\mathcal{X}}_{N_r}(t+1) \quad (5.13)$$

The algorithm can be summarized as follows:

1. Update $\mathbf{Z}(t) = \left(\mathcal{G}_{N_r}^H(t) \mathcal{G}_{N_r}(t) \right)^\#$
2. Update $\mathcal{Q}_z(t+1)$ using (5.13)
3. Update $\mathbf{h}(t+1)$ using (5.6) and (5.7)
4. Normalize $\mathbf{h}(t+1)$ such that $\|\mathbf{h}(t+1)\|_2 = 1$

Note that the proposed algorithm can be modified by using another optimization descent method. We can also change the sparsity prior which would lead us to change the final objective function. Next, we will provide two ideas that are used to extend this work: derive an optimal gradient step and approximate the update of $\mathbf{Z}(t)$ in order to further reduce the computational complexity.

5.2.1 Computational complexity reduction

The complexity of the proposed algorithm is dominated by the computation of the pseudo inverse $\mathbf{Z}(t) = \left(\mathcal{G}_{N_r}^H(t) \mathcal{G}_{N_r}(t) \right)^\#$. One way to reduce the cost of this step is to use the previous gradient step and the fact that we are using a small optimization step μ to approximate the pseudo inverse. Actually, one can use the first order approximation of the pseudo inverse of the sum of two matrices $\mathcal{A} + \mu\mathcal{B}$ of size $(n \times m)$ which is given by :

$$\begin{aligned} (\mathcal{A} + \mu\mathcal{B})^\# &\approx \mathcal{A}^\# - \mu\mathcal{A}^\#\mathcal{B}\mathcal{A}^\# \\ &+ \mu\mathcal{A}^\#\mathcal{A}^{\#T}\mathcal{B}^T(\mathbf{I}_n - \mathcal{A}\mathcal{A}^\#) \\ &+ \mu(\mathbf{I}_m - \mathcal{A}^\#\mathcal{A})\mathcal{B}^T\mathcal{A}^{\#T}\mathcal{A}^\# + \mathcal{O}(\mu^2) \end{aligned} \quad (5.14)$$

In our case, we have

$$\mathbf{h}(t) = \frac{\mathbf{h}(t-1) - \mu\nabla\mathcal{J}(\mathbf{h}(t-1))}{\left\| \mathbf{h}(t-1) - \mu\nabla\mathcal{J}(\mathbf{h}(t-1)) \right\|_2} \quad (5.15)$$

The linear construction of $\mathcal{G}_{N_r}^H(t)$ from $\mathbf{h}(t)$ as entry allows us to write :

$$\mathcal{G}_{N_r}^H(t) = \frac{\mathcal{G}_{N_r}^H(t-1) - \mu \nabla \mathcal{G}_{N_r}^H(t-1)}{\left\| \mathbf{h}(t-1) - \mu \nabla \mathcal{J}(\mathbf{h}(t-1)) \right\|_2} \quad (5.16)$$

with $\nabla \mathcal{G}_{N_r}^H(t-1)$ has the same construction as $\mathcal{G}_{N_r}^H(t-1)$ with the gradient $\nabla \mathcal{J}(\mathbf{h}(t-1))$ as entry instead of $\mathbf{h}(t-1)$. which leads to:

$$\begin{aligned} \mathcal{G}_{N_r}^H(t) \mathcal{G}_{N_r}(t) \approx & \frac{1}{\left\| \mathbf{h}(t-1) - \mu \nabla \mathcal{J}(\mathbf{h}(t-1)) \right\|_2^2} \left\{ \mathcal{G}_{N_r}^H(t-1) \mathcal{G}_{N_r}(t-1) \right. \\ & \left. - \mu \mathcal{G}_{N_r}^H(t-1) \nabla \mathcal{G}_{N_r}(t-1) - \mu \nabla \mathcal{G}_{N_r}^H(t-1) \mathcal{G}_{N_r}(t-1) \right\} + \mathcal{O}(\mu^2) \end{aligned} \quad (5.17)$$

Separating terms with and without μ in (5.17) and using them as \mathcal{B} and \mathcal{A} respectively in (5.14) enables us to approximate $\left(\mathcal{G}_{N_r}^H(t) \mathcal{G}_{N_r}(t) \right)^\#$ without an expensive complexity.

Remark: Another way to reduce the numerical cost would be to choose a noise subspace generating matrix $\tilde{\mathcal{G}}_{N_r}$ that is 'non redundant' so that matrix $\tilde{\mathcal{G}}_{N_r}^H \tilde{\mathcal{G}}_{N_r}$ is invertible which allows us to replace the pseudo-inversion by the relatively simpler matrix inversion. To build matrix $\tilde{\mathcal{G}}_{N_r}$, one can follow similar steps as for the minimum CR method in [76].

5.2.2 Gradient step optimization

The choice of the optimization step μ is really important to achieve good convergence performance. Choosing μ too large can cause the divergence of the algorithm and at the same time, a too small μ will induce a poor convergence rate. To avoid these problems, one can use the fact that we are using a gradient descent method which allows us to derive an optimal step that minimizes:

$$\hat{\mu} = \arg \min_{\mu} \mathcal{J}(\mathbf{h}(t+1)) \quad (5.18)$$

Let's start by replacing $\mathbf{h}(t+1)$ by its formula from (5.6) in (5.5) which yields:

$$\begin{aligned} \mathcal{J}(\mathbf{h}(t+1)) = & \left(\mathbf{h}(t) - \mu \nabla \mathcal{J}(\mathbf{h}(t)) \right)^H \mathcal{Q}_z(t+1) \left(\mathbf{h}(t) - \mu \nabla \mathcal{J}(\mathbf{h}(t)) \right) \\ & + \lambda \left\| \mathbf{h}(t) - \mu \nabla \mathcal{J}(\mathbf{h}(t)) \right\|_p^p \end{aligned} \quad (5.19)$$

hence, the derivative of the previous formula w.r.t. μ is:

$$\begin{aligned} \frac{\partial \mathcal{J}(\mathbf{h}(t+1))}{\partial \mu} &= \mathcal{K}(\mu) \\ &= \left\{ 2 \left(\mu \nabla \mathcal{J}(\mathbf{h}(t)) - \mathbf{h}(t) \right)^H \mathbf{Q}_z(t+1) - \mu \lambda \tilde{\mathbf{r}}^H \right\} \nabla \mathcal{J}(\mathbf{h}(t)) \end{aligned} \quad (5.20)$$

where

$$\tilde{r}_i = \text{sign} \left(h_i(t) - \mu \nabla \mathcal{J}(\mathbf{h}(t))_i \right) \left| h_i(t) - \mu \nabla \mathcal{J}(\mathbf{h}(t))_i \right|^{p-1}$$

for $i = 1, \dots, N_r(L+1)$.

Finally, we can use a Newton method to approximate the optimal solution of (5.18) at every iteration with

$$\mu_t = \mu_{t-1} - \mathcal{K}(\mu_{t-1}) \frac{\mu_{t-1} - \mu_{t-2}}{\mathcal{K}(\mu_{t-1}) - \mathcal{K}(\mu_{t-2})} \quad (5.21)$$

The resulting algorithm is summarized in the table below.

Algorithm 13 blind sparse channel identification algorithm based on (approximated) adaptive maximum a posteriori approach MAP-adapt & AMAP-adapt

Require: $\mathbf{x}(t)$ data vector, β the forgetting factor, λ the sparsity parameter, $\mathbf{h}(t-1)$, $\mathbf{Q}_z(t-1)$ and $\mathbf{Z}(t-1)$ from the previous iteration.

Ensure: $\mathbf{Q}_z(t)$, $\mathbf{Z}(t)$ and the sparse channel $\mathbf{h}(t)$

- 1: Update $\mathbf{Z}(t)$ by $\begin{cases} \left(\mathcal{G}_{N_r}^H(t) \mathcal{G}_{N_r}(t) \right)^\# & \text{if MAP-adapt} \\ \text{use (5.14) and (5.17)} & \text{if AMAP-adapt} \end{cases}$
 - 2: Build $\bar{\mathcal{X}}_{N_r}(t)$ as explained in (5.10) and (5.11)
 - 3: Update $\mathbf{Q}_z(t)$ using (5.13)
 - 4: Calculate the gradient $\nabla \mathcal{J}(\mathbf{h}(t-1))$ given by (5.7)
 - 5: Update $\mathbf{h}(t)$ with (5.6) $\begin{cases} \text{fixed } \mu \\ \text{optimal } \mu \text{ using (5.21)} \end{cases}$
 - 6: Normalize $\mathbf{h}(t+1)$ w.r.t. $\|\mathbf{h}(t+1)\|_2 = 1$
-

5.3 Regularized deterministic maximum likelihood based joint estimation of MIMO channels and input data

In this section, we consider the problem of blind estimating both multiple-input multiple-output (MIMO) finite impulse response (FIR) channels and the transmitted data. Blind identification of MIMO FIR channels has been deeply studied most

of the times by generalization of the simple-input multiple-output (SIMO) solutions. Some solutions considered the extensions of various 'higher-order' methods such as [111, 112]. However, most of these methods have a lack of global convergence or/and poor estimation accuracy. Under some mild conditions, solutions have been proposed to identify MIMO-FIR systems up to a constant matrix within the framework of second order statistics. The subspace-based methods such as [83] are not robust in noisy scenarios that lack for a good disparity of channels. The linear prediction methods such as [113] are less sensitive to the presence of noise, they require large sample size even in the noiseless case.

Among the blind channel methods, we focus on deterministic maximum likelihood (DML) methods since they have the additional advantage of being high signal-to-noise ratio (SNR) efficient [114]. In addition, the input signals are considered as part of the unknown parameters with the channel coefficients, which is equivalent to the joint estimation. As major contributions to DML methods, we can cite the two-step maximum likelihood (TSML) [78], the iterative quadratic maximum likelihood (IQML) [115] and its dual algorithm proposed in [116] which considered simple-input multiple-output (SIMO) FIR channels. Another DML method, the maximum likelihood block algorithm (MLBA), has been proposed in [117] where for both the channels and in the symbols, least squares estimation is performed in an alternating manner. Following the same formulation, the Maximum Likelihood Adaptive Algorithm (MLAA) is derived in [118] which presents low-complexity in computation. The ML methods usually cannot be obtained in closed form and require an optimization in presence of local minima. In addition, the dimension of the problem increases with the sample size, which makes this approach not practical for large data size applications. However, ML approaches can be made very effective by including initialization procedure such as the subspace method or other sub-optimal approaches. Another important feature of the alternative formulation of DML is the facility to introduce any further information about the channel impulse response or the input signal to the cost function. For example, the finite alphabet properties was first considered with DML in [119–121]. However, the convergence of such methods is not guaranteed in general and the incorporation of the finite alphabet property often increases the number of local minima. Later, the authors in [122] proposed to use the Bayesian maximum a posteriori approach with a continuous probability distribution function that reflects the prior knowledge on the input sequence. We propose in this section to use the DML formulation for MIMO channels with different regularization such as the simplicity (instead of the finite alphabet property) or the sparsity of the transmitted the data and the sparsity of channels.

5.3.1 Blind deterministic maximum likelihood DML estimation approach

The DML approach assumes no statistical model for the input sequences. In other words, both the channel matrix \mathbf{H} and the input source vectors $\mathbf{s}_i(t)$ $i = 1, \dots, N_t$ are parameters to be estimated. Considering the MIMO FIR model expressed in Section 2.4, the DML problem can be stated as: given the observation $\mathbf{x}_N(t)$, we want to estimate:

$$\{\hat{\mathbf{H}}, \hat{\mathbf{s}}_N(t)\} = \arg \max f(\mathbf{x}_N; \mathbf{H}, \mathbf{s}_N) \quad (5.22)$$

where $f(\mathbf{x}_N; \mathbf{H}, \mathbf{s}_N)$ is the probability density function of the observation vectors parameterized by both the channel matrix \mathbf{H} and the input sources vector \mathbf{s}_N . In the case of zero-mean Gaussian noise with covariance $\sigma^2 \mathbf{I}$, the above DML estimator leads to the nonlinear least squares optimization:

$$\{\hat{\mathbf{H}}, \hat{\mathbf{s}}_N(t)\} = \arg \min_{\mathcal{T}(\mathbf{H}, \mathbf{s}_N(t))} \left\{ \left\| \mathbf{x}_N(t) - \mathcal{T}(\mathbf{H}) \mathbf{s}_N(t) \right\|_2^2 \right\} \quad (5.23)$$

The above function can also be written as :

$$\{\hat{\mathbf{H}}, \hat{\mathbf{s}}_N(t)\} = \arg \min_{\mathcal{T}(\mathbf{H}, \mathbf{s}_N(t))} \left\{ \left\| \mathbf{x}_N(t) - \mathcal{F}(\mathbf{s}_N(t)) \mathbf{h} \right\|_2^2 \right\} \quad (5.24)$$

where $\mathbf{h} = \text{vec}(\mathbf{H})$ is the vectorized version of the matrix \mathbf{H} . The operator $\mathcal{F}(\cdot)$ transforms a vector $\mathbf{s}_N(t)$ into an $NNr \times (L + N)Nt$ matrix, in such a way that: $\mathcal{F}(\mathbf{s}_N(t)) \mathbf{h} = \mathcal{T}(\mathbf{H}) \mathbf{s}_N(t)$.

Under the assumptions expressed in Chapter 5, $\mathcal{T}(\mathbf{H})$ is full rank column and the variables $(\mathbf{H}, \mathbf{s}_N(t))$ are identifiable up to a $N_t \times N_t$ constant full rank matrix [83] which we denote \mathbf{Q} . The identifiability condition for the DML approach is the same as that for the deterministic second-order subspace methods. The reason is that, when the noise is Gaussian (assumed true in DML), all information about the channel in the likelihood function resides in the second-order moments of the observations. Readers are referred to [83] for more detailed discussion about the identifiability of the MIMO FIR channel with the noise subspace method.

Resolving the ambiguity caused by the matrix \mathbf{Q} in second order based blind channel estimation of MIMO-FIR is equivalent to the instantaneous Blind Source Separation BSS problem [123]. Hence, the indeterminacy can be reduced to a complex-valued diagonal matrix and a real-valued permutation matrix.

The blind DML criterion as stated in Eq. (5.23) and Eq. (5.24) is complicated and non-convex for estimating jointly both parameters $(\mathbf{H}, \mathbf{s}_N(t))$. However, it is convex for each unknown parameter alone by supposing the other one fixed. Hence,

Eq. (5.23) and Eq. (5.24) can be resolved by alternatively optimizing over \mathbf{H} and $\mathbf{s}_N(t)$. This idea was proposed in many previous papers [115, 117, 118, 122] but for the SIMO case.

5.3.2 Regularized blind deterministic maximum likelihood DML estimation approach

In the case where the system is not time-varying and if the data sequence is long enough so that a reliable statistical model can be built, then, the SML method should be used, since in that case the statistical method outperforms the deterministic one in terms of estimation accuracy. However, in a fast fading environment, the data related to a given channel are not numerous, which makes a reliable statistical estimation less effective. In such a situation, the symbols are assumed arbitrary and a DML method is used. The regularized DML approach is a trade-off between DML and SML approaches, where we take advantage of some prior information about input data or/and transmission channel to enhance the DML results. Next we present different types of priors and how to include them to the DML criterion.

Simplicity and the finite alphabet property

The finite alphabet property in digital communication signals was considered in [119–121] with the DML approach. In this case, an alternating optimization is used to minimize the criterion given by:

$$\hat{\mathbf{s}}_N(t) = \arg \min_{\mathbf{s}_N(t) \in \mathcal{S}} \left\| \mathbf{x}_N(t) - \mathcal{T}(\mathbf{H})\mathbf{s}_N(t) \right\|_2^2 \quad (5.25)$$

$$\hat{\mathbf{H}} = \arg \min_{\mathbf{h}} \left\| \mathbf{x}_N(t) - \mathcal{F}(\mathbf{s}_N(t))\mathbf{h} \right\|_2^2 \quad (5.26)$$

where \mathcal{S} is the (discrete) domain of $\mathbf{s}_N(t)$ of cardinal $p^{Nt(N+L)}$ for a finite alphabet $f = \{\alpha_1, \dots, \alpha_p\}$ of cardinal p . The optimization in Eq. (5.26) is a linear least squares problem whereas the optimization in Eq. (5.25) is computationally expensive and can be achieved by using the Viterbi algorithm. The convergence of such approaches are not guaranteed due to the numerous local minima induced by the discrete set constraint. We propose to replace this constraint by the signal simplicity. The simplicity property was first introduced in [124] where we say that a signal is *simple* if most of its elements are equal to the extremes of the finite alphabet. Recently, the authors in [110] proposed a simplicity-based detector for finite alphabet source separation in both determined and underdetermined large-scale MIMO systems. They relaxed the problem of the finite alphabet constraint as stated in Eq. (5.25)

to a convex box constraint depending only of the constellation extremes $\{\alpha_1, \alpha_p\}$. The new optimization problem is given by:

$$\hat{\mathbf{r}} = \arg \min_{\mathbf{r}} \left\| \underline{\mathbf{x}}_N(t) - \underline{\mathcal{T}}(\mathbf{H}) \mathbf{B}_\alpha \mathbf{r} \right\|_2^2 \quad \text{subject to} \quad \mathbf{B}_1 \mathbf{r} = \mathbf{1}_{2N}, \quad r \geq 0 \quad (5.27)$$

where $\underline{\mathbf{s}}_N(t) = \mathbf{B}_\alpha \mathbf{r}$. The Matrices \mathbf{B}_α and \mathbf{B}_1 are defined by: $\mathbf{B}_\alpha = I_{2Nt(N+L)} \otimes [\alpha_1, \alpha_p]$ and $\mathbf{B}_1 = I_{2Nt(N+L)} \otimes [1, 1]$. The underlined notation is reserved to the complex-real transformation where $\underline{\mathcal{T}}(\mathbf{H})$, $\underline{\mathbf{x}}_N(t)$ and $\underline{\mathbf{s}}_N(t)$ are given by

$$\underline{\mathcal{T}}(\mathbf{H}) = \begin{bmatrix} \mathcal{R}(\mathcal{T}(\mathbf{H})) & -\mathcal{I}(\mathcal{T}(\mathbf{H})) \\ \mathcal{I}(\mathcal{T}(\mathbf{H})) & \mathcal{R}(\mathcal{T}(\mathbf{H})) \end{bmatrix} \quad \underline{\mathbf{x}}_N(t) = \begin{bmatrix} \mathcal{R}(\mathbf{x}_N(t)) \\ \mathcal{I}(\mathbf{x}_N(t)) \end{bmatrix} \quad \underline{\mathbf{s}}_N(t) = \begin{bmatrix} \mathcal{R}(\mathbf{s}_N(t)) \\ \mathcal{I}(\mathbf{s}_N(t)) \end{bmatrix}$$

In addition to the convexity of this formulation, the computation cost of the resulting detector does not depend on the constellation size [110].

Sparsity of the input signals

The sparsity property of the input signals was introduced earlier as a contrast function for blind source separation. Now, it is introduced as a regularization on Eq. (5.23) which will enhance the estimation and improve the robustness to outliers. If the sources are sufficiently sparse, the regularization can be carried out directly in the time domain by considering the LASSO problem (or basis pursuit equivalent problem). In this case, an alternating optimization is used to minimize the criterion given by:

$$\hat{\mathbf{s}}_N(t) = \arg \min_{\mathbf{s}_N(t)} \left\| \mathbf{x}_N(t) - \mathcal{T}(\mathbf{H}) \mathbf{s}_N(t) \right\|_2^2 + \lambda_s \left\| \mathbf{s}_N(t) \right\|_1 \quad (5.28)$$

$$\hat{\mathbf{H}} = \arg \min_{\mathbf{h}} \left\| \mathbf{x}_N(t) - \mathcal{F}(\mathbf{s}_N(t)) \mathbf{h} \right\|_2^2 \quad (5.29)$$

where λ_s is a weighting parameter which controls the trade-off between approximation error and sparsity level of the input signals. This formulation can also be interpreted as linear regression for which the coefficients have Laplace prior distributions (special case of GGD model introduced in Eq. (5.4) with $p = 1$ because of the convexity of the ℓ_1 -norm) that tends to set most of the coefficients close or equal to zero. The problem in Eq. (5.28) is convex but has no closed form solution. The Least Angle Regression (LARS) is a less greedy version of traditional forward selection methods for model selection problems and solves the LASSO problem efficiently.

In case where the input signals are not sufficiently sparse in the time domain, we can use sparse representations methods in order to transform the signals into a dictionary where they are more sparse. For instance, speech signals have more sparse representations in the time-frequency domain than in the time domain, therefore,

the STFT is used in this case. If we denote by Φ the considered transformation (dictionary) matrix, then the problem in Eq. (5.28) can be rewritten as:

$$\hat{\mathbf{r}} = \arg \min_{\mathbf{r}} \left\| \mathbf{x}_N(t) - \mathcal{T}(\mathbf{H})\Phi\mathbf{r} \right\|_2^2 + \lambda_r \|\mathbf{r}\|_1 \quad (5.30)$$

with $\underline{\mathbf{s}}_N(t) = \Phi\mathbf{r}$.

Representing the sparsity with the ℓ_1 -norm minimization is suitable due to the convexity property. However, other heuristic penalization functions (generally non-convex) were used in the literature to enhance the sparsity such as the Reweighted- ℓ_1 [43].

Sparsity of the channel impulse response

The sparsity of the channel impulse response was first studied in case of SIMO systems, then extended to the MIMO case such as in [50]. In order to exploit the sparsity *a priori* information of the channel impulse response, we introduce an additional cost function based on the GGD model of channel coefficients in the same manner as we did previously in case of sparse input signals. Under the assumption that all the components of \mathbf{H} are i.i.d, the GGD model is expressed in the same way as in Eq. (5.4). This model encourages the values that are close to zero and the sparsity of the channel \mathbf{H} . Taking the logarithm of the a posteriori estimator, leads to the objective function:

$$\hat{\mathbf{H}} = \arg \min \left\| \mathbf{x}_N(t) - \mathcal{F}(\mathbf{s}_N(t))\mathbf{h} \right\|_2^2 + \lambda_h \|\mathbf{h}\|_q^q \quad (5.31)$$

where λ_h is a weighting parameter which controls the trade-off between approximation error and sparsity represented by the ℓ_q -norm of the channel impulse response. This function has LASSO-like formulation and it is convex only for the case $q = 1$.

Other heuristic penalization functions can be used to enhance the sparsity such as the Reweighted ℓ_1 criterion [43], which generally outperforms the ℓ_1 -based criterion. The cost function in this case is given by:

$$\hat{\mathbf{H}} = \arg \min \left\| \mathbf{x}_N(t) - \mathcal{F}(\mathbf{s}_N(t))\mathbf{h} \right\|_2^2 + \lambda_h \sum_{i=1}^{N_r N_t (L+1)} \log(|h(i)| + \varepsilon) \quad (5.32)$$

where $\varepsilon > 0$ is a relatively small positive constant. Both cost functions in Eq. (5.31) and Eq. (5.32) are optimized under the constraint $\|\mathbf{h}\|_2^2 = 1$ to avoid the trivial null solutions.

5.3.3 Initialization and resolving ambiguities in subspace-based blind identification of MIMO channels

The ML method solutions usually cannot be obtained in closed form and require an optimization in presence of local minima. In addition, the dimension of the problem depends on the sample size, which makes this approach not practical for large data size applications. However, ML approaches can be made very effective by including some initialization procedure. In our case we have chosen the MIMO second-order based subspace method [83] because of its nice convergence properties.

Another problem in our formulation is the ambiguity of the blind identification MIMO problem itself. In fact, as we stated before the channel matrix \mathbf{H} is estimated up to a $N_t \times N_t$ full rank matrix \mathbf{Q} i.e.

$$\mathbf{H} = \hat{\mathbf{H}}_{\text{CS}} \mathbf{Q} \quad (5.33)$$

Hence, we cannot introduce directly penalty functions such as simplicity without resolving this ambiguity. The authors in [123] shows that resolving the ambiguity is equivalent to instantaneous Blind Source Separation BSS problem and they solve it using independent component analysis (ICA) under the assumption that transmitted sequences are statistically independent and non-Gaussian (which is generally true for communication sources). Hence, the indeterminacy can be reduced to a complex-valued diagonal scaling matrix and a permutation matrix.

In case of sparse MIMO channel \mathbf{H} , it is clear that this problem is similar to the sparse principal subspace estimation problem discussed in Chapter 3. In this case the subspace is represented by the estimation $\hat{\mathbf{H}}_{\text{CS}}$ and we search for the rotation matrix \mathbf{Q} that leads to the sparse channel \mathbf{H} . If the recovery conditions (high level of sparsity and $(L + 1)N_r > CN_t \log(N_t)$), as stated in the results of Chapter 3, are satisfied, then we can estimate the sparse channel \mathbf{H} up to a complex diagonal scaling matrix and a permutation matrix. We can use the second step of algorithms SS-FAPI or SGSS-FAPI in order to accomplish this task.

Finally, the resulting scaling and permutation indeterminacy is more complicated and requires additional information in order to be resolved. It is equivalent to the instantaneous BSS indeterminacy problem. In our case, we generalize the same assumptions used in the SIMO case such as having the first row of \mathbf{H} equal to ones and sort its columns depending on their ℓ_2 -norm.

5.4 Simulation results

Blind sparse SIMO channel identification

To assess the performance of the proposed solutions, we consider first the SIMO system with N_r outputs represented by a polynomial transfer function of degree L . The channel impulse response is a sparse sequence of random variables generated according to the Bernoulli-Gaussian distribution. In our simulation, we have used a sparsity level of 30%, which means that 30% of the vector \mathbf{h} entries are nonzeros as illustrated in Figure 5.1.

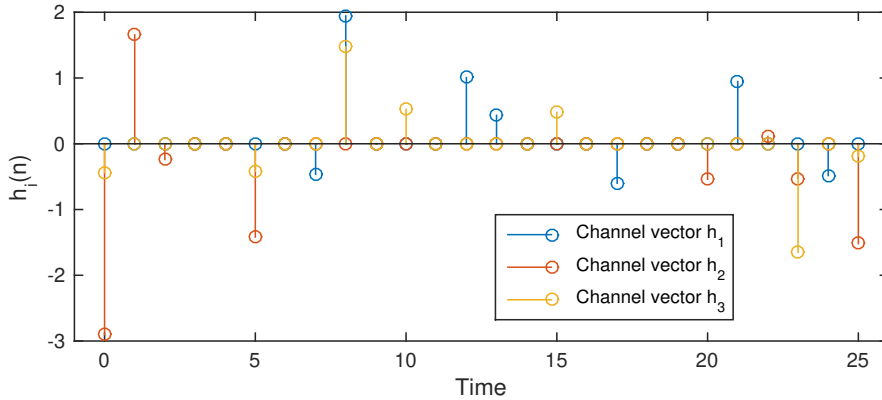


Figure 5.1: Example of sparse SIMO channel used in simulation with $N_r = 3$ and $L = 25$.

The input signal is a random binary sequence and the additive white Gaussian noise has a variance σ^2 chosen according to the target signal to noise ratio $SNR = 10 \log(\frac{\|\mathbf{h}\|_2^2}{\sigma^2})$. The used performance factor is the normalized mean-square error criterion given by

$$NMSE = \frac{1}{K} \sum_{k=1}^K 1 - \left(\frac{\hat{\mathbf{h}}_k^H \mathbf{h}}{\|\hat{\mathbf{h}}_k\|_2 \|\mathbf{h}\|_2} \right)^2 \quad (5.34)$$

with $K = 100$ is the number of Monte-Carlo runs. For the comparison, we use the CR-based algorithm [50] which we will refer to as SCR-adapt. MAP-adapt will refer to the first proposed algorithm and AMAP-adapt will refer to the version that uses the pseudo inverse approximation.

Figure 5.2 shows the NMSE evolution as function of time for the parameters $N_r = 3, L = 15, \beta = 0.98$ and $SNR = 20dB$. The optimization step is chosen fixed to $\mu = 0.0001$, then we use the optimal one calculated according to Eq. (5.21). It is clearly shown that the proposed algorithms outperform the SCR-adapt algorithm. In addition, the following observations can be made out of this experiment: (i) the

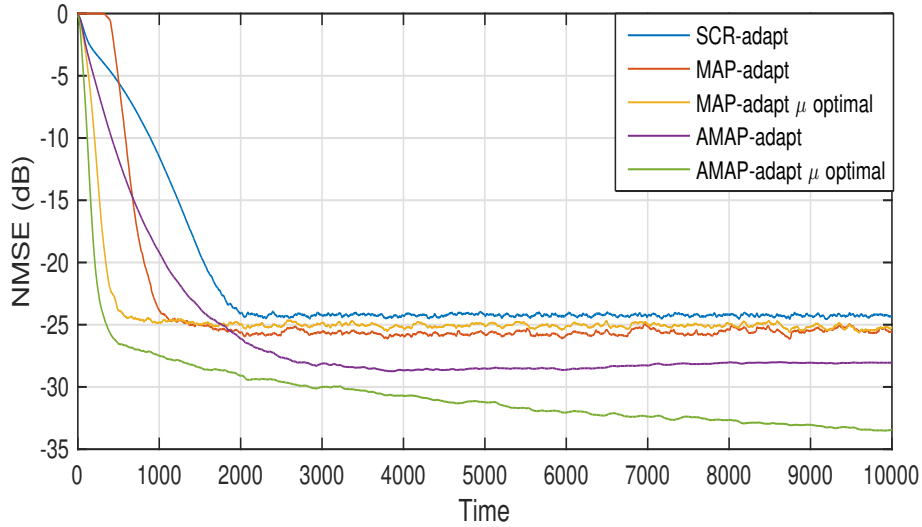


Figure 5.2: NMSE in dB versus time for $(N_r = 3, L = 15)$ and $SNR = 20dB$.

AMAP method is better than the MAP one due to the fact that the considered approximation allows us to control the slow variation of the update vector estimate contrary to the adaptive MAP using exact (batch) pseudo-inversion. In other words, the AMAP-adapt is better aligned with the spirit of the gradient method than the MAP-adapt. (ii) As expected, the optimal step size allows increasing the convergence rate of the considered algorithms. (iii) the best results are obtained by the AMAP-adapt with optimal step size which has the joint advantages of reduced complexity, faster convergence rate and lower steady state error as compared to the other methods.

Although we have changed the parameters to $N_r = 3, L = 30, \gamma = 0.95$ and $SNR = 20$, we can see in Figure 5.3 relatively the same NMSE evolution over time. The AMAP-adapt algorithm with optimal μ remains the best among all considered algorithms.

In Figure 5.4, the NMSE is plotted versus the SNR after $T = 10000$ snapshots for a SIMO system with $N_r = 3$ and $L = 15$. Generally, our algorithms MAP-adapt and AMAP-adapt keep having better performance than the SCR-adapt algorithm for moderate and high SNRs.

In order to illustrate the behavior of the AMAP algorithm in case of overestimation of the channel order, we consider a system with $N_r = 3, L = 60$ and $SNR = 20$. Figure 5.5 shows the robustness of the AMAP-adapt algorithm for a channel order overestimation by 15 and 30, respectively.

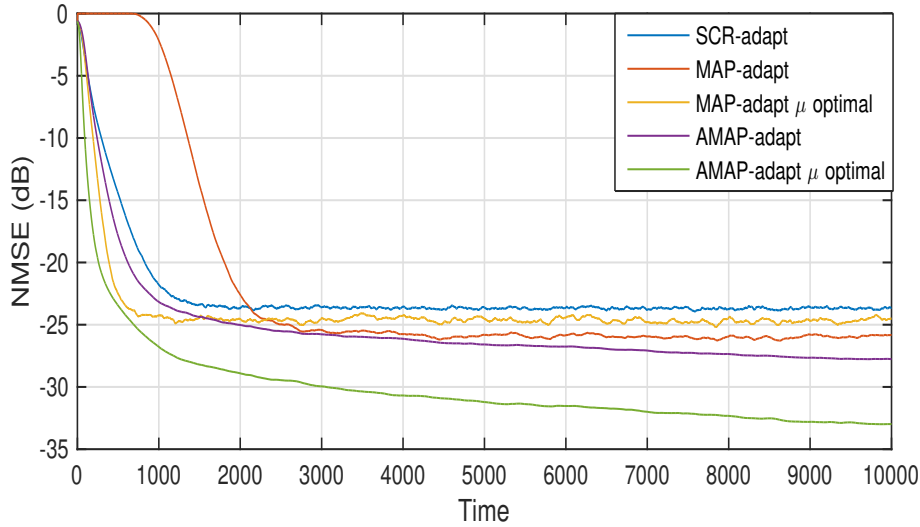


Figure 5.3: NMSE in dB versus time for $(N_r = 3, L = 30)$ and $SNR = 20dB$.

Blind joint estimation of MIMO channels and input data

We consider now the MIMO problem with N_t transmitters and N_r receivers and the channels are represented by a polynomial transfer function of maximum degree L . The channels impulse responses are generated randomly according to a Gaussian distribution in the non-sparse case. Sparse channels impulse responses are generated according to the Bernoulli-Gaussian distribution with 30% of non-zeros elements.

All the proposed criteria for the MIMO problem are convex with respect to the channel or the input data separately. Hence, for the optimization, we have used the Matlab CVX toolbox [125].

In the first simulation, we consider a real-valued case with a Gaussian noise, a real non-sparse channel with $N_t = 3, N_r = 8, L = 10$. We consider a BPSK constellation which will be used for the simplicity prior with $T = 1000$ received symbols. We have used as performance factors the NMSE (generalized from the SIMO case to the MIMO) of the estimated channels and the Bit Error Rate (BER) of the estimated input signals. The proposed regularized DML method which in this case consider the simplicity prior (BPSK constellation) is compared to the initialization subspace method, the least squares LS solution and the oracle solution. We have considered two iterations for the regularized DML and the LS solutions.

It is clear in Fig. 5.6 that using the simplicity prior in the DML formulation enhances the performance in terms of NMSE and BER. Furthermore, we can reach the oracle performance for a certain SNR level (above 13dB). Same observations can be made in Fig. 5.7 where we have considered a 4-QAM modulation, circularly

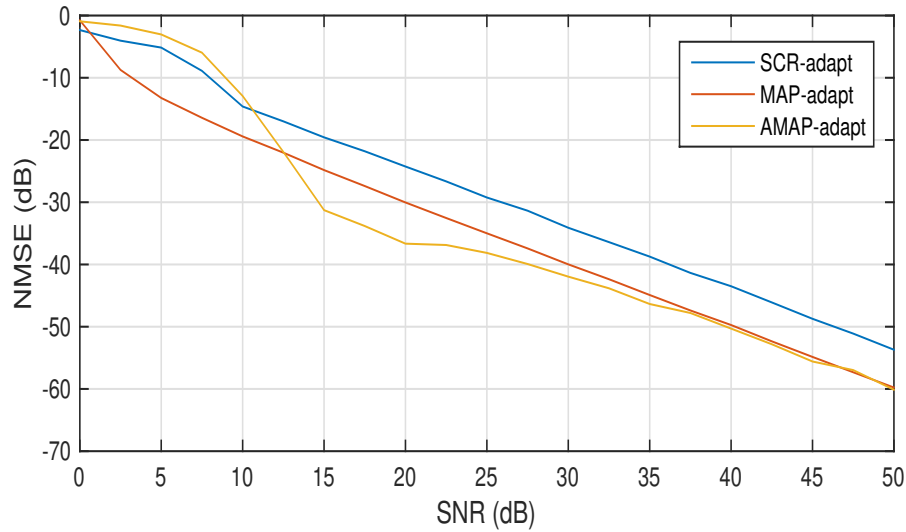


Figure 5.4: NMSE in dB versus SNR en dB for $(N_r = 3, L = 15)$.

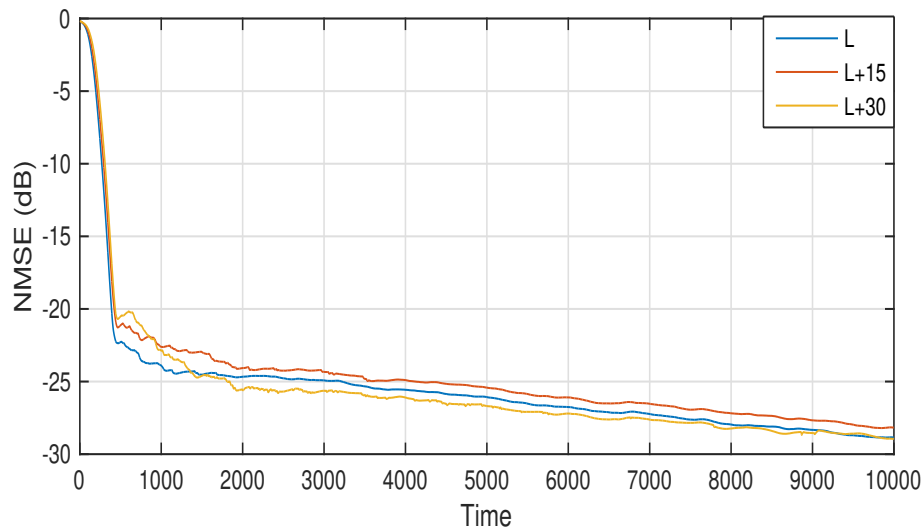


Figure 5.5: NMSE in dB of AMAP-adapt algorithm versus time for $(N_r = 3, L = 60)$ and $SNR = 20dB$.

symmetric complex Gaussian noise and a complex non-sparse channel with $(N_t = 3, N_r = 8, L = 10)$ and $T = 1000$. In this case, we need a much higher SNR level to see the impact of the proposed approach.

In both previous simulations, we have considered only one iteration in our regularized DML approach. However, we can use multiple iterations to have a better performance.

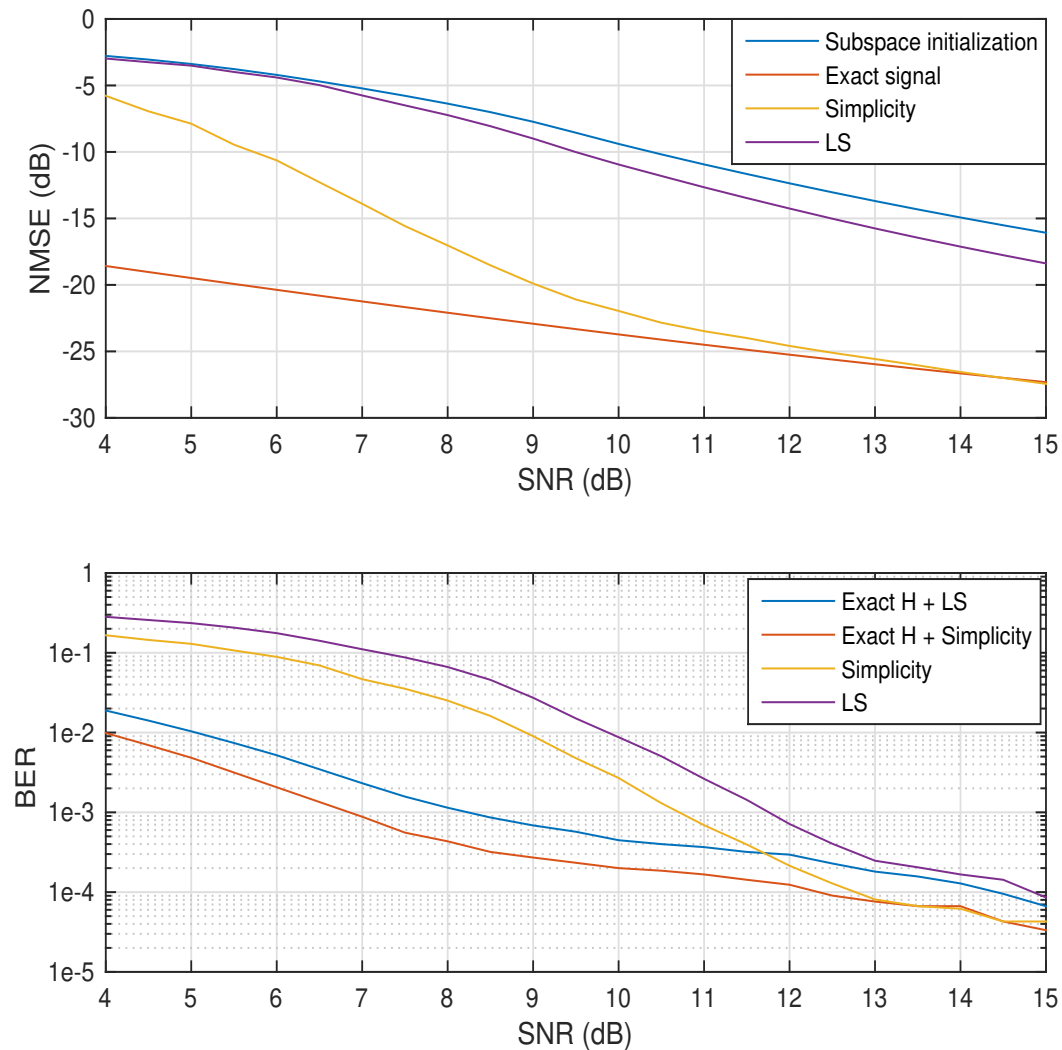


Figure 5.6: NMSE in dB and BER performance of the regularized-DML proposed approach versus SNR for BPSK modulation and $(N_t = 3, N_r = 8, L = 10)$ and $T = 1000$.

Fig. 5.8 shows the results of using 1, 2, 5 and 10 iterations of the simplicity prior for the case of $(N_t = 3, N_r = 8, L = 10)$ and $T = 1000$. It is clear how increasing the number of iterations improves the performance especially for the first ones. In terms of NMSE, we can observe that the amount of SNR needed to reach the oracle performance is going lower with the increase of the iterations number. In terms of BER, same can be made in addition to outperforming the LS oracle performance.

Now we consider, in addition to the simplicity prior, the sparsity of the channels impulse responses. We reuse the same parameters of the first simulation with longer channels $L = 20$ which have 30% of their elements non-zeros. Fig. 5.9 shows

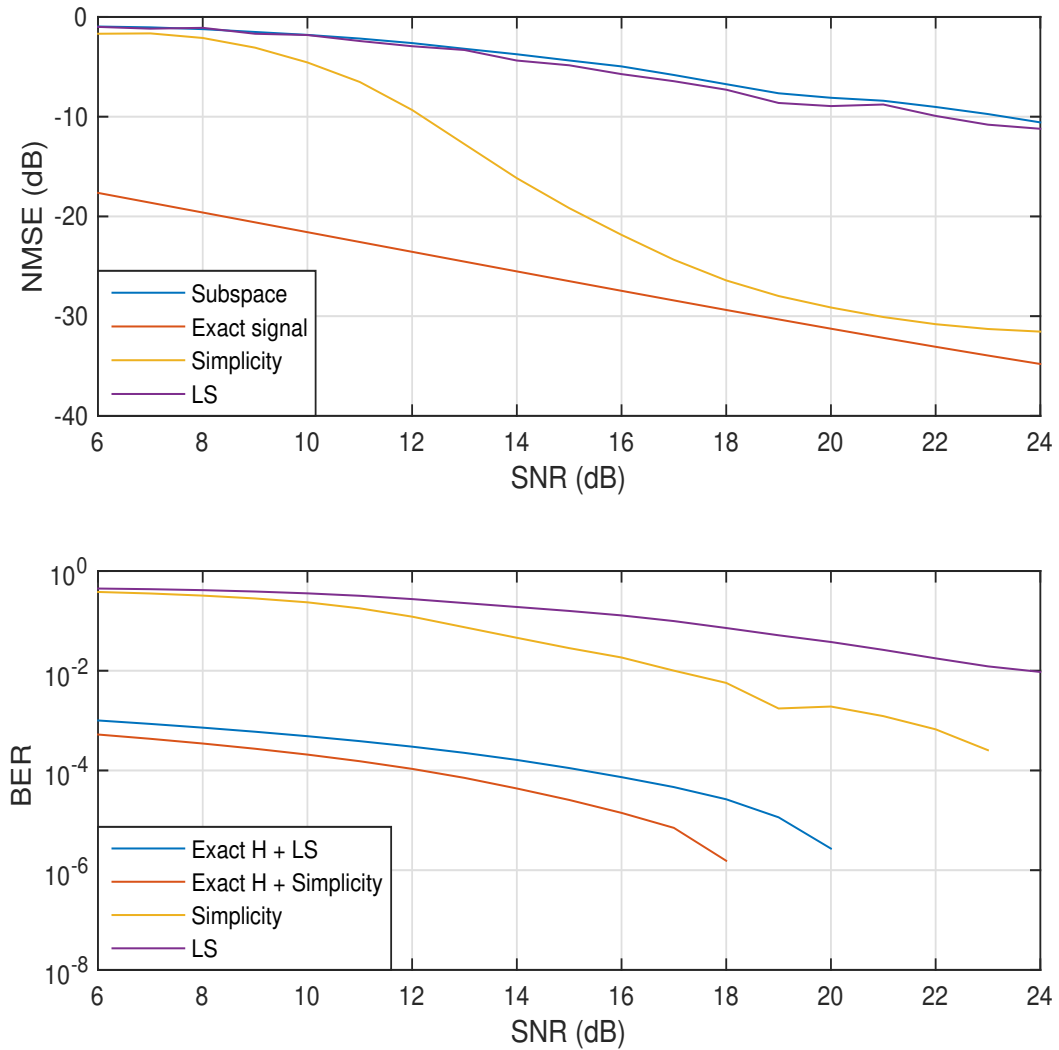


Figure 5.7: NMSE in dB and BER performance of the regularized-DML proposed approach versus SNR for 4-QAM modulation and $(N_t = 3, N_r = 8, L = 10)$ and $T = 1000$.

the influence of combining both simplicity and sparsity of channels ($\lambda_h = 0.5$) on the NMSE and the BER. Adding the sparsity prior allows us to reach even better performance in terms of NMSE and BER in both the oracle case and the full blind case.

In the case of sparse signals, we will use the mean squared error (MSE) $MSE = \frac{1}{T} \mathbb{E} \left\{ \|\mathbf{s}_N - \hat{\mathbf{s}}_N\|_2^2 \right\}$ between the original signal and the estimated one as a performance factor. Fig. 5.10 shows the improved performance of the proposed approach in case of sparse *a priori* on the input signals compared to the least-squares method with $(N_t = 3, N_r = 8, L = 10)$ and $T = 1000$.

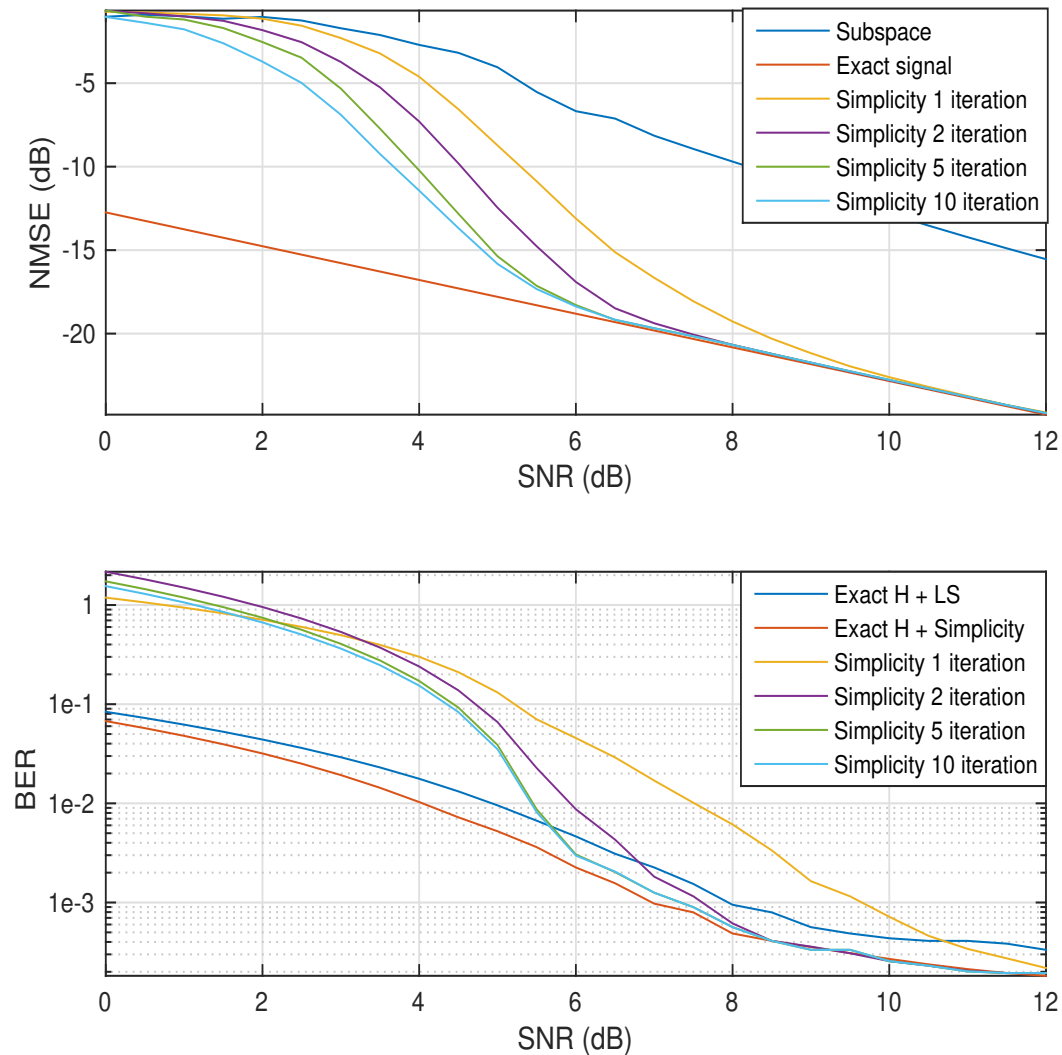


Figure 5.8: NMSE in dB and BER performance of the regularized-DML proposed approach with different number of iterations versus SNR for BPSK modulation and $(N_t = 3, N_r = 8, L = 10)$ and $T = 1000$.

In the next simulation, in addition to the sparsity of the input signals, we consider longer $L = 20$ and sparse channels with 30% of non-zeros elements. Hence, we will use the sparse regularization DML approach on both the channels and the signals. Fig. 5.11 illustrates how introducing the double sparsity prior enhances the performance.

In the previous simulations, we have chosen ad-hoc parameters λ_s and λ_h . This choice has an important influence of the performance of the proposed formulation. Some solutions can be adopted from the literature [7] for choosing the "best" LASSO regularization parameter.

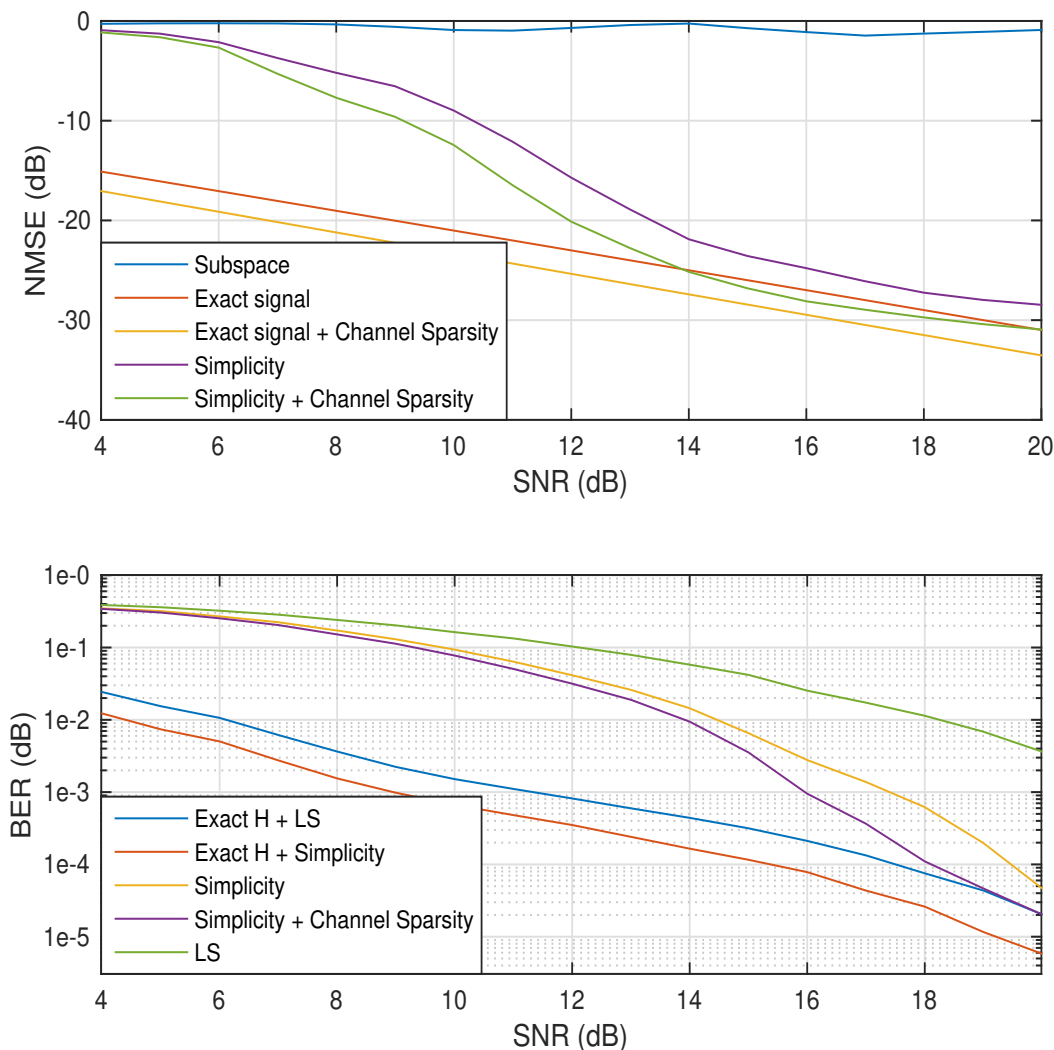


Figure 5.9: NMSE in dB and BER performance of the regularized-DML proposed approach versus SNR for BPSK modulation and sparse channel with $(N_t = 3, N_r = 8, L = 20)$ and $T = 1000$.

5.5 Conclusion

In this chapter, we have considered the problem of blind identification of FIR systems. First, we consider the SIMO case, where the sparsity a priori on the channel coefficients channel is used to adaptively estimate the channel impulse response. A MAP approach combined with an adaptive gradient descent method is applied to solve the problem. We have also proposed improvements to enhance the computational complexity and the convergence speed of our solution. The proposed algorithms MAP-adapt and AMAP-adapt have improved the estimation accuracy

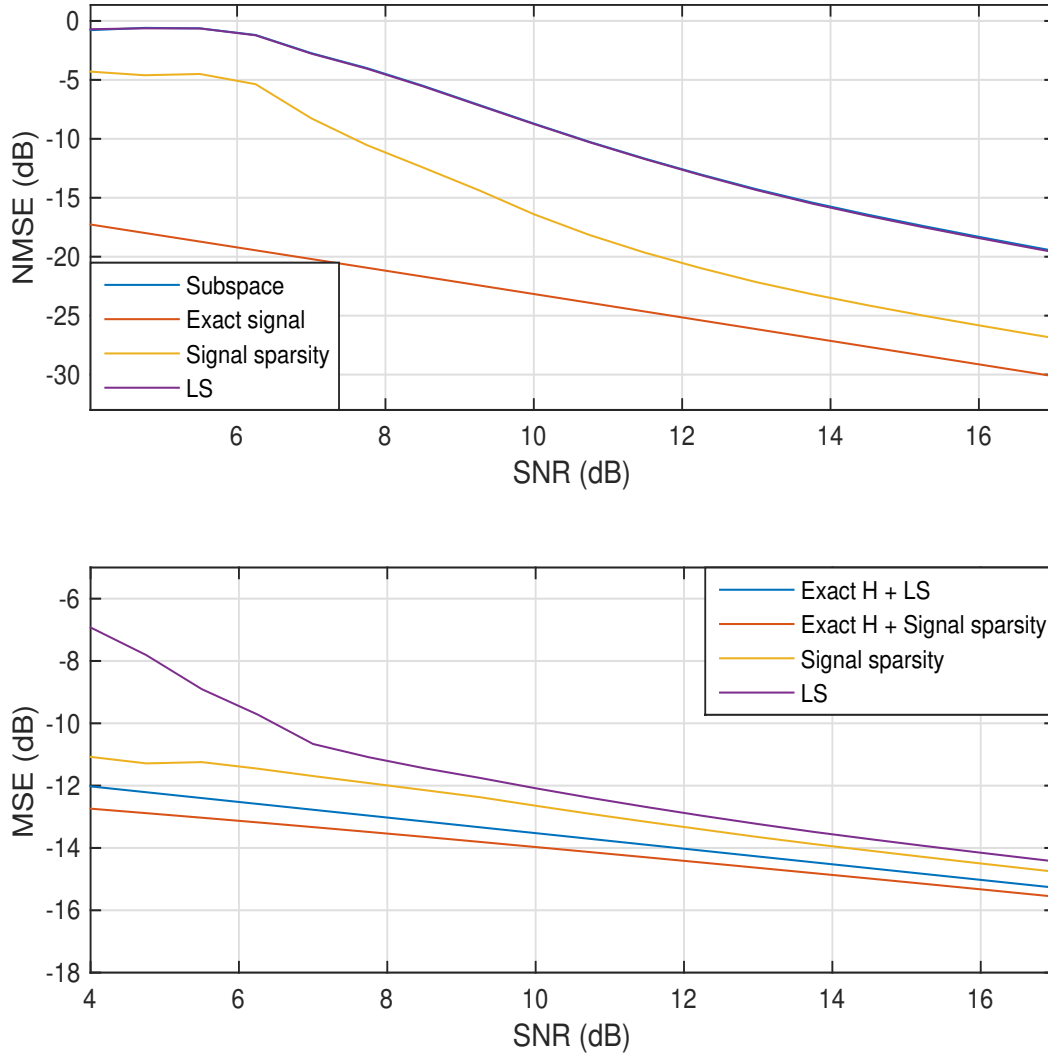


Figure 5.10: NMSE in dB and MSE in dB performance of the regularized-DML proposed approach versus SNR for sparse signals with $(N_t = 3, N_r = 8, L = 10)$ and $T = 1000$.

as compared to the adaptive CR method. For the MIMO case, we have presented a bilinear approach based on the regularized DML formation of the problem. This formulation has the advantage of alternatively estimating the channel impulse responses and the transmitted data while adding the *a priori* information about the problem as a regularization penalty. Different *a priori* are considered: the finite alphabet simplicity or the sparsity of the transmitted data, the sparsity of the channels finite responses. As an initialization of our blind framework, we have proposed to use the subspace blind identification channel method followed by a step to resolve its full rank matrix ambiguity. An iterative convex optimization is applied

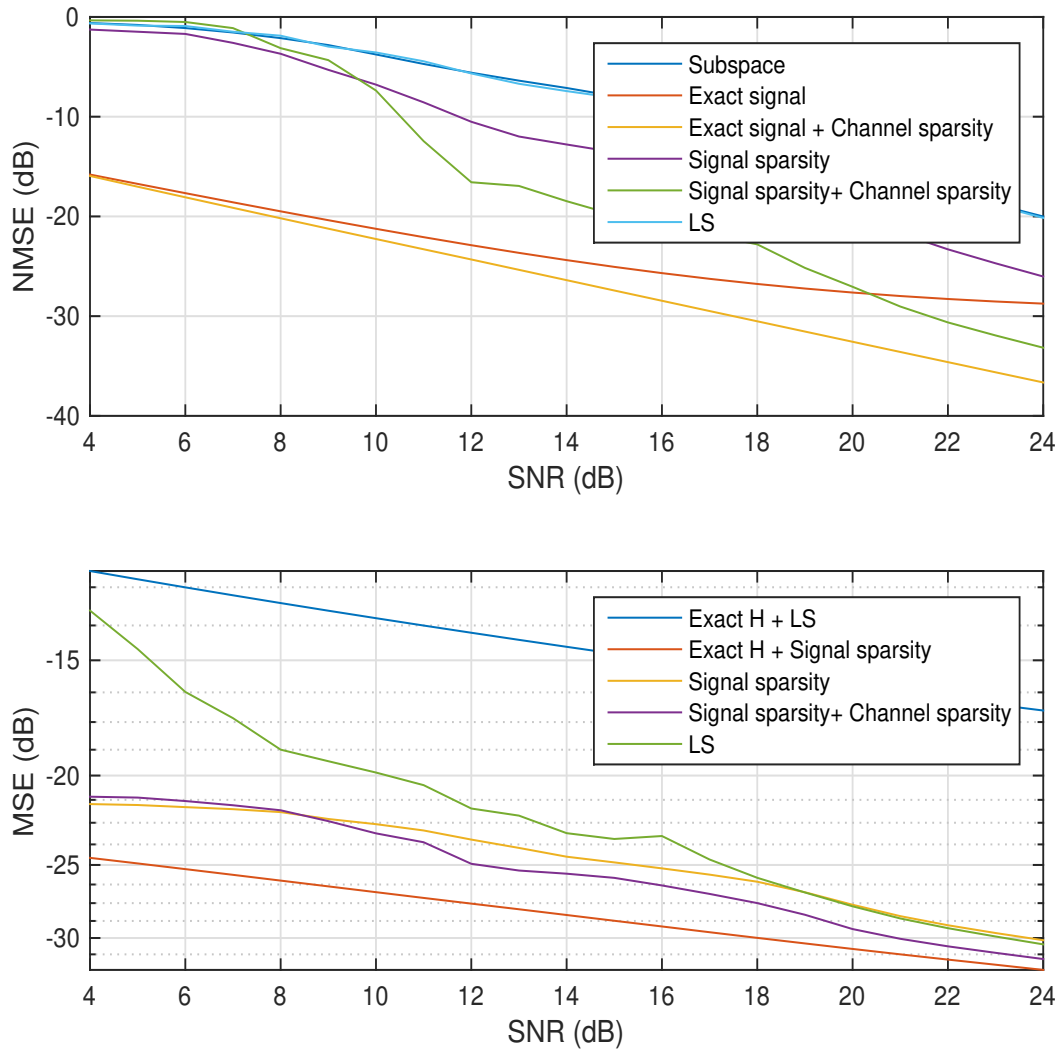


Figure 5.11: NMSE in dB and MSE in dB performance of the regularized-DML proposed approach versus SNR for sparse signals and sparse channels with $(N_t = 3, N_r = 8, L = 20)$ and $T = 1000$.

over the channel and the transmitted data. The proposed method has improved the estimation accuracy in terms of both NMSE and BER.

Conclusions & Perspectives

Contents

6.1	Conclusions	113
6.2	Perspectives	115

6.1 Conclusions

Blind methods are seen as the answer to many of modern signal and image processing problems. This interest arises from a number of applications such as in data communications, speech recognition, image restoration, seismic signal processing, etc. At the same time, the new advances in sparse representations theory and applications make them attractive to signal processing researchers. This thesis is motivated by the new opportunities in sparse representations field applied to blind system identification problems and the different challenges to be addressed to make them operational. Also, as we are expecting more and more notable increase in the dimensions of multidimensional signal processing problems, we have focused on solutions that have low computational cost and can be used in an adaptive scheme. Hence, the key objective of this thesis is to analyze the effect of sparsity prior information on blind system identification problems and to propose new low cost solutions suitable for adaptive applications. The PhD report can be summarized as follows:

In Chapter 1, we have first introduced the motivations and the objective of this thesis in general. Then, we gave a scope of the problems that have been studied in this thesis. We presented a brief development chronology of the multidimensional and array signal processing, especially subspace methods which have been used in many of the proposed solutions. We have also discussed how the sparsity was first introduced to statistical and signal processing fields and the most famous application where the sparsity integration was impressive.

In Chapter 2, we have introduced the three main investigated problems in this thesis and the corresponding state-of-the-art. First, the problem of subspace track-

ing algorithms under a sparsity constraint on the weight matrix is discussed. We introduced different solutions from the state-of-the-art such as classical principal subspace trackers (PAST, OPAST and FAPI), SPCA algorithms and the ℓ_1 -PAST method. The second discussed problem was blind source separation where we have introduced the classical ICA based separation solutions. Then, we showed how sparse decomposition techniques affected this problem and led to SCA and MCA based separation solutions. The third problem treated is blind FIR channel identification where we exposed the SIMO/MIMO model. We presented three classical approaches to this problem: the TSML method, CR method and noise subspace method. For the sparse channel problem, we have presented some methods from the state-of-the-art, which are, in general, just an adaptation of the classical methods with additional constraints to induce the sparsity. In each discussed problem, We have stressed weak and strong points of the presented literature solutions from point of performance and computational complexity.

Chapter 3 was dedicated to the principal subspace tracking problem under sparsity constraint of the weight matrix. We exploit the sparsity information to design multiple algorithms. First, the sparse subspace is considered non-orthogonal which is most likely the case in blind source separation with a sparse mixing matrix. We have proposed three algorithms in this case: SS-FAPI, SS-FAPI2 and SGSS-FAPI. Then, we consider the orthogonal case which is much closer to SPCA case and we have proposed two algorithms: OSS-FAPI and GSS-FAPI. Compared to the literature, our algorithms have the advantage of low computational cost and improved performances in terms of subspace estimation accuracy and the sparsity of the results. They allow us to recover the ground truth sparse mixing matrix under some mild constraints which we have discussed. The diversity of the proposed methods makes them adaptable to many applications depending on the problem's imposed constraints.

In chapter 4, the problem of blind adaptive sparse source separation has been studied. The sparsity prior information about the sources is used to allow an adaptive blind separation. Based on a two step approach, we project the data on the signal subspace in the first step. In the second step, we enhance the sparsity of the source signals which is represented by an ℓ_1 criterion. This criterion is optimized by the Natural gradient method in DS-OPAST algorithm. An adaptive method based on Shear and Givens rotations is used in SGDS-FAPI algorithm. Different extensions of these two algorithms were also presented to reduce the complexity and enhance the tracking capabilities. In addition to the low computational cost, numerical simulations have shown improved performance as compared to state-of-the-art solutions.

Chapter 5 is devoted to the problem of blind identification of FIR systems. First, we consider the SIMO case, where the sparsity a priori on the channel coefficients channel is used to adaptively estimate the channel impulse response. A MAP approach is applied to solve the problem based on an adaptive gradient decent method. Improvements have been also proposed to enhance the computational complexity and the convergence speed of our solution. The proposed algorithms MAP-adapt and AMAP-adapt have improved the estimation accuracy as compared to the adaptive CR method.

For the MIMO case, we present a bilinear approach based on a regularized DML formulation of the problem. This formulation allows us to alternatively estimate the channel impulse responses and the transmitted data using the *a priori* information about the problem as a regularization penalty. Different *a priori* are considered: the finite alphabet simplicity or the sparsity of the transmitted data, the sparsity of the channels finite responses. We proposed to use as an initialization a subspace method followed by a step to resolve its full rank matrix ambiguity. Then, an iterative convex optimization is done over the channel and the transmitted data. The proposed method has improved the estimation accuracy in terms of both NMSE and BER.

6.2 Perspectives

Short-term perspectives

Our short-term perspectives generally aim to improve the performance of the proposed algorithms for each problem treated in terms of estimation efficiency and computational cost.

First, for the sparse subspace tracking problem, both algorithms GSS-FAPI and SGSS-FAPI use predefined Matlab optimization functions. We can develop the calculation even further and propose a less time consuming solution based on gradient descent method or a Newton method if we replace the ℓ_1 -norm with a more smooth penalty function. This suggestion holds also for the other proposed algorithms such as SGDS-FAPI. The proposed methods where based on a two step approach which leads to similar subspace performance as the subspace tracker used in the first step. We are interested to discuss the situations where solving the problem in a unique step may be more efficient than doing it in a two-step scheme as we suggested.

Second, for the blind source separation problem, we have some ideas about the combination of priors information and their impact of the performance. For instance, the sources can be sparse and independent at the same time. Would the combination of the two priors enhance the separation performance ?. This can also include the

simplicity prior and the sparsity of the mixing matrix.

Third, further investigation is necessary for the proposed regularized DML solution to the blind joint data estimation and channel identification problem. We suggest to study the parameter's influence on the performance and to design more adapted optimization methods (we have used the CVX Matlab toolbox [125]).

Mid-term perspectives

Noise (minor) subspace tracking is directly related to adaptive blind MIMO channel identification problem. Unlike the principal subspace, the noise subspace is more difficult to track. Hence, it is challenging to develop sparse noise subspace tracking methods and apply them in the context of blind channel identification.

The exact recovery of the ground truth sparse mixing matrix discussed in Chapter 3 is a powerful result which needs further investigations. We should be able to give more tight necessary conditions and use this result in practical applications.

We are interested also in the underdetermined model for the blind source separation as an extension to our work. Until now, we have been using subspace methods which force us to consider only overdetermined systems. However, sparsity has been already successfully applied to such systems, and we should give this case more thoughts.

Connexion with the Natural Gradient

It was shown in [90] that natural gradient learning is stable, statistically efficient and works better than ordinary gradient learning, thus, it is widely used in the field of blind source separation. Therefore, we want to show that the gradient step used in SS-FAPI is similar to the natural gradient step introduced in [126] [90].

We now define a Riemannian structure of the set of all $d \times d$ non-singular matrices, which forms a Lie group denoted by $Gl(d)$, for the purpose of introducing the natural gradient learning rule. Let \mathbf{dQ} be a small deviation of a matrix from \mathbf{Q} to $\mathbf{Q} + \mathbf{dQ}$. First, we need to introduce an inner product at \mathbf{Q} which defines the squared norm of \mathbf{dQ} as $\langle \mathbf{dQ}, \mathbf{dQ} \rangle_{\mathbf{Q}}$.

After multiplying by \mathbf{Q}^{-1} from the left, \mathbf{Q} is mapped to $\mathbf{Q}^{-1}\mathbf{Q} = \mathbf{I}_p$, and $\mathbf{Q} + \mathbf{dQ}$ is mapped to $\mathbf{Q}^{-1}(\mathbf{Q} + \mathbf{dQ}) = \mathbf{I}_p + \mathbf{Q}^{-1}\mathbf{dQ}$. The Lie group invariance requires that the metric is kept invariant under this change and leads to the Riemannian metric structure:

$$\langle \mathbf{dQ}, \mathbf{dQ} \rangle_{\mathbf{Q}} = \langle \mathbf{Q}^{-1}\mathbf{dQ}, \mathbf{Q}^{-1}\mathbf{dQ} \rangle_{\mathbf{I}} \quad (\text{A.1})$$

$$= \text{Tr}(\mathbf{dQ}^T \mathbf{Q}^{-T} \mathbf{Q}^{-1} \mathbf{dQ}) \quad (\text{A.2})$$

On the other hand, for the objective function $J_{SS}(\mathbf{Q}) = \|\mathbf{W}_{PS}\mathbf{Q}\|_1$, the gradient $\partial J_{SS}(\mathbf{Q})$ is defined by

$$J_{SS}(\mathbf{Q} + \mathbf{dQ}) = J_{SS}(\mathbf{Q}) + \partial J_{SS} \circ \mathbf{dQ} \quad (\text{A.3})$$

with

$$\partial J_{SS} \circ \mathbf{dQ} = \text{Tr}(\partial J_{SS}^T \mathbf{dQ}) = \langle \partial J_{SS}, \mathbf{dQ} \rangle_{\mathbf{I}} \quad (\text{A.4})$$

Hence, the natural gradient $\partial \tilde{J}_{SS}$ should verify

$$\langle \partial J_{SS}, \mathbf{dQ} \rangle_{\mathbf{I}} = \langle \partial \tilde{J}_{SS}, \mathbf{dQ} \rangle_{\mathbf{Q}} \quad (\text{A.5})$$

$$= \text{Tr}(\partial \tilde{J}_{SS}^T \mathbf{Q}^{-T} \mathbf{Q}^{-1} \mathbf{dQ}) \quad (\text{A.6})$$

which leads to

$$\partial \tilde{J}_{SS} = \mathbf{Q}\mathbf{Q}^T \partial J_{SS} \quad (\text{A.7})$$

This result is inspired from [90, theorem 6], where the author gives the relation between the natural gradient and the ordinary gradient for learning by means of information geometry in the matrix space (also explained in [126, Appendix B]). Finally, if we calculate $\frac{\partial J_{SS}}{\partial \mathbf{Q}} = \mathbf{W}_{PS}^T \text{sign}(\mathbf{W}_{PS}\mathbf{Q})$, then the natural gradient is given by $\frac{\partial \tilde{J}_{SS}}{\partial \mathbf{Q}} = \mathbf{Q}\mathbf{Q}^T \mathbf{W}_{PS}^T \text{sign}(\mathbf{W}_{PS}\mathbf{Q})$ which is exactly the gradient update that we have used in SS-FAPI :

$$\mathbf{Q}_{t+1} = \mathbf{Q}_t - \mu \mathbf{Q}_t \mathbf{Q}_t^T \mathbf{W}_{PS}^T \text{sign}(\mathbf{W}_{PS}\mathbf{Q}_t) \quad (\text{A.8})$$

Bibliography

- [1] Cisco, “Cisco visual networking index: Forecast and trends, 2017-2022,” Cisco, Tech. Rep., February 2019. (Cited on page 5.)
- [2] M. Aharon, M. Elad, and A. Bruckstein, “K-SVD: An algorithm for designing overcomplete dictionaries for sparse representation,” *Signal Processing, IEEE Transactions on*, vol. 54, pp. 4311 – 4322, 12 2006. (Cited on pages 6 and 14.)
- [3] Y. Li, S. Amari, A. Cichocki, and D. W. C. H. and, “Underdetermined blind source separation based on sparse representation,” *IEEE Transactions on Signal Processing*, vol. 54, no. 2, pp. 423–437, Feb 2006. (Cited on pages 6 and 14.)
- [4] M. Zibulevsky, “Sparse source separation with relative Newton method,” *Proc. ICA2003*, pp. 897–902, 01 2003. (Cited on pages 6 and 32.)
- [5] M. Elad and M. Aharon, “Image denoising via learned dictionaries and sparse representation,” in *2006 IEEE Computer Society Conference on Computer Vision and Pattern Recognition (CVPR’06)*, vol. 1, June 2006, pp. 895–900. (Cited on pages 6 and 14.)
- [6] J. Bobin, J. Starck, J. Fadili, and Y. Moudden, “Sparsity and morphological diversity in blind source separation,” *IEEE Transactions on Image Processing*, vol. 16, no. 11, pp. 2662–2674, Nov 2007. (Cited on pages 6, 14 and 32.)
- [7] T. Hastie, R. Tibshirani, and M. Wainwright, *Statistical Learning with Sparsity: The LASSO and Generalizations*. Chapman & Hall/CRC, 2015. (Cited on pages 6 and 108.)
- [8] E. Giusti, P. Samczynski, M.-P. Jarabo-Amores, and A. Capria, “Recent advances in array antenna and array signal processing for radar,” *International Journal of Antennas and Propagation*, vol. 1, 2018. [Online]. Available: <https://doi.org/10.1155/2018/6195704> (Cited on page 7.)
- [9] M. Viberg and P. Stoica, “Editorial note,” *Signal Processing*, vol. 50, no. 1-2, pp. 1–3, 1996. (Cited on page 8.)
- [10] R. Schmidt, “Multiple emitter location and signal parameter estimation,” *IEEE Transactions on Antennas and Propagation*, vol. 34, no. 3, pp. 276–280, March 1986. (Cited on pages 8, 20, 42 and 51.)

- [11] T. Tuncer and B. Friedlander, *Classical and Modern Direction-of-Arrival Estimation*. Elsevier Science, 2009. [Online]. Available: <https://books.google.fr/books?id=1aQbxKJI2CsC> (Cited on page 8.)
- [12] Z. Chen, G. Gokeda, and Y. Yu, *Introduction to Direction-of-arrival Estimation*, ser. Artech House signal processing library. Artech House, 2010. [Online]. Available: https://books.google.fr/books?id=_63d0OKsDsAC (Cited on page 8.)
- [13] H. Ghauch, T. Kim, M. Bengtsson, and M. Skoglund, “Subspace estimation and decomposition for large millimeter-wave MIMO systems,” *IEEE Journal of Selected Topics in Signal Processing*, vol. 10, no. 3, pp. 528–542, April 2016. (Cited on page 8.)
- [14] F. H. C. Tivive, A. Bouzerdoum, and M. G. Amin, “A subspace projection approach for wall clutter mitigation in through-the-wall radar imaging,” *IEEE Transactions on Geoscience and Remote Sensing*, vol. 53, no. 4, pp. 2108–2122, April 2015. (Cited on page 8.)
- [15] L. Gao, J. Li, M. Khodadadzadeh, A. Plaza, B. Zhang, Z. He, and H. Yan, “Subspace-based support vector machines for hyperspectral image classification,” *IEEE Geoscience and Remote Sensing Letters*, vol. 12, no. 2, pp. 349–353, Feb 2015. (Cited on page 9.)
- [16] B. Yang, “Projection approximation subspace tracking,” *IEEE Transactions on Signal Processing*, vol. 43, no. 1, pp. 95–107, 1995. (Cited on pages 9, 10, 21, 22, 23, 24, 27, 55 and 71.)
- [17] K. Abed-Meraim, A. Chkeif, and Y. Hua, “Fast orthonormal PAST algorithm,” *IEEE Signal Processing Letters*, vol. 7, no. 3, pp. 60–62, 2000. (Cited on pages 9, 10, 22, 23, 24, 43, 71, 75 and 78.)
- [18] P. Strobach, “Low-rank adaptive filters,” *IEEE Transactions on Signal Processing*, vol. 44, no. 12, pp. 2932–2947, 1996. (Cited on pages 9, 46, 66 and 71.)
- [19] Y. Hua, X. Yong, T. Chen, K. Abed-Meraim, and Y. Miao, “A new look at the power method for fast subspace tracking,” *Digit. Signal Process.*, vol. 9, no. 4, pp. 297–314, 1999. (Cited on pages 9, 10, 22 and 55.)
- [20] R. Badeau, G. Richard, B. David, and K. Abed-Meraim, “Approximated power iterations for fast subspace tracking,” in *Seventh International Symposium on Signal Processing and Its Applications, 2003. Proceedings.*, 2003. (Cited on pages 9, 24, 25, 54, 66 and 78.)

- [21] R. Badeau, B. David, and G. Richard, "Fast approximated power iteration subspace tracking," *IEEE Transactions on Signal Processing*, vol. 53, no. 8, pp. 2931–2941, 2005. (Cited on pages 9, 10, 24, 25, 42, 43, 53, 54, 58, 60, 70, 71, 75 and 78.)
- [22] P. Strobach, "Square-root QR inverse iteration for tracking the minor subspace," *IEEE Transactions on Signal Processing*, vol. 48, no. 11, pp. 2994–2999, 2000. (Cited on page 9.)
- [23] S. Attallah and K. Abed-Meraim, "Low-cost adaptive algorithm for noise subspace estimation," *Electronics Letters*, vol. 38, no. 12, pp. 609–611, 2002. (Cited on page 9.)
- [24] S. Attallah, "The generalized Rayleigh's quotient adaptive noise subspace algorithm: a Householder transformation-based implementation," *IEEE Transactions on Circuits and Systems II: Express Briefs*, vol. 53, no. 1, pp. 3–7, 2006. (Cited on page 9.)
- [25] E. Oja, "Simplified neuron model as a principal component analyzer," *Journal of Mathematical Biology*, vol. 15, no. 3, pp. 267–273, 1982. (Cited on pages 9 and 26.)
- [26] S. Attallah and K. Abed-Meraim, "Fast algorithms for subspace tracking," *IEEE Signal Processing Letters*, vol. 8, no. 7, pp. 203–206, 2001. (Cited on page 9.)
- [27] X. G. Doukopoulos and G. V. Moustakides, "Fast and stable subspace tracking," *IEEE Transactions on Signal Processing*, vol. 56, no. 4, pp. 1452–1465, 2008. (Cited on page 9.)
- [28] R. Badeau, G. Richard, and B. David, "Fast and stable YAST algorithm for principal and minor subspace tracking," *IEEE Transactions on Signal Processing*, vol. 56, no. 8, pp. 3437–3446, 2008. (Cited on page 9.)
- [29] M. Moonen, P. V. Dooren, and J. Vandewalle, "An SVD updating algorithm for subspace tracking," 1992. (Cited on page 9.)
- [30] E. M. Dowling, L. P. Ammann, and R. D. DeGroat, "A TQR-iteration based adaptive SVD for real time angle and frequency tracking," *IEEE Transactions on Signal Processing*, vol. 42, no. 4, pp. 914–926, April 1994. (Cited on page 9.)
- [31] G. W. Stewart, "An updating algorithm for subspace tracking," *IEEE Transactions on Signal Processing*, vol. 40, no. 6, pp. 1535–1541, June 1992. (Cited on page 9.)

- [32] I. Karasalo, “Estimating the covariance matrix by signal subspace averaging,” *IEEE Transactions on Acoustics, Speech, and Signal Processing*, vol. 34, no. 1, pp. 8–12, February 1986. (Cited on page 9.)
- [33] C. S. MacInnes, “Fast, accurate subspace tracking using operator restriction analysis,” in *Proceedings of the 1998 IEEE International Conference on Acoustics, Speech and Signal Processing, ICASSP '98 (Cat. No.98CH36181)*, vol. 3, May 1998, pp. 1357–1360 vol.3. (Cited on page 9.)
- [34] M. Elad, *Sparse and Redundant Representations: From Theory to Applications in Signal and Image Processing*, 1st ed. Springer Publishing Company, Incorporated, 2010. (Cited on pages 12 and 13.)
- [35] E. J. Candès, M. B. Wakin, and S. P. Boyd, “Enhancing sparsity by reweighted ℓ_1 minimization,” *Journal of Fourier Analysis and Applications*, vol. 14, no. 5, pp. 877–905, Dec 2008. (Cited on pages 12, 13, 38, 54 and 71.)
- [36] G. H. Mohimani, M. Babaie-Zadeh, and C. Jutten, “A fast approach for overcomplete sparse decomposition based on smoothed L0 norm,” *CoRR*, vol. abs/0809.2508, 2008. [Online]. Available: <http://arxiv.org/abs/0809.2508> (Cited on page 13.)
- [37] S. G. Mallat and Z. Zhang, “Matching pursuits with time-frequency dictionaries,” *IEEE Transactions on Signal Processing*, vol. 41, no. 12, pp. 3397–3415, Dec 1993. (Cited on page 14.)
- [38] Y. C. Pati, R. Rezaifar, and P. S. Krishnaprasad, “Orthogonal matching pursuit: recursive function approximation with applications to wavelet decomposition,” in *Proceedings of 27th Asilomar Conference on Signals, Systems and Computers*, Nov 1993, pp. 40–44 vol.1. (Cited on page 14.)
- [39] S. Chen, D. Donoho, and M. Saunders, “Atomic decomposition by basis pursuit,” *SIAM Journal on Scientific Computing*, vol. 20, no. 1, pp. 33–61, 1998. (Cited on page 14.)
- [40] I. Drori and D. L. Donoho, “Solution of ℓ_1 minimization problems by lars/homotopy methods,” in *2006 IEEE International Conference on Acoustics Speech and Signal Processing Proceedings*, vol. 3, May 2006, pp. III–III. (Cited on page 14.)
- [41] B. A. Olshausen, P. Sallee, and M. S. Lewicki, “Learning sparse image codes using a wavelet pyramid architecture,” in *Advances in Neural Information Processing Systems 13*, T. K. Leen, T. G. Dietterich, and V. Tresp, Eds. MIT

- Press, 2001, pp. 887–893. [Online]. Available: <http://papers.nips.cc/paper/1878-learning-sparse-image-codes-using-a-wavelet-pyramid-architecture.pdf> (Cited on page 14.)
- [42] E. J. Candes, J. Romberg, and T. Tao, “Robust uncertainty principles: exact signal reconstruction from highly incomplete frequency information,” *IEEE Transactions on Information Theory*, vol. 52, no. 2, pp. 489–509, Feb 2006. (Cited on page 14.)
- [43] E. J. Candes and M. B. Wakin, “An introduction to compressive sampling,” *IEEE Signal Processing Magazine*, vol. 25, no. 2, pp. 21–30, March 2008. (Cited on pages 14 and 100.)
- [44] D. L. Donoho, “Compressed sensing,” *IEEE Transactions on Information Theory*, vol. 52, no. 4, pp. 1289–1306, April 2006. (Cited on page 14.)
- [45] I. T. Jolliffe, N. T. Trendafilov, and M. Uddin, “A modified principal component technique based on the LASSO,” *Journal of Computational and Graphical Statistics*, vol. 12, no. 3, pp. 531–547, 2003. (Cited on page 15.)
- [46] A. d’Aspremont, L. E. Ghaoui, M. I. Jordan, and G. R. G. Lanckriet, “A direct formulation for sparse PCA using semidefinite programming,” *SIAM Review*, vol. 49, no. 3, pp. 434–448, 2007. (Cited on page 15.)
- [47] H. Zou, T. Hastie, and R. Tibshirani, “Sparse principal component analysis,” *Journal of Computational and Graphical Statistics*, vol. 15, no. 2, pp. 265–286, 2006. (Cited on page 15.)
- [48] M. Journée, Y. Nesterov, P. Richtik, and R. Sepulchre, “Generalized power method for sparse principal component analysis,” *Journal of Machine Learning Research*, vol. 11, pp. 517–553, 2008. (Cited on pages 15, 26, 58, 65 and 70.)
- [49] K. Benidis, Y. Sun, P. Babu, and D. P. Palomar, “Orthogonal sparse PCA and covariance estimation via procrustes reformulation,” *IEEE Transactions on Signal Processing*, vol. 64, no. 23, pp. 6211–6226, 2016. (Cited on pages 15, 26, 54, 58, 65, 70 and 71.)
- [50] A. Aïssa-El-Bey, D. Kimura, H. Seki, and T. Taniguchi, “Blind and semi-blind sparse channel identification in MIMO OFDM systems,” in *2011 IEEE International Conference on Communications (ICC)*, June 2011, pp. 1–5. (Cited on pages 15, 38, 90, 100 and 102.)

- [51] C. R. Berger, Z. Wang, J. Huang, and S. Zhou, "Application of compressive sensing to sparse channel estimation," *IEEE Communications Magazine*, vol. 48, no. 11, pp. 164–174, November 2010. (Cited on page 15.)
- [52] R. Roy and T. Kailath, "ESPRIT-estimation of signal parameters via rotational invariance techniques," *IEEE Transactions on Acoustics, Speech, and Signal Processing*, vol. 37, no. 7, pp. 984–995, July 1989. (Cited on page 20.)
- [53] Z. Lu and Y. Zhang, "An Augmented Lagrangian Approach for Sparse Principal Component Analysis," *arXiv e-prints*, p. arXiv:0907.2079, Jul 2009. (Cited on page 26.)
- [54] C. Wang and Y. M. Lu, "Online learning for sparse PCA in high dimensions: Exact dynamics and phase transitions," in *2016 IEEE Information Theory Workshop (ITW)*, 2016, pp. 186–190. (Cited on pages 26 and 70.)
- [55] W. Yang and H. Xu, "Streaming sparse principal component analysis," in *Proceedings of the 32Nd International Conference on International Conference on Machine Learning - Volume 37*, 2015, pp. 494–503. (Cited on pages 26, 58 and 70.)
- [56] X. Yang, Y. Sun, T. Zeng, T. Long, and T. K. Sarkar, "Fast STAP method based on PAST with sparse constraint for airborne phased array radar," *IEEE Transactions on Signal Processing*, vol. 64, no. 17, pp. 4550–4561, 2016. (Cited on pages 27, 60 and 69.)
- [57] P. Comon and C. Jutten, *Handbook of Blind Source Separation, Independent Component Analysis and Applications*. Academic Press (Elsevier), 2010. (Cited on pages 27, 28, 31, 73 and 82.)
- [58] M. Congedo, C. Gouy-Pailler, and C. Jutten, "On the blind source separation of human electroencephalogram by approximate joint diagonalization of second order statistics." *Clinical Neurophysiology*, vol. 119, no. 12, pp. 2677–2686, 2008. (Cited on page 27.)
- [59] A. Ozerov and C. Fevotte, "Multichannel nonnegative matrix factorization in convolutive mixtures for audio source separation," *IEEE Transactions on Audio, Speech, and Language Processing*, vol. 18, no. 3, pp. 550–563, 2010. (Cited on page 28.)
- [60] M. Valkama, M. Renfors, and V. Koivunen, "Advanced methods for I/Q imbalance compensation in communication receivers," *IEEE Transactions on Signal Processing*, vol. 49, no. 10, pp. 2335–2344, 2001. (Cited on page 28.)

- [61] G. Darmois, “Analyse générale des liaisons stochastiques: etude particulière de l’analyse factorielle linéaire,” *Revue de l’Institut International de Statistique / Review of the International Statistical Institute*, vol. 21, no. 1/2, pp. 2–8, 1953. [Online]. Available: <http://www.jstor.org/stable/1401511> (Cited on page 29.)
- [62] J.-F. Cardoso, “Dependence, correlation and Gaussianity in independent component analysis,” *J. Mach. Learn. Res.*, vol. 4, pp. 1177–1203, Dec. 2003. [Online]. Available: <http://dl.acm.org/citation.cfm?id=945365.964302> (Cited on page 30.)
- [63] A. Hyvarinen, “Fast and robust fixed-point algorithms for independent component analysis,” *IEEE Transactions on Neural Networks*, vol. 10, no. 3, pp. 626–634, May 1999. (Cited on page 30.)
- [64] J. F. Cardoso and A. Souloumiac, “Blind beamforming for non-Gaussian signals,” *IEE Proceedings F - Radar and Signal Processing*, vol. 140, no. 6, pp. 362–370, Dec 1993. (Cited on page 30.)
- [65] S. Amari, A. Cichocki, and H. H. Yang, “A new learning algorithm for blind signal separation,” in *Proceedings of the 8th International Conference on Neural Information Processing Systems*, ser. NIPS’95. Cambridge, MA, USA: MIT Press, 1995, pp. 757–763. [Online]. Available: <http://dl.acm.org/citation.cfm?id=2998828.2998935> (Cited on page 30.)
- [66] J. . Cardoso and B. H. Laheld, “Equivariant adaptive source separation,” *IEEE Transactions on Signal Processing*, vol. 44, no. 12, pp. 3017–3030, Dec 1996. (Cited on page 30.)
- [67] A. J. Bell and T. J. Sejnowski, “An information-maximization approach to blind separation and blind deconvolution,” *Neural Comput.*, vol. 7, no. 6, pp. 1129–1159, Nov. 1995. [Online]. Available: <http://dx.doi.org/10.1162/neco.1995.7.6.1129> (Cited on page 31.)
- [68] M. Zibulevsky and B. A. Pearlmutter, “Blind source separation by sparse decomposition in a signal dictionary,” *Neural Computation*, vol. 13, no. 4, pp. 863–882, April 2001. (Cited on pages 31, 73 and 90.)
- [69] J. Bobin, Y. Moudden, J. . Starck, and M. Elad, “Morphological diversity and source separation,” *IEEE Signal Processing Letters*, vol. 13, no. 7, pp. 409–412, July 2006. (Cited on page 32.)

- [70] J. Bobin, J.-L. Starck, Y. Moudden, and J. M. Fadili, “Blind Source Separation: the Sparsity Revolution,” in *Advances in Imaging and Electron Physics*, e. Peter Hawkes, Ed. Academic Press, Elsevier, 2008, vol. 152, pp. 221–306. (Cited on pages 32 and 73.)
- [71] B. Muquet, M. de Courville, and P. Duhamel, “Subspace-based blind and semi-blind channel estimation for OFDM systems,” *IEEE Transactions on Signal Processing*, vol. 50, no. 7, pp. 1699–1712, 2002. (Cited on page 33.)
- [72] Y. Huang, J. Benesty, and J. Chen, “A blind channel identification-based two-stage approach to separation and dereverberation of speech signals in a reverberant environment,” *IEEE Transactions on Speech and Audio Processing*, vol. 13, no. 5, pp. 882–895, 2005. (Cited on page 33.)
- [73] D. Kundur and D. Hatzinakos, “Blind image deconvolution,” *IEEE Signal Processing Magazine*, vol. 13, no. 3, pp. 43–64, 1996. (Cited on page 33.)
- [74] A. K. Takahata, E. Z. Nadalin, R. Ferrari, L. T. Duarte, R. Suyama, R. R. Lopes, J. M. T. Romano, and M. Tygel, “Unsupervised processing of geophysical signals: A review of some key aspects of blind deconvolution and blind source separation,” *IEEE Signal Processing Magazine*, vol. 29, no. 4, pp. 27–35, 2012. (Cited on page 33.)
- [75] K. Abed-Meraim, W. Qiu, and Y. Hua, “Blind system identification,” *Proceedings of the IEEE*, vol. 85, no. 8, pp. 1310–1322, 1997. (Cited on page 33.)
- [76] A. Aïssa-El-Bey, M. Grebici, K. Abed-Meraim, and A. Belouchrani, “Blind system identification using cross-relation methods: further results and developments,” in *7th International Symposium on Signal Processing and Its Applications (ISSPA)*, vol. 1, July 2003, pp. 649–652. (Cited on pages 33 and 94.)
- [77] E. Moulines, P. Duhamel, J. F. Cardoso, and S. Mayrargue, “Subspace methods for the blind identification of multichannel FIR filters,” *IEEE Transactions on Signal Processing*, vol. 43, no. 2, pp. 516–525, 1995. (Cited on pages 33, 35 and 36.)
- [78] Y. Hua, “Fast maximum likelihood for blind identification of multiple FIR channels,” *IEEE Transactions on Signal Processing*, vol. 44, no. 3, pp. 661–672, 1996. (Cited on pages 33, 35, 36 and 96.)
- [79] A. Aïssa-El-Bey, K. Abed-Meraim, and Y. Grenier, “Blind audio source separation using sparsity based criterion for convolutive mixture case,” in *Indepen-*

- dent Component Analysis and Signal Separation (ICA)*, vol. 4666, 2007, pp. 317–324. (Cited on pages 33 and 73.)
- [80] A. Aïssa-El-Bey and K. Abed-Meraim, “Blind SIMO channel identification using a sparsity criterion,” in *9th IEEE Workshop on Signal Processing Advances in Wireless Communications (SPAWC)*, Recife, Brazil, July 2008, pp. 271–275. (Cited on pages 33 and 38.)
- [81] ———, “Blind identification of sparse SIMO channels using maximum a posteriori approach,” in *16th European Signal Processing Conference (EUSIPCO)*, August 2008, pp. 1–5. (Cited on pages 33, 38 and 90.)
- [82] A. Aïssa-El-Bey, K. Abed-Meraim, and C. Laot, “Adaptive blind estimation of sparse SIMO channels,” in *International Workshop on Systems, Signal Processing and their Applications (WOSSPA)*, May 2011, pp. 348–351. (Cited on page 33.)
- [83] K. Abed-Meraim, P. Loubaton, and E. Moulines, “A subspace algorithm for certain blind identification problems,” *IEEE Transactions on Information Theory*, vol. 43, no. 2, pp. 499–511, March 1997. (Cited on pages 34, 35, 37, 90, 96, 97 and 101.)
- [84] L. Perros-Meilhac, E. Moulines, K. Abed-Meraim, P. Chevalier, and P. Duhamel, “Blind identification of multipath channels: a parametric subspace approach,” *IEEE Transactions on Signal Processing*, vol. 49, no. 7, pp. 1468–1480, 2001. (Cited on page 38.)
- [85] J. P. Delmas, “Subspace tracking for signal processing,” in *Adaptive signal processing : next generation solutions*. Wiley-IEEE Press, 2010, pp. 211 – 270. (Cited on page 42.)
- [86] D. Lee, W. Lee, Y. Lee, and Y. Pawitan, “Super-sparse principal component analyses for high-throughput genomic data,” *BMC Bioinformatics*, vol. 11, no. 1, p. 296, Jun 2010. [Online]. Available: <https://doi.org/10.1186/1471-2105-11-296> (Cited on page 42.)
- [87] A. Hyvarinen and K. Raju, “Imposing sparsity on the mixing matrix in independent component analysis,” *Neurocomputing*, vol. 49, no. 1, pp. 151 – 162, 2002. [Online]. Available: <http://www.sciencedirect.com/science/article/pii/S092523120200512X> (Cited on page 42.)

- [88] R. Kumaresan and D. W. Tufts, "Estimating the angles of arrival of multiple plane waves," *IEEE Transactions on Aerospace and Electronic Systems*, vol. AES-19, no. 1, pp. 134–139, 1983. (Cited on pages 42 and 51.)
- [89] C. Ramirez, V. Kreinovich, and M. Argaez, "Why l1 is a good approximation to l0: A geometric explanation," *Journal of Uncertain Systems*, vol. 7, pp. 203–207, 2013. (Cited on pages 44 and 75.)
- [90] S. Amari, "Natural gradient works efficiently in learning," *Neural Computation*, vol. 10, no. 2, pp. 251–276, 1998. (Cited on pages 45, 75, 117 and 118.)
- [91] J. Cardoso, "High-order contrasts for independent component analysis," *Neural Computation*, vol. 11, no. 1, pp. 157–192, 1999. (Cited on pages 48, 79, 82 and 87.)
- [92] S. A. W. Shah, K. Abed-Meraim, and T. Y. Al-Naffouri, "Blind source separation algorithms using hyperbolic and givens rotations for high-order qam constellations," *IEEE Transactions on Signal Processing*, vol. 66, no. 7, pp. 1802–1816, 2018. (Cited on pages 48 and 79.)
- [93] C. Riou and T. Chonavel, "Fast adaptive eigenvalue decomposition: A maximum likelihood approach," in *1997 IEEE International Conference on Acoustics, Speech, and Signal Processing*, vol. 5, 1997, pp. 3565–3568. (Cited on page 51.)
- [94] P. Georgiev, F. Theis, and A. Cichocki, "Sparse component analysis and blind source separation of underdetermined mixtures," *IEEE Transactions on Neural Networks*, vol. 16, no. 4, pp. 992–996, 2005. (Cited on pages 56 and 57.)
- [95] M. Aharon, M. Elad, and A. M. Bruckstein, "On the uniqueness of overcomplete dictionaries, and a practical way to retrieve them," *Linear Algebra and its Applications*, vol. 416, no. 1, pp. 48 – 67, 2006. (Cited on pages 56 and 57.)
- [96] D. A. Spielman, H. Wang, and J. Wright, "Exact recovery of sparsely-used dictionaries," *CoRR*, vol. abs/1206.5882, 2012. [Online]. Available: <http://arxiv.org/abs/1206.5882> (Cited on pages 56, 57 and 70.)
- [97] A. Agarwal, A. Anandkumar, P. Jain, and P. Netrapalli, "Learning Sparsely Used Overcomplete Dictionaries via Alternating Minimization," *ArXiv e-prints*, Oct. 2013. (Cited on pages 56 and 57.)
- [98] A. Agarwal, A. Anandkumar, P. Jain, P. Netrapalli, and R. Tandon, "Learning sparsely used overcomplete dictionaries via alternating minimization," *CoRR*, 2013. (Cited on pages 56 and 57.)

- [99] R. Gribonval and K. Schnass, “Dictionary identification sparse matrix factorization via ℓ_1 -minimization,” *IEEE Transactions on Information Theory*, vol. 56, no. 7, pp. 3523–3539, 2010. (Cited on pages 56 and 57.)
- [100] Q. Geng, H. Wang, and J. Wright, “On the local correctness of ℓ_1 minimization for dictionary learning,” *CoRR*, vol. abs/1101.5672, 2011. (Cited on pages 56 and 58.)
- [101] R. Gribonval, R. Jenatton, and F. Bach, “Sparse and spurious: Dictionary learning with noise and outliers,” *IEEE Transactions on Information Theory*, vol. 61, no. 11, pp. 6298–6319, 2015. (Cited on pages 56 and 58.)
- [102] A. Belouchrani, K. Abed-Meraim, J. F. Cardoso, and E. Moulines, “A blind source separation technique using second-order statistics,” *IEEE Transactions on Signal Processing*, vol. 45, no. 2, pp. 434–444, 1997. (Cited on page 59.)
- [103] V. Perrone, P. A. Jenkins, D. Spano, and Y. Whye Teh, “Poisson Random Fields for Dynamic Feature Models,” *arXiv e-prints*, p. arXiv:1611.07460, Nov. 2016. (Cited on page 67.)
- [104] A. Mesloub, K. Abed-Meraim, and A. Belouchrani, “A new algorithm for complex non-orthogonal joint diagonalization based on shear and givens rotations,” *IEEE Transactions on Signal Processing*, vol. 62, no. 8, pp. 1913–1925, 2014. (Cited on page 74.)
- [105] M. Abuthinien, S. Chen, and L. Hanzo, “Semi-blind joint maximum likelihood channel estimation and data detection for mimo systems,” *IEEE Signal Processing Letters*, vol. 15, pp. 202–205, 2008. (Cited on page 90.)
- [106] H. R. Palally, S. Chen, W. Yao, and L. Hanzo, “Particle swarm optimisation aided semi-blind joint maximum likelihood channel estimation and data detection for mimo systems,” in *2009 IEEE/SP 15th Workshop on Statistical Signal Processing*, Aug 2009, pp. 309–312. (Cited on page 90.)
- [107] M. Abuthinien, S. Chen, A. Wolfgang, and L. Hanzo, “Joint maximum likelihood channel estimation and data detection for MIMO systems,” in *2007 IEEE International Conference on Communications*, June 2007, pp. 5354–5358. (Cited on page 90.)
- [108] C. Wen, C. Wang, S. Jin, K. Wong, and P. Ting, “Bayes-optimal joint channel-and-data estimation for massive MIMO with low-precision adcs,” *IEEE Transactions on Signal Processing*, vol. 64, no. 10, pp. 2541–2556, May 2016. (Cited on page 90.)

- [109] J. Ma and L. Ping, "Data-aided channel estimation in large antenna systems," in *2014 IEEE International Conference on Communications (ICC)*, June 2014, pp. 4626–4631. (Cited on page 90.)
- [110] Z. Hajji, A. Aïssa-El-Bey, and K. Amis, "Simplicity-based recovery of finite-alphabet signals for large-scale mimo systems," *Digital Signal Processing*, vol. 80, pp. 70 – 82, 2018. (Cited on pages 90, 98 and 99.)
- [111] A. Swami, G. Giannakis, and S. Shamsunder, "Multichannel ARMA processes," *IEEE Transactions on Signal Processing*, vol. 42, no. 4, pp. 898–913, April 1994. (Cited on page 96.)
- [112] V. Zarzoso and A. K. Nandi, "Exploiting non-Gaussianity in blind identification and equalisation of MIMO FIR channels," *IEE Proceedings - Vision, Image and Signal Processing*, vol. 151, no. 1, pp. 69–75, Feb 2004. (Cited on page 96.)
- [113] A. Gorokhov and P. Loubaton, "Blind identification of MIMO-FIR systems: A generalized linear prediction approach," *Signal Processing*, vol. 73, no. 1, pp. 105 – 124, 1999. (Cited on page 96.)
- [114] L. Tong and S. Perreau, "Multichannel blind identification: from subspace to maximum likelihood methods," *Proceedings of the IEEE*, vol. 86, no. 10, pp. 1951–1968, Oct 1998. (Cited on page 96.)
- [115] D. T. M. Slock and C. B. Padias, "Further results on blind identification and equalization of multiple FIR channels," in *1995 International Conference on Acoustics, Speech, and Signal Processing*, vol. 3, May 1995, pp. 1964–1967 vol.3. (Cited on pages 96 and 98.)
- [116] M. Feder and J. A. Catipovic, "Algorithms for joint channel estimation and data recovery-application to equalization in underwater communications," *IEEE Journal of Oceanic Engineering*, vol. 16, no. 1, pp. 42–55, Jan 1991. (Cited on page 96.)
- [117] D. Gesbert, P. Duhamel, and S. Mayrargue, "Blind least-squares approaches for joint data/channel estimation," in *1996 IEEE Digital Signal Processing Workshop Proceedings*, Sep. 1996, pp. 450–453. (Cited on pages 96 and 98.)
- [118] F. Alberge, P. Duhamel, and M. Nikolova, "Adaptive solution for blind identification/equalization using deterministic maximum likelihood," *IEEE Transactions on Signal Processing*, vol. 50, no. 4, pp. 923–936, April 2002. (Cited on pages 96 and 98.)

- [119] N. Seshadri, “Joint data and channel estimation using fast blind trellis search techniques,” in *[Proceedings] GLOBECOM '90: IEEE Global Telecommunications Conference and Exhibition*, Dec 1990, pp. 1659–1663 vol.3. (Cited on pages 96 and 98.)
- [120] C. L. W. Monisha Ghosh, “Maximum-likelihood blind equalization,” *Optical Engineering*, vol. 31, pp. 31 – 31 – 5, 1992. (Cited on pages 96 and 98.)
- [121] S. Talwar, M. Viberg, and A. Paulraj, “Blind estimation of multiple co-channel digital signals using an antenna array,” *IEEE Signal Processing Letters*, vol. 1, no. 2, pp. 29–31, Feb 1994. (Cited on pages 96 and 98.)
- [122] F. Alberge, M. Nikolova, and P. Duhamel, “Blind identification/equalization using deterministic maximum likelihood and a partial prior on the input,” *IEEE Transactions on Signal Processing*, vol. 54, no. 2, pp. 724–737, Feb 2006. (Cited on pages 96 and 98.)
- [123] S. Visuri and V. Koivunen, “Resolving ambiguities in subspace-based blind receiver for MIMO channels,” in *Conference Record of the Thirty-Sixth Asilomar Conference on Signals, Systems and Computers, 2002.*, vol. 1, Nov 2002, pp. 589–593 vol.1. (Cited on pages 97 and 101.)
- [124] D. L. Donoho and J. Tanner, “Counting faces of randomly projected polytopes when the projection radically lowers dimension,” *Journal of the American Mathematical Society*, vol. 22, no. 1, pp. 1–53, 2009. [Online]. Available: <http://www.jstor.org/stable/40587224> (Cited on page 98.)
- [125] M. Grant and S. Boyd, “CVX: Matlab software for disciplined convex programming, version 2.1,” <http://cvxr.com/cvx>, Mar. 2014. (Cited on pages 104 and 116.)
- [126] H. H. Yang and S. Amari, “Adaptive online learning algorithms for blind separation: Maximum entropy and minimum mutual information,” *Neural Computation*, vol. 9, no. 7, pp. 1457–1482, 1997. (Cited on pages 117 and 118.)

Résumé des Travaux de Thèse

Introduction

Au cours des dernières années, nos besoins en matière de transmission de données avec moins de latence et d'une manière efficace ne font qu'augmenter. Les communications sans fil et les services Internet ont infiltré la société et ont changé notre vie en dépassant toutes les attentes. En outre, la demande de traitement du signal de réseau fiable et efficace continue de croître rapidement, en particulier avec les nouveaux contextes de communication entre machines M2M et internet des objets (IoT). Selon les prévisions de Cisco, d'ici 2022, on déplacera les 28 milliards d'appareils connectés dans le monde avec plus de la moitié consacré aux applications des communications entre machines. Malheureusement, la nécessité de systèmes de traitement et de transmission plus efficaces continue à drainer des ressources qui sont limitées telles que la bande spectrale, la densité des composants des circuits intégrés et leur consommation d'énergie. Il est donc impératif de développer de nouvelles techniques de traitement du signal multidimensionnel pour relever ces défis.

Un problème majeur des communications sans fil est l'estimation de l'information d'état du canal (CSI). Malgré la perte d'efficacité de la bande passante, les solutions basées sur des séquences pilotes sont généralement utilisées. Du point de vue de l'efficacité spectrale, les solutions basées sur des méthodes aveugles ou semi-aveugles sont les plus appropriées, car elles donnent à l'émetteur plus de flexibilité en lui permettant de réduire ou de supprimer totalement les séquences pilotes afin d'avoir une occupation optimale de la bande passante. Les techniques aveugles sont également recommandées pour traiter des problèmes pour lesquels nous ne pouvons pas influencer les entrées, tels que l'extraction de l'électrocardiogramme fœtal (FECG) ou dans le cas des communications militaires.

Afin d'améliorer le traitement des signaux reçus par les capteurs, toute l'information à priori disponible doit être utilisée. Dans diverses applications, l'à priori de parcimonie a été utilisé avec succès et il a beaucoup attiré l'attention des chercheurs dans les domaines du traitement du signal et des images, de la vision par ordinateur et de la reconnaissance des formes. Malgré l'ampleur des recherches consacrées aux méthodes basées sur la parcimonie, le potentiel de cet à priori n'est pas pleinement exploité et certains problèmes restent largement ouverts.

Du point de vue du traitement du signal, les solutions algorithmiques futures doivent présenter une complexité de calcul faible et suivre des approches adaptatives

dans lesquels les sorties peuvent être mises à jour sur la base des sorties précédentes sans répéter tous les traitements. Ceci est important afin de réduire la consommation énergétique des calculateurs et pour pouvoir garder un traitement efficace même dans des environnements non stationnaires.

Motivée par les idées ci-dessus, cette thèse combine les dernières avancées en matière de représentation / estimation parcimonieuse et de méthodes de traitement du signal multidimensionnel, en particulier celles basées sur des techniques sous-espace, afin de relever le défi de développer de meilleures solutions aveugles à faible coût calculatoire. Nous avons étudié trois axes principaux: la poursuite du sous-espace principal parcimonieux, la séparation aveugle de sources parcimonieuses et l'identification aveugle de canaux parcimonieux. Nous avons à chaque fois visé des solutions adaptatives à faible coût calculatoire.

La parcimonie et l'identification aveugle de système : état de l'art

L'identification aveugle des systèmes est une technologie fondamentale du traitement du signal et fait l'objet d'un intérêt croissant pour la recherche. Au même temps, l'utilisation de l'information de parcimonie dans certaines applications de traitement du signal a connu un grand succès. Par conséquent, la combinaison de ces deux idées semble intéressante, en particulier pour répondre au défi de développement d'algorithmes plus efficaces avec des contraintes de «temps réel». Les trois sujets principaux de cette thèse sont: la poursuite du sous-espace principal parcimonieux, où nous considérons un mélange instantané avec une information de parcimonie sur la matrice de mélange du système. Le deuxième sujet est la séparation aveugle de sources parcimonieuses où nous considérons le même mélange instantané, mais avec une information de parcimonie sur les signaux sources. Le troisième sujet est l'identification aveugle du canal, où nous adoptons le modèle à réponse impulsionnelle finie (RIF) et un mélange convolutif, ce qui rend le problème plus complexe par rapport aux deux problèmes précédents. Dans ce cas, l'information a priori utile peu différée d'un cas à un autre. Nous avons considéré trois différents a priori: la parcimonie du canal RIF, la parcimonie des signaux sources et la simplicité du signal source.

La poursuite du sous-espace principal et la parcimonie

L'estimation de sous-espace joue un rôle important dans diverses applications modernes de traitement du signal. L'application la plus connue est l'estimation des directions d'arrivée (DOA) d'ondes planes reçues par un réseau d'antennes avec les

algorithmes MUSIC et ESPRIT. Lorsque nous considérons un contexte de suivi dans lequel les sources se déplacent, nous devons estimer plus fréquemment les DOA. Cependant, cela pourrait être compliqué en raison de la complexité de calcul de la décomposition nécessaire. En effet, l'implémentation de ces techniques est basée soit sur la décomposition en valeurs propres EVD soit sur la décomposition en valeurs singulières SVD. Dans un contexte de traitement adaptatif, l'utilisation de ces techniques est déconseillée vu la nécessité d'exécuter plusieurs décompositions EVD ou SVD, ce qui est très complexe et coûteux en temps de calcul. Afin de surmonter cette difficulté, un certain nombre d'algorithmes adaptatifs pour la poursuite de sous-espaces ont été développés. Les algorithmes de poursuite de sous-espace peuvent être classés en fonction du sous-espace recherché en algorithmes de poursuite du: sous-espace principal (signal, dominant), sous-espace mineurs (bruit) et les algorithmes qui peuvent être utilisés pour estimer les sous-espaces mineurs et principaux. Ils peuvent également être classés en fonction de leur complexité en trois classes. Si p indique le rang du sous-espace principal ou mineur que nous aimerions estimer, étant généralement $p \ll d$, il est fréquent de se référer aux trois classes par leur complexité de calcul, c'est-à-dire des algorithmes qui ont une complexité de calcul d'ordre $\mathcal{O}(d^2)$ ou $\mathcal{O}(pd^2)$, les algorithmes ayant une complexité de calcul d'ordre $\mathcal{O}(dp^2)$ et les algorithmes moins gourmands en temps de calcul, qui présentent une complexité de calcul linéaire d'ordre $\mathcal{O}(dp)$ tels que PAST, OPAST et FAPI.

L'analyse en composantes principales (PCA) a aussi une relation directe avec l'estimation du sous-espace principale. En effet, la PCA est largement utilisée pour le traitement des données et la réduction de dimension du problème étudié. Cependant, elle souffre du fait que chaque composante principale est une combinaison linéaire de toutes les variables d'origine. Il est donc souvent difficile d'interpréter les résultats du point de vue physique. De plus, les bases de données ont souvent un nombre de variables d'entrée comparable, voire beaucoup plus grand, que le nombre d'échantillons. Il a été démontré que si leur rapport ne converge pas à zéro, la PCA classique n'est pas cohérente. Pour remédier à ces inconvénients, différentes méthodes connues sous le nom de Sparse PCA (SPCA) ont été proposées pour former des composantes principales, chacune étant la combinaison linéaire d'un petit sous-ensemble de variables pouvant encore expliquer un pourcentage élevé de variance des données. On peut mentionner par exemple les algorithmes SCoTLASS, SPCA développée par Zou, Elastic-net SPCA, GPower et IMRP. La plupart des solutions proposées pour SPCA sont des algorithmes de traitement par bloc qui traitent toutes les données reçues en un seul bloc. Cependant, dans les systèmes non stationnaires, les paramètres à estimer changent avec le temps et le résultat d'une telle approche

est sous-optimal. Par conséquent, le traitement adaptatif doit être effectué après réception de chaque échantillon de données. Il est à noter que le problème de l'analyse adaptative en composantes principales est équivalent au problème de poursuite de sous-espace à des contraintes près. Parmi les solutions adaptatives existantes, on peut citer l'algorithme d'Oja avec seuillage progressif itératif (OIST) et l'algorithme streaming SPCA. L'algorithme ℓ_1 -PAST est proposé pour résoudre le principal problème de poursuite du sous-espace principal sous une contrainte de parcimonie sur la matrice des poids. Il a été développé pour l'application STAP (traitement adaptatif spatio-temporel) du radar à dispersion de phase aéroporté.

La séparation aveugle de sources et la parcimonie

La séparation aveugle de sources (BSS) est une technologie de traitement du signal qui a été utilisée de manière intensive dans plusieurs domaines, tels que le génie biomédical, le traitement audio (musique et parole) et les applications de communications numériques. L'objectif principal de la séparation de source est de récupérer des signaux inconnus à partir d'observations reçues sur un ensemble de capteurs. Dans la BSS, ni les sources ni la matrice de mélange ne sont connues, c'est-à-dire que nous exploitons uniquement les informations transportées par les signaux reçus et une information préalable sur les statistiques ou la nature des signaux sources transmis (par exemple, décorrélation, indépendance, parcimonie, diversité morphologique, etc). Dans le cas où l'indépendance des signaux d'entrées est considérée comme à priori, nous parlons alors de l'analyse en composante indépendantes (ICA). Contrairement à la PCA où nous chercherons des composantes ayant la plus grande variance mais qui n'ont aucune signification physique directe, la technique ICA tente de récupérer les sources d'origine en estimant une transformation linéaire et en supposant une indépendance statistique entre les sources inconnues. L'ICA est clairement liée au problème de séparation aveugle de sources, où les signaux sources sont supposés être i.i.d (distribués de manière identique et indépendante) et non Gaussiennes.

Les techniques de représentations parcimonieuses des signaux et des images ont connu un développement considérable au cours de l'essor des méthodes de compression et de débruitage à base d'ondelettes au début des années 90. Plus tard, ces techniques ont été exploitées pour la séparation aveugle de sources. Leur principal impact est qu'elles fournissent un cadre relativement simple pour séparer un nombre de sources supérieur au nombre de mélanges observés. En outre, elles améliorent grandement la qualité de la séparation dans le cas d'une matrice de mélange carrée (ou surdéterminée). La parcimonie a été introduite pour la première fois comme alternative aux fonctions de contraste standard d'ICA en utilisant une approche en-

tièrement Bayésienne. En parle alors d'analyse en composante parcimonieuse (SCA). Chaque source est supposée être parcimonieusement représentée dans une base (par exemple, une base d'ondelettes orthogonale) avec des coefficients qui suivent une certaine distribution qui force les éléments à être le plus proche de zéro. L'estimateur au sens du Maximum A Posteriori (MAP) peut être utilisé pour estimer la matrice de mélange et les signaux de coefficients. De nombreuses recherches récentes en SCA ont étendu la base à un dictionnaire sur-complet et utilisent la redondance pour améliorer la parcimonie des coefficients. La combinaison des résultats antérieurs de la BSS basés sur l'ICA et des récents progrès dans le domaine des représentations parcimonieuses a beaucoup aidé à développer de nouvelles techniques SCA. Le cas parcimonieux parfait suppose que les sources ont des supports mutuellement disjoints (ensembles d'échantillons non nuls) dans le domaine temporel ou transformé. Néanmoins, ce cas simple nécessite des signaux très parcimonieux. Malheureusement, ce n'est pas le cas pour une grande classe de données hautement structurées et en particulier dans le traitement d'images. De plus, au cours des dix dernières années, de nouveaux outils sont apparus à partir de l'analyse harmonique moderne: wavelets, ridgelets, curvelets, bandlets, contourlets, etc. Il était tentant de combiner plusieurs représentations pour créer un dictionnaire plus large de formes d'ondes qui permettrait la représentation parcimonieuse d'une plus large classe de signaux. Un algorithme pratique connu sous le nom d'Analyse en Composantes Morphologique (MCA) visant à décomposer les signaux dans des dictionnaires sur-complets composés d'une union de bases. Par exemple, une source lisse par morceaux (image de bande dessinée) est bien éparse dans un cadre serré en courbes alors qu'une source oscillante globalement déformée (texture) est mieux représentée à l'aide d'une transformée en cosinus discrète (DCT). La diversité morphologique repose alors sur la rareté de ces composants morphologiques dans des bases spécifiques.

L'identification aveugle de système et la parcimonie

Une communication fiable nécessite souvent l'identification de la réponse impulsionnelle du canal. Une telle identification peut faciliter l'égalisation de canal ainsi que la détection de séquence avec le maximum de vraisemblance. L'identification dite de canal aveugle signifie que le canal est identifié sans utiliser de signal d'apprentissage; Au lieu de cela, l'identification est réalisée en utilisant uniquement la sortie du canal avec certaines informations statistiques a priori sur l'entrée. Ces méthodes peuvent potentiellement augmenter la capacité de transmission du fait de l'élimination des signaux d'apprentissage. Le problème d'identification du canal aveugle a fait l'objet de beaucoup d'attention au cours des deux dernières décennies et de nombreuses solutions efficaces existent pour les systèmes à entrée unique, à sorties multiples

(SIMO) et à entrées multiples, à sorties multiples (MIMO) dans la littérature. Nous pouvons distinguer deux classes principales de méthodes d'identification de système aveugle BSI: les techniques de statistiques d'ordre supérieur (HOS) et de statistiques de second ordre (SOS). En général, les méthodes basées sur HOS nécessitent des échantillons de grande taille pour obtenir de meilleures performances d'estimation que les méthodes basées sur SOS. Parmi les célèbres techniques basées sur SOS, on peut citer la méthode des relations croisées (CR), la méthode des sous-espaces et la méthode en deux étapes maximum de vraisemblance (TSML). Malheureusement, il semble probable qu'en cas de réponse impulsionnelle très longue et d'un canal parcimonieux, ces méthodes fonctionnent mal. Ces canaux parcimonieux peuvent être rencontrés dans de nombreuses applications de communication, y compris les canaux de télévision haute définition (HDTV) et les canaux acoustiques sous-marins. Récemment, des solutions ont été proposées pour traiter ce cas en adaptant les méthodes d'identification à l'aveugle «classiques» au cas parcimonieux. Parmi les solutions qui tiennent compte de la parcimonie du canal, on cite la méthode CR sparse, la méthode MAP et sa version adaptative pour le cas d'un canal SIMO. Pour le cas d'un canal MIMO le problème est plus complexe et il existe peu de solution qui considère la parcimonie du canal avec un modèle convolutif.

Algorithmes de poursuite du sous-espace principal parcimonieux à faible coût calculatoire

Dans ce chapitre, notre objectif est de résoudre le problème de poursuite du sous-espace principal sous une contrainte de parcimonie sur la matrice de pondération. Cela sera crucial dans deux cas majeurs: lorsque nous traiterons le manque d'interprétabilité physique des résultats de la PCA, par exemple, dans la recherche génomique en haute dimension. Dans le second cas, où nous souhaiterions récupérer la matrice de mélange originale comme c'est le cas dans la séparation de source lorsque la matrice de mélange est parcimonieuse. De nombreuses solutions ont été proposées pour l'estimation de sous-espaces parcimonieux par bloc, généralement appelées méthodes SPCA. Contrairement au problème pas bloc, peu de solutions ont été proposé pour le schéma adaptatif.

Nous présentons ici les méthodes proposées pour résoudre le problème considéré dans les deux cas: orthogonal et non orthogonal, c'est-à-dire s'il existe des contraintes d'orthogonalité sur la matrice de pondération ou pas. Le cas non orthogonal correspond au problème de l'identification aveugle du système parcimonieux. Le cas orthogonal est nécessaire pour traiter les applications qui nécessitent ou préfèrent utiliser une matrice de pondération orthogonale, par ex. les algorithmes MUSIC et

minimum-norm dans le contexte de l'estimation de la DOA. La plupart des méthodes proposées dans la littérature souffrent d'un compromis entre la performance du sous-espace et le niveau de parcimonie visée. Pour résoudre ce problème, nous avons proposé une approche en deux étapes: dans la première on utilise l'algorithme de poursuite de sous-espace de l'état de l'art FAPI pour une estimation adaptative d'une base orthonormale du sous-espace principal. Ensuite, sous la contrainte de parcimonie, une estimation de la matrice de pondération souhaitée est effectuée dans la deuxième étape en utilisant différentes techniques d'optimisation tel que le gradient naturel et les rotations de Shear et Givens.

Une étude de performance est effectuée en utilisant des données synthétiques (avec des matrices de mélange orthogonal et non orthogonal) et des données réels a confirmé la supériorité des algorithmes proposés par rapport à ceux de l'état de l'art. Les algorithmes résultants ont différentes caractéristiques telles que la performance de parcimonie (vitesse et limite de convergence), la complexité de calcul et l'orthogonalité de la solution. Le tableau A.1 résume la complexité de calcul par itération des algorithmes et s'il considère la contrainte d'orthogonalité avec l'algorithme FAPI comme témoin des algorithmes de poursuite de sous-espace sans parcimonie et l'algorithme ℓ_1 -PAST pour représenter l'état de l'art.

Algorithme	Complexité de calcul par itération	Orthogonalité
FAPI	$3dp + \mathcal{O}(p^2)$	Oui
ℓ_1 -PAST	$3dp^2 + 3dp + \mathcal{O}(p^2)$	Oui
SS-FAPI	$2dp^2 + 4dp + \mathcal{O}(p^2)$	Non
OSS-FAPI	$2dp^2 + 3dp + \mathcal{O}(p^3)$	Oui
SS-FAPI2	$4dp + \mathcal{O}(p^2)$	Non
SGSS-FAPI	$4dp + 8\alpha d + \mathcal{O}(p^2)$	Non
GSS-FAPI	$4dp + 4\alpha d + \mathcal{O}(p^2)$	Oui

Table A.1: Résumé des complexités de calcul par itération des algorithmes proposés et s'il considère la contrainte d'orthogonalité

Une étude théorique est aussi proposée pour confirmer l'unicité et la convergence locale de la solution donnée par nos algorithmes. Nous avons pu conclure que, sous certaines contraintes, la méthode de descente de gradient proposée convergera asymptotiquement vers les minima locaux équivalant à la matrice du mélange originale à une matrice de permutation et signe prés. Ces contraintes concernent la taille du système ($d > Cp \log(p)$), la parcimonie de la vérité de terrain (la matrice du mélange originale) et sa cohérence.

Comparés aux méthodes proposées dans la littérature, nos algorithmes présen-

tent l'avantage d'un faible coût de calcul avec des performances améliorées en termes de précision de l'estimation de sous-espace et de parcimonie des résultats. Nous avons aussi fait l'étude théorique qui montrent que nos algorithmes nous permettent de récupérer la matrice de mélange parcimonieuse originale sous certaines contraintes légères. Enfin, la diversité des méthodes proposées les rend adaptables à de nombreuses applications en fonction des contraintes imposées au problème, telles que la complexité de calcul et l'orthogonalité de la matrice de pondération.

Séparation aveugle de sources parcimonieuses

Bien que la séparation aveugle de sources parcimonieuses puisse être particulièrement utile pour séparer des mélanges sous-déterminés (plus de sources que de capteurs), elle est également potentiellement intéressante pour le mélange bruité sur-déterminé (plus de capteurs que de sources), auquel cas la parcimonie est exploitée pour améliorer la qualité de séparation. Dans ce chapitre, nous abordons le problème de la séparation aveugle adaptative de sources parcimonieuses dans le cas sur-déterminé bruité. Nous avons proposé deux algorithmes basés sur la même approche en deux étapes que nous utilisions précédemment pour la poursuite du sous-espace principal parcimonieux. Dans la première étape on utilise l'algorithme OPAST ou FAPI pour estimer adaptativement une base orthogonale du sous-espace principale. Dans la deuxième étape, on estime la matrice du poids parcimonieuse recherchée en utilisant différentes méthodes d'optimisation pour minimiser une fonction de coût qui représente la norme ell_1 des signaux séparés.

Le premier algorithme proposé est DS-OPAST (DS signifie Data Sparsity) basé sur un schéma de gradient naturel et qui utilise aussi une technique de projection approximée pour garder un coût calculatoire indépendant du temps et donc adéquat pour un contexte adaptatif. Une autre version nommée DS-OPAST2 est aussi proposée en utilisant plus d'approximation dans le but de réduire encore plus le temps de calcul. Le deuxième algorithme SGDS-FAPI se base sur les rotations Shear et Givens pour la minimisation de la norme ell_1 . Différentes versions ont été proposées, toutes dépendent de la stratégie de sélection des indices de rotations Shear and Givens considérée ou en utilisant une optimisation jointe ou séparées des paramètres des rotations.

Des simulations numériques sont présentées en utilisant des données synthétique parcimonieuse dans le domaine temporel ou des signaux de paroles où la parcimonie est obtenue après une l'application du transformation DCT. Nous avons montré que les algorithmes proposés surpassent les solutions existantes à la fois en vitesse de convergence et en qualité d'estimation.

Algorithme	étape 1	étape 2	Complexité de calcul par itération
DS-OPAST	OPAST	Gradient naturel	$dp^2 + 4dp + \mathcal{O}(p^3)$
DS-OPAST2	OPAST	Gradient naturel	$5dp + \mathcal{O}(p^3)$
SGDS-FAPI	FAPI	Rotations de Shear et Givens	$5dp + 2dL + 8\alpha_1d + \mathcal{O}(p^2)$
SGDS-FAPI2	FAPI	Rotations de Shear et Givens	$5dp + 2dL + 8\alpha_2d + \mathcal{O}(p^2)$

Table A.2: Résumé des Complexités de calcul par itération pour les algorithmes proposés pour la séparation aveugle de sources parcimonieuses

Identification aveugle des systèmes parcimonieux

Dans ce chapitre, nous présentons nos contributions à la résolution du problème d'identification de canal parcimonieux dans les cas d'entrée simple, de sorties multiples (SIMO) et d'entrées multiples, de sorties multiples (MIMO). Contrairement aux deux problèmes précédents où nous avons considéré des mélanges instantanés, cette fois nous considérons des mélanges convolutifs avec un modèle de réponses impulsionnelles finis pour les canaux.

Tout d'abord, dans le cas d'un canal SIMO parcimonieux, on considère un canal variant dans le temps et on propose deux solutions adaptatives qui se basent sur une approche de maximum a posteriori MAP. On considère que les coefficients de la réponse impulsionnelle du canal suivent une distribution Laplacienne généralisée qui donne plus de probabilité aux éléments proche du zéro pour améliorer la parcimonie. Ensuite, une méthode de descente de gradient est utilisée pour proposer le premier algorithme MAP-adapt en utilisant des approximations liées à la fenêtre exponentielle considérée pour rendre la complexité de calcul indépendante du temps et donc adéquate pour un schéma adaptative. Un deuxième algorithme AMAP-adapt est proposé pour réduire encore la complexité du calcul en utilisant une approximation pour le calcul de la pseudo-inverse d'une matrice de grande taille. Les simulations ont montré que nos algorithmes améliorent clairement l'estimation du canal par rapport aux méthodes d'état de l'art en gardant un coût de calcul plus faible. On a aussi testé nos algorithmes dans le cas d'une surestimation de l'ordre du canal, où on a remarqué leur robustesse contre les erreurs due à ce problème.

Même si une séquence d'entraînement existe, leur combinaison avec des techniques aveugles entraîne souvent une amélioration des performances, ce qui explique l'intérêt croissant que suscitent l'estimation conjointe des canaux et des données, également appelées estimation de canal assistée par données. Notre deuxième con-

tribution vise à estimer conjointement les informations sur l'état du canal et les données transmises dans le cas d'un canal MIMO à l'aide d'une approche de maximum de vraisemblance déterministe (DML) régularisée basée sur différents types d'a priori. Dans le cas où le système ne varie pas dans le temps et si la séquence de données est suffisamment longue pour pouvoir construire un modèle statistique fiable, il convient d'utiliser une méthode SML, car dans ce cas, la méthode statistique surpasse la méthode déterministe en qualité de l'estimation. Toutefois, dans un environnement à évanouissements rapides, les données relatives à un canal donné ne sont pas nombreuses, ce qui rend une estimation statistique fiable moins efficace. Dans une telle situation, les symboles sont supposés arbitraires et une méthode DML est utilisée. L'approche DML régularisée est un compromis entre les approches DML et SML, où nous tirons parti de certaines informations préalables sur les données d'entrée et / ou le canal de transmission pour améliorer les résultats de la DML.

Le premier à priori utilisé est la simplicité d'un signal à alphabet finis. En effet, la plupart des communications numériques sont basées sur des signaux transmis appartenant à un ensemble d'alphabets finis. L'introduction de la contrainte d'alphabet finis aux détecteur est compliqué vu le nombre de minima locaux introduits par l'ensemble discret des solutions. Nous avons considéré la propriété de simplicité qui est une sorte de relaxation de la contrainte de l'alphabet finis. Un signal est dit simple si la majorité de ses éléments sont égales aux bornes de son alphabet finis. Le taux de simplicité est donc liée à la modulation considérée. Cette relaxation a pour but de rendre le problème d'optimisation convexe et le coût calculatoire ne dépend pas de la taille de la constatation. Le deuxième à priori considéré est la parcimonie des signaux sources. Comme dans le chapitre précédent cette parcimonie peut être dans le domaine temporel ou dans le domaine de la transformée. On utilise la norme ℓ_1 pour représenter la parcimonie des coefficient du signal et avoir un critère d'optimisation convexe de type LASSO avec un paramètre de régularisation entre un terme des données et le terme de la parcimonie du signal. Comme dans le cas SIMO, les canaux peuvent aussi être parcimonieux dans le cas MIMO. C'est le troisième à priori considéré et de la même manière que pour signaux on va utilisé une formulation de type LASSO pour avoir un critère convexe avec un paramètre de régularisation entre un terme des données et un terme de la parcimonie du canal.

Pour l'initialisation de notre solution aveugle, nous proposons d'utiliser la méthode du sous-espace de bruit, suivie d'une étape de résolution d'ambiguïté induite par la méthode sous-espace. Cette ambiguïté est résolue soit en utilisant la parcimonie du canal, soit en utilisant une hypothèse d'indépendance des signaux sources lorsque le canal est non-parcimonieux. Ensuite une optimisation itérative convexe

est faite par rapport au canal et les signaux transmis. Les simulations numériques ont montré que la solution proposée surpasse les méthodes existantes en termes de NMSE et BER dans les différentes cas de figure.

Conclusions

Cette thèse cherche à trouver des solutions aveugles et à faible coût pour résoudre les problèmes de traitement du signal en combinant les progrès récents des méthodes d'estimation et de réduction de la dimensionnalité basées sur les sous-espaces avec l'information a priori de parcimonie. Ceci dans le but d'améliorer les performances des méthodes classiques de traitement du signal. Notre travail s'articule autour de trois axes principaux : - Le premier défi concerne la poursuite du sous-espace principal parcimonieux. Après une analyse approfondie de l'état de l'art, nous avons proposé des solutions peu coûteuses en calcul basées sur une approche en deux étapes dans lesquelles, à chaque donnée reçue, nous actualisons l'estimation du sous-espace principal, puis de la base parcimonieuse recherchée. Les algorithmes proposés ont différentes caractéristiques en termes de performance, la complexité de calcul et l'orthogonalité de la solution. De plus, nous montrons que sous certaines conditions modérées, ils sont capables de récupérer la matrice de mélange originale. - Le deuxième axe de recherche est la séparation adaptative aveugle de sources parcimonieuses. Notre objectif est d'utiliser l'information de parcimonie des signaux source afin de les séparer aveuglément de manière adaptative. Contrairement à la plupart des travaux sur la séparation aveugle de sources parcimonieuses, nous nous intéressons au cas surdéterminé où des méthodes de sous-espace peuvent être utilisées pour estimer le sous-espace principal des données reçues. Nous avons suivi une approche en deux étapes similaire à celle utilisée pour le suivi de sous-espace principal parcimonieux: nous commençons par estimer le sous-espace principal, puis nous calculons la matrice de séparation recherchée. Nous avons proposé deux algorithmes peu coûteux en calcul, ce qui les rend convenables pour des applications nécessitant un traitement adaptatif. - Le troisième sujet que nous avons traité est l'identification aveugle des systèmes à réponse impulsionnelle finie (FIR). Nous avons commencé par proposer une nouvelle solution permettant d'estimer de manière adaptative la réponse impulsionnelle d'un canal SIMO en utilisant la parcimonie du canal. L'algorithme proposé a une faible complexité de calcul. De plus, il est robuste aux erreurs dues à la surestimation de l'ordre du canal. Nous avons ensuite étudié le problème dans le cas d'un canal MIMO. Nous nous sommes basés sur une formulation régularisée du maximum de vraisemblance déterministe (DML) en ajoutant différentes fonctions de pénalité pour exploiter les informations a priori

disponibles, telles que la propriété de simplicité d'un source à alphabet fini ou / et la parcimonie du canal. Après une initialisation effectuée à l'aide d'une méthode de l'état de l'art, le critère résultant est optimisé alternativement par rapport au canal et les données en raison de la convexité de la formation utilisée pour chaque paramètre séparément. Les deux algorithmes proposés sont comparés à des solutions de l'état de l'art.

Titre : Représentations parcimonieuses et analyse multidimensionnelle : méthodes aveugles et adaptatives.

Mots clés : Traitement multidimensionnel, parcimonie, méthode aveugle, estimation adaptative, poursuite de sous-espace, identification du canal de transmission, séparation de sources.

Résumé : Au cours de la dernière décennie, l'étude mathématique et statistique des représentations parcimonieuses de signaux et de leurs applications en traitement du signal audio, en traitement d'image, en vidéo et en séparation de sources a connu une activité intensive. Cependant, l'exploitation de la parcimonie dans des contextes de traitement multidimensionnel comme les communications numériques reste largement ouverte. Au même temps, les méthodes aveugles semblent être la réponse à énormément de problèmes rencontrés récemment par la communauté du traitement du signal et des communications numériques tels que l'efficacité spectrale. Aussi, dans un contexte de mobilité et de non-stationnarité, il est important de pouvoir mettre en œuvre des solutions de traitement adaptatives de faible complexité algorithmique en vue d'assurer une consommation réduite des appareils. L'objectif de cette thèse est d'aborder ces challenges de traitement multidimensionnel en proposant des solutions aveugles de faible coût de calcul en utilisant a priori de parcimonie. Notre travail s'articule autour de trois axes principaux : la poursuite de sous-espace principal parcimonieux, la séparation adaptative aveugle de sources parcimonieuses et l'identification aveugle des systèmes parcimonieux. Dans chaque problème, nous avons proposé de nouvelles solutions adaptatives en intégrant l'information de parcimonie aux méthodes classiques de manière à améliorer leurs performances. Des simulations numériques ont été effectuées pour confirmer l'intérêt des méthodes proposées par rapport à l'état de l'art en termes de qualité d'estimation et de complexité calculatoire.

Title : Sparse multidimensional analysis using blind and adaptive processing.

Keywords : Multidimensional processing, sparsity, blind method, adaptive estimation, subspace tracking, channel identification, source separation

Abstract : During the last decade, the mathematical and statistical study of sparse signal representations and their applications in audio, image, video processing and source separation has been intensively active. However, exploiting sparsity in multidimensional processing contexts such as digital communications remains a largely open problem. At the same time, the blind methods seem to be the answer to a lot of problems recently encountered by the signal processing and the communications communities such as the spectral efficiency. Furthermore, in a context of mobility and non-stationarity, it is important to be able to implement adaptive processing solutions of low algorithmic complexity to ensure reduced consumption of devices. The objective of this thesis is to address these challenges of multidimensional processing by proposing blind solutions of low computational cost by using the sparsity a priori. Our work revolves around three main axes: sparse principal subspace tracking, adaptive sparse source separation and identification of sparse systems. For each problem, we propose new adaptive solutions by integrating the sparsity information to the classical methods in order to improve their performance. Numerical simulations have been conducted to confirm the superiority of the proposed methods compared to the state of the art.

